SINGLE CRYSTAL FACEPLATE EVALUATION

Final Report to

NAVAL TRAINING SYSTEMS CENTER
12350 Research Parkway
Orlando, FL 32826-3224

Contract N61339-90-C-0047

Presented to: Richard Hebb, Code 263

Prepared by:

TRIDENT INTERNATIONAL, INC.
Central Florida Research Park
3251 D Progress Drive
Orlando, FL 32826
407-282-3344
Fax 407-282-3343

October, 1993

DISCLAIMER NOTICE

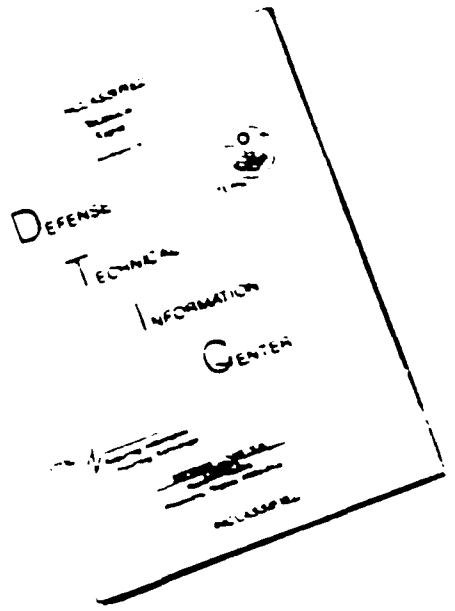

THIS DOCUMENT IS BEST QUALITY AVAILABLE. THE COPY FURNISHED TO DTIC CONTAINED A SIGNIFICANT NUMBER OF PAGES WHICH DO NOT REPRODUCE LEGIBLY.

REPORT DOCUMENTATION PAGE

1a. REPORT SECURITY CLASSIFICATION Unclassified	1b RESTRICTIVE MARKINGS
2a. SECURITY CLASSIFICATION AUTHORITY	3. DISTRIBUTION/AVAILABILITY OF REPORT Approved for Public Release Distribution is Unlimited
2b. DECLASSIFICATION/DOWNGRADING SCHEDULE	
4. PERFORMING ORGANIZATION REPORT NUMBER(S)	5. MONITORING ORGANIZATION REPORT NUMBER(S)
6a. NAME OF PERFORMING ORGANIZATION Trident International, Inc. 6b. OFFICE SYMBOL (*If applicable*)	7a. NAME OF MONITORING ORGANIZATION Naval Training Systems Center Sensor Simulation Branch, Code 263
6c. ADDRESS (*City, State, and ZIP Code*) 3251 D Progress Drive Orlando, FL 32826	7b. ADDRESS (*City, State, and ZIP Code*) 12350 Research Parkway Orlando, FL 32826-3224
8a. NAME OF FUNDING/SPONSORING ORGANIZATION Naval Air Systems Command 8b. OFFICE SYMBOL (*If applicable*)	9. PROCUREMENT INSTRUMENT IDENTIFICATION NUMBER N61339-90-C-0047
8c. ADDRESS (*City, State, and ZIP Code*)	10. SOURCE OF FUNDING NUMBERS PROGRAM ELEMENT NO. 0605502N; PROJECT NO.; TASK NO.; WORK UNIT ACCESSION NO.

11. TITLE (*Include Security Classification*)
Single Crystal Faceplate Evaluation

12. PERSONAL AUTHOR(S)
Tucker, A. R. and Kindl, H. J.

13a. TYPE OF REPORT	13b. TIME COVERED	14. DATE OF REPORT (*Year, Month, Day*)	15 PAGE COUNT
Final	FROM Nov. 90 TO Oct. 93	93 Oct. 25	

16. SUPPLEMENTARY NOTATION
Final Report for Single Crystal Faceplate Evaluation

17. COSATI CODES		
FIELD	GROUP	SUB-GROUP
09	05	

18. SUBJECT TERMS (*Continue on reverse if necessary and identify by block number*)
Video Projectors, Single Crystal Phosphor, CRTs, Flight Simulators

19. ABSTRACT (*Continue on reverse if necessary and identify by block number*) Single crystal phosphor faceplates are epitaxial phosphor grown crystalline substrates with the advantages of high light output, resolution and extended operational life. Single crystal phosphor faceplate industrial technology in the United States is capable of providing faceplates appropriate to the projection industry up to four (4) inches in diameter.

During the physical implementation phase of this program; ie, fabrication of SCFP CRTs, great difficulty was experienced in attempting to bond the SCFP to the CRT due to differences in the coefficients of expansion between the two. Although two (2) of the leading U.S. CRT manufacturers attempted to fabricate the units, both had only limited success. The units fabricated allowed confirmation of SCFP performance and life characteristics; however, the proces problems remaining are of such variable nature and definition as to preclude any recommendation for further development effort leading toward production.

Further, the high power that will be required to generate the desired light output at the SCFP efficiency levels (less than 5 lumens per watt) limits the practicality of usefulness in projector applications.

20. DISTRIBUTION/AVAILABILITY OF ABSTRACT ☐ UNCLASSIFIED/UNLIMITED ☒ SAME AS RPT. ☐ DTIC USERS	21. ABSTRACT SECURITY CLASSIFICATION Unclassified
22a. NAME OF RESPONSIBLE INDIVIDUAL Richard C. Hebb	22b. TELEPHONE (*Include Area Code*) (407) 380-4578 22c. OFFICE SYMBOL NTSC/Code 263

☆U.S. Government Printing Office: 1986—607-047

N61339-90-C-0047

TABLE OF CONTENTS

SINGLE CRYSTAL FACEPLATE EVALUATION

Final Report to:

Naval Training Systems Center
12350 Research Parkway
Orlando, FL 32826-3224
Code 263, Richard Hebb

25 October 1993

1.0 Introduction

The Naval Training Systems Center under separate development contract to Allied Signal Corp. (See Enclosure #11.1) developed single crystal faceplates which held promise of providing significantly improved life span over conventional powder phosphor cathode ray tubes (CRT) while maintaining acceptable resolution and light output characteristics. Single crystal faceplates being evaluated are composed of yttrium aluminum garnet (YAG) with an epitaxial cerium phosphor layer grown on the YAG substrate producing a cathodoluminescent material (CE:YAG). The single crystal nature of these faceplates should allow higher resolution (no phosphor grains) and higher thermal conductivity. (See Study submitted by Allied-Signal, Inc., Morristown, NJ, P.O. #9166, Enclosure #11.2). Determination of the characteristics of the single crystal faceplate in a CRT configuration was considered the next necessary technical objective of this program. To insure maximum usefulness of the data, the test evaluation was conducted as close to normal CRT operating conditions as was considered practical and cost effective to achieve. This was accomplished by assembly of a CRT Test Bed based upon the T1080 ultra-high resolution projection system which had been developed by Trident International, Inc. The subsystems incorporated into the test bed; i.e., power, deflection, focus, etc., were compatible with the range of parameters necessary to be exercised and varied for proper faceplate evaluation. The CRT Test Bed constituted a deliverable item.

During the initial phase of the program, a manufacturer was selected to fabricate Single Crystal Faceplate (SCFP) based CRT's using faceplates supplied to Trident International, Inc. by the Naval Training Systems Center. The criteria for selection of a CRT manufacturer to support the Single Crystal Faceplate Evaluation program were:

A. Experience with high power CRT design and fabrication.

B. Capability to conduct demountable faceplate test and evaluations.

C. Engineering capability to participate in electronic gun selection and to assist in specifying physical characteristics of faceplates of production tubes.

D. Participate in follow-on program as a CRT production source.

Four manufacturers were evaluated: Thomas Electronics, Inc., (Reference #10.1), Clinton Electronics, (Reference #10.2), Hughes Display Products, (Reference #10.3), and G. E. C. of England (Reference #10.4). Thomas Electronics, Inc. was initially selected. The problems encountered, the corrective actions taken and the ultimate selection of an alternate manufacturer are described in the following sections.

This report has been organized to reflect the fact that a change in the CRT manufacturer was effected during the program: i.e., Thomas Electronics was replaced by Hughes Display Products. In addition, comparative test data was utilized that was taken by Allied Signal, Inc., Hughes Display Products, Division of Hughes Aircraft Corp. and Trident International, Inc. The incorporation of liquid cooling by Trident International, Inc. produced test data at significantly higher power.

1.1 Single Crystal Faceplate Developments

Allied Signal, Inc. has done extensive development work in epitaxial layering of yttrium aluminum garnet (YAG) substrate and also etched retro-reflective reticulated surfaces unto the phosphor crystals in an attempt to improve the light conservation from the crystal faceplates. These techniques are described in their report titled Epitaxial Phosphor Faceplates for High Resolution High Intensity Cathode Ray Tubes, dated August, 1991, Contract N61339-90-C-0046 prepared for the Naval Training System Center, Orlando, FL. (Enclosure #1.1.1).

In implementing the contract, Trident International, Inc. utilized G.F.P. crystals which had been fabricated by Allied Signal, Inc. and furnished to Trident by the Navy. Subsequently, Trident contracted with Thomas Electronics, Inc. and Hughes Display Products to incorporate the crystals faceplates in various cathode ray tubes (CRT) glass envelopes.

Projection CRT's, contemporarily used, are constructed by depositing powder phosphors on the inside of a glass envelope. The glass faceplates have limited (poor) thermal conductivity. Also, the powder phosphor grains do not conduct heat well. With the advent of liquid cooling of CRT faceplates, some increase in power loading has been achieved. Conventional projectors have an average phosphor loading of 4 to 5 watts per square inch developing 12,000 to 15,000 foot lamberts of light from the green phosphor (typically P53). The luminous efficiency is approximately 20 lumens per watt. At 5 watts per square inch the powder phosphor's (P53, green) life expectancy has shown 50% decrease in brightness in the first 1,000 hours of high power operation.

In the search for improved life and possible other advantages in CRT developments, the utilization of single crystal faceplates composed of Y(3)AL(5)O(12) (YAG) that have been doped with rare-earth elements is being evaluated. The process used is to grow the phosphor materials as epitaxial layers on YAG substrate. The single crystal nature of the epitaxial faceplate allows higher resolution (no grain size) and intimate thermal conductivity. YAG is a comparatively good thermal conductor compared to glass which in operational use is liquid cooled.

The limitations on the size of faceplates have been the size of the garnets grown and the high temperature furnaces needed to process the crystals. Single sapphire crystals have been grown ten (10) inches in diameter. It is possible to conceive of larger YAG crystals being grown in the future. The current opinion is that a 4" limitation exists on YAG. An additional limitation is that YAG has a high refractive index (1.84 @ 550 um). This causes total internal reflection to occur at approximately 33 degrees (critical angle); therefore, considerable light energy is light piped to the edges of the faceplate, not to the optical entrance pupil.

Attempts to increase the optical efficiency of the faceplates by stippling (sandblasting) the phosphor side of the crystal and by various sophisticated reticulating methods to produce small retro-reflective pyramids on the epitaxial layer have been tried by Allied Signal (See Allied Signal, Inc. Report Enclosure #10.1).

Conventional aluminization of the epitaxial layer was found necessary to prevent creating a surface charge while electron beam scanning. The aluminization also improved the light reflection to the front of the crystal faceplate.

1.2 Background

Trident International, Inc. entered into this contract with the Naval Training Systems Center to incorporate and test SCFP CRT's in a high-powered projector.

Trident International, Inc. has extensive background in television projection. Their areas of development are:

A. High power, high resolution simulation projectors using standard sweep techniques as well as calligraphic (stroke written) methods.

B. Special optics developed for these applications.

C. Special CRT's in various colors using conventional powder phosphors.

D. Digital control of the geometry and operation of high power electron beams used in cathode ray tube television projectors.

Trident contracted with Thomas Electronics, Inc., Wayne, NJ., for the initial CRT construction using a 2" diameter Ce:YAG crystal that was stippled (sandblasted) and then aluminized. The detailed results of Thomas' test are discussed later in this report; however, in summary, they revealed light output efficiencies of approximately 4.8 lumens per watt. Subsequent testing by Trident using liquid cooling and with high voltages up to 40 kv and power densities of 90 watts per square inch generated brightness reaching 62,700 foot lamberts with no indication of phosphor saturation. The liquid cooling chamber utilizing only convection limited temperature to 113 degrees F., 30 degrees F. above ambient (82.4 degrees F.) High voltage increases during the test on this particular CRT, Serial #154871, appeared to increase the lumen efficiency from 4.35 lumens per watt to 4.84 lumens per watt. As the program progressed, initial performance data were successfully obtained from several CRT's assembled by Thomas Electronics using faceplates furnished as GFP material. These CRT's had a very limited life; i.e., failure of the frit seal interface became a major problem. After many attempts, Thomas concluded that they were unable to solve this problem and they were dropped from the program.

Trident then initiated an industry wide search for an alternate CRT manufacturing source. It was determined that competence with gradient seals and the ability to formulate frit material was necessary in order to cope with the problem of bonding the faceplates to the glass CRT bulb with the different expansion coefficients involved. The only manufacturer located who expressed confidence in his ability to solve the problem was Hughes Display Products, a subdivision of Hughes Aircraft Corp, Carlsbad, CA. A contract was let to them. The results of their efforts are reported hereinafter.

1.3 Objectives of the Program

A. To integrate GFP furnished single crystal (Ce:YAG) faceplates into cathode ray tubes to test performance characteristics.

B. To install SCFP CRT's in a high performance video projection system.

C. Test objectives are:

(1) To determine lumen efficiencies of Ce:YAG faceplate CRT's as constructed.

(2) To compare equivalent lumen output of SCFP CRT's versus powder phosphor CRT's.

(3) To measure equivalent resolution of SCFP CRT's at various power levels.

(4) To discover practical operational problems if SCFP's were used with projection CRT's.

(5) To ascertain manufacturing problems and their solutions, if possible.

D. To deliver an operational high definition television projector with an SCFP CRT installed.

E. To deliver test data, conclusions and recommendations as to future programs or product developments.

2.0 Construction of Cathode Ray Tubes Utilizing Single Crystal Faceplates.

2.1 Problems and Actions

2.1.1 Thomas Electronics, Inc.

A contract was let to Thomas Electronics, Inc. It included the test of four (4) each 1" diameter Ce:YAG crystal samples in their demountable vacuum chamber.

These tests were to evaluate the epitaxial phosphor layer versus electron beam (E beam) high voltage penetration to see if any correlation could be made.

The results of these tests are shown in Section #3.0. In the process of conducting the tests, aluminization of the rear surface of the crystals was found necessary to eliminate the buildup of surface charge. This technique is standard with powder phosphor CRT construction. No cooling was possible in the demountable vacuum chamber; so only low power readings were taken.

Thomas then used two 2" diameter SCFP's to construct two CRT's. The electron gun design was intended to operate at 1.5 ma @ 40 kv (60 watts) average beam power with a peak of approximately 3 ma (120 watts) (See Paragraph 2.2) The electron beam line width was expected to be approximately .003" at 1.5 ma @ 35 kv. The 2" diameter CRT (Thomas' designation 3M320YAG, Ser. #SCFP 00606-1-1) was tested at Thomas' facility without liquid cooling. The results are shown in Fig. 1 and 2 and Enclosure #11.3. The CRT's were delivered to Trident who incorporated a cooling chamber that would dissipate the heat energy anticipated. (See Para. 6.1).

After several CRT failures and rebuild attempts, Thomas concluded they could not match the expansion coefficient of the crystal faceplate with the glass envelope although several variationa of conventional frit seals were used.

2.1.2 Hughes Display Products

Trident researched the field again and found Hughes Display Products were willing to try the construction of several CRT's. Trident furnished Hughes with Ser. #10122-1-2, #10212-1-2 and #10214-1-1 Ce:YAG SCFP's for integration into CRT's. The electron gun specifications developed by Thomas were given to Hughes for their gun construction.

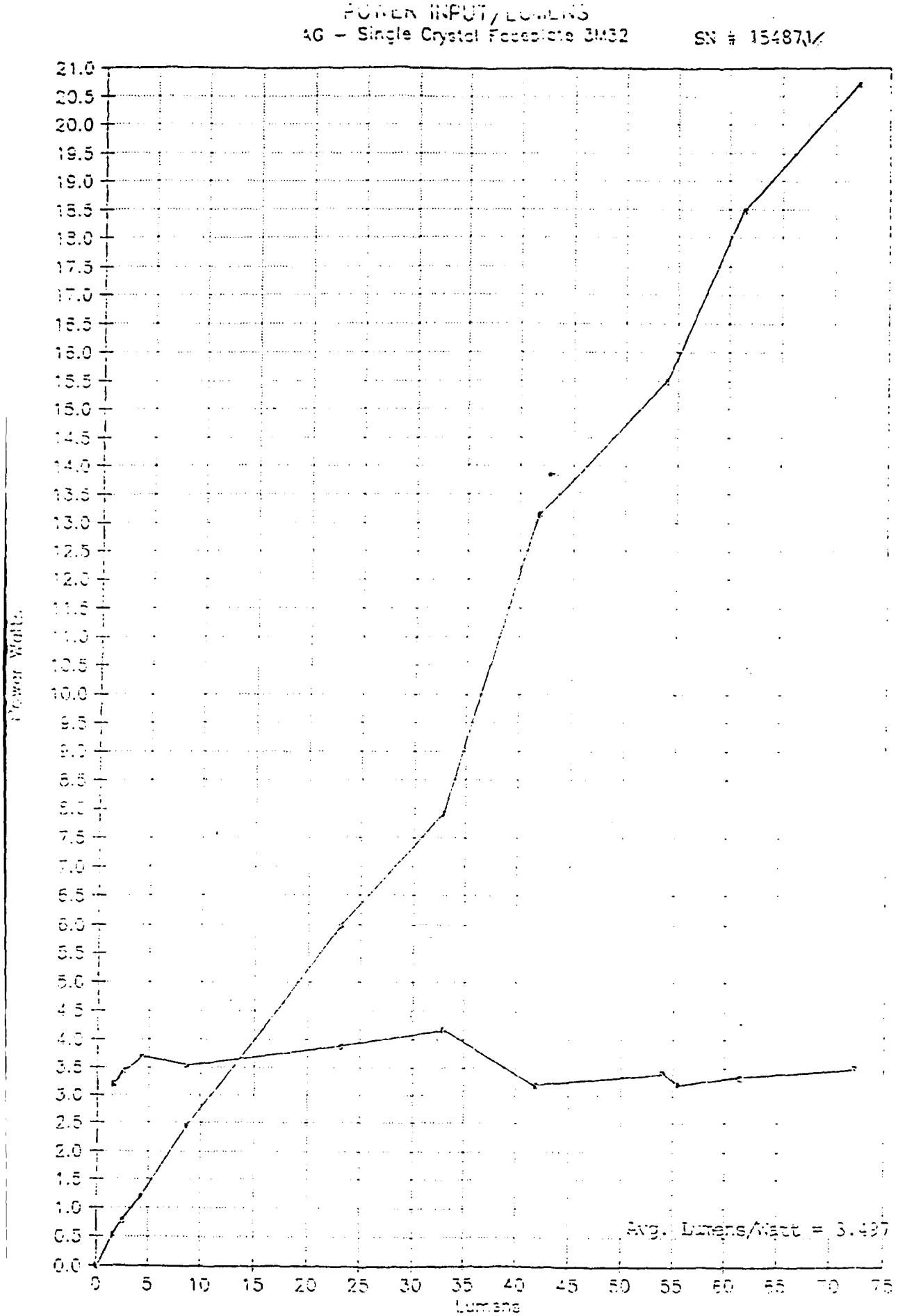
POWER INPUT/LUMENS
AG – Single Crystal Faceplate 3M32
SN # 15487(1)
Power Watts
Lumens
Avg. Lumens/Watt = 3.497

Figure 1

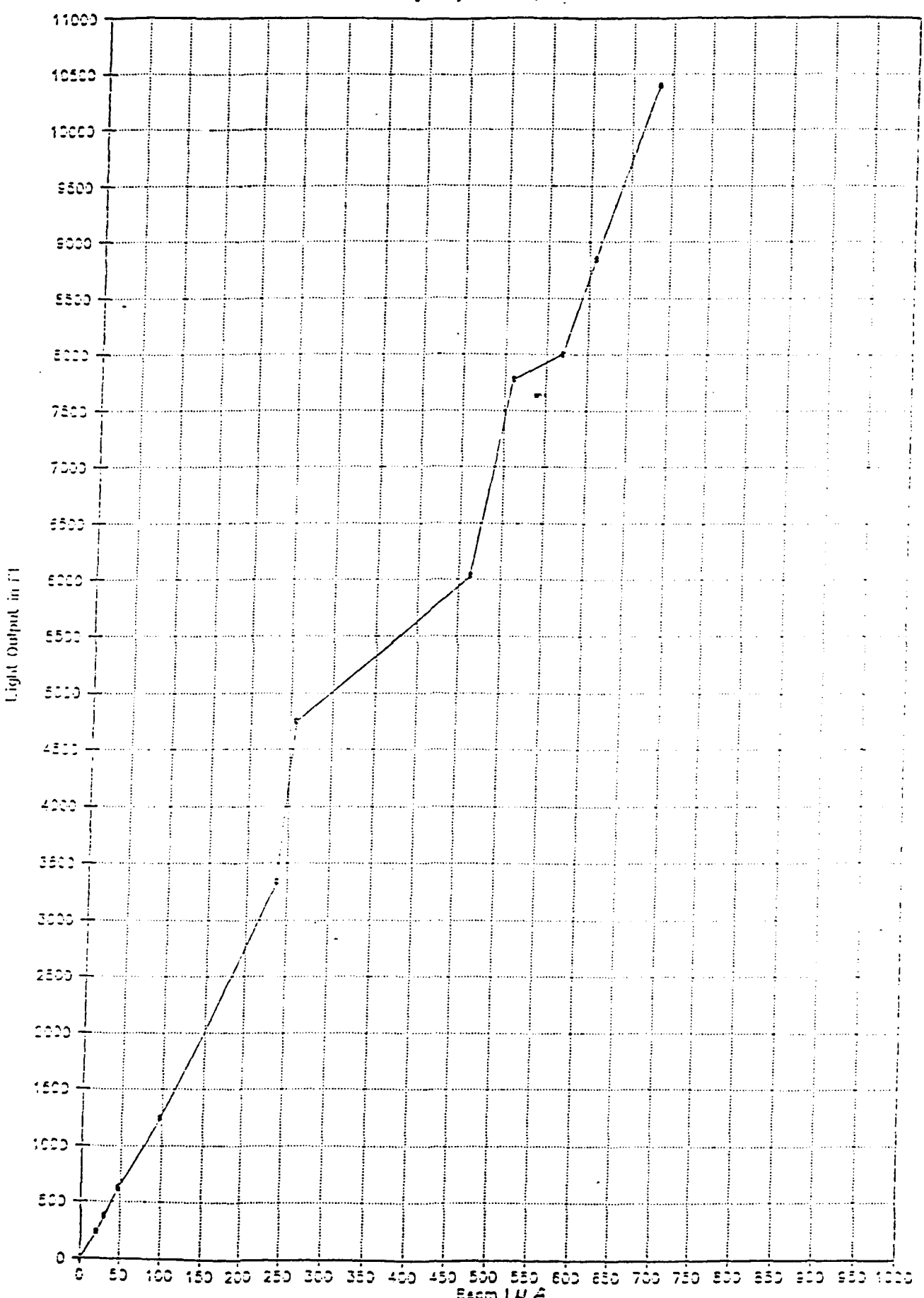
Light Output FL/BEAM I
YAG – Single Crystal Faceplate 3M320
SN # 154871
Light Output in FL
11000
10500
10000
9500
9000
8500
8000
7500
7000
6500
6000
5500
5000
4500
4000
3500
3000
2500
2000
1500
1000
500
0
0 50 100 150 200 250 300 350 400 450 500 550 600 650 700 750 800 850 900 950 1000
Beam I μA

Figure 2

Several attempts at sealing were made by Hughes before a successful CRT was able to be tested at Trident's facility in their test bed.

2.2 Electron Gun Design

Trident requested Thomas Electronics, Inc. to select an electron gun to incorporate in the CRT's to be used with single crystal faceplates. The performance desired was .0038 mil spot size at 112 watts (37 Kv at 3 ma peak beam current), and at 37 kv @ 1.5 ma, an .0015" average line width. The specification, noted below, was incorporated into the Hughes subcontract.

SPECIFICATIONS

TYPE 3M320YAG

Description

The 3M320YAG is a 3" diameter projection tube designed for high performance applications. It features a high resolution magnetic focus electron gun which, when employed in conjunction with a high quality focus coil, will display well over 1000 peak brightness elements. CRT uses a YAG faceplate.

Detailed Characteristics

Electrical Requirements

Focusing Method	Magnetic
Deflection Method	Magnetic
Heater Voltage	6.3 Volts
Heater Current @ 6.3 Volts	300 ma
Phosphor	Ce:YAG
Maximum Accelerator Voltage	45.000 Volts
Faceplate Power Dissipation Capability	Above 1 Watt/sq.in. External cooling Necessary

Mechanical Data

Overall Length	12" +/- .250 in.
Faceplate Thickness	.110 +/- .015 in.
Deflection Angle	45 Degrees
Maximum Outside Diameter	3.00" +/- .100 in.
Maximum Useful Screen Diameter	2.6"

Electrical Operating Conditions and Performance Requirements

Accelerator Voltage	37.000 Volts
Grid #1 Voltage	-200 Volts
Grid #2 Voltage	700 to 1,000 Volts
Line Width	.0015 in. maximum
Spot Position Error	.250" Radius Circle
Acceleration Current	1.5 ma

2.3 Glass Envelopes

The following Figures #3 and #4 are envelope design drawings used by Hughes Display Products to produce the various sized single crystal faceplate CRT's for Trident.

2.4 Cooling Chamber

A detailed analysis was performed to determine the amount of conduction and radiation necessary to transfer the heat generated by the high electron beam power needed to take advantage of the SCFP's characteristics.

A liquid cooling chamber was designed to be incorporated on the CRT assembly (See Figs. #5 and #6). The fluid used was a mixture of ethylene glycol (80%) and glycerine (20%). This mixture is necessary to achieve acceptable indices of refraction (approximately 1.48) to reduce first surface internal reflections between the SCFP and the optics. The resulting fluid combination is non-inflammable, crystal clear, low viscosity, low freezing point and high boiling point.

Analysis of the heat dissipating chamber revealed that forced air flow across the fins is required if operated above 100 watts per CRT. (See Paragraph 6.1)

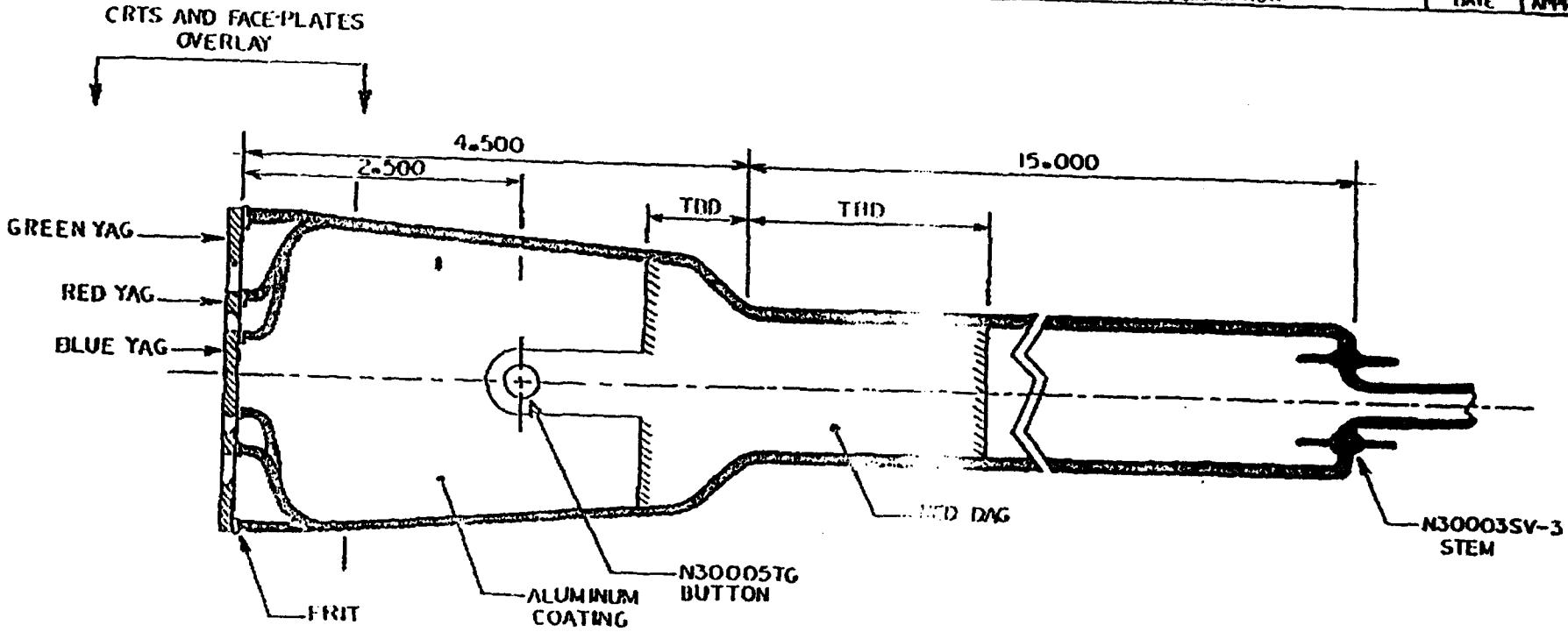

Figure 3 ▲
12

N61339-90-C-0047

1. CRTS WILL USE "PROJECTRON'S" HIGH RESOLUTION GUN

NOTES.

QTY REQD	FSCM NO	PART NO OR IDENTIFYING NO	NOMENCLATURE OR DESCRIPTION	ITEM OR FIND NO

PARTS LIST

	EXCEPT AS NOTED DIM ARE IN INCHES AND PER ANSI Y14.5 .XXX ± .XX ± ANGLES ±	CONTRACT:	HUGHES — HUGHES AIRCRAFT COMPANY INDUSTRIAL PRODUCTS DIVISION CARLSBAD, CALIFORNIA
	MATERIAL	DR Amelia Dolli CHK 4/4/91	CRT DESIGN FOR YAG FACE PLATES (CROSS SECTION)
NEXT ASSY	USED ON	NA APPD	SIZE B · FSCM NO 99816 · DWG NO AD92004

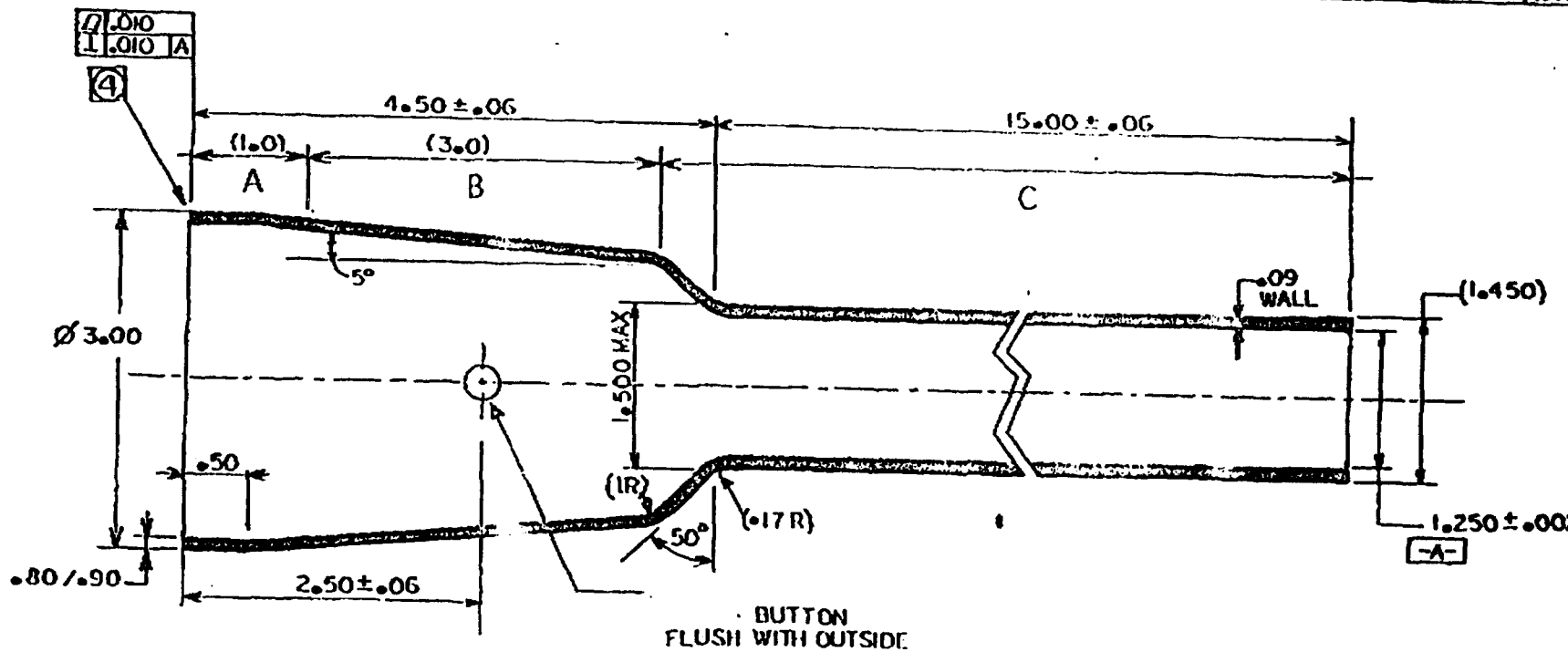

Figure 4
13

5 MATERIAL. GLASS

4 SURFACE OF END TO BE GROUND WITH 440 GRIT AND ACID FORTIFIED FOR FRIT SEALING

3. ANNEALING AND STRAIN. THE ENVELOPE ASSEMBLY SHALL BE GIVEN A GOOD COMMERCIAL ANNEALING

2. OUTSIDE BUTTON FLAT SURFACE (INSIDE ENVELOPE) TO BE FREE OF GLASS

1. BUTTON SEAL. COLOR-UNIFORM GREY (NOT METALLIC OR BLACK, SEALS TO BE CLEAN AND CLEAR, NO GLASS BUILD UP AT SEAL INSIDE OR OUTSIDE.

NOTES.

QTY REQD	FSCM NO	PART NO OR IDENTIFYING NO	NOMENCLATURE OR DESCRIPTION	ITEM (FIND)
		PARTS LIST		

EXCEPT AS NOTED DIM ARE IN INCHES AND PER ANSI Y14.5
.XXX .XX ANGLES
± ±.01 °

MATERIAL
(SEE NOTES)
5

NEXT ASSY | USED ON
APPLICATION

CONTRACT

DR Andy Self
CHK 4/20/92
APPD

HUGHES — HUGHES AIRCRAFT COMPANY, INDUSTRIAL PRODUCTS DIVISION, CARLSBAD, CALIFORNIA

CRT FUNNEL 3.000
(CROSS SECTION)

SIZE	FSCM NO	DWG NO
B	00816	AD92001X

SCALE | SHEET

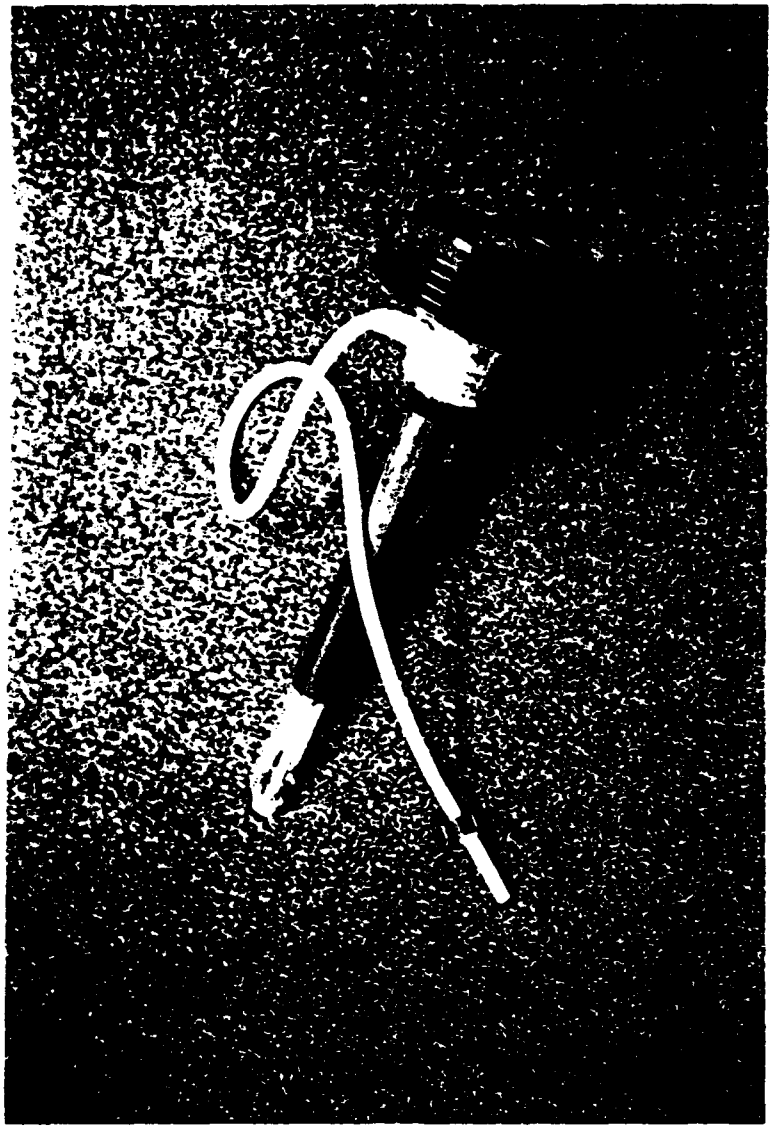

Figure 5

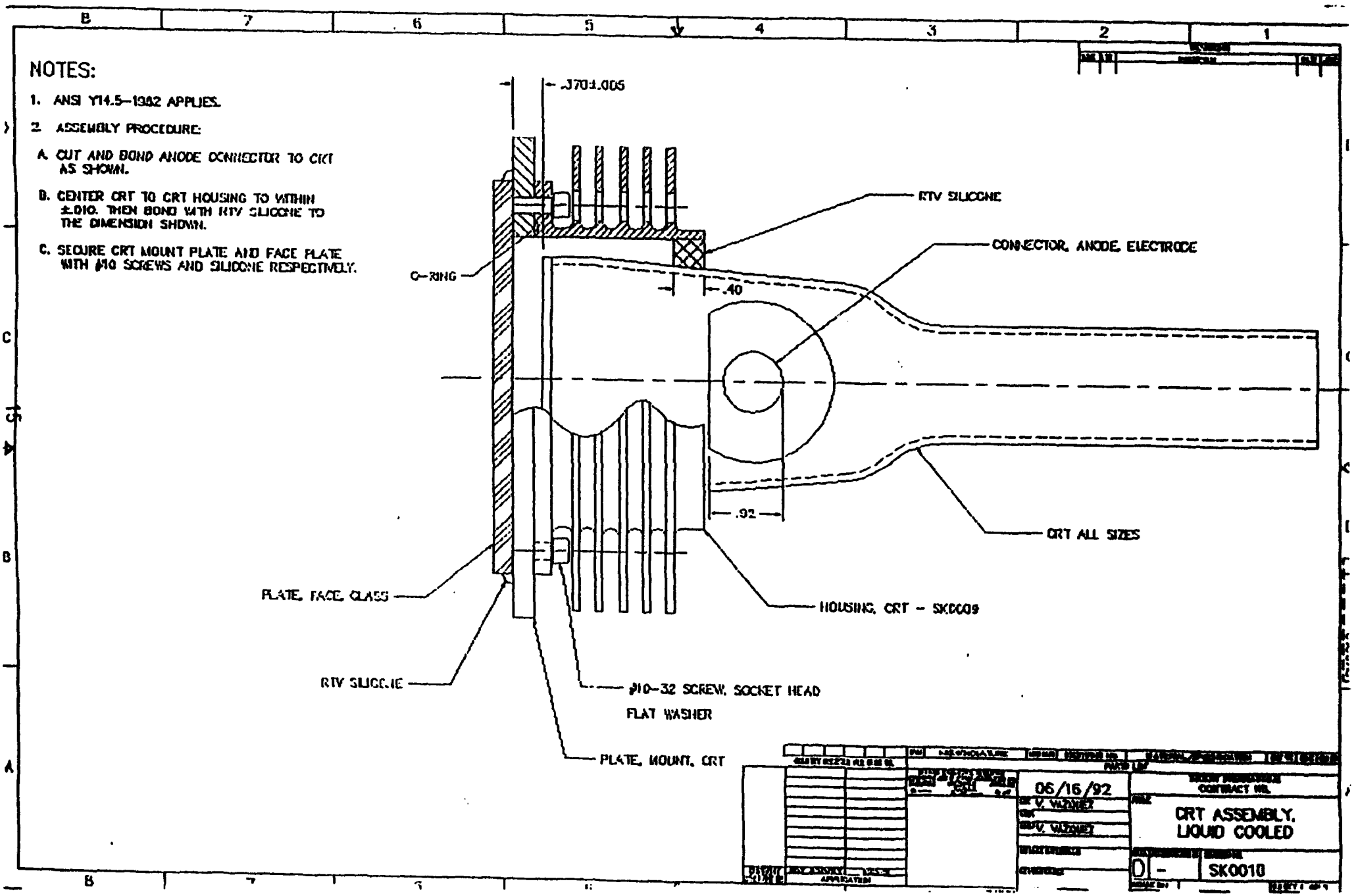
NOTES:
1. ANSI Y14.5–1982 APPLIES.
2. ASSEMBLY PROCEDURE:
A. CUT AND BOND ANODE CONNECTOR TO CRT AS SHOWN.
B. CENTER CRT TO CRT HOUSING TO WITHIN ±.010. THEN BOND WITH RTV SILICONE TO THE DIMENSION SHOWN.
C. SECURE CRT MOUNT PLATE AND FACE PLATE WITH #10 SCREWS AND SILICONE RESPECTIVELY.
.3704.005
RTV SILICONE
CONNECTOR, ANODE, ELECTRODE
O-RING
.40
.92
CRT ALL SIZES
PLATE, FACE, GLASS
HOUSING, CRT – SK0009
RTV SILICONE
#10-32 SCREW, SOCKET HEAD
FLAT WASHER
PLATE, MOUNT, CRT
06/16/92
CRT ASSEMBLY, LIQUID COOLED
SK0010

Figure 6

3.0 Tests of Unmounted Ce:YAG Crystals

Tests on four (4) 1" Ce:YAG crystals were run to gather additional data and evaluate the epitaxial layer thickness relationships with high voltage penetration. Tests were run by both Allied Signal, Inc. and Thomas Electronics, Inc. in their respective demountable vacuum chambers.

3.1 Tests Run at Allied Signal, Inc., 1" Diameter

Ce:YAG, Non-Reticulated #00320-2-1

High Voltage 20,000 V

Beam Current (ma)	W/Sq.Cm	FL	Lumens	Lu/W
0.16	9.52	28	.008	2.5
0.52	30.95	79	.023	2.2
0.68	40.47	115	.033	2.4
0.88	52.38	159	.046	2.6
1.04	61.90	192	.055	2.6
1.28	76.19	234	.068	2.6
1.44	85.71	286	.083	2.8
1.60	95.23	309	.089	2.8
1.84	109.52	370	.107	2.9
2.16	128.57	420	.121	2.8

There were no transmission losses in this demountable chamber because the crystal is sealed externally.

3.2 Tests Run at Thomas Electronics, Inc., 1" Diameter

The following is an evaluation of four (4) one inch Ce:YAG faceplates. These were study samples, manufactured by Allied Signal, which were non-reticulated, non-aluminized and of varying phosphor layer thicknesses.

The luminance efficiency (lumens/watt) was calculated and listed by the following methodology:

Step 1. Obtain power by multiplying current by voltage; i.e.,

30 ua @ 20 kv = .03 x 20 = .6 w
60 ua @ 20 kv = .06 x 20 = 1.2 w
90 ua @ 20 kv = .09 x 20 = 1.8 w
30 ua @ 30 kv = .03 x 30 = .9 w
60 ua @ 30 kv = .06 x 30 = 1.8 w
90 ua @ 30 kv = .09 x 30 = 2.7 w

Step 2. Convert 1 sq. cm. to square feet

1 sq. cm. = .155 sq. in.

$$\frac{.155 \text{ sq. in.}}{144 \text{ sq.in./sq.ft.}} = .0010763 \text{ sq. ft.}$$

Step 3. Determine total lumens

Multiply light output by area in sq. ft.

e.g. Sample #00320-2-3 @ 90 ua
.0010763 sq ft X 4330 fl =
lumens = 4.66 lumens

Step 4. Luminance efficiency = lumens/watt

e.g. Sample 00320-2-3
90 ua @ 30 kv = 2.7 w

$$\frac{4.66 \text{ lumens}}{2.7 \text{ w}} = 1.726 \text{ lumens/watt}$$

3.2.1 SCFP #00319-2-1
Phosphor Layer Thickness, 7.0 um

All testing was done in an electron gun demountable test fixture. Initial testing was of faceplate as received in a non-aluminized state. Initial conditions were:

Anode voltage	20,000 v
Raster size	1 cm X 1 cm

Beam Current	Light Output	Lumens/Watt
30 ua	63.5 fl	.11
60 ua	130.0 fl	.12
90 ua	141.0 fl	.08

The tests were then conducted under the following conditions:

Anode voltage	30,000 v
Raster size	1 cm X 1 cm

Beam Current	Light Output	Lumens/Watt
30 ua	39.4 fl	.05
60 ua	68.1 fl	.04
90 ua	105.0 fl	.04

The sample was then aluminized and the test rerun under identical conditions:

Anode voltage	20,000 v
Raster size	1 cm X 1 cm

Beam Current	Light Output	Lumens/Watt
30 ua	744 fl	1.33
60 ua	1240 fl	1.112
90 ua	1920 fl	1.148

The tests were then rerun using:

Anode voltage	30,000 v
Raster Size	1 cm X 1 cm

Beam Current	Light Output	Lumens/Watt
30 ua	1120 fl	1.339
60 ua	2040 fl	1.219
90 ua	2480 fl	.988

3.2.2 SCFP #00320-2-1
Phosphor Layer Thickness, 17.6 um

Initial test conditions:

Anode voltage	20,000 v
Raster Size	1 cm X 1 cm

Beam Current	Light Output	Lumens/Watt
30 ua	116.0 fl	.208
60 ua	140.0 fl	.125
90 ua	177.0 fl	.100

Test then conducted under following conditions:

Anode Voltage	30,000 v
Raster Size	1 cm X 1 cm

Beam Current	Light Output	Lumens/Watt
30 ua	41.4 fl	.05
60 ua	73.5 fl	.04
90 ua	77.8 fl	.03

The samples were then aluminized and the tests rerun under the identical conditions:

Anode Voltage	20,000 V
Raster Size	1 cm X 1 cm

Beam Current	Light Output	Lumens/Watt
30 ua	711 fl	1.275
60 ua	1550 fl	1.39
90 ua	2590 fl	1.548

The tests were then rerun as follows:

Anode Voltage	30,000 V
Raster Size	1 cm X 1 cm

Beam Current	Light Output	Lumens/Watt
30 ua	1040 fl	1.243
60 ua	3020 fl	1.805
90 ua	4020 fl	1.602

3.2.3 SCFP #00320-2-2
Phosphor Layer Thickness, 19.2 um

Initial tests were run as follows:
Anode Voltage 20,000 V
Raster Size 1 cm X 1 cm

Beam Current	Light Output	Lumens/Watt
30 ua	82.2 fl	.15
60 ua	106.0 fl	.10
90 ua	80.0 fl	.05

The tests were then conducted under the following conditions:
Anode Voltage 30,000 V
Raster Size 1 cm X 1 cm

Beam Current	Light Output	Lumens/Watt
30 ua	31.4 fl	.04
60 ua	57.3 fl	.03
90 ua	120.0 fl	.05

The samples were then aluminized and the test rerun under the identical conditions:
Anode Voltage 20,000 V
Raster Size 1 cm X 1 cm

Beam Current	Light Output	Lumens/Watt
30 ua	841 fl	1.508
60 ua	1810 fl	1.62
90 ua	2520 fl	1.506

The tests were then rerun as follows:
Anode Voltage 30,000 V
Raster Size 1 cm X 1 cm

Beam Current	Light Output	Lumens/Watt
30 ua	1450 fl	1.73
60 ua	1690 fl	1.01
90 ua	2920 fl	1.163

3.2.4 SCFP # 00320-2-3
Phosphor Layer Thickness, 17.1 um

Initial tests were run under the following conditions:
Anode Voltage 20,000 V
Raster Size 1 cm X 1 cm

Beam Current	Light Output	Lumens/Watt
30 ua	44.7 fl	.08
60 ua	71.9 fl	.06
90 ua	60.8 fl	.04

The tests were then conducted as follows:

Anode Voltage	30,000 V
Raster Size	1 cm X 1 cm

Beam Current	Light Output	Lumens/Watt
30 ua	33.3 fl	.04
60 ua	67.7 fl	.04
90 ua	60.8 fl	.02

The samples were then aluminized and the test rerun under identical conditions:

Anode Voltage	20,000 V
Raster Size	1 cm X 1 cm

Beam Current	Light Output	Lumens/Watt
30 ua	828 fl	1.48
60 ua	1740 fl	1.56
90 ua	2600 fl	1.55

The test was repeated under the following conditions:

Anode Voltage	30,000 V
Raster Size	1 cm X 1 cm

Beam Current	Light Output	Lumens/Watt
30 ua	1240 fl	1.48
60 ua	2700 fl	1.61
90 ua	4330 fl	1.726

Conclusions:

A. In the non-aluminized state, there is a space charge buildup at the faceplate. This space charge renders all data variable and significantly decreases luminance efficiency; therefore, all faceplates should be aluminized prior to further testing or evaluation.

B. It would appear that phosphor layer thickness is an important factor in the luminance efficiency of faceplates; e.g., samples 00320-2-1 and 00320-2-3 produced the highest luminance efficiency results; i.e., 1.6 to 1.8 lumens/watt at 30 kv. The high voltage penetration will increase with increased anode voltage.

These readings must be adjusted to reflect the 85% transmissibility factor of the test fixture. This is done by multiplying all the readings by the constant 1.176. The result with a 1.0 transmissibility factor is 1.88 to 2.17 lumens/watt. These samples were not cooled while in the vacuum chamber resulting in the relatively low readings. Graphs to show relationships of thickness of the phosphor layer versus efficiency are shown in Figure 7.

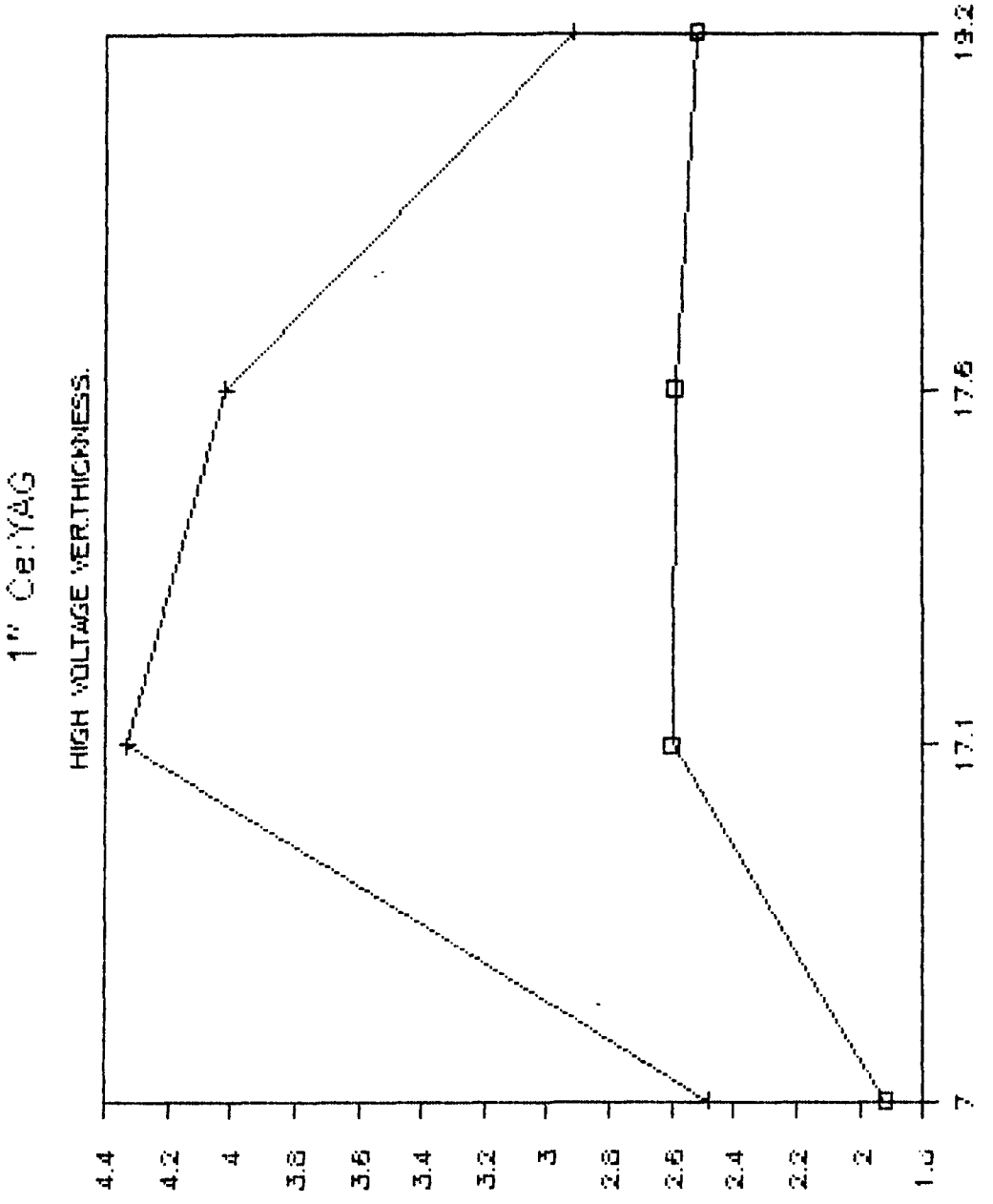
1" Ce:YAG
HIGH VOLTAGE VER.THICKNESS.
FOOTLAMBERTS
(Thousands)
4.4
4.2
4
3.8
3.6
3.4
3.2
3
2.8
2.6
2.4
2.2
2
1.8
7
17.1
17.6
19.2
PHOSPHOR THICKNESS
□ 20KV + 30KV

Figure 7

4.0 Test Results of 2" Diameter Cathode Ray Tube Manufactured by Thomas Electronics, Inc. (3M320YAG) SCFP #00606-1-1 and SCFP # 00608-1-1

4.1 Test Equipment Used

A. CRT Test Bed Projector (See Fig. #27, Pg 47)

B. Tektronix one degree angle luminance probe (J6523)

C. Omega surface temperature measuring probe

D. Fluke digital voltmeters

4.2 Background

There were two (2) 2" CRT's fabricated using GFP furnished faceplates. The initial testing program was established as follows:

A. Test 1 was oriented toward thermal mapping of the faceplate. The faceplate was not liquid cooled since temperature measurements can only be directly taken from the surface of the faceplate.

B. Test 2 was oriented toward obtaining of luminance data with the cooling subsystem attached.

As events described herein evolved, both units failed during the test program. The failure mode is described herein. The units were subsequently repaired and the tests program rerun; however, the sequence was reversed; i.e., luminance data, under cooling conditions, was taken first, followed by thermal mapping testing.

4.3 Procedure

The CRT test bed was set up for operation with the 2" single crystal faceplate CRT installed. The CRT was turned on and a 1" x 1" raster set up on the faceplate. The raster was generated at a 525 line, 60 Hertz interlaced rate.

Measurements of luminance were made under varying conditions of beam current and anode voltage. Based on this data, included herein, calculations were made of luminance efficiency (lumens/watt).

4.4 Summary of Test Operation and Performance

A. Initial Test Program

CRT #1. Thermal mapping of the faceplate was initiated at low power levels with no liquid cooling. The temperature of the faceplate at startup was 77.7 degrees F. Prior to any data accumulation, the tube failed. Visual inspection lead to the initial conclusion that the tube frit (seal between faceplate and tube) had failed under power loading. The tube was returned to Thomas Electronics for analysis and repair.

CRT #2 was then assembled into the test bed with the cooling system attached. Light output (foot lamberts) was measured as a function of the beam current of the CRT. Performance of single crystal faceplate 3M320 (154871) crystal #00606-1-1 as measured against these parameters is shown on Table #1. Note that the above measurements were made prior to failure of the CRT and subsequent repair per the recommended corrective active.

The maximum power induced was 20.7 watts/sq.in. This is higher than the maximum allowed on a 5" x 7" glass CRT, which is 18 watts/sq.in.

The tube frit failed on the second tube while at a reduced power input operating condition. Given essentially the same operation of both tubes at failure, an electrically induced frit failure mode was considered the most probable cause of failure. This opinion was subsequently proven incorrect. Failure mode analysis concluded that an inadequate aquadag existed in both CRT's. Both units were repaired and the test program rerun.

Thermal mapping was attempted on the second CRT. The cooling subsystem was not attached after taking superficial data, the CRT exhibited corona discharge at a single point of the CRT frit followed by faceplate fracture along a single line across the face of the faceplate. It is concluded that a thermally induced frit failure occurred, almost immediately followed by fracture of the faceplate. Maximum temperature recorded on the faceplate was 137 degrees F.

Initial test results of 2" CRT with cooling system attached.

Ce:YAG - Single Crystal Faceplate 3M320 SN 154871

Read No.	HV (kv)	Iv	FL (x 10)	Beam Iua	Power Watts	Lumens	Lumens/ Watts*
1	25.24	.215	23.8	20.41	.515	1.653	3.200
2	25.25	.317	37.5	30.10	.760	2.604	3.420
3	25.03	.499	62.8	47.38	1.186	4.360	3.670
4	25.06	1.030	125.0	97.82	2.451	8.680	3.540
5	25.20	2.500	334.0	237.41	5.982	23.192	3.877
6	30.90	2.700	475.0	256.40	7.920	32.980	4.160
7	28.30	4.890	604.0	464.38	13.140	41.900	3.190
8	30.32	5.380	778.0	510.92	15.490	54.020	3.400
9	30.32	6.000	800.0	569.80	17.270	55.500	3.200
10	30.40	6.400	885.0	607.78	18.476	61.450	3.326
11	30.30	7.200	1040.0	683.70	20.710	72.200	3.488

* Avg 3.497 Lu/W

Table 1

B. Retesting of Repaired Tubes.

Luminance data, lumens/watt, was taken on the repaired CRT with the cooling system attached. The data recorded is shown in Table #2. (Initial testing was witnessed by Rich Hebb/Code 253 of Naval Training Systems Center.) Upon completion of the luminance evaluation, the CRT test bed was set up with a power input of 21 watts. The system was operated continuously for fourteen (14) hours before frit failure occurred.

Data Taken on 2" SCFP #00606-1-1, Aluminized and Slightly Stippled. Phosphor Thickness 35 um.

High Voltage (kv)	Beam Current (ma)	Watts/ Sq. In.	Brightness (fl)	Lumens/ Watt
36.3	.0236	.8559	594	4.81
36.4	.0530	1.9300	1365	4.91
36.4	.0821	2.9880	2104	4.89
36.4	.1268	4.6144	3267	4.91
36.5	.1837	6.7043	4785	4.95
36.5	.2553	9.3184	6501	4.84
36.5	.3298	12.0369	8602	4.96
36.6	.4432	16.2211	11308	4.84
36.6	.5851	21.4146	14806	4.80
36.6	.7801	28.5516	19558	4.76
36.6	1.0000	36.6000	25300	4.80
36.7	1.4184	52.0550	36080	4.81
36.7	1.5070	55.3060	37620	4.72
36.8	1.6310	60.0200	39050	4.52
36.8	1.7907	65.8977	42570	4.48
36.8	1.8617	68.5100	44000	4.45
36.8	1.9500	71.7600	45650	4.42
36.9	2.0390	75.2191	47190	4.35
36.9	2.2160	81.7770	52250	4.44
36.9	2.2830	84.2427	52800	4.35
40.0	2.2510	90.0400	62700	4.83

Note: These brightness readings were corrected for losses of 10% through the X-ray window and coolant fluid.

Table 2

C. Conclusions of the 2" CRT Tests

Of all the CRT's tested, the tests on this 2" CRT resulted in the highest brightness being obtained with the highest power density reached.

The electron gun (Thomas') performed very well, allowing high peak beam currents.

The phosphor thickness (35 um) was greater than subsequent SCFP CRT's tested .

Utilizing a higher anode voltage (40 kv) resulted in an increase in efficiency. At 84 watts per square inch, the crystal was starting to exhibit coulombic effects. Increasing the voltage to 40 kv from 36.9 kv showed a marked increase in efficiency (4.35 to 4.83 l/w).

It is concluded that liquid cooling and pressure relief of the liquid chamber is mandatory if single crystal faceplates are to be operated at useful power levels.

Based on the data as shown, a comparison with existing 5 inch and 9 inch CRT performance was made at the 19,000 ft. lambert level for 20% of the 3" x 4" raster size. At this operating level, the power required to generate 19,000 fl for a conventional (P53 green) powder phosphor CRT is 18 watts/sq.in. Over a 20% size raster of 2.4 sq. in., a total of 43.2 watts would be required to generate an average of 19,000 fl over the 2.4 sq in.

An equivalent single crystal faceplate would require 68.4 watts to generate 19,000 fl over a 2.4 sq in equivalent area. (19,000 fl/sq in. requires 28.5 watts; therefore, 28.5 watt x 2.4 sq in. equals total watts for an equivalent comparison value.)

5.0 Tests of 3" Diameter Ce:YAG Cathode Ray Tubes Manufactured by Hughes Display Products

Trident delivered to Hughes Display Products seven (7) Ce:YAG 3" single crystal faceplates for integration into cathode ray tubes. Several of the crystals were damaged while trying to frit seal them to the glass envelopes. Others cracked during the bake cycle and two had the frit material punctures resulting from high voltage during testing. Trident has the two remaining Ce:YAG faceplate CRT's. One has been installed in the deliverable test bed projector. During testing, the CRT's were mounted in the Trident test bed with the liquid cooling chamber attached. The readings were taken through the X-ray windows which have a transmission of approximately .9.

5.1. Test Results

5.1.1 CRT #1, SCFP #10122-1-2

Aluminized, reticulated surface of 3" Ce:YAG epitaxial phosphor faceplate, phosphor thickness 16 um. (See Figure 8 showing electron microscope, reticulated surface and Figure 9 showing Allied-Signal's test of this faceplate in their demountable chamber.)

Test conditions:
Scan rates 15,750 Hz/60 Hz, interlaced,
Raster Size: 1" x 1"
Image Size: 1" x 1"

High Voltage (kv)	Beam Current (ma)	Watts/ Sq. In.	Brightness (fl)	Lumens/ Watt
29.81	.037	1.10	85	.53
29.90	.045	1.35	172	.88
30.29	.056	1.69	282	1.16
30.26	.090	2.72	680	1.73
29.98	.125	3.74	1,075	2.00
29.98	.185	5.54	1,720	2.15
29.98	.234	7.01	2,460	2.43

Notes:
1. This CRT appeared gassy (blue glow in gun area). Readings erratic.

5.1.2 CRT #2, SCFP #10212-1-2

Aluminized, reticulated surface of 3" Ce:YAG epitaxial phosphor faceplate, phosphor thickness 17 um. (See Figure 10 showing electron microscope, reticulated surface and Figure 11 showing Allied-Signal's test of this faceplate in their demountable chamber.)

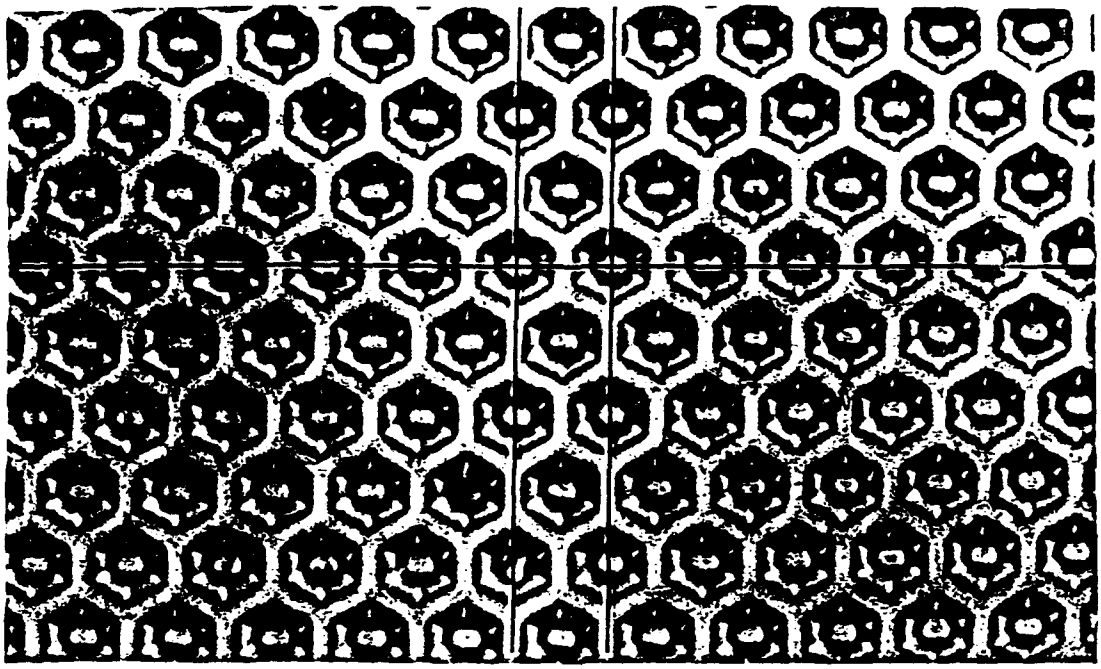

Fig. 8 Reticulated surface of the three-inch Ce:$Y_3Al_5O_{12}$ epitaxial phosphor faceplate number 10122-1-2.

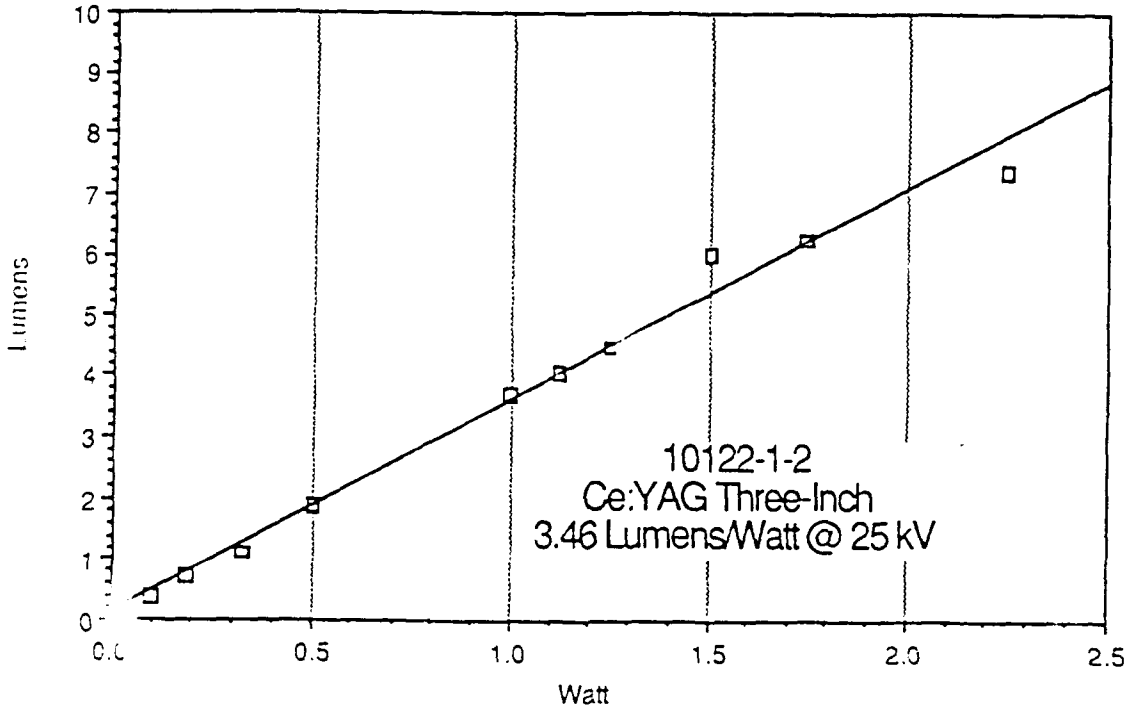

Fig. 9 Cathodoluminescence efficiency at 25 kV for the three-inch Ce:$Y_3Al_5O_{12}$ epitaxial phosphor faceplate number 10122-1-2.

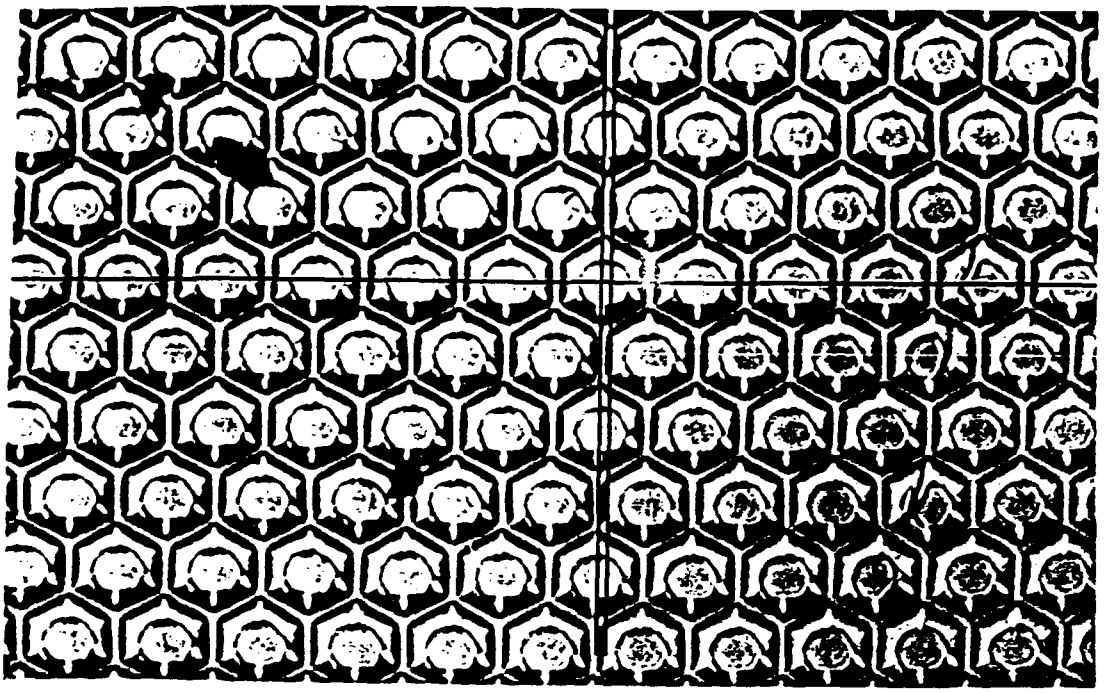

Fig. 10 Reticulated surface of the three-inch Ce:$Y_3Al_5O_{12}$ epitaxial phosphor faceplate number 10212-1-2.

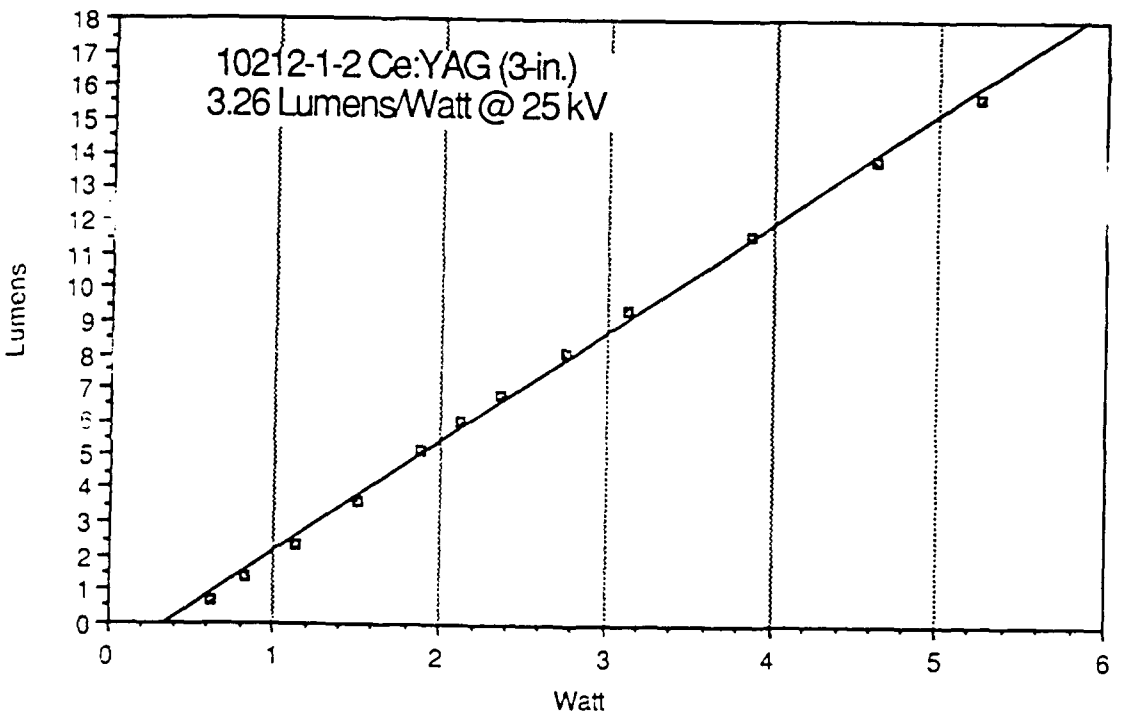

Fig. 11 Cathodoluminescence efficiency at 25 kV for the three-inch Ce:$Y_3Al_5O_{12}$ epitaxial phosphor faceplate number 10212-1-2.

5.1.2 CRT #2, SCFP #10212-1-2 (Cont.)

Test conditions:
Scan rates: 32,000 Hz/60 Hz, interlaced
Raster Size: 2.8" x 1.78"
Image Size: 1.25" x 1.98"

High Voltage (kv)	Beam Current (ma)	Watts/ Sq. In.	Brightness (fl)	Lumens/ Watt
27.0	.114	.80	400	2.22
27.0	.164	1.79	600	2.33
27.0	.210	2.29	932	2.83
27.0	.256	2.80	1,200	3.23
27.0	.360	3.91	1,700	3.01
27.0	.734	8.00	3,400	2.95
Note: Image size changed to .0127 sq.ft.				
30.0	.200	3.39	1,200	2.35
30.0	.480	7.86	2,700	2.28
30.0	.870	14.26	4,800	2.24
Note: Image size changed to .0098 sq. ft.				
34.0	.200	4.80	1,500	2.16
34.0	.500	12.00	3,500	2.00
34.0	.940	22.60	6,600	2.15

Notes:
1. These tests were run at a higher scan rate and a larger raster size to simulate a 4" CRT capability. The image was blanked so that it would only turn on in a small white square as per the areas indicated. The technique was implemented in an attempt to establish that a higher scan rate (inches/second) would increase the luminous efficiency. No correlation could be made.

5.1.3 CRT #3, SCFP #10214-1-1

Aluminized, reticulated surface of 3" Ce:YAG epitaxial phosphor, faceplate phosphor thickness 11.9 um. (See Figure 12 showing electron microscope, reticulated surface and Figure 13 showing Allied-Signal's test of this faceplate in their demountable chamber.)

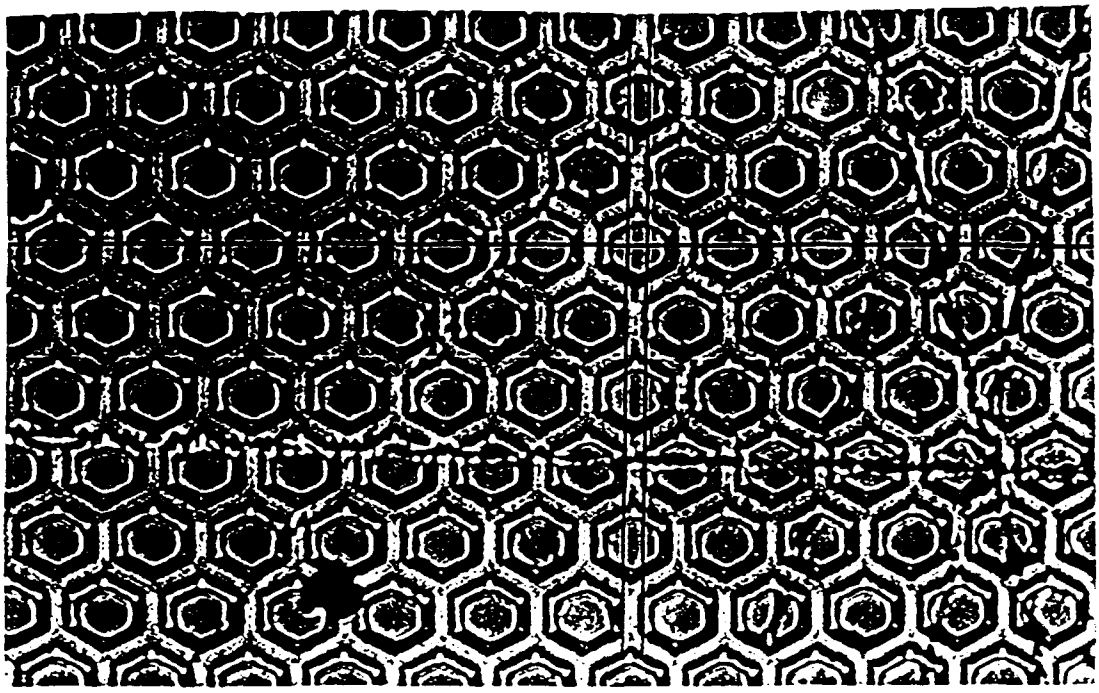

Fig. 12 Reticulated surface of the three-inch $Ce:Y_3Al_5O_{12}$ epitaxial phosphor faceplate number 10214-1-1.

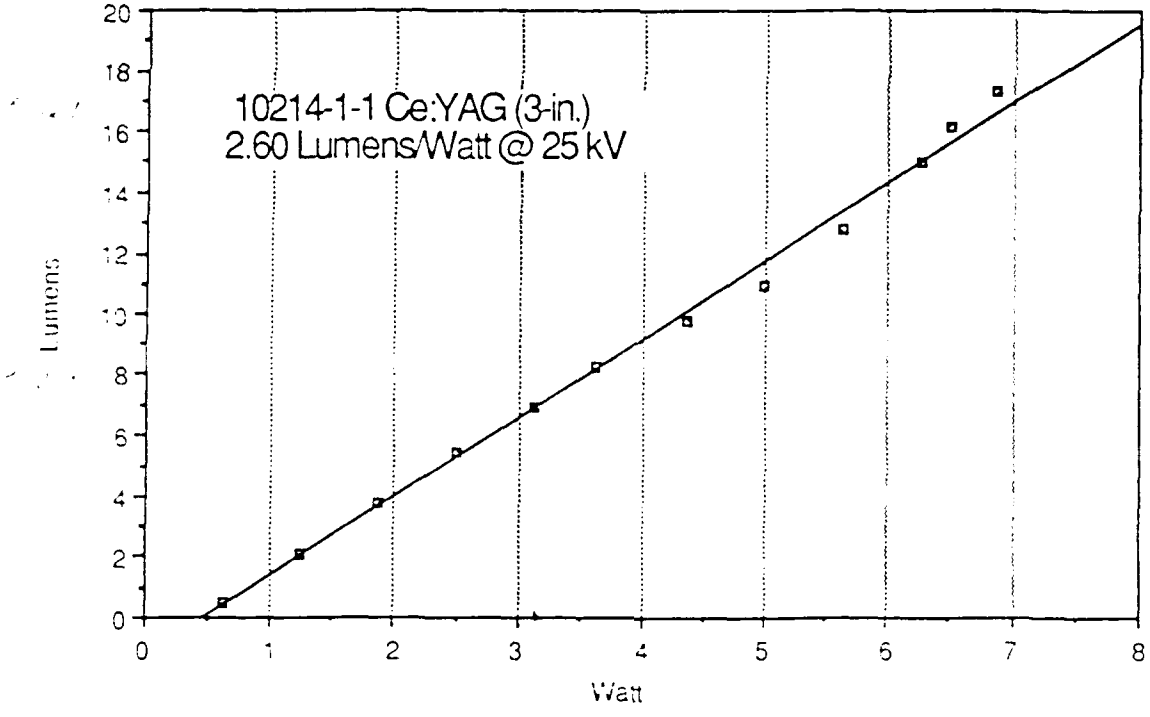

Fig. 13 Cathodoluminescence efficiency at 25 kV for the three-inch $Ce:Y_3Al_5O_{12}$ epitaxial phosphor faceplate number 10214-1-1.

5.1.3 CRT #3, SCFP #10214-1-1 (Cont.)

First Test:

Scan Rates 15,750 Hz/60 Hz, interlaced, 1" x 1" raster.

High Voltage (kv)	Beam Current (ma)	Watts/ Sq. In.	Brightness (fl)	Lumens/ Watt
28.0	.103	2.88	710	1.70
28.8	.142	4.09	999	1.72
29.3	.250	7.32	1,783	1.69
29.0	.335	9.71	2,820	2.00
28.6	.400	11.40	3,550	2.15
27.8	.480	13.30	4,550	1.73
28.9	.514	14.80	4,350	2.00
35.2	1.200	42.24	10,500	1.73

Notes:

1. The frit punctured at 35.2 kv, 35 minutes into the test.
2. The tube was returned for rebuild.

Second Test

Same CRT after rebuild, silicon insulation added to the frit area in attempt to prevent puncturing. Test conditions same as test #1.

High Voltage (kv)	Beam Current (ma)	Watts/ Sq. In.	Brightness (fl)	Lumens/ Watt
30.5	.375	11.4	4,150	2.54
30.5	.400	12.2	5,250	2.98
30.5	.130	13.0	1,080	---
31.5	.523	16.8	6,300	2.60
31.0	.711	22.0	8.800	2.77
31.0	.923	28.6	13,300	3.23
31.0	.904	28.0	13,400	3.32
32.3	1.300	41.9	17,900	3.96
31.0	1.200	37.0	17,300	3.24
35.0	1.330	11.5	24,500	---
35.0	.974	34.0	17,700	3.60
34.7	1.500	52.0	25,300	3.39

Notes:

1. This CRT failed after 40 minutes of operation because of outgassing.
2. The maximum current at 0 grid bias that could be drawn at 35,000 v and 1,100 v G2 was 1.5 ma. The attempt to draw more current caused the grid to draw current, probably causing the outgassing.

Tests run by Allied-Signal on remaining faceplates #10123-1-1, #10122-1-3, #01214-1-1 and #10109-1-2 are shown in Figures #14 through #21. Successful CRT's were not produced by these crystals.

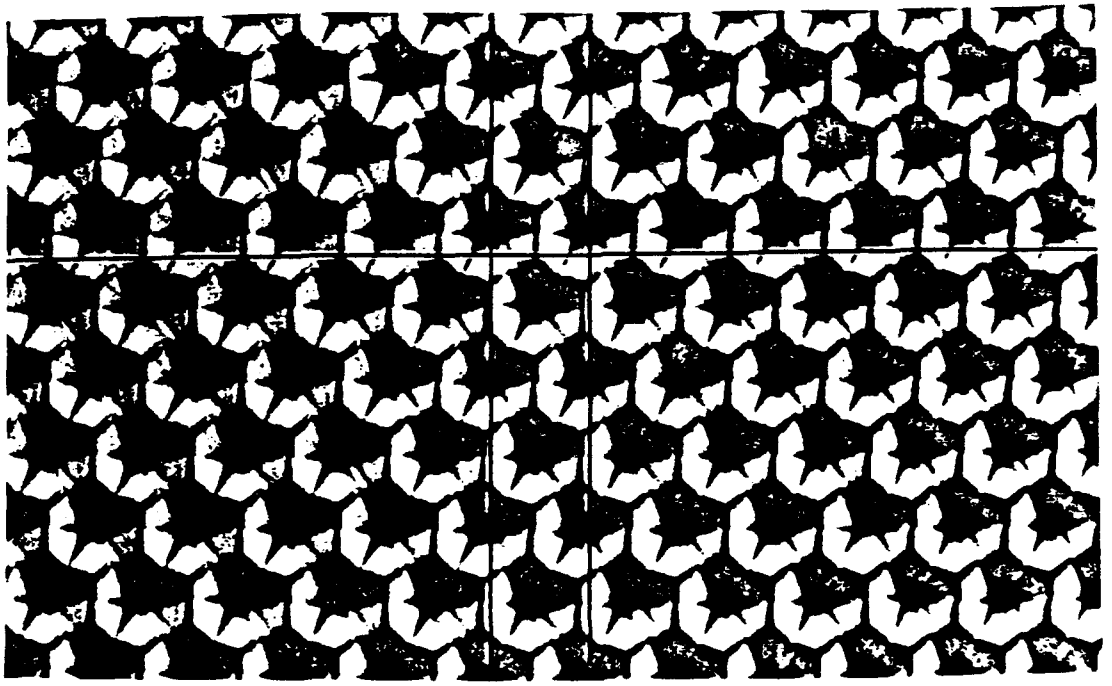

Fig. 14 Reticulated surface of the three-inch Ce:$Y_3Al_5O_{12}$ epitaxial phosphor faceplate number 10123-1-1.

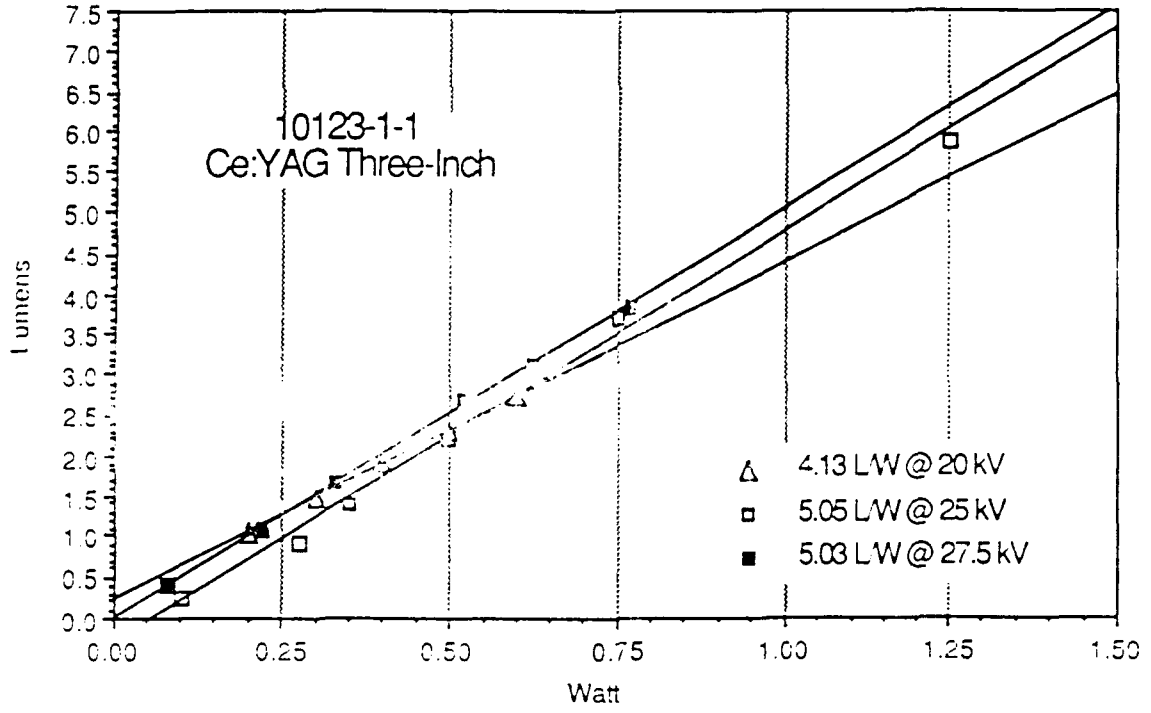

Fig. 15 Cathodoluminescence efficiency at 25 kV for the three-inch Ce:$Y_3Al_5O_{12}$ epitaxial phosphor faceplate number 10123-1-1.

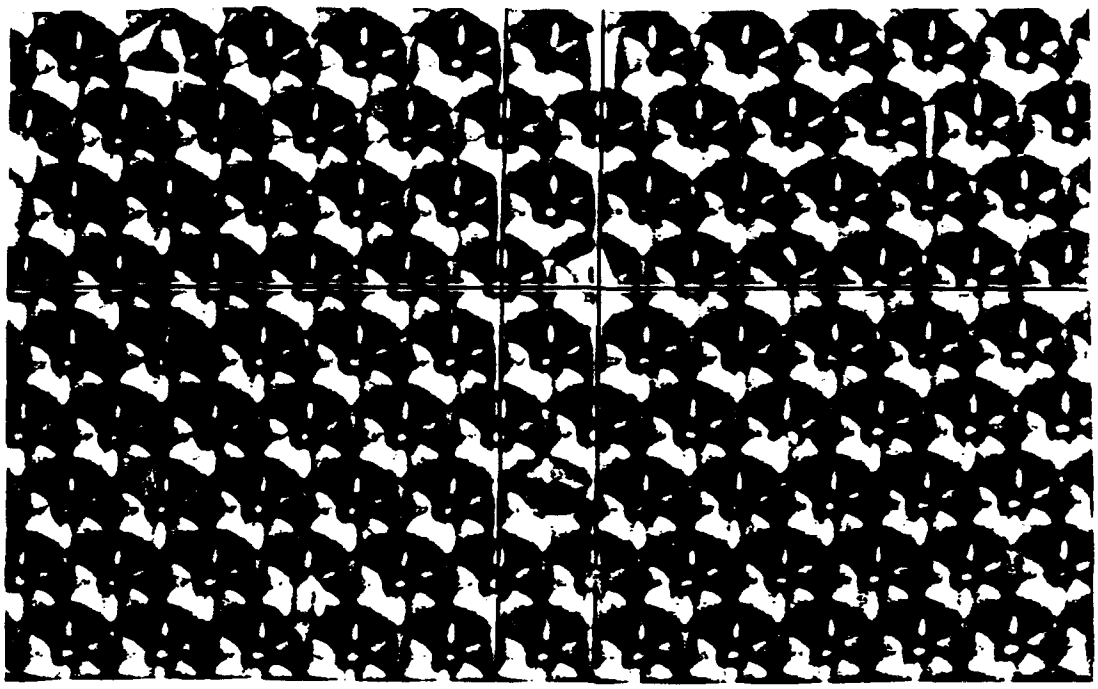

Fig. 16 Reticulated surface of the three-inch Ce:$Y_3Al_5O_{12}$ epitaxial phosphor faceplate number 10122-1-3.

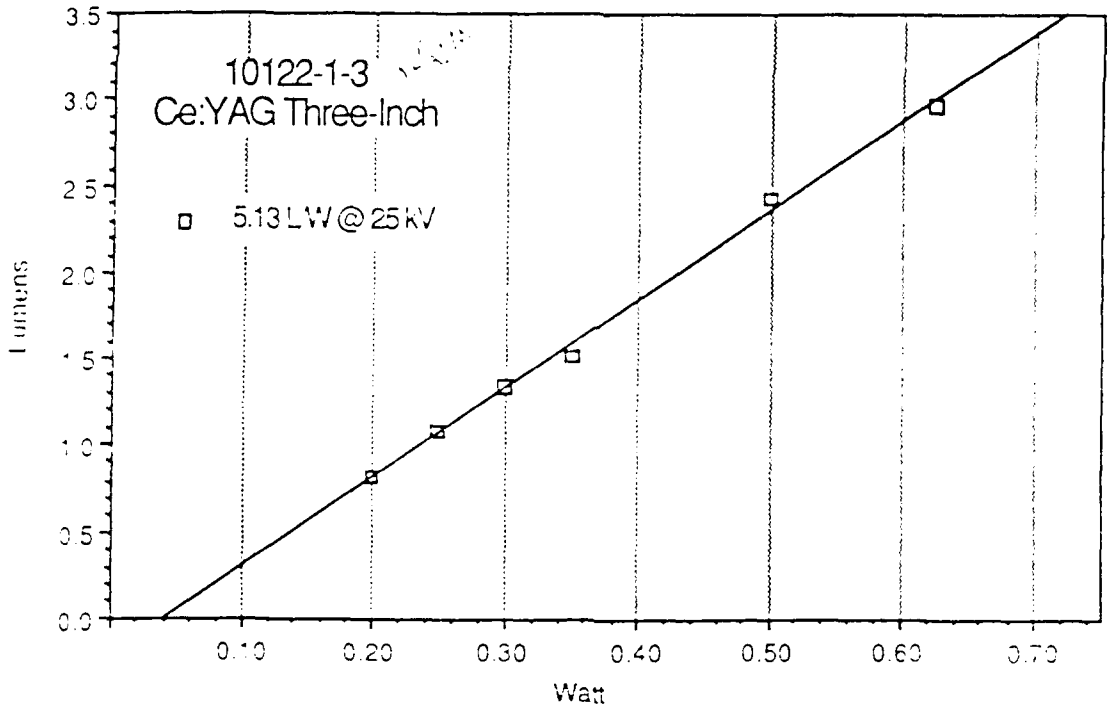

Fig. 17 Cathodoluminescence efficiency at 25 kV for the three-inch Ce:$Y_3Al_5O_{12}$ epitaxial phosphor faceplate number 10122-1-3.

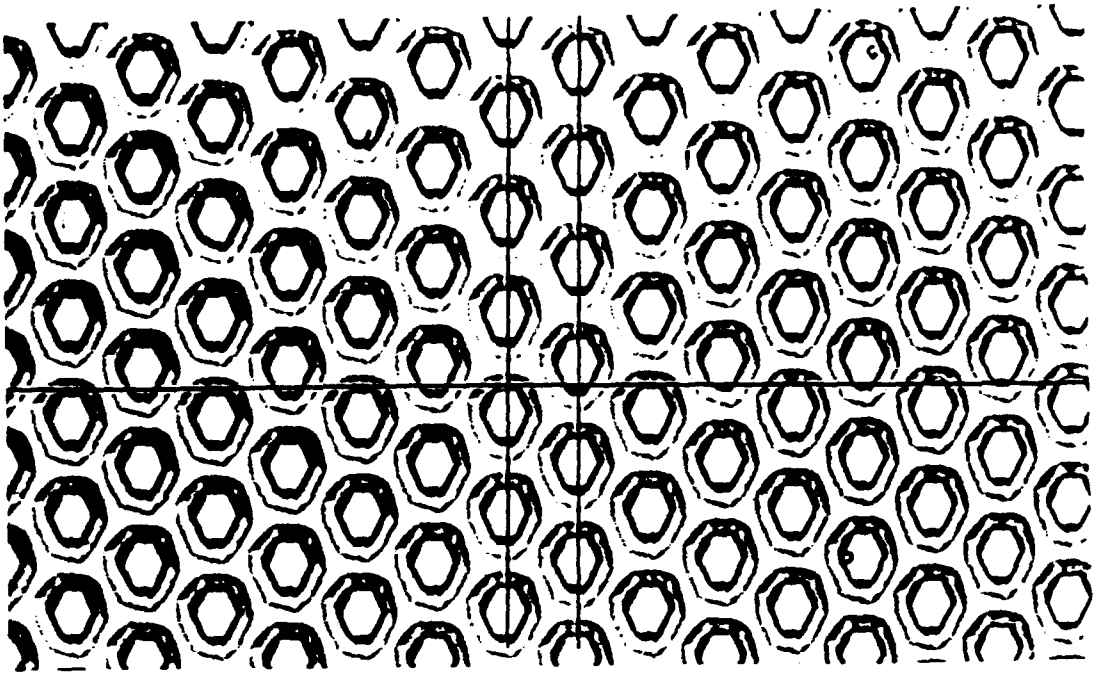

Fig. 18 Reticulated surface of the three-inch Ce:$Y_3Al_5O_{12}$ epitaxial phosphor faceplate number 01214-1-1.

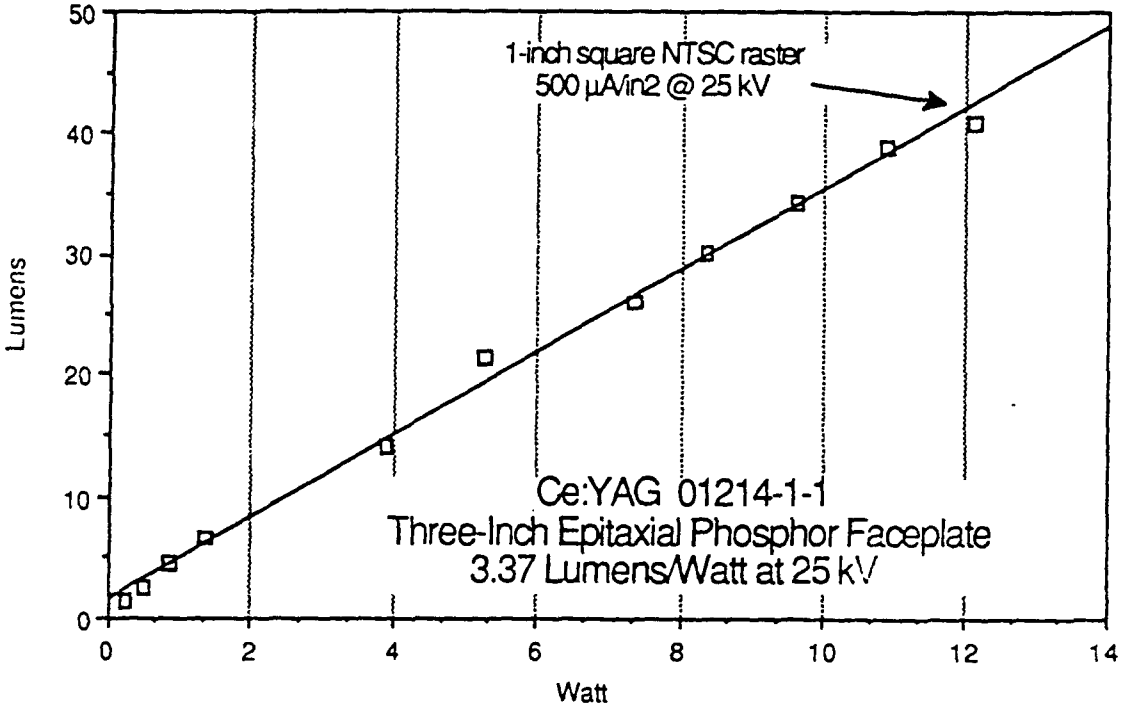

Fig. 19 Cathodoluminescence efficiency at 25 kV for the three-inch Ce:$Y_3Al_5O_{12}$ epitaxial phosphor faceplate number 01214-1-1.

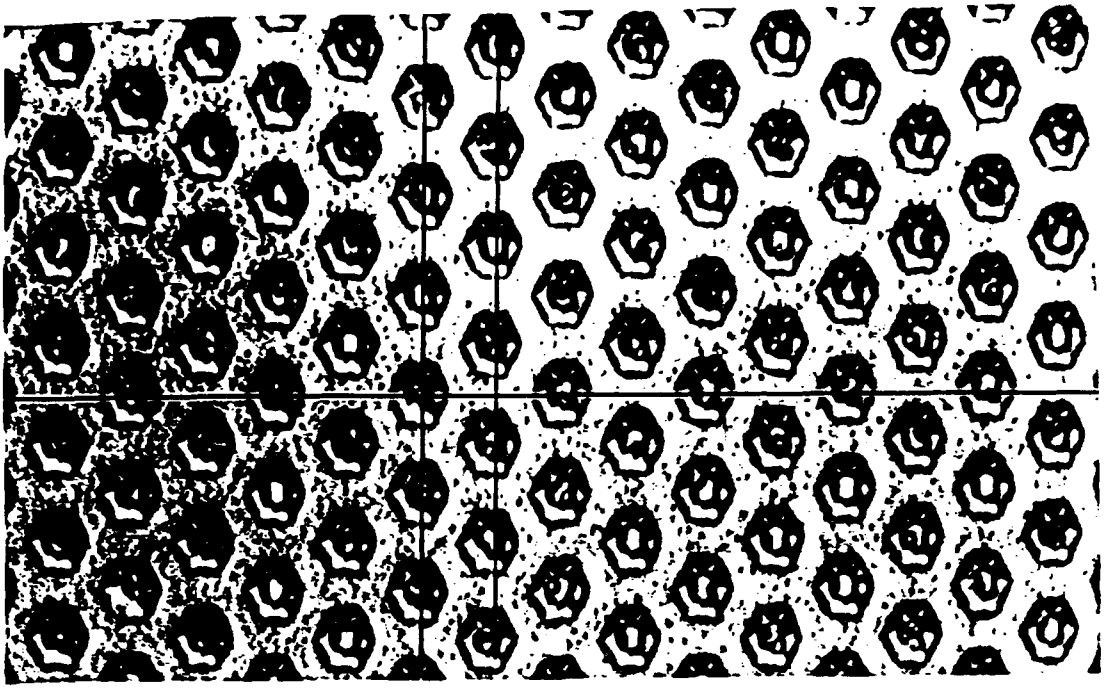

Fig. 20 Reticulated surface of the three-inch Ce:$Y_3Al_5O_{12}$ epitaxial phosphor faceplate number 10109-1-2.

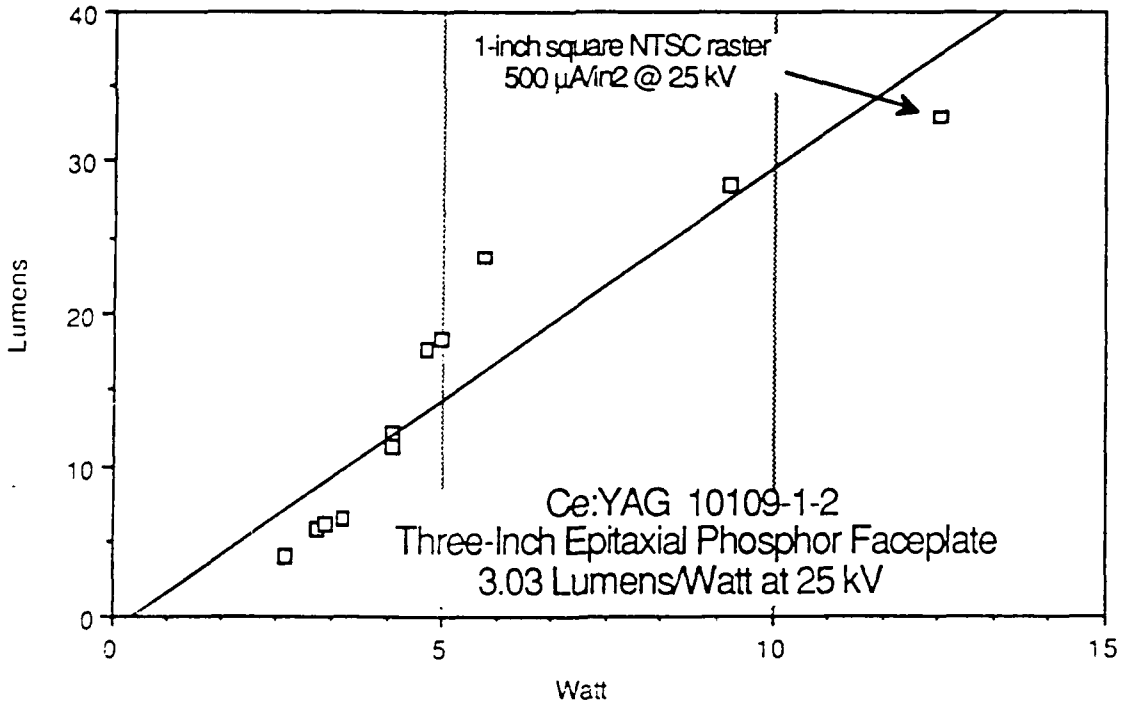

Fig. 21 Cathodoluminescence efficiency at 25 kV for the three-inch Ce:$Y_3Al_5O_{12}$ epitaxial phosphor faceplate number 10109-1-2.

5.2 Test Results of Deliverable Monochrome Projector (Green)

The raster line width measurement was conducted by projecting on a screen. The green (CE:YAG) SCFP projector had an HD6 (U.S. Precision, Inc.) wide angle lens installed. A square image was projected. The image size on the SCFP CRT was 1.626" square. The projected image was 28.625".

$$\frac{28.625"}{1.626"} = 17.6 \text{ X magnification}$$

The line width at various beam currents and high voltages were measured. Faceplate brightness was taken using a Tektronix luminous probe J6523 1 degree spot brightness meter. The CRT brightness was measured through the lens while looking at the CRT. This measurement does include all the losses of the lens, X-ray glass, fluid and YAG faceplate. Measurements were then taken at the screen. A standard magnesium flashed block was used at the screen surface to measure foot lamberts. The test results are shown in Table 4. Considerable crystal edge illumination was noted and also there was noticeable halation on the highlights. The test setup did not have liquid coupling to the lens but did have fluid to the X-ray window. The lens was coated for first surface reflections, but the X-ray window was not.

The graphs in Figures 22 and 23 were derived from data shown on Page 38, Tables 3 and 4. The test results shown by Table 3 were run to measure spot (line width) growth at constant power with high voltage change. The line width decreased from .0046" to .0034" with high voltage increase from 20 kv to 30 kv indicating improved resolution possible with higher anode voltages. The line width measurements were taken by projecting the image on a screen to enable the individual scan lines to be observed. A micrometer was used to measure from skirt to skirt. Several lines were measured in the center of the image. This technique will give larger line width readings than those normally quoted when a slit scanner is used. Measurements shown in Table 4 were an attempt to verify losses through the optical system. Discrepancies occur because of the poor measurement ability in taking the faceplate brightness through the projection optics. The Tektronix one (1) degree spot brightness probe's subtense is not accurate under these conditions, but the screen measurements are correct.

Example pertaining to data in Figure 13:

The transmission should be as follows:
(HD6 lens .91)(X-ray glass .894)(Fluid .99) = Total .8054

F:1 lens efficiency .2

113.80 lu at the CRT face should generate 3.5 fl at the screen.
(113.8)(.8054)(.2) = 18.60 divided by screen area 5.3166 sq.ft. = 3.5 fl.

Ce:YAG Single Crystal Faceplate Resolution (Line Width)
Versus High Voltage @ Constant Power
Epitaxial Thickness 17 um

Watts	Beam Current	H.V. (kv)	Line Width @ Screen	Line Width @ CRT
1.8	.09 ma	20	.081"	.0046"
1.8	.08 ma	22.5	.079"	.0045"
1.8	.072 ma	25	.068"	.0039"
1.8	.065 ma	27.5	.060"	.0035"
1.8	.060 ma	30	.059"	.0034"

Table 5

Ce:YAG Single Crystal Faceplate CRT Mounted in Trident
Test Bed Projector
CRT Crystal #10212-1-2 3"
Epitaxial Thickness 17 um

Brightness Measurements

Faceplate Image Size: 1.25" Wide x 1.98" High
2.475 sq. in. .0172 sq. ft.
Screen Image Size: 22" Wide x 34.8" High
5.3166 sq. ft.

H.V. (kv)	Faceplate Lumens*	Watts	Faceplate Brightness (fl)	Lu/W**	Screen Brightness	Screen Lumens*
27	6.88	3.10	400	2.22	.21 FL	1.11 Lu
27	10.32	4.43	600	2.33	.32 FL	1.70 Lu
27	16.03	5.67	932	2.83	.50 FL	2.66 Lu
27	22.36	6.92	1300	3.23	.70 FL	3.72 Lu
27	29,24	9.69	1700	3.01	.90 FL	4.78 Lu
27	58.48	19.84	3400	2.95	1.80 FL	9.56 Lu
30	19.51	6.21	1134***	3.14	.60 FL	3.19 Lu
30	45.50	14.40	2645***	3.25	1.40 FL	7.44 Lu
30	81.30	26.10	4726***	3.11	2.50 FL	13.29 Lu
34	25.90	6.80	1511***	3.80	.80 FL	4.25 Lu
34	59.80	17.00	3488***	3.52	1.85 FL	9.80 Lu
34	113.80	32.00	6616***	3.55	3.50 FL	18.60 Lu

* Lumen calculation: Brightness X sq. ft. screen image area
** Lu/W calculation: Lumens divided by watts
*** Calculated number based on optical efficiency of .1635

Table 6

CE: YAG SINGLE CRYSTAL FACEPLATE RESOLUTION (LINE WIDTH) VERSUS H.V. @ CONSTANT POWER

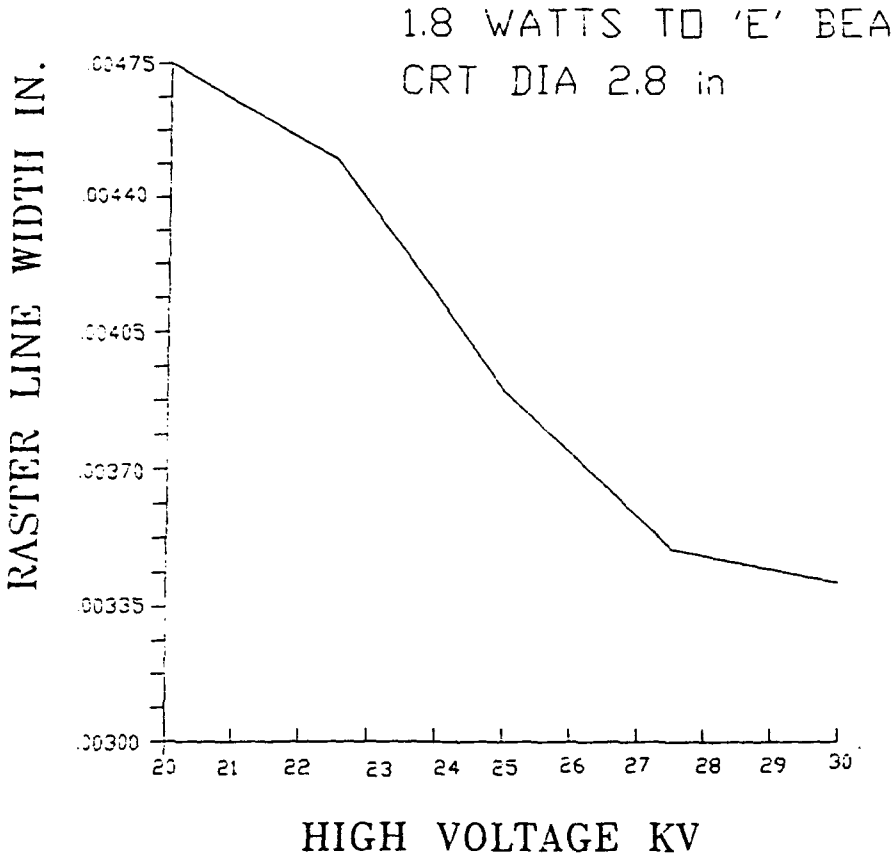

Figure 22

CE: YAG SINGLE CRYSTAL FACEPLATE CRT MOUNTED IN TRIDENT TEST BED PROJECTOR

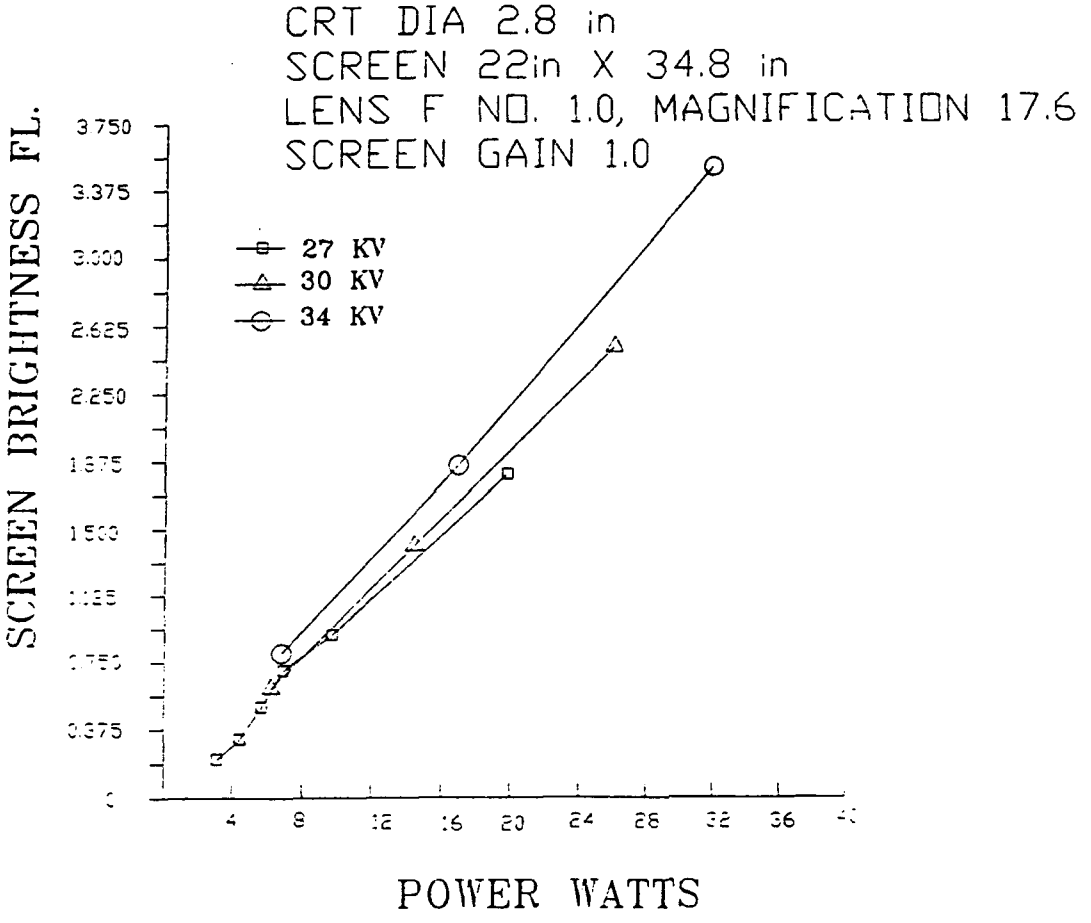

Figure 23.

5.3 Comparisons between Allied and Trident Tests

The graph in Figure 24 compares tests run at Allied-Signal, Inc and tests run by Trident with the CRT's constructed with the same crystals. The high voltage and powers used by Trident were considerably higher and liquid cooling was incorporated on the CRT's.

The CRT's tested by Trident had the cooling chamber with X-ray window and high refractive index optical coupling cooling fluid incorporated. The readings were factored for the optical losses of these elements.

5.4 Crystal Efficiency Comparison

Comparisons of normalized data taken of the 3" SCFP's were made to try to correlate differences in test conditions. Utilizing data taken by Allied Signal, Inc. in their demountable vacuum chamber and data taken from CRT's manufactured with the 3" Ce:YAG single crystal faceplates, a comparison of the crystals efficiency versus epitaxial phosphor layer thickness is shown in Figure #25.

The crystal efficiencies varied over a range of 2.6 l/w to 5 l/w. High voltage penetration versus phosphor (epitaxial layer) thickness is important in future design parameters. Fifteen (15 um) to seventeen (17 um) at the 30 kv to 35 kv voltage level appear to be optimum.

Comparison Chart

Crystal #	Tester	HV	Watts	Lu/W	Remarks
10123-1-1	Allied	20.0 kv	.60	4.13	
10123-1-1	Allied	25.0 kv	1.25	5.05	
10123-1-1	Allied	27.5 kv	.75	5.03	All Allied tests run
01214-1-1	Allied	25.0 kv	12.00	3.37	in demountable vacuum
10109-1-2	Allied	25.0 kv	12.00	3.03	chamber
10122-1-3	Allied	25.0 kv	.62	5.13	
10122-1-2	Allied	25.0 kv	2.25	3.46	
10212-1-2	Allied	25.0 kv	5.20	3.26	
10214-1-1	Allied	25.0 kv	6.80	2.60	
10122-1-2	Trident	30.0 kv	7.00	2.69*	Crystals incorporated
10212-1-2	Trident	27.0 kv	8.00	3.33*	in CRT's tested by
retested	Trident	30.0 kv	14.26	2.53*	Trident
retested	Trident	34.0 kv	22.60	2.33*	
10214-1-1	Trident	32.5 kv	42.24	2.22*	Rebuilt CRT's were
retested	Trident	35.0 kv	52.00	3.93*	retested

* Numbers corrected for optical losses (.898)

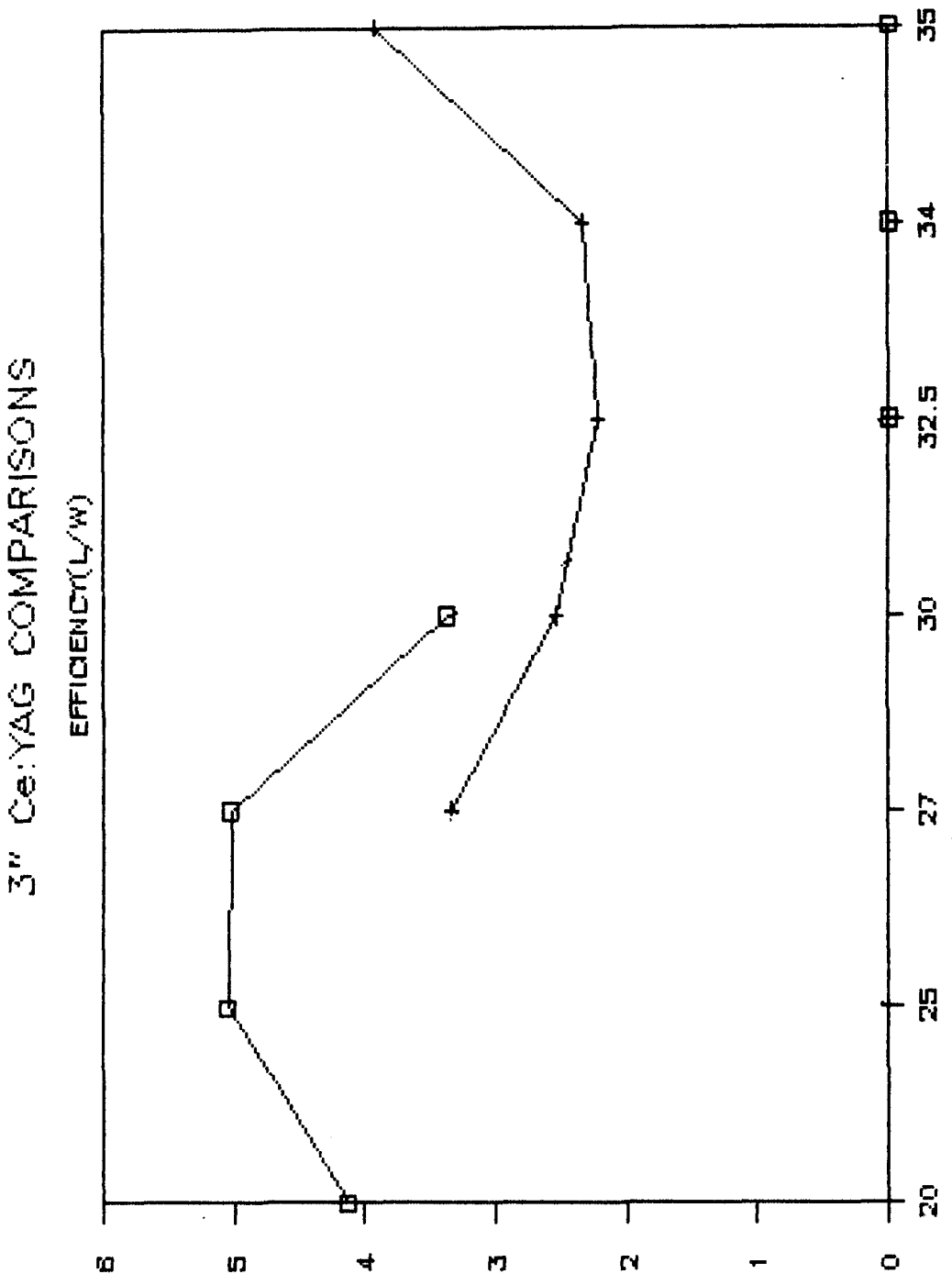
3" Ce:YAG COMPARISONS
EFFICIENCY(L/W)
LUMENS PER WATT
0
1
2
3
4
5
6
20
25
27
30
32.5
34
35
HIGH VOLTAGE
□ ALLIED
+ TRIDENT

Figure 24

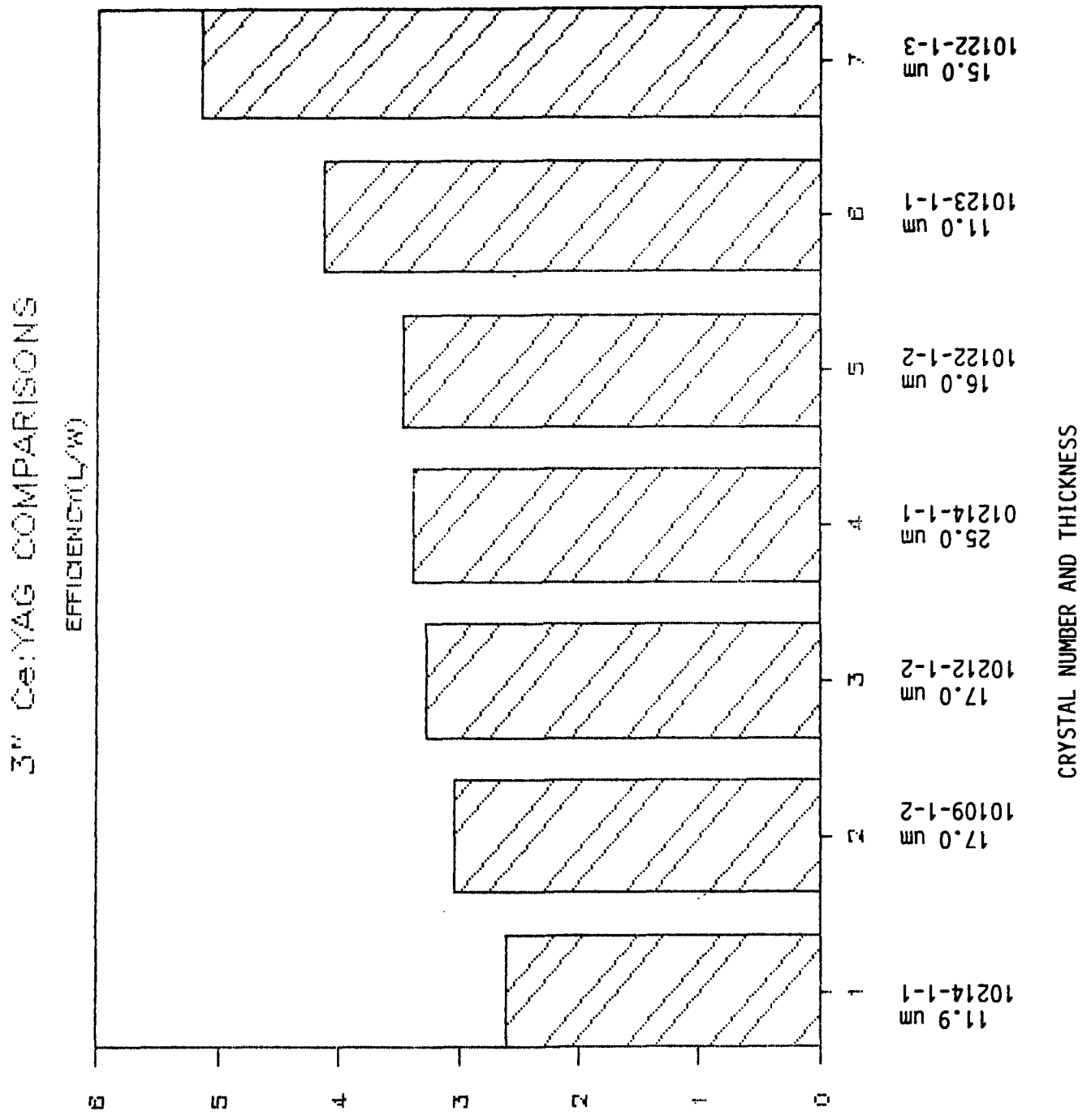
3" Ce:YAG COMPARISONS
EFFICIENCY(LM/W)
LUMENS PER WATT
0
1
2
3
4
5
6
1
2
3
4
5
6
7
11.9 um
10214-1-1
17.0 um
10109-1-2
17.0 um
10212-1-2
25.0 um
10214-1-1
16.0 um
10122-1-2
11.0 um
10123-1-1
15.0 um
10122-1-3
CRYSTAL NUMBER AND THICKNESS

Figure 25

6.0 Optical Coupling and Cooling of Single Crystal Faceplate Cathode Ray Tube

To improve the optical coupling of the single crystal faceplate to the projection optical system, a thick lens composed of a high refractive index fluid is used as the first element. This fluid also conducts the heat generated by the high power levels needed to utilize the SCFP. Analyses of the heat transfer as well as the optical benefits are shown below.

6.1 CRT Faceplate Cooling

The amount of heat produced by the CRT's is approximately equal to the input power. It is necessary to remove this heat. The CRT assembly design consists of a CRT mounted in a fin heat exchanger, an aluminum mounting plate, a glass window and a housing that supports the CRT assembly by the front plate. This assembly is filled with a cooling fluid. A liquid mixture of 80% ethylene-glycol and 20% glycerin surrounds the CRT (See Figure #26). Supplied air removes heat from the heat exchanger and its mounting components. Almost all the CRT's heat is removed by the aluminum components due to the thermal conductive property of the glass window being .15% of the aluminum components. A power range of 100-350 watts has been calculated for the CRT assembly. Enclosure 11.4, Table #1 gives a step by step calculation of the method used to derive the temperature of the heat exchanger and the required air flow. For a maximum power input of 350 watts the heat exchanger's root temperature is approximately 84 degrees C. This temperature is applied to the calculation on Enclosure 11.4, Table #2 to derive the CRT's skin temperature. The resulting skin temperature is approximately 197 degrees C. At this temperature the cooling liquid will start to boil, because the boiling point for ethylene-glycol is 198 degrees C. The results of this analysis reveal that additional cooling of the liquid is necessary if the CRT power is above 300 watts. An additional heat exchanger outside the CRT assembly will be needed if higher powers are used.

6.2 "Optical Research Associates'" Study

Trident International, Inc. contracted with Optical Research Associates, Pasadena, CA. to do a study of optical couplings and coatings which could improve transmission and reduce scattering. A copy of the results of this study is included as Enclosure #11.5.

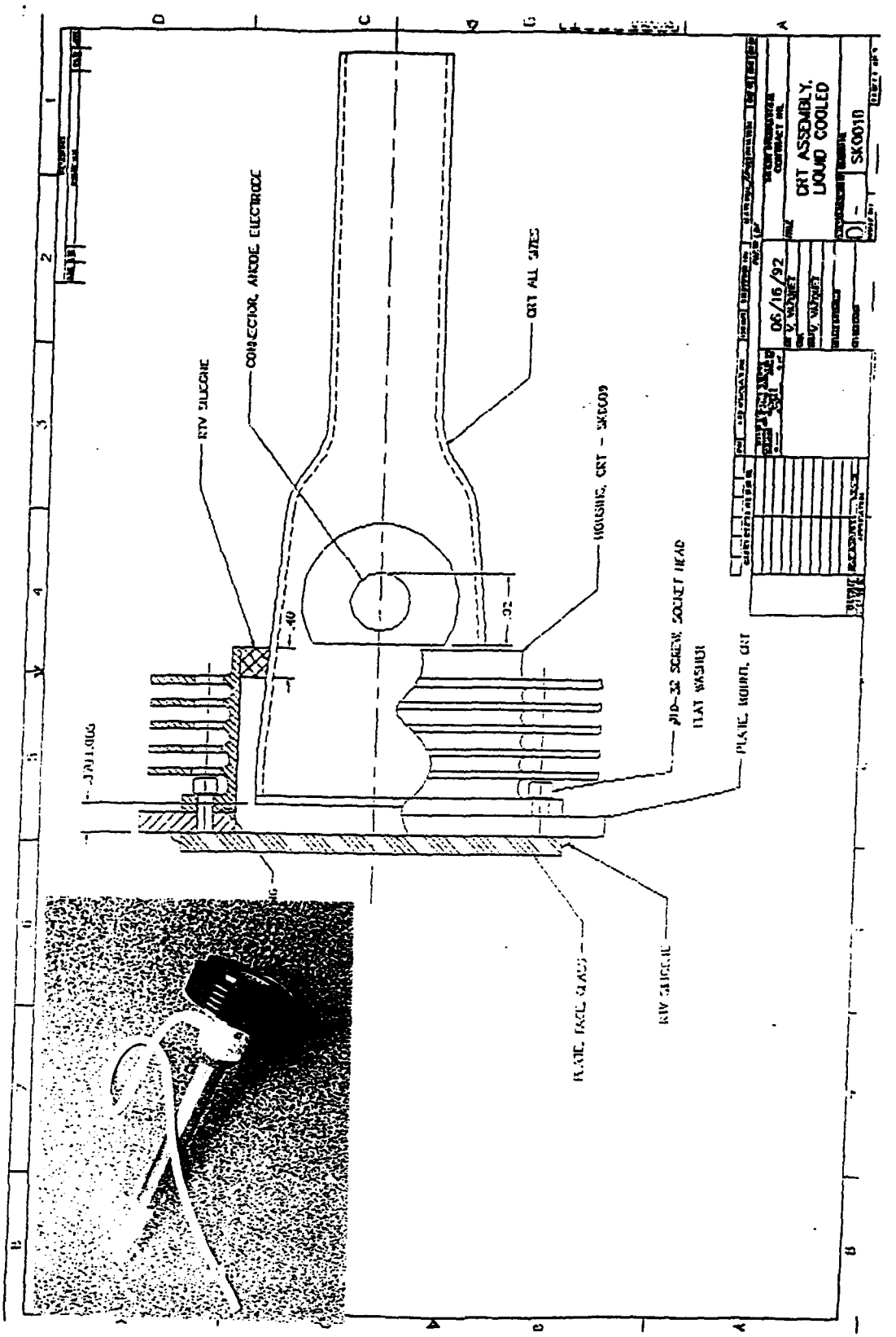
CRT ASSEMBLY, LIQUID COOLED
SK00310
06/16/92
CONNECTOR, ANODE ELECTRODE
RTV SILICONE
CRT ALL SIZES
HOUSING, CRT - SK0009
PLATE, FACE GLASS
PLATE, MOUNT, CRT
FLAT WASHER

Figure 26

7.0 Test Bed Projector

The test bed projector was modified from a Trident high resolution color projector Model T1080. The CRT mounting area was removed and a clear acrylic box was made to enclose the Ce:YAG CRT, yoke, focus coil and shielding. This box is necessary because this area is at 10,000 volts above ground. (WARNING!!) The CRT assembly is floated above ground to reduce the anode voltage stress across the frit seal area on the CRT.

To match the yoke impedances and reduce the image size without major modification, Trident used redundant yokes mounted to the case.

The front panel has additional controls and test points as well as a beam current meter. The isolated beam current meter can be viewed through the window in the front panel.

The high voltage control was configured so that it can be varied from the front panel and high voltage is measurable by a standard Fluke or equivalent voltmeter. Calibrated divider resisters reduce the meter voltage by 1,000:1; i.e., 30 kv = 30 volts. The resistance error build-up requires that the voltmeter reading be multiplied by 1.115 to obtain the correct high voltage; i.e., 29 v = 32.33 kv.

The test does not have liquid coupling to the lens; therefore, the lens is removable without complications.

Figure #27 shows test set-up.

See photograph Figure #28.

See Test Bed Projector Operator's Manual Enclosure #11.6.

SINGLE CRYSTAL FACE-PLATE TEST

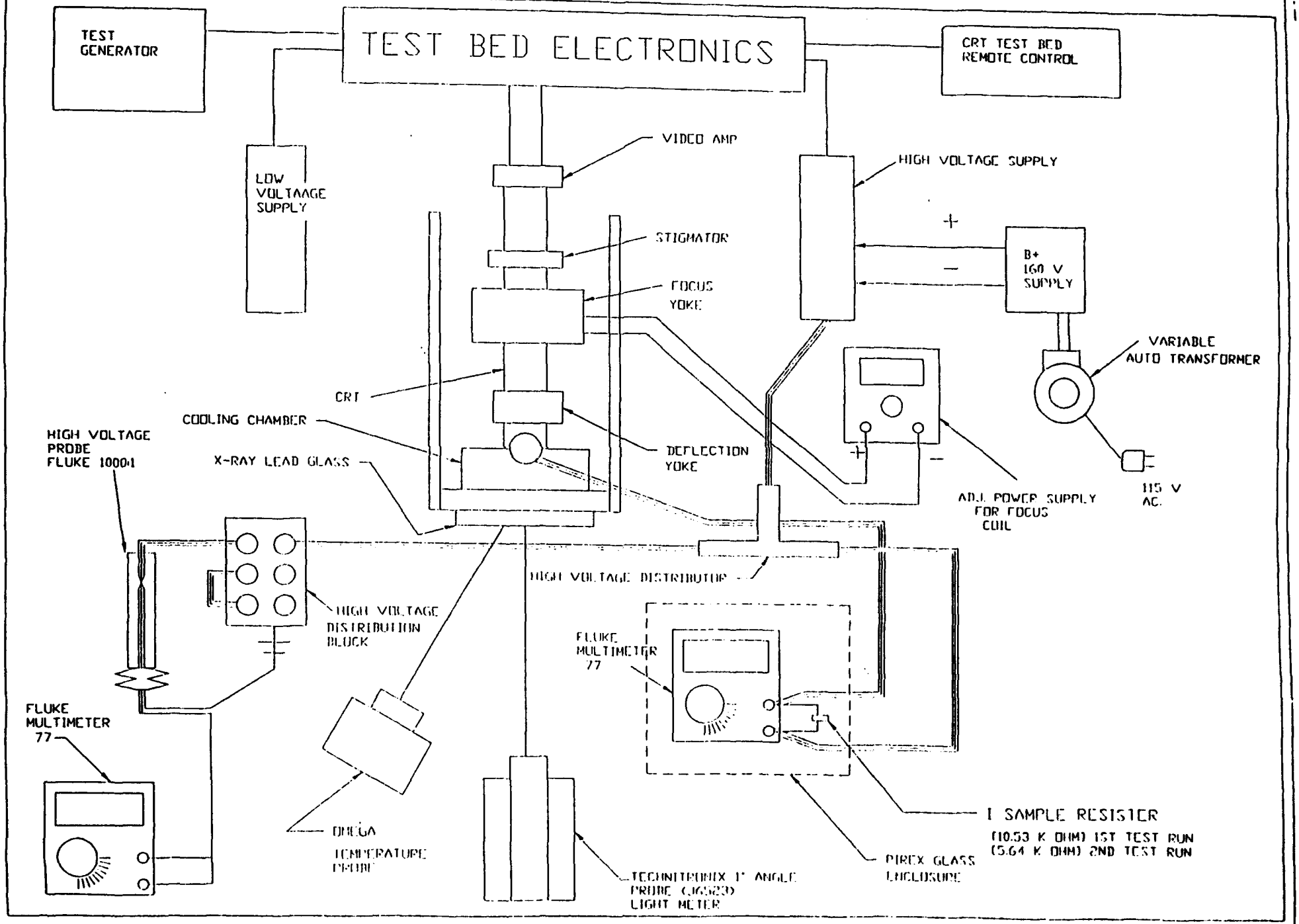

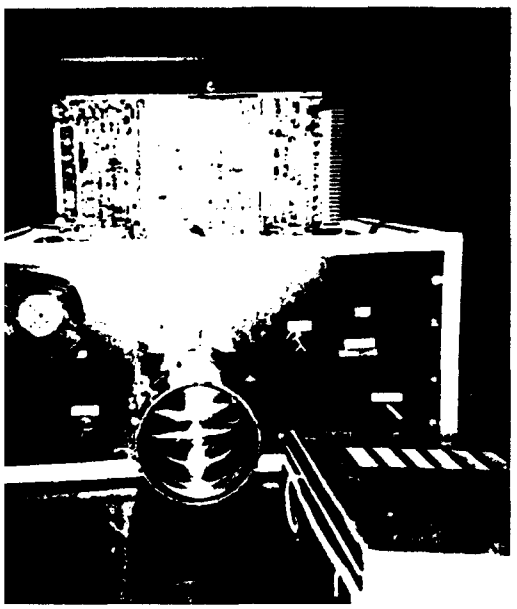

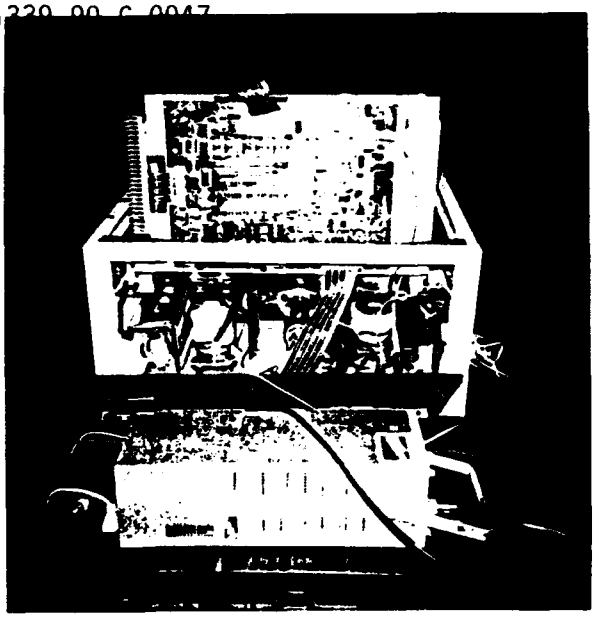

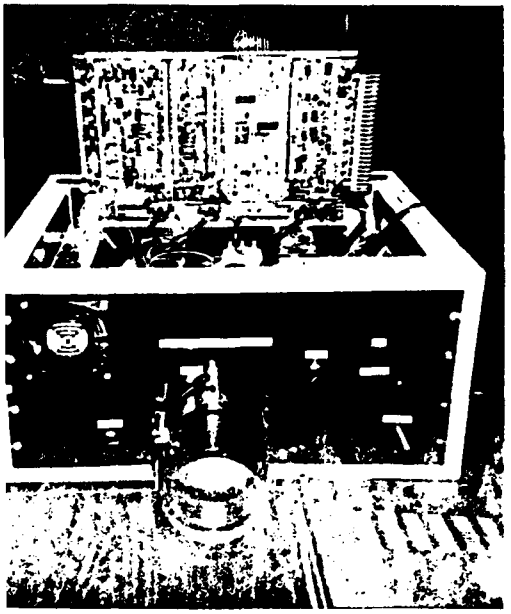

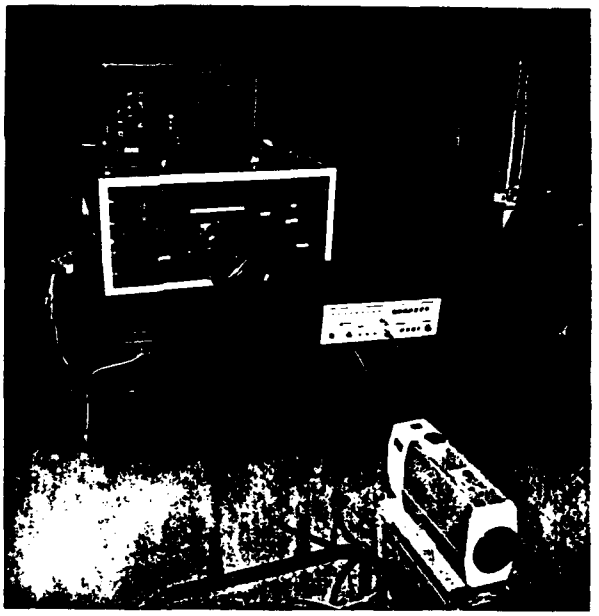

Figure 28

8.0 Summary and Conclusions

Single crystal faceplates have performance characteristics of luminance efficiency approximately 80% less than currently available powder phosphor deposited on glass faceplates. The possible advantage of the crystal faceplate is its lack of coulombic saturation and non-burning capability; therefore, its application in stationary images such as status boards and stroke written images, where small characters or spots of high intensity, stationary or non-raster scanned, graphics is required may offset the lack of luminance efficiency.

Tests of several unmounted crystal faceplates and SCFP's integrated into CRT envelopes resulted in luminous efficiencies under the varying conditions of phosphor thickness, reticulated or stippled surface, aluminization and high voltage combinations, produced luminous efficiencies between 3.5 to 5 lumens per watt. The efficiencies varied between test articles.

Life of the single crystal faceplate CRT's was anticipated to exceed those of current technology Crt's which have a "browning" factor that causes a decrease in luminance efficiency. This is characteristic of powder phosphor deposited glass faceplate CRT's; but at comparable light levels to powder phosphors, the higher electron beam energy required by the SCFP CRT will cause early CRT out-gassing and cathode deterioration. It is doubtful, therefore, that any overall increase in life expectancy would result.

Crystal growing sources advise that the current crystal boule size is limited to 4" in diameter. Projecting a faceplate of this dimension and the peak efficiencies determined by Trident's and others' tests will require approximately 700 watts electron energy to the faceplates to generate 590 lumens from an F:1 with 85% transmission optical system in green light from a Ce:YAG faceplate CRT. This amount of E-beam power will produce an electron beam spot size at reasonable high voltages when scanned upon a limited sized faceplate (4") will result in limited resolution capabilities plus generate considerable heat. None of the crystals tested showed any deterioration caused by X-ray bombardment at the voltages and powers used.

The major problem encountered in manufacturing SCFP CRT's by both Thomas Electronics and Hughes Display Products was matching the expansion characteristics of the Ce:YAG compared to the glass envelopes. Ce:YAG to glass frit material to make a gradient seal was finally developed and the last CRT's received are still operating as of this report. Other methods of sealing the faceplates to the CRT envelopes are possible but were not attempted.

9.0 Recommendations

While the data obtained during this evaluation theoretically projects the potential for limited applications from the use of SCFP in a CRT application, the probability of achieving a high yield, reliable product is considered low. The manufacturing problems; specifically, differences in coefficients of expansion between faceplate, frits and glass, remain a "yet to be solved" process. This problem was unsuccessfully addressed by two (2) of the leading CRT manufacturers in the United States. Compounding this problem is the fact that the problem must be addressed three times; i.e., with red, green and blue faceplate material if a full color projector were to be developed. In addition to the problem of differential material coefficient of expansion, the system implications of increased operating high voltage and power requirements dictates increases in cost per lumen which would require significant development effort to allow a reasonable system to be configured. Utility of existing high voltage and beam current capability within a reasonable form factor would require reduction in system light output by a factor of 5. Given this situation, further system development could not be justified.

In lieu of the problems remaining to be solved and the limited potential for their solution, further development effort on application of SCFP to projection CRT's is not recommended.

10.0 References

10.1 Thomas Electronics, Inc., 100 Riverview Drive, Wayne, NJ 07470

10.2 Clinton Electronics Corp., 6701-T Clinton Road,Rockford, IL 61131

10.3 Hughes Display Products, subsidiary of Hughes Aircraft Co., 1501 Newton Parkway, Lexington, KY 40511

11.0 Enclosures

11.1 Epitaxial Phosphor Faceplates for High Resolution High Intensity Cathode Ray Tubes, dated August 1991, by Allied-Signal, Inc., Research and Technology, P. O. Box 1021, Morristown, NJ. 07960

11.2 Single Crystal Phosphor Faceplates for High Resolution, High Intensity Cathode Ray Tubes, Purchase Order No. 9166, dated February, 1992, by Applied Physics Laboratory, Allied-Signal, Inc., Research and Technology, P.O. Box 1021, Morristown, NJ 07962

11.3 Test Data Report, dated September 26, 1990, on 3M320 YAG, by Thomas Electronics, Inc., 100 Riverview Drive, Wayne, NJ 07470

11.4 CRT Cooling Analysis by Trident International, Inc., Central Florida Research Park, 3290 Progress Drive, Suite 155, Orlando, FL 32826

11.5 The Study of the Performance of a YAG Faceplate, dated February 3, 1992, by Optical Research Associates, 550 N. Rosemead Boulevard, Pasadena, CA 91107

11.6 Test Bed Projector, Operator's Manual, Trident International, Inc., Central Florida Research Park, 3290 Progress Drive, Suite 155, Orlando, FL 32826

ENCLOSURE 11.1

FINAL REPORT
EPITAXIAL PHOSPHOR FACEPLATES FOR HIGH RESOLUTION HIGH INTENSITY CATHODE RAY TUBES

AUGUST 1991

Epitaxial Phosphor Faceplates for High Resolution High Intensity Cathode Ray Tubes

N61339-90-C-0046

Final Report to

Naval Training Systems Center
12350 Research Parkway
Orlando, Florida 32826-3224
Code 253, Richard Hebb

by

D.M. Gualtieri and H. van de Vaart
Allied-Signal, Inc.
Research and Technology
P.O. Box 1021-R
Morristown, NJ 07962

August 199

0.0 CONTENTS

0.2 List of Tables.

0.3 List of Figures

Final Report

EPITAXIAL PHOSPHOR FACEPLATES FOR HIGH RESOLUTION HIGH INTENSITY CATHODE RAY TUBES

prepared for

Naval Training Systems Center
Code 271, Richard Hebb
12350 Research Parkway
Orlando, Florida 32826-3224

Contract N61339-90-C-0046

by

ALLIED-SIGNAL INC.
Research and Technology
P.O. Box 1021
Morristown, NJ 07960-1021

August 1991

Allied Signal

N61339-90-C-0046

Epitaxial Phosphor Faceplates for High Resolution High Intensity Cathode Ray Tubes

Final Report to

Naval Training Systems Center
12350 Research Parkway
Orlando, Florida 32826-3224
Code 253, Richard Hebb

August 1991

1. INTRODUCTION

1.1 Summary

1.1.1 Objectives of Program.

The primary objective of this program was the development of a monochromatic epitaxial phosphor faceplate of 1000 lines resolution in a 2.75-inch diagonal raster. Targeted light output was 2000 lumens of visible light at a beam power of 10-20 W/cm^2. This specification was set by the largest available substrate wafers of YAG, three inches in diameter at present. Since some of the wafer periphery must be used in bonding the epitaxial phosphor faceplate to the electron gun neck, the excited area in a finished CRT would be a 2.75-inch diagonal raster, or an excited area of about 20 cm^2 in a 3:4 raster.

Ce:YAG epitaxial phosphors were selected as capable of operation at the power levels required for such a light output. The faceplate reticulation techniques of physical structuring and ion implantation were investigated as a means of increasing the external efficiency of such epitaxial phosphor faceplates. Only physical structuring by acid etching was found to be suitable. A total of twelve epitaxial phosphor faceplates were to be delivered to NTSC, six of which were to be 3 inches in diameter and of sufficient thickness to be incorporated into CRT's.

A secondary objective was the identification of candidate red, green, and blue phosphors compatible with the epitaxial phosphor faceplate process for color projection faceplates. Yttrium aluminum garnet (YAG) and other activator host materials were to be considered. Ce:$Gd_3Ga_5O_{12}$ and (Ce,Cr):$Gd_3Ga_5O_{12}$ were evaluated as potential epitaxial phosphors, but their efficiency was found to be far lower than that for Ce:YAG. A redshifted Ce:YAG phosphor, Ce:$Y_2Gd_1Al_5O_{12}$, was developed. The efficiency of a new blue phosphor, Ce:BEL, was increased by annealing in a reducing atmosphere. The best reticulated efficiency of Ce:YAG, as measured at 25 kV anode potential at power

loadings to 5 watt/cm^2, was 5.4 lumens/watt. This is sufficient to reach the goal of 2000 lumens in a 2.75-inch diagonal raster at a beam power of 16 watt/cm^2.

Four one-inch diameter study samples, two two-inch diameter faceplates, and six three-inch diameter faceplates were delivered to NTSC for testing.

1.1.2 Conventional CRT Faceplates

Conventional CRT faceplates are formed by the deposition of phosphor powder on the inside of a glass envelope of limited thermal conductivity. The image resolution and power capabilities of these faceplates are limited, and many applications now require CRT performance at the limits of phosphor faceplate technology. For example, sunlight-readable head-up displays (HUDs) for aircraft require a brightness of 10,000 foot-lamberts, a performance just achieved by conventional CRTs in stroke mode, and a factor of ten beyond that achieved in raster mode. The resolution of conventional faceplates is limited by phosphor particle size to twenty micrometers. High intensity operation is limited by a decomposition threshold of about 1 watt/cm^2. The phosphor particles will actually melt at about 5 watts/cm^2. High intensity operation also limits phosphor lifetime by a process called coulombic degradation. This failure mode reduces the intensity of P53, a standard phosphor, to 50% of its initial value after an electron dosage of 140 coulombs/cm^2. This leads to a CRT lifetime in a high luminance application of about 1000 hours under the best conditions.

1.1.3 Garnet Crystals

Garnets are crystalline materials with many technologically useful properties. Garnets are oxides of the general composition $R_3T_5O_{12}$ (R and T are large and small metal or metalloid elements) which are resistant to chemical attack and high temperatures. There is much diversity in garnet composition since R and T can be combinations of one or several elements cohabiting a crystal sublattice, and R and T range over much of the Periodic Table. As an example, the yttrium in $Y_3Al_5O_{12}$ (YAG) can be partially replaced with neodymium to form the useful laser crystal Nd-YAG. $Y_3Fe_5O_{12}$ (YIG), which can be considered to be YAG with the aluminum atoms completely replaced by iron, is an important microwave material because of its combined magnetic, dielectric, and insulating properties. Bismuth-substituted YIG, $(Bi,Y)_3Fe_5O_{12}$, is an important optical material because of its large Faraday rotation.

YAG is used not only as a laser material, but as a substrate for the deposition of other garnet compositions. In particular, YAG doped with rare-earth elements, when grown as epitaxial layers on YAG substrates, is a cathodoluminescent material. Such layers can be used as phosphor faceplates in cathode ray tubes with significant advantages over standard, powder phosphor, faceplates. The single crystal nature of such epitaxial faceplates allows a higher resolution, and the intimate thermal contact between the epitaxial phosphor and the thermally conductive substrate allows operation of cathode ray tubes at power levels which would destroy a conventional powder phosphor.

The utility of garnets is amplified by the high state of the art of liquid phase epitaxy (LPE). Liquid phase epitaxy of garnets reached a high level of capability in the development of magnetic bubble memory materials, which are highly substituted rare-earth iron garnets (for example, $(Y,Sm,Lu,Tm,Ca)_3(Fe,Ge)_5O_{12}$). In liquid phase epitaxy, a crystalline garnet substrate, usually (111)-oriented $Gd_3Ga_5O_{12}$, is "dipped" into a

supersaturated solution of garnet oxides dissolved in a solvating flux. A crystalline garnet layer, typically YIG, is grown in perfect registry to the substrate. In this way a garnet with specific properties and many constituent elements can be grown easily on a substrate of a simpler composition. Magnetic bubble memory materials utilize iron garnet layers of about one micrometer thickness, and magnetostatic wave devices utilize YIG layers from 10 to 100 micrometers.

Epitaxial phosphors are fluorescent crystalline layers which are grown on crystalline substrates. The usual case is homoepitaxial growth, in which a fluorescent ion is susbtituted for another ion in a host composition epitaxially grown onto a substrate of the host composition. An example is Ce:YAG epitaxially grown on YAG substrates, where cerium is incorporated into the layer on yttrium sites. The more unusual case is heteroepitaxy, in which a layer is grown on a substrate of different crystal structure; for example, zinc suphide deposited on sapphire. Since electrons penetrate only a few microns into epitaxial phosphors, the epitaxial layer need not be very thick, 5-20 microns are usually sufficient. Epitaxial layers can be grown on top of other epitaxial layers to form penetration phosphors, in which different colors are excited at different anode potentials.

1.1.4 Epitaxial Phosphor Faceplates.

Epitaxial phosphor faceplates (EPF) have several significant advantages, which are summarized below:

1) *Ultra-High Resolution.* Resolution is limited only by electron beam size.

2) *Fast Decay Time.* Fluorescence decay of Ce:YAG (10 nsec), a standard epitaxial phosphor, is an order of magnitude faster than conventional powder phosphors.

3) *High Power Operation.* Epitaxial phosphors will not decompose at high power levels. There is no "burn". Thermal quench temperature is much higher than for powder phosphors.

4) *Superior Ageing Characteristics.* No coulombic degradation.

5) *Superior Mechanical Properties.* Single crystals have high strength. Faceplates resist scratching.

Since epitaxial phosphors are single crystals with no granulation, resolution is limited only by the dimension of the electron beam. Prof. Albert Crewe of the Fermi Institute, University of Chicago, has tested a Ce:YAG epitaxial phosphor faceplate fabricated by Allied-Signal, Inc. in a high resolution electron microscope and found no granulation to 0.1 μm spot size. This Ce:YAG epitaxial phosphor faceplate was further tested to a current density of 1000 A/cm^2 at 5 kV without permanent damage. M.W. van Tol and J. van Esdonk operated epitaxial phosphor faceplates at power levels of 10 W/cm^2 [1]. J.M. Robertson and M.W. van Tol tested epitaxial phosphor faceplates of Ce:YAG, Tb:YAG, and Eu:YAG at power levels to 10^4 W/cm^2 [2]. They found that Ce:YAG is linear to the highest power levels, but that the light output of Tb:YAG and Eu:YAG saturates at power levels above 1 W/cm^2. Thus, Ce:YAG is preferred as a high intensity monochrome phosphor. The saturation in Tb:YAG arises from excited state absorption and cross-relaxation processes and it is a general feature of many phosphors, for example Mn:$BaAl_{12}O_{19}$ [3,4]. AT&T Bell Laboratories has developed a modified terbium

composition, $Tb_{0.2}Y_{0.1}Lu_{2.7}Al_3Ga_2O_{12}$, with improved saturation characteristic [5]. Such a phosphor has shown a peak line brightness of 28,000 fL at a 25,000 inch/sec writing speed when excited with a 25 kV, 2 mA beam. This is equivalent to 594 lumens in a 2.75 inch diagonal raster.

Levy and Yaffe have shown that the thermal quenching temperature of Ce:YAG is about 400°C, and that a decrease in light output is first evident at 200°C [6]. They determined that it is safe to operate an EFP at thermal gradients up to 150°C/inch, and that a three inch diameter epitaxial phosphor faceplate can be operated at 25 watts excitation with no cooling. Since the thermal conductivity of YAG is high, forced-air cooling is very effective at higher excitation levels. Forced-air cooling can extract about 60% of the heat, radiation can dissipate about 20% of the heat, and conduction down the neck can dissipate the remaining 20%. Coulombic degradation does not occur in epitaxial phosphor faceplates, whereas 0.5 W/cm^2 is the conventional limit for projection CRTs. Operation of P53 at 0.5 W/cm^2 results in an extremely short lifetime.

Ce:YAG, a standard epitaxial phosphor, has the disadvantage of lower external efficiency than the best powder phosphors due to the waveguide trapping of light in the layer-substrate composite. Research in epitaxial phosphor faceplates would focus on improving the efficiency. It would also try to model the spectral output of the phosphor to match potential applications.

1.1.5 Epitaxial Processing and Faceplate Characterization.

Garnet layers are generally grown by liquid phase epitaxy, usually by the horizontal dipping technique with rotation [7]. Much the research at Allied-Signal, Inc. in garnet layer growth has been involved with the kinetics of crystallization of garnet from LPE melts and its affect on layer composition and site selectivity of substituent atoms [8,9,10]. As an example, LPE growth of YIG layers results in a small substitution of yttrium onto iron lattice sites, and a small incorporation of lead from the growth solution onto yttrium lattice sites.

In the case of mixed garnets, such as bismuth substituted YIG, the composition of the growing crystal does not mirror the composition of the growth solution. Instead, the crystal composition is a strong function of the growth rate and the segregation coefficients of the atomic species.

The liquid phase epitaxy technique was developed to a high state of the art in research on magnetic bubble memory materials. Magnetic bubble memory devices utilize epitaxial layers of rare earth iron garnet on gadolinium gallium garnet (GGG) substrates. Such layers must be nearly defect-free for proper device operation. The growth of an epitaxial layer of YAG by liquid phase epitaxy proceeds as follows. A substrate of YAG is carefully cleaned and mounted in a substrate holder which allows horizontal rotation and vertical translation. The substrate is then "dipped" by vertical translation into a tube furnace containing a platinum crucible holding the molten constituent oxides of the garnet. These oxides are dissolved in a lead oxide based solvent first heated to 1050°C and then supercooled to about 10°C below the temperature at which garnet crystals will grow (the saturation temperature).

After the substrate is dipped into the growth solution, it is rotated at about 100-250 rev/min, and an aluminum garnet layer is epitaxially grown on the substrate at a rate of about 0.5-1.0 μm/min. After a time sufficient for growth of the desired layer thickness, the

substrate is pulled vertically from the growth solution, and the clinging solution is "spun-off" at high speed. The substrate, now with an epitaxial layer, is removed from the furnace, and remaining traces of solidified growth solution are removed in hot nitric acid. This entire process is done in a class 100 laminar flow hood, allowing growth of garnet layers by liquid phase epitaxy with less than 10 defects/cm^2.

Characterization of epitaxial phosphor faceplates consists of measurements related to the layer epitaxy, and measurements of the optical and cathodoluminescent properties of the layers. Epitaxial crystal growth requires substrates of known orientation and polish. Layers are grown to a specified thickness and lattice constant match to the substrate. Substrate crystallographic orientation and lattice constant measurements are made by X-ray diffraction. Epitaxial layer thickness can be measured by guided wave optical techniques, or by weight and reference to the layer density. Optical properties, including the cathodoluminescent spectrum, are measured by a spectrometer. Cathodoluminescent efficiency is measured by photometry with reference to the cathode ray beam power (anode current x anode voltage). Since faceplate resolution is gun-limited for these faceplates, resolution is not typically measured.

Phosphor layers must be thick enough to absorb the total electron flux, but not as thick as to absorb the emitted light, thus the need for an accurate thickness measurement. Also, many layer properties depend on the growth rate, which is calculated from the thickness and growth time. Allied-Signal,Inc. has a commercial guided wave thickness and refractive index measurement apparatus (Metricon) which has been fitted with an infra-red laser for more accurate measurement of absorptive garnet layers.

Accurate measurement of the lattice constant is essential for calculation of epitaxial layer misfit to the substrate, and for measurement of temperature coefficients of thermal expansion. Allied-Signal, Inc. has a computerized Blake double crystal X-ray diffractometer which allows measurement of the (444) garnet reflection to arc-sec resolution, and calculation of lattice constant to 0.00001 Angs. by the Bond technique. Lattice constant can also be indicative of activator concentration (e.g., Ce in Ce:YAG). This Blake diffractometer further allows measurement of the X-ray linewidth of epitaxial layers, an indicator of their crystalline perfection or degree of faceting.

Cathodoluminescence of epitaxial phosphor faceplates is measured at Allied-Signal, Inc. on a demountable faceplate characterization station consisting of a high vacuum pumping station, an electron gun, and a demountable faceplate assembly. This electron-beam excitation station is capable of 30 kV anode potential at 2 mA beam current, or about sixty watts of beam power. This is combined with a computer controlled spectrometer system to capture and analyze the cathodoluminescence spectra of faceplates to nanometer wavelength resolution. Faceplates are first coated with an aluminum anode in a vacuum metallization station before electron excitation. Cathodoluminescent efficiency is measured by a Tektronix J16 Photometer and J6523 Narrow Angle Luminance Probe, calibrated to within 5% of N.I.S.T. standards.

1.2 Summary of Results.

1.2.1 2000 Lumen Faceplate.

Cathodoluminescence measurements of Ce:YAG faceplates, both at Allied-Signal and at Trident International, another contractor to the NTSC, have shown that the goal of 2000 lumens in a three-inch faceplate can be achieved. Trident International obtained 62,700 fL (435 lumens) from a one-inch square raster on a Ce:YAG faceplate. This faceplate was not reticulated, but it was produced with a slight facet texture, produced by epitaxial growth on a roughly polished faceplate, which also increases the external efficiency. The facets are natural faces of the YAG crystal which scatter the cathodoluminescence out of the phosphor layer towards the front of the faceplate.

A slightly higher electron beam power density than used in the test of the two-inch faceplate will give more than 2000 lumens from the 3.6 square inches of a 3:4 raster of 2.75-inch diagonal on a three-inch faceplate. Reticulated faceplates would require less power for 2000 lumens, or they will have more than 2000 lumens light output at the same excitation. Data for the two-inch faceplates appear in section 2.7.

1.2.2 Red/Green/Blue Phosphors.

A partial substitution of Gd for Y in Ce:YAG has red-shifted the cerium emission to give 50% greater light intensity at the red wavelength of 650 nm. Ce:BEL has a spectral characteristic suitable for a blue epitaxial phosphor; namely, high blue output peaking at 480 nm, with significant intensity at 450 nm.

1.3 Conclusions

1.3.1 2000 Lumen Faceplate.

Ce:YAG epitaxial phosphor faceplates are capable of 2000 lumens light output in either their reticulated or facet-textured form in a 2.75-inch diagonal raster. Although the reticulated faceplates are expected to operate at power levels below 10 W/cm^2, the facet-textured faceplates would require 18 W/cm^2 excitation.

1.3.2 Red/Green/Blue Phosphors.

$Ce:Gd_3Al_5O_{12}$ (Ce:GdAG, red), $Ce:Y_3Al_5O_{12}$ (Ce:YAG, green), and $Ce:La_2Be_2O_5$ (Ce:BEL, blue), appear to be an appropriate trio of epitaxial phosphors for a high intensity color projection display. Figure 1 shows the spectra of these phosphors.

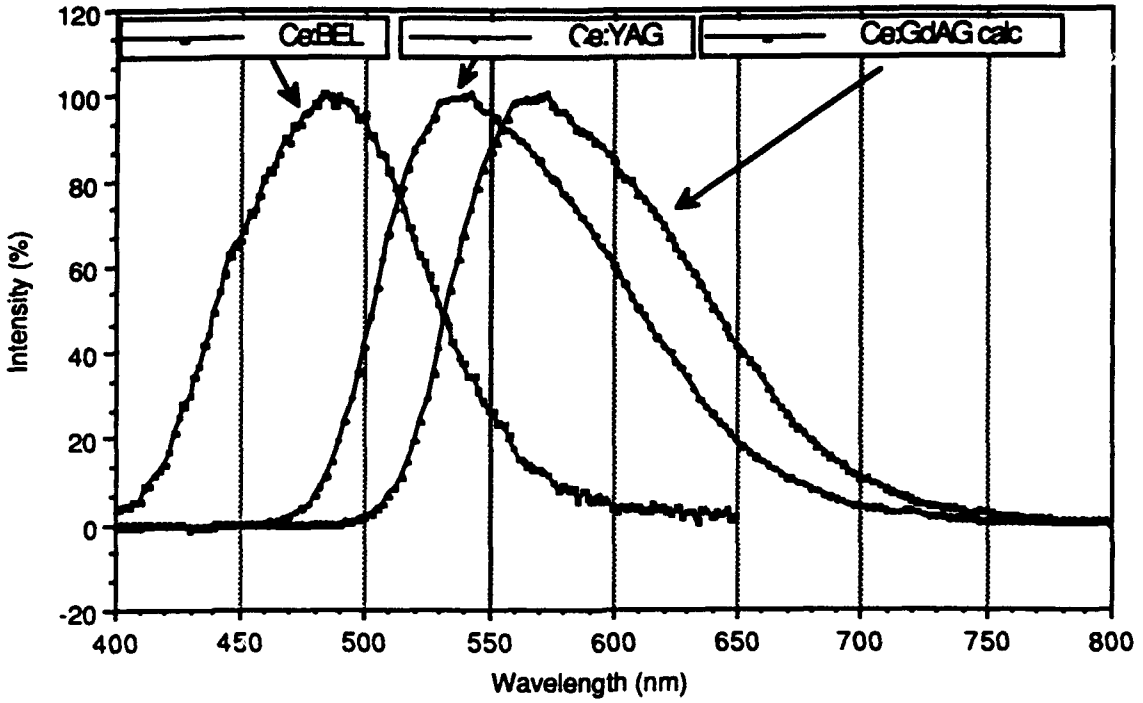

Fig. 1. Spectra of Ce:BEL (blue), Ce:YAG (green) and Ce:GdAG (red) phosphors.

2. EXPERIMENTAL DATA.

2.1 Epitaxial Layer Growth of YAG.

The following is a general procedure for the growth of epitaxial layers of Ce:YAG on YAG substrates. A single crystal wafer of YAG is prepared from a cylindrical crystal boule by slicing, lapping, and polishing. Polishing proceeds through finer grit, and a final polish is done with a colloidal silica mixture, as is common for the polish of garnet crystal wafers. The wafer is carefully cleaned and mounted in a substrate holder which allows rotation and translation. Epitaxy is achieved by dipping the substrate into a platinum crucible holding the molten constituent oxides of the Ce:YAG composition in the proportions listed in Table I.

Table I. Melt for the growth of epitaxial layers of Ce:YAG on YAG substrates at 980 °C. Note that cerium oxide, the dopant, is not included in the mole fraction calculation.

Oxide	Mole Fraction	Moles	Grams
PbO	0.90282	3.44684	769.299
Al_2O_3	0.01737	0.06632	6.762
B_2O_3	0.07524	0.28724	19.998
Y_2O_3	0.00457	0.01745	3.941
CeO_2		0.00581	1.000
	1.00000	3.82367	801.000

The melt composition of Table I can be specified by the following molar ratios of its constituents:

$R_1 = Al_2O_3/Y_2O_3 = 3.8$

$R_3 = PbO/2B_2O_3 = 6.0$

$R_4 = (Y_2O_3 + Al_2O_3)/(Y_2O_3 + Al_2O_3 + B_2O_3 + 1/2PbO)$

$= 0.04.$

The platinum crucible, 3-inches high by 2.25-inch diameter, is placed in a vertical furnace as shown in fig. 2. These powders are heated to 1050 °C, a temperature well above the melting point of the mixture, and allowed to "soak" for 24 hours. The melt is stirred for one hour at 1050 °C and 200 rev/min just before each layer growth. After stirring, the melt is cooled to the growth temperature of about 980°C in 45 minutes (melt saturation occurs at about 990°C).

The YAG faceplate wafers, 2-inch in diameter by 0.100 inch thickness, are thermally equilibrated above the melt surface for ten minutes, dipped to the melt surface, and rotated at 200 rev/min. for about ten minutes. The Ce:YAG epitaxial phosphor layer grows at a rate of about 1.5 μm/min. After growth, the substrate with the epitaxial layer is raised above the melt, and the residual flux is spun-off by rapid rotation of 500 rev/min. Removal of the faceplate from the furnace to room temperature proceeds over the course of 90 minutes. This slow exit rate prevents thermal shock and cracking of the wafers. This entire process is done in a class 100 laminar flow hood. Remaining traces of solidified growth solution on the wafers are removed in a 40% solution of nitric acid at 90 °C. Layer thickness is measured by weight, using a density of 4.565 g/cc, the density of pure $Y_3Al_5O_{12}$. Optical thickness measurement is not possible since there is no refractive index difference between the layer and the substrate.

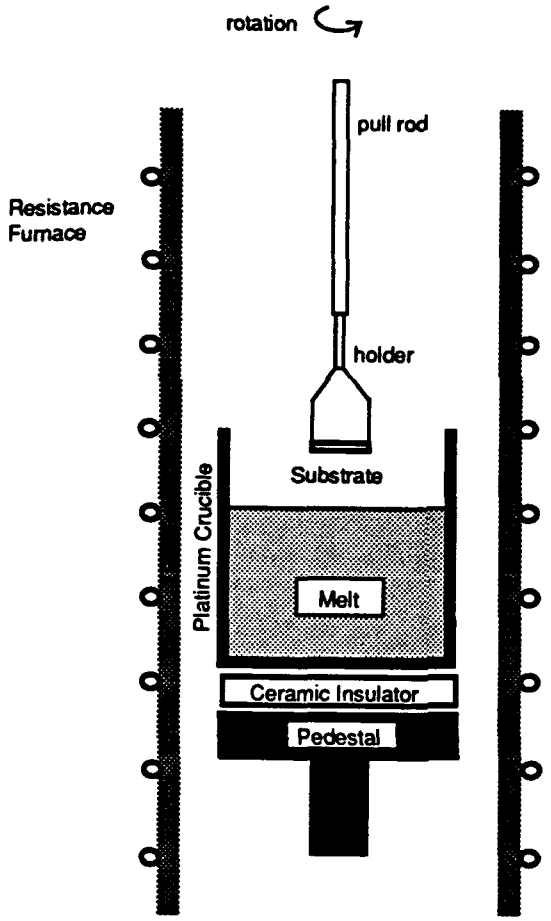

Fig. 2. Schematic diagram of system for liquid phase epitaxial growth of single crystal phosphors of Ce-YAG on YAG substrates.

2.2 Increasing the Internal Efficiency of Ce:YAG

Experiments were performed to find the epitaxial growth conditions which would give the maximum internal efficiency of Ce:YAG. Internal efficiency is the efficiency of the phosphor material composition itself, as distinct from effects relating to the problem of coupling light out of the material. A photometer with calibration traceable to the NIST was used in conjunction with a demountable faceplate electron gun station to measure cathodoluminescent efficiency. An effort was made to incorporate more cerium into the epitaxial phosphor layers with a higher cerium concentration in the melt, and to attempt epitaxial growth at higher growth rates and higher growth temperatures. Higher cerium content in the melt will increase cerium incorporation into the epitaxial layers up to a certain point, at which the melt will become saturated in cerium and further additions of cerium will have no other effect than to increase the defect density of the layers. Increasing growth rate will also increase cerium content, up to the point at which the growth interface becomes saturated with cerium. High temperature growth reduces the concentration of lead in the epitaxial layers. Lead is always present to a small extent, since it is a constituent of the flux, but it is not thermodynamically favorable for lead to enter the crystal lattice of YAG at high temperatures.

Since lead is a doubly-charged cation, it is expected that the deleterious effect of lead on the cathodoluminescent efficiency is due to its forcing of Ce^{3+} into the inactive Ce^{4+} charge state. As an attempt to reduce any Ce^{4+} present in the faceplates to Ce^{3+}, a Ce:YAG faceplate was annealed at 1150 °C in a reducing atmosphere of 10% hydrogen in argon. The cathodoluminescent efficiency was unchanged.

Steps were taken to verify that the melt composition that was used for epitaxy of the Ce:YAG phosphor layer on single crystal YAG faceplates is indeed saturated with respect to cerium oxide. Five epitaxial layers were grown near 1076 °C at growth rates of 1.65-2.30 μm/min and cerium oxide concentration Ce/(Ce+Y) from 0.16 to 0.23. The growth temperature of 1076 °C, the highest temperature possible with our furnaces, was chosen to ensure the lowest concentration of lead in the epitaxial phosphor. Melt precipitation of cerium oxide was evident to the eye at concentrations of 0.23, and there was no change in cathodoluminescent efficiency in this range. It is clear that the cerium ion concentration is optimized at its value of 0.16, and this concentration will be used in all subsequent work. Cathodoluminescence measurements showed the point at which the melts were saturated with cerium, since melts with Ce/(Ce+Y) = 0.15 and 0.22 had essentially identical efficiencies. Growth rate was found to have but a small effect on efficiency, which is consistent with the small fraction of cerium incorporated and the Burton-Prim-Slichter model of segregation [11]. Faceting was found to occur at growth rates above 4 μm/min. Scanning electron microscopy showed cerium oxide crystals precipitating out of the growth interface at a growth rate of 5.4 μm/min (fig. 3). One undesirable side-effect of the high growth temperature was the evaporation of lead oxide from the melts, which approached 25 g/day from the 2-1/4 inch diameter crucibles. Since the melts initially contain 800 grams of lead oxide, such loss has a significant effect on the saturation temperature. Too high a growth rate leads to faceting. Growth rates of about 3 μm/min are optimum.

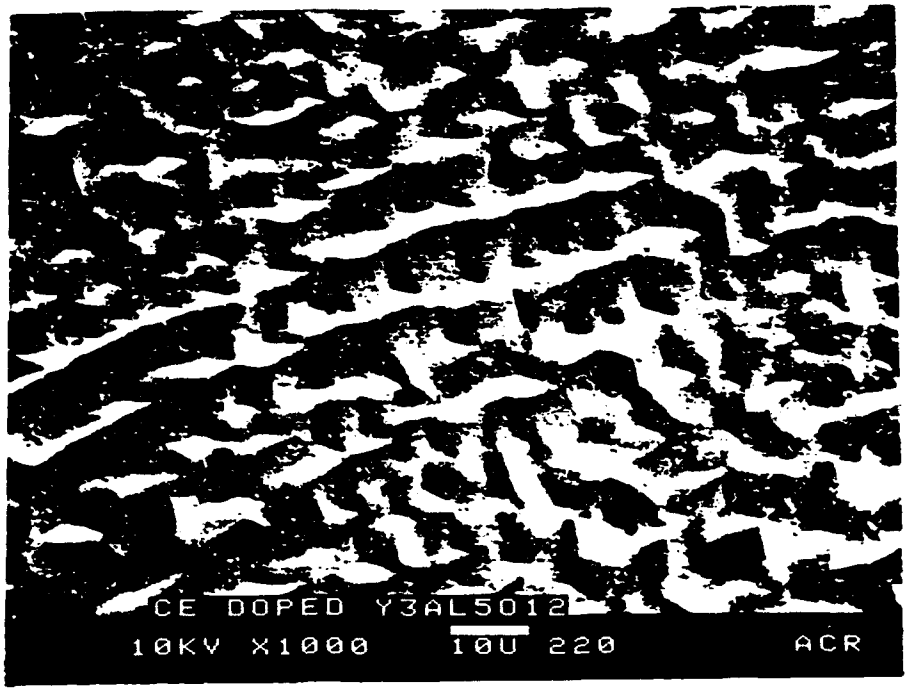

Fig. 3 Scanning electron micrograph of a Ce:YAG epitaxial phosphor faceplate showing precipitates of cerium oxide.

2.3 Increasing the External Efficiency of Ce:YAG

The major factor limiting the external efficiency of Ce:YAG phosphors is the high refractive index of the YAG substrate (1.84), which allows only rays less than a critical angle of 33° to be emitted from the faceplate. The remaining rays are waveguided to the edges, so that only 16% of the cathodoluminescence is emitted from the faceplate. Higher external efficiencies can be expected from Ce:YAG through reticulation, a texturing of the epitaxial phosphor into structures which will focus the cathodoluminescence towards the observer. Non-reticulated epitaxial phosphors have low external efficiencies, since the cathodoluminescence is waveguided by the high refractive index of YAG to the edge of the faceplate.

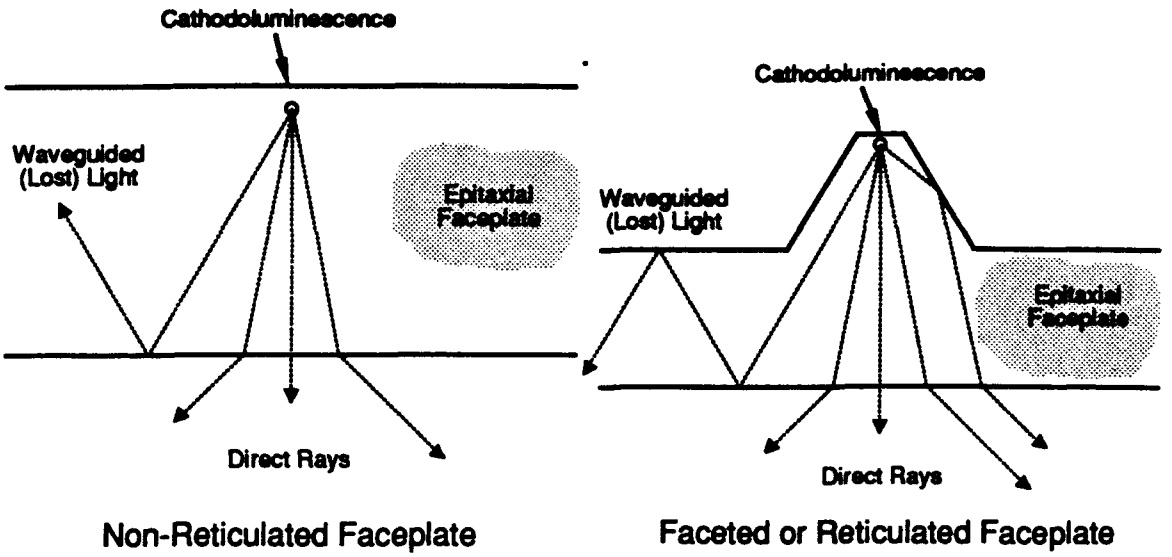

Fig. 4. Schematic illustration of waveguiding effect in epitaxial faceplates, and the role of reticulation in directing light into the critical cone.

P.F. Bongers, et al., [12] have etched grooves in the phosphor to increase the external efficiency. D.M. Gualtieri, et al. [13] have used a faceted epitaxial layer for the same purpose. D.T.C. Huo and T.W. Hou [14], have used photolithographic techniques to pattern a Ce:YAG epitaxial phosphor faceplate with an array of rectangular mesas. They were able to increase the external efficiency by a factor of three. A truncated cone geometery can increase the external efficiency by a factor of 5.5, if such a shape can be formed in the phosphor layer. Such reticulation will not limit the faceplate resolution if a small mesa size is used.

In the present study, five techniques were investigated for the reticulation of Ce:YAG faceplates. These were diffusion processing, reaction processing, physical masking, ion-implantation, and physical structuring. These techniques are examined in the following sections.

2.3.1 Reticulation by Diffusion Processing

One possible technique for reticulating epitaxial phosphor faceplates of Ce:YAG is through selective area modification of the composition of the YAG wafer before epitaxial growth. If the lattice constant of the wafer differs from that of the epitaxial layer by more than 0.5%, nucleation and growth of the epitaxial layer are inhibited. Titanium diffusion is well utilized in lithium niobate, another oxide crystal, to form optical waveguides. For this reason, titanium diffusion was attempted to change the lattice constant of YAG in selected areas to achieve reticulation in the epitaxial layer.

In an initial experiment, a (111)-oriented wafer of YAG was overcoated with a 60 nm layer of titanium and photolithographically prepared to produce an array of titanium stripes 2.5 μm in width by 25 μm center-to-center spacing. The wafer was annealed in air at 1000°C for four hours, and optical microscopy revealed some reaction between the

titanium and YAG at closely spaced points along the lines. Subsequent growth of a 12.5 μm thick YAG layer on this wafer produced an array of three-fold symmetric facets in the same pattern as the titanium lines. This experiment indicated that titanium could be a suitable masking agent for producing the facet island structures required to increase the external cathodoluminescent efficiency of Ce:YAG.

Further YAG wafers of (111)-orientation were overcoated with 150 nm layers of titanium and photolithographically prepared to produce arrays of titanium stripes 2.5 μm in width by 25 μm center-to-center spacing. Two of these wafers were annealed in air at 850°C and 1100°C for four hours, and one wafer was left unannealed. Subsequent growth of 20 μm thick Ce:YAG layers on these wafers produced no pattern on the unannealed wafer, a poorly defined pattern on the 850 °C annealed wafer, and a clearly defined pattern on the 1100°C annealed wafer (fig. 4).

A YAG wafer of (111)-orientation was photolithographically prepared to produce a square mesh of titanium stripes 2.5 μm in width by 25 μm center-to-center spacing, and it was then annealed in air at 1100°C for four hours. Subsequent growth of a thick Ce:YAG layer produced a checkerboard pattern of islands on the wafer. The cathodoluminescent efficiency of this wafer was found to 2.1 lumens/watt, about the efficiency of an unpatterned wafer. A titanium patterned YAG substrate was annealed at 1150 °C in an argon atmosphere. It showed a frosty appearance similar to the air-annealed wafers.

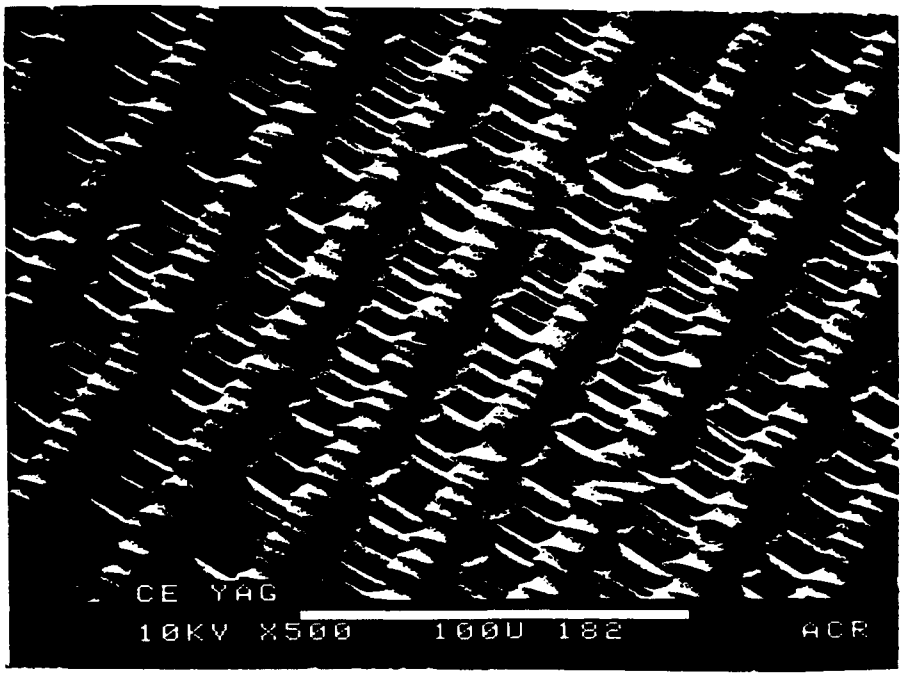

Fig. 5. Scanning electron micrograph of a Ce:YAG epitaxial layer grown on a titanium diffused YAG wafer.

Profilometer measurements of air-annealed YAG wafers with titanium stripes 2.5 μm in width by 25 μm center-to-center spacing, overgrown with Ce:YAG layers, showed a peak-to-valley depth of about 2 μm, or about 20% of the epitaxial layer thickness. Further analysis by scanning electron microscopy of tilted wafers confirmed the profilometry result which showed a small peak-valley excursion. On final analysis it can be said that the titanium diffusion process inhibits epitaxy of Ce:YAG on YAG, but only slightly. A maximum peak-to-valley thickness difference of only ten percent has been observed, which is not sufficient to increase the external efficiency of the faceplates. Cathodoluminescent efficiency increased slightly after hydrogen anneal, but only to 2.6 lumens/watt (fig. 5). Moreover, the resultant pattern is not as sharp as the pattern of the original titanium overlayer.

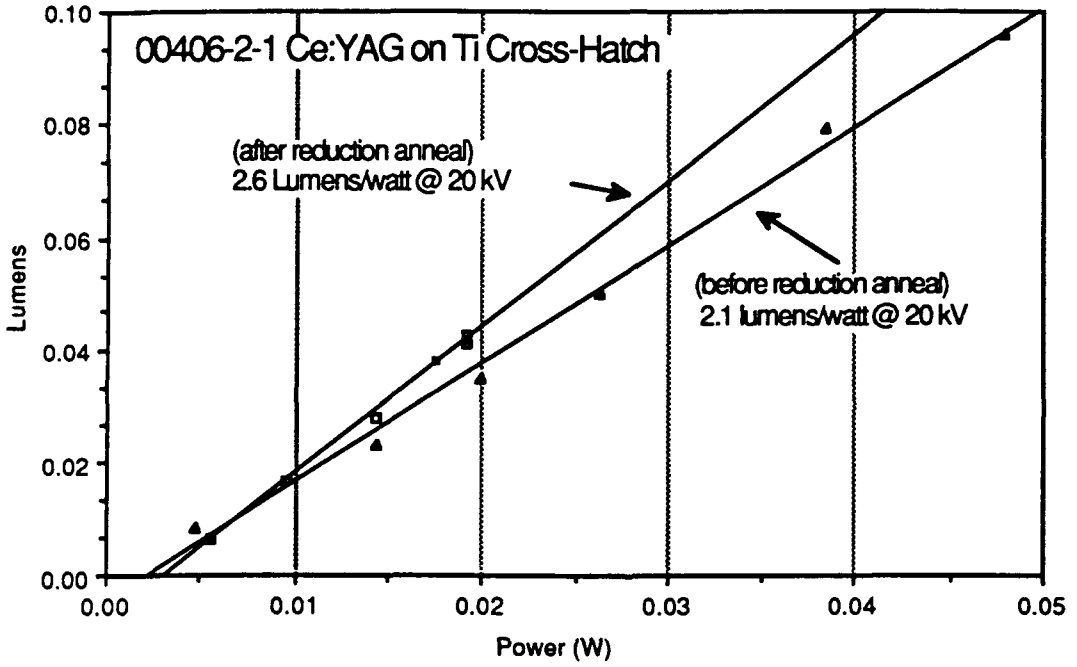

Fig. 6. Cathodoluminescent efficiency of a titanium patterned Ce:YAG epitaxial phosphor layer before and after hydrogen anneal.

2.3.2 Reticulation by Reaction Processing

Another possible reticulation technique is to chemically react the surface of the YAG wafers with another material in selected areas before epitaxy. Ce:YAG will nucleate and epitaxially grow on YAG substrates, but not on other crystals. Such reactions were attempted with layers of silica, indium oxide, and boron oxide. In these experiments, half of the YAG wafer was coated with the reactant material, the other half was left in its pristine state, and the wafers were heated to high temperatures. Silica was deposited in a plasma reactor; indium oxide was prepared by depositing indium metal by vacuum evaporation followed by oxidation in air; boron oxide was deposited by dip-coating in a molten bath of boron oxide. Reaction was evident in all cases, but epitaxy was not inhibited. Epitaxial growth resulted in a faceted layer in all cases. It appears that the lead

oxide flux dissolves away the reacted surface, leaving a damaged surface of YAG which can support faceted epitaxial growth.

2.3.3 Reticulation by Physical Masking

The alternative approach of physically masking the substrate against epitaxy was tried. A physical mask will produce reticulation by separating the YAG wafer from the epitaxial solution. This process requires a masking material which is resistant to the lead oxide melt and adherent to the YAG substrate at high temperatures. Titanium was tried as a masking layer, but to no effect. Also, Ce:YAG was epitaxially grown on a YAG wafer which was partially overcoated with a 0.1 μm layer of rhenium. The rhenium layer offered no resistance to epitaxy. Since the ionic radius of Re is identical to Al, rhenium was not investigated as a diffusion agent.

Silica, deposited in a CVD reactor from silane in oxygen, was also tried as a masking material, as were platinum on thick and thin chromium layers, and thick(> 1 μm) and thin (< 0.5 μm) platinum. As in the other experiments, half of the YAG wafer was coated with the masking material, and the other half was left in its pristine state. Only thick platinum layers showed growth inhibition. Profilometry showed that the thick platinum layers inhibited epitaxy for a short time (2-5 minutes), but not for the time required to reticulate the surface. Chromium is commonly used to promote adhesion of metals to oxide crystals, but platinum layers with thin or thick chromium showed essentially no growth inhibition.

2.3.4 Reticulation by Ion Implantation

YAG wafers, one-inch diameter by 0.020 inch thickness, were x-ray oriented, prepared with aluminum ion-implantation masks of square and triangle reticulation patterns, and sent to Implant Sciences Corporation, Danvers MA, for implantation of boron at a dosage of 5×10^{15} atoms/cm^2 at 80 keV. Ion implantation is intended to inhibit epitaxy in selected areas to form reticulation patterns during epitaxial growth. Ion implantation with boron (B^+, 80 KeV, 5×10^{15} atoms/cm^2) has been shown to inhibit epitaxy of iron garnet on gadolinium gallium garnet [15]. Epitaxial growth experiments on these wafers showed no patterning of Ce:YAG phosphor layers on these wafers, although a small optical density difference could be detected under a microscope. It appears that the ion implant damage, which should inhibit epitaxy, is annealed out of the wafer at the growth temperature.

2.3.5 Reticulation by Physical Structuring

A Ce:YAG epitaxial layer (00425-2-1) was grown on a YAG substrate roughened by sandblasting, a crude reticulation technique. Sandblasting exposes the facet faces of the YAG wafer, and the subsequent epitaxy propagates the facet structure. The facet texture helps to scatter the cathodoluminescence into the critical cone of allowed light transmission through the faceplate. This roughening process reduced the resolution proportionate to the grit size, but the efficiency was increased to 5.7 lumens/watt at 20 kV (fig. 7). Although the efficiency was high, the resolution was too poor to be useful in a CRT, and halation was quite severe.

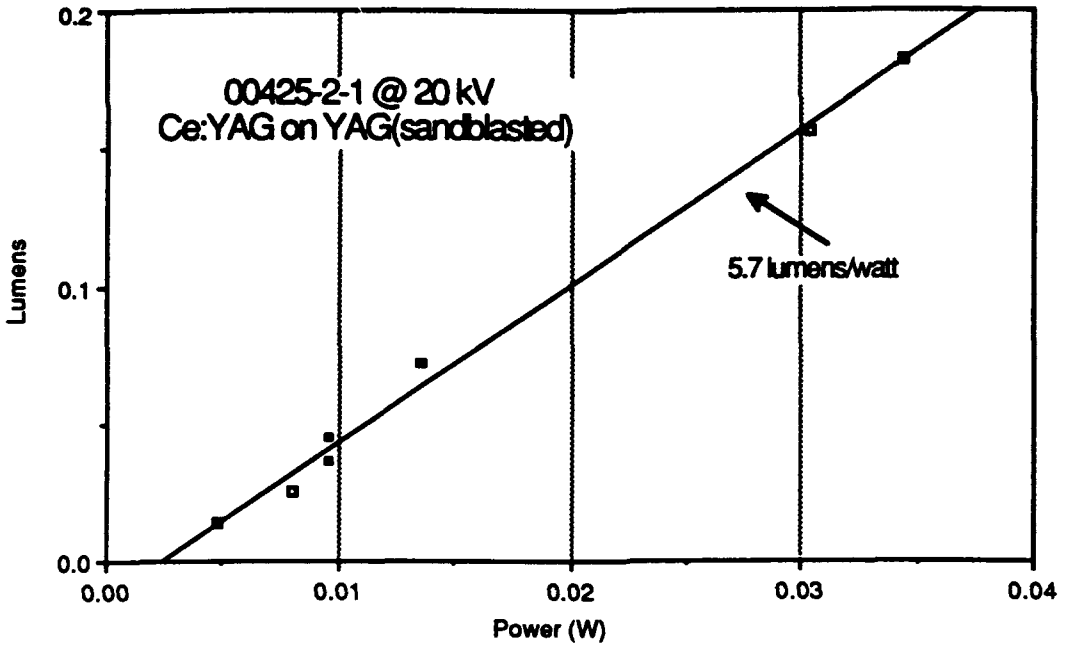

Fig. 7. Cathodoluminescent efficiency of a Ce:YAG epitaxial layer grown on a sandblasted YAG substrate.

Acid etching of YAG was investigated. YAG wafers were placed in an etchant bath of 3:1 by volume phosphoric acid:sulfuric acid for various times at temperatures between 175 and 300 °C to accurately determine etching rate. This was in preparation for the etching of reticulation structures on YAG substrates and on epitaxial Ce:YAG layers. The data are summarized by the equation

$$f = 1.34 \times 10^{-4}\, e^{0.0364\, T}$$

where f is the etching rate in μm/min, and T is the temperature in Centigrade. The etching rate of YAG is less than a tenth that of GGG at a given temperature. At 250°C the etching rate of YAG is only 1.25 μm/min. Etching temperatures above 250 °C should be avoided, since the phosphoric acid tends to polymerize ("gel").

Mesa structures were etched into plain YAG wafers by this etchant using an SiO_2 mask of 22 μm squares on 25 μm centers, the separation of adjacent squares being 3 μm. The (211) facet faces of YAG were revealed upon etching as the mask was undercut, so that a pyramidal reticulation was obtained. Subsequent epitaxial growth of Ce:YAG on these wafers preserved the pyramidal structure, and capped the truncated tops of partially formed pyramids. Cathodoluminescent efficiency of these reticulated arrays was essentially the same as for unreticulated faceplates. This may be a result of a decreased cerium incorporation for growth on the (211) crystal face. For Tb:YAG, growth on the (111) face gives a significantly higher efficiency than growth on the (211) face, and the same may be true for Ce:YAG. In that case, growth of Ce:YAG on (111)-oriented wafers, followed by etching to reveal the pyramidal structure, could give a higher efficiency, and this was tried next.

Nine epitaxial layers of Ce:YAG were grown single-sided on one-inch diameter YAG wafers, chosen for extreme flatness, for photolithographic etching of reticulation patterns in the Ce:YAG layer itself. Epitaxial layer thickness was between 5 - 14 μm at growth temperatures of 1083 - 1093 °C and growth rates of 1.0 - 2.8 μm/min. This series also gave an opportunity to confirm the temperature sensitivity of growth rate of the Ce:YAG melt, $\partial f/\partial T$, as -0.165 μm/min/deg.

In the simple model in which the cathodoluminescence is emitted as a point source in the phosphor, he external efficiency of a Ce:YAG epitaxial faceplate would be greatest when the reticulation pattern resembles a parabolic reflector. In practice, only an approximation to this shape can be made. In the case of YAG, the (211) facets of the crystal form a six-fold tent shape which approximates a paraboloid when truncated.

These epitaxial wafers of Ce:YAG were reticulated by acid etching using two techniques. In one, a shallow etch of a few micrometers resulted in an array of square mesas (fig. 8) and a cathodoluminescent efficiency of up to 4.0 lumens/watt at 25 kV and a beam power of 5 watt/cm^2. The other etching was a deep etching which undercut the SiO_2 mask to reveal the six-fold symmetric facets of the YAG crystal structure. The resulting pattern for the deep etch was an array of truncated six-sided pyramids (fig. 9), which was found to give 5.4 lumens/watt at 25 kV and a beam power of 5 watt/cm^2. A beam power of 16 watt/cm^2 would be required for 2000 lumen output at such an efficiency, although extrapolation to the 40 kV anode potential which will be used in the prototype projection tube gives a higher efficiency of 7 lumens/watt. This efficiency would require 12.5 watt/cm^2 beam power for 2000 lumens output.

Gold (200 nm) on chromium (100 nm) was found to be an effective mask for the high temperature phosphoric acid etching of reticulation patterns. A one-inch uncoated YAG wafer was reticulated with such a masking layer. This gives an alternative to masking with plasma-deposited SiO_2.

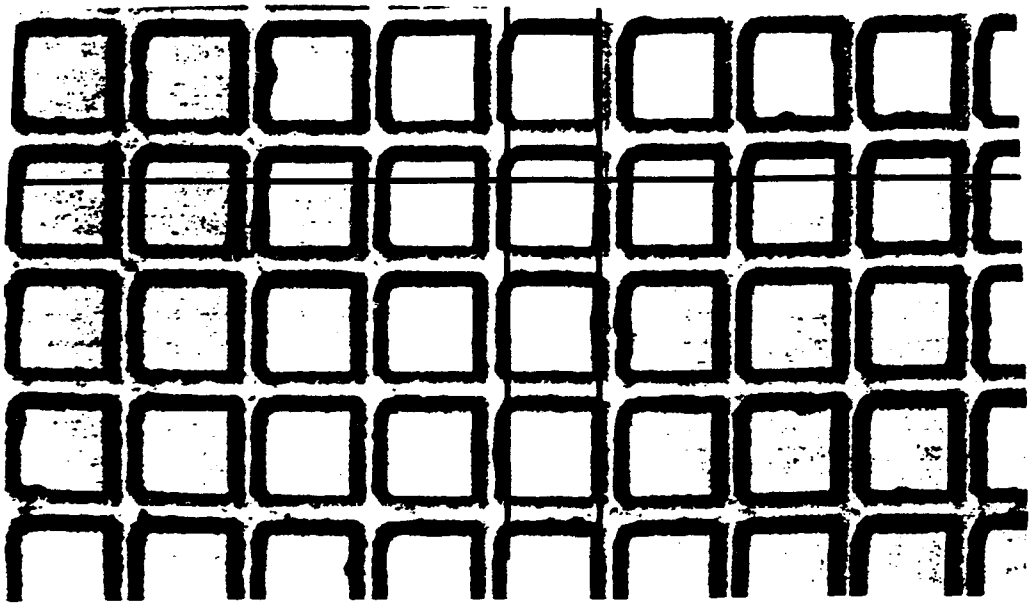

Fig. 8. Reticulation pattern of square mesas etched into epitaxial layer 00807-2-2.

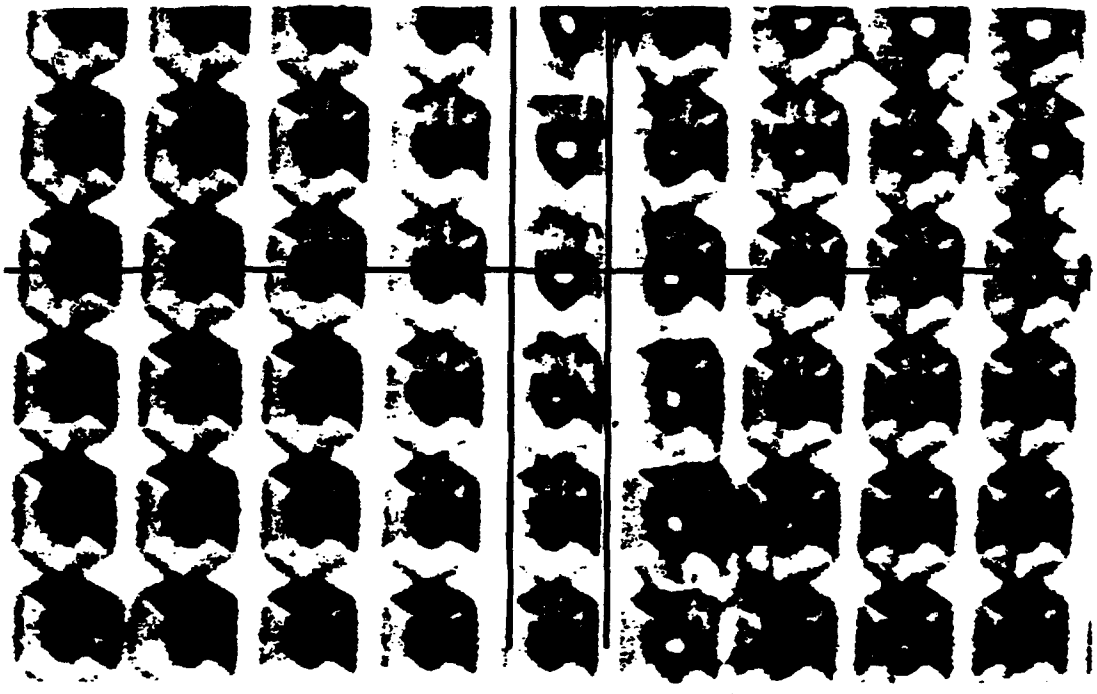

Fig. 9 Reticulation pattern of six-fold pyramids etched into epitaxial layer 00807-2-1.

Non-reticulated faceplates of Ce:YAG have an NTSC raster efficiency at 25 kV of 1.9 - 2.0 lumens/watt, when measured in our characterization station, so that at a beam power of 10 watts/cm^2 an NTSC raster of 2.75-inch diagonal on a *non-reticulated* Ce:YAG faceplate will have a luminance of 450 lumens. The best *reticulated* faceplate was found to give 5.38 lumens/watt at a beam power of 5 watt/cm^2. A beam power of 16 watt/cm^2 will be required for 2000 lumen output at such an efficiency. Figs. 9 - 11 show the results of cathodoluminescent measurements on the faceplates shown in figs. 7 - 8.

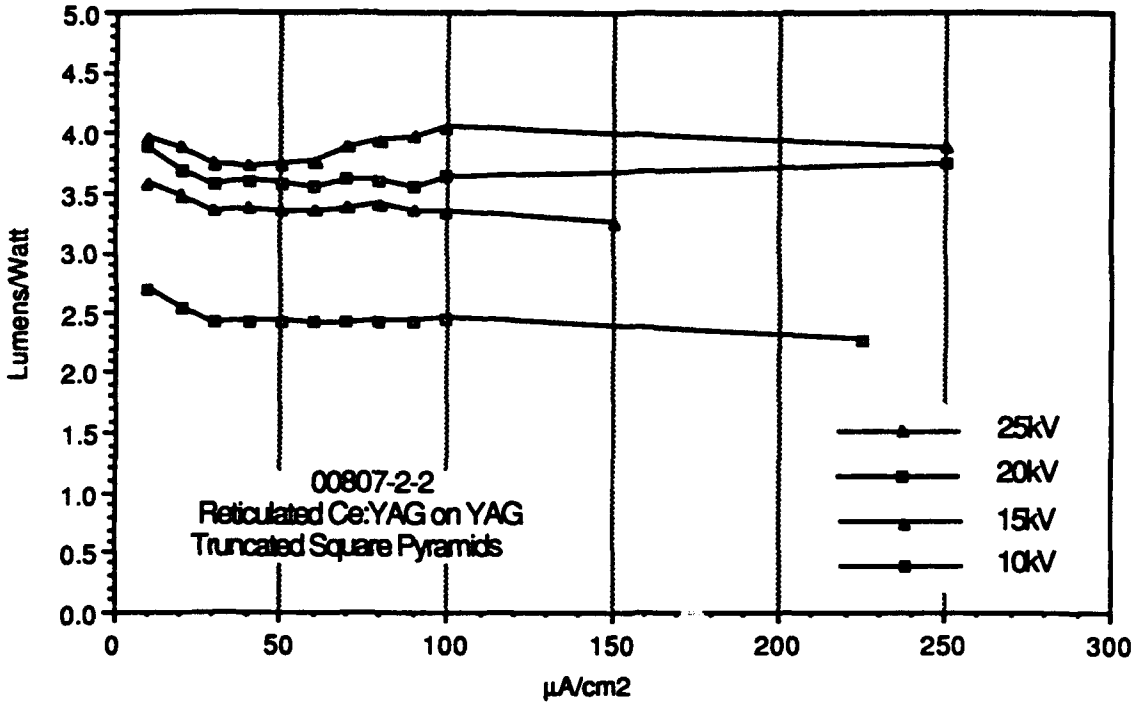

Fig. 10 Efficiency data for square mesa reticulation on epitaxial layer 00807-2-2.

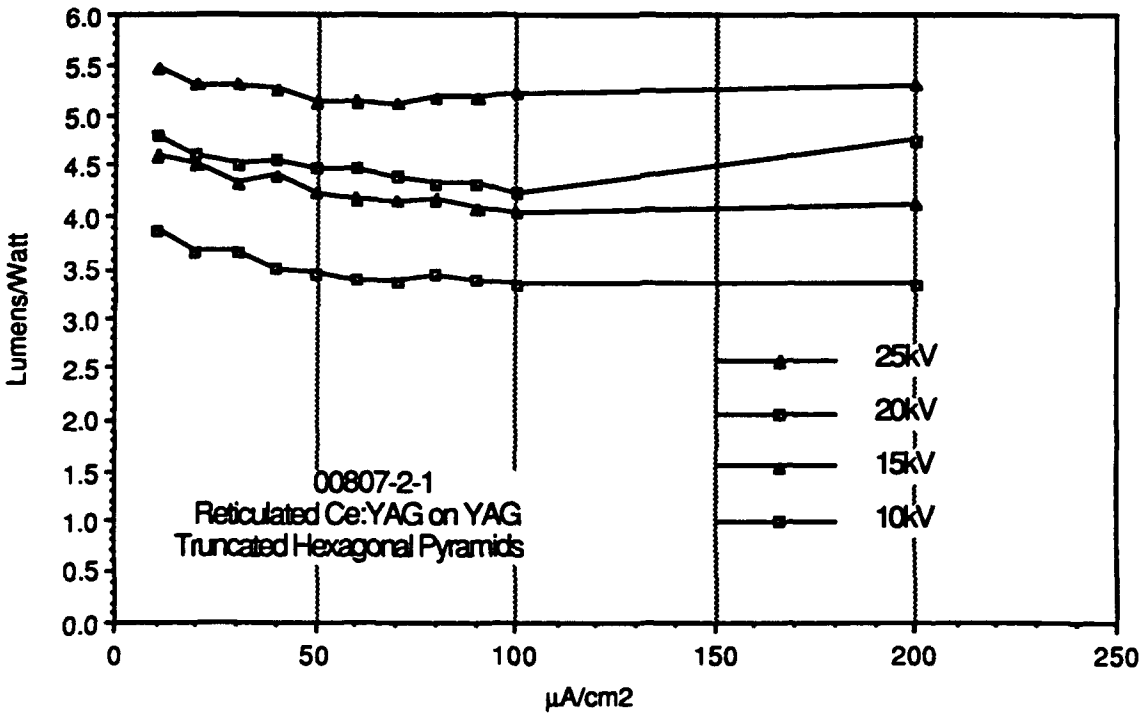

Fig. 11 Efficiency data for six-fold pyramid reticulation on epitaxial layer 00807-2-1.

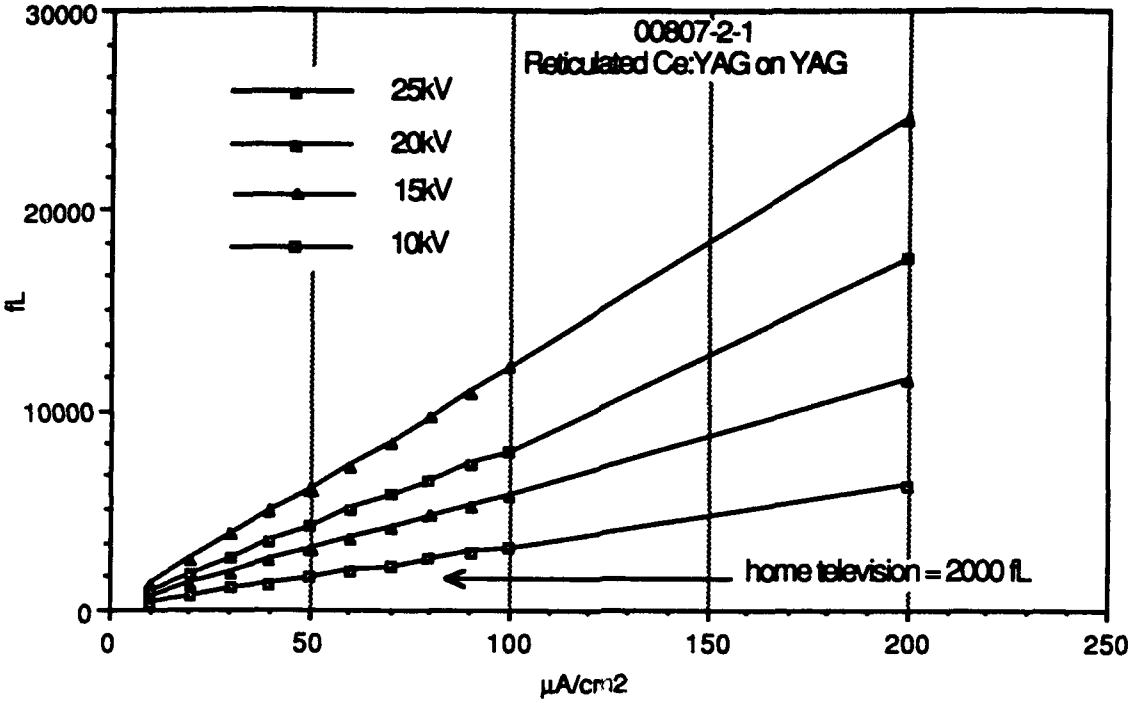

Fig. 12 Luminance data for six-fold pyramid reticulation on epitaxial layer 00807-2-1.

2.4 Scale-Up of Faceplate Diameter

A large furnace was installed for the epitaxial coating of two-inch and three inch Ce:YAG faceplates. A large platinum crucible and platinum wafer holder were purchased for the growth of these large diameter faceplates. Discussions about the mechanical properties of YAG between Allied-Signal, Trident International, and Thomas Electronics led to a wafer thickness specification of 0.110 inch at three inch diameter.

As could be expected, scale-up from one-inch to three-inch faceplates had its own special problems. First, three-inch diameter YAG is not available as a commercial product. Fortunately, a laser materials group at Allied-Signal was able to produce such a crystal. Second, it was difficult to polish the large wafers to the same "epi" polish as the small wafers, but an external polishing shop (Commercial Crystal Laboratories, Naples, Florida), was able to do the job. Third, thermal gradients in the furnace caused cracking of the faceplates during withdrawal to room temperature. This problem was solved by removing all heat-shielding baffles from the furnace. Fourth, the flatness of the epitaxial phosphor layer was not sufficient to allow the fine-line lithography needed for the reticulation pattern. This lack of flatness was caused by the non-ideal fluid flow in the limited dimensions of the crucible. This problem was solved by a polish of the epitaxial layer before epitaxy. The thermal expansivity of YAG has also caused problems for Trident International and Thomas Electronics in bonding the faceplate to the CRT neck assembly.

2.5 High Intensity Blue Phosphors

2.5.1 Blue-Shifted Ce:YAG

An epitaxial phosphor faceplate of (Ce,Lu,In)-YAG was prepared as a candidate blue-enriched phosphor. Large cations on the octahedral lattice sites and small cations on the dodecahedral lattice sites are known to blue-shift the cerium emission. In this case, the novel octahedral substituent In was combined with dodecahedral Lu to blue shift the cerium. UV excitation of the cerium fluorescence indicated low efficiency. It appears that substitutions for aluminum reduce the efficiency of cerium YAG.

2.5.2 Ce:BEL

The cathodoluminescence of Ce:BEL was characterized. A thin wafer of a Czochralski boule prepared from a melt of 0.5% cerium content was used in the analysis [16]. Ce:BEL proved to be an excellent blue phosphor with a peak fluorescence at 485 nm and a fluorescence bandwidth (FWHM) of 80 nm (fig. 13). Thus, there is significant light energy at the extremely blue wavelength 445 nm. The measured cathodoluminescent efficiency of the available, as-grown Czochralkski crystal was 0.1 lumen/watt, weighted according to the C.I.E. photoptic curve. It was found that annealing at 1150 °C in a reducing atmosphere of 10% hydrogen in argon doubles the efficiency of Ce:BEL to 0.2 lumens/watt (fig. 14). Annealing also changes the appearance of the crystals from an orange color to transparent. It was also found that the light output of Ce:BEL does not saturate up to an electron beam power of 19 watt/cm^2.

Mass spectroscopy of the Ce:BEL crystal revealed a cerium content of 3.9×10^{18} atoms/cc, as compared with 23×10^{18} atoms/cc for YAG. If the cerium content of Ce:BEL can be increased to the level of cerium in YAG, this six-fold increase in concentration could increase the C.I.E. weighted efficiency of Ce:BEL to 1.2 lumens/watt. Since the refractive indices of Ce:BEL are about the same value as the refractive index of YAG, reticulation will yield the same increase in external efficiency.

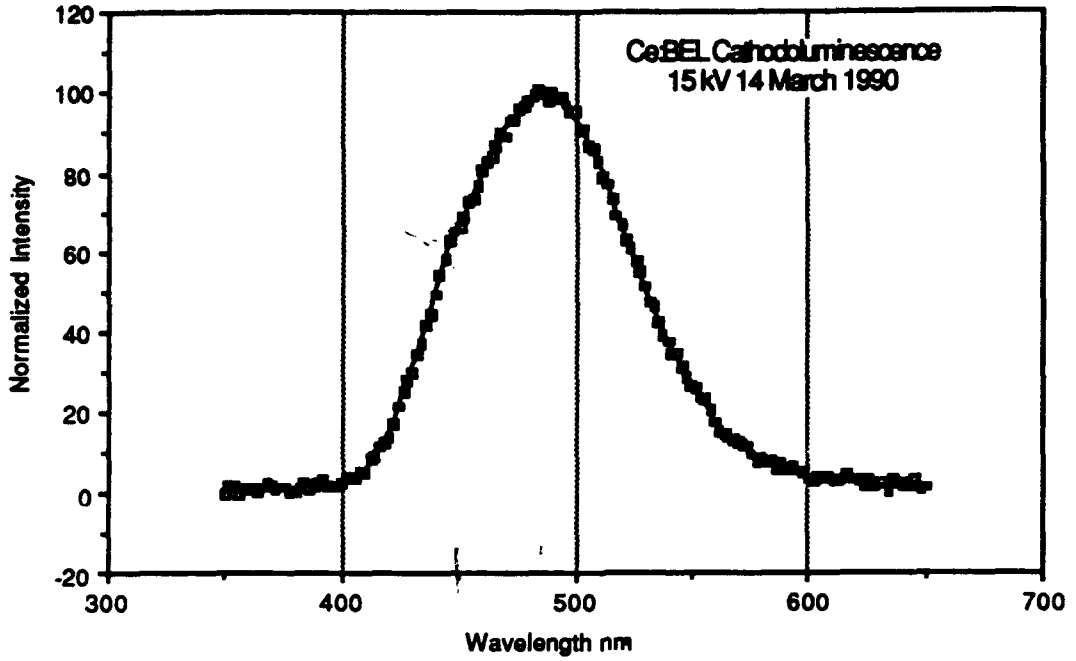

Fig. 13. Cathodoluminescence spectrum of Ce:BEL.

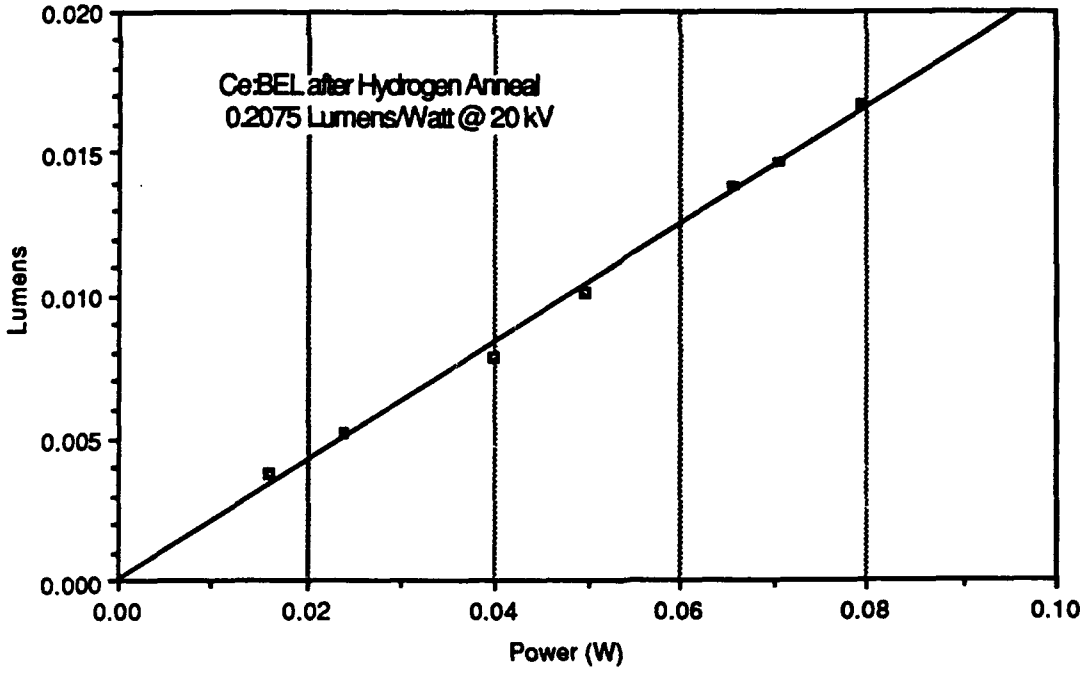

Fig. 14. Cathodoluminescent efficiency of Ce:BEL after hydrogen anneal.

2.6 Red Phosphors

2.6.1 (Ce,Cr):Gadolinium Gallium Garnet Red Phosphor

Epitaxial layers of gadolinium gallium garnet ($Gd_3Ga_5O_{12}$, GGG), Ce:GGG, and (Ce,Cr):GGG were grown on GGG substrates to assess the cathodoluminescent potential of GGG as a cerium host. AT&T Bell Laboratories has reported that the cathodoluminescent efficiency of Tb:GGG is, at best, only 15% that of Tb:YAG, but there has been no comparison of Ce:GGG and Ce:YAG. The efficiency of Ce:GGG was found to be too small for a quantitative measurement, but it was possible to obtain a spectrum showing a broad emission peak at 625 nm, a considerable red-shift from the Ce:YAG peak at 550 nm (fig. 15). (Ce,Cr):GGG had about fifty times the cathodoluminescence of Ce:GGG, but this was due to a broad Cr emission at 725 nm, and the efficiency was still too small to measure (fig. 16).

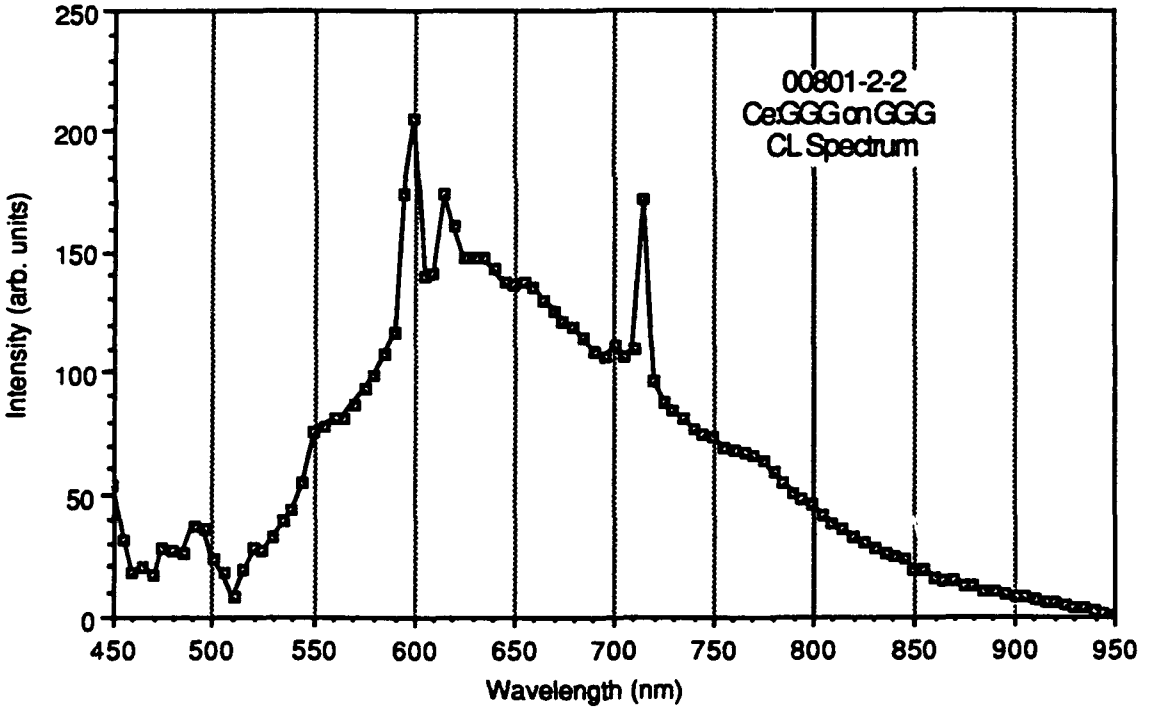

Fig. 15 Cathodoluminescence spectrum of a Ce:GGG epitaxial layer.

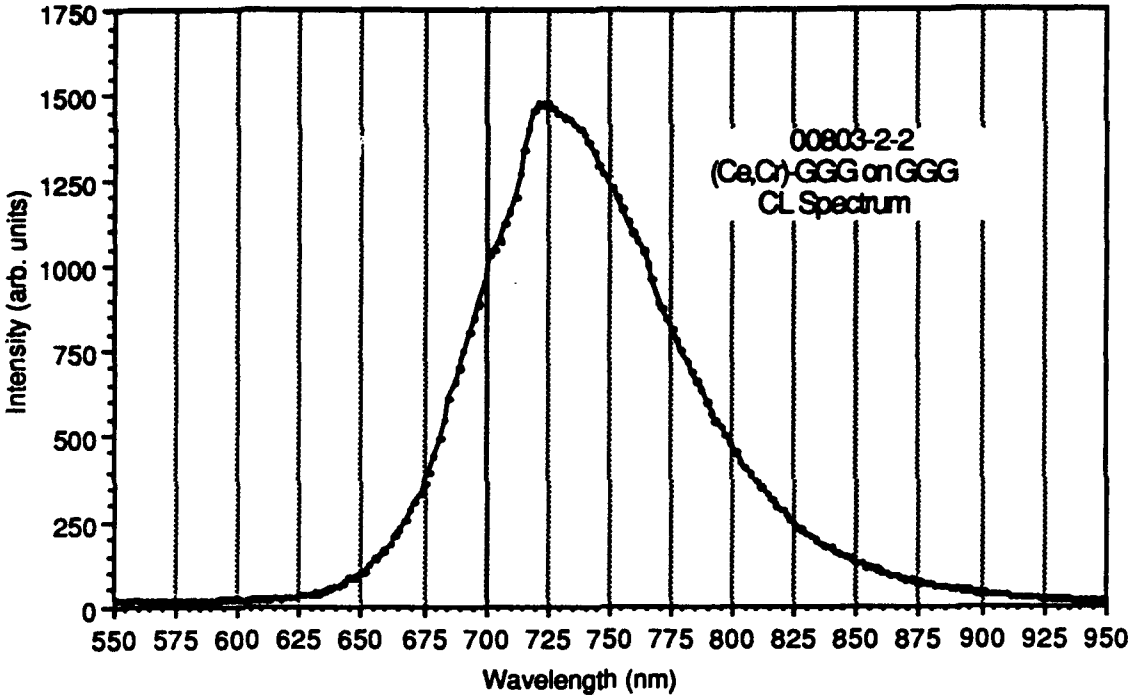

Fig. 16 Cathodoluminescence spectrum of a (Ce,Cr):GGG epitaxial layer.

2.6.2 Redshifted Ce:YAG Phosphor

Red-shifting of the cerium emission in YAG was investigated. A melt was formulated for the epitaxial growth of the cerium-doped garnet Ce:$Y_2Gd_1Al_5O_{12}$ on YAG. The melt composition appears in Table II.

Table II. Melt for the growth of epitaxial layers of Ce:$Y_2Gd_1Al_5O_{12}$, a red-shifted Ce:YAG phosphor, on YAG substrates.

Oxide	Mole Fraction	Moles	Grams per Mole	Grams
PbO	0.89503	3.42367	223.189	764.12800
Al_2O_3	0.02406	0.09202	101.960	9.38236
B_2O_3	0.07459	0.28531	69.620	19.86310
Y_2O_3	0.00411	0.01574	225.810	3.55431
Gd_2O_3	0.00222	0.00848	225.810	3.07237
CeO_2		0.00930	172.120	1.60000
	1.00000	3.82367		801.00000

This composition with a [Gd] concentraion of 0.35 has a lattice constant (measured perpendicularly at the (444) reflection) about 0.4% greater than YAG, which is just under the typical facet limit of 0.5%. Layers of 7.9 μm and 12 μm were faceted after growth, but a 2.2 μm layer grown at 0.44 μm/min was continuous. It is likely that a gadolinium content of 0.25 would give continuous, unfaceted layers under all growth conditions, but with less red-shift. Table III lists the growth conditions for the Ce:$Y_2Gd_1Al_5O_{12}$ phosphor layers grown on YAG substrates. Fig. 17 shows the growth rate dependence on temperature.

Table III. Properties of epitaxial layers of Ce:$Y_2Gd_1Al_5O_{12}$, a red-shifted Ce:YAG phosphor, on YAG substrates.

Layer No.	Growth Temp(°C)	Thickness (μm)	Growth Rate (μm/min)
01017-2-1	1085.8	-7.77*	-1.55*
01017-2-2	1060.5	2.18	0.44
01018-2-1	1052	12.25	1.23
01019-2-1	1061.5	7.92	0.53

* Substrate etched-back.

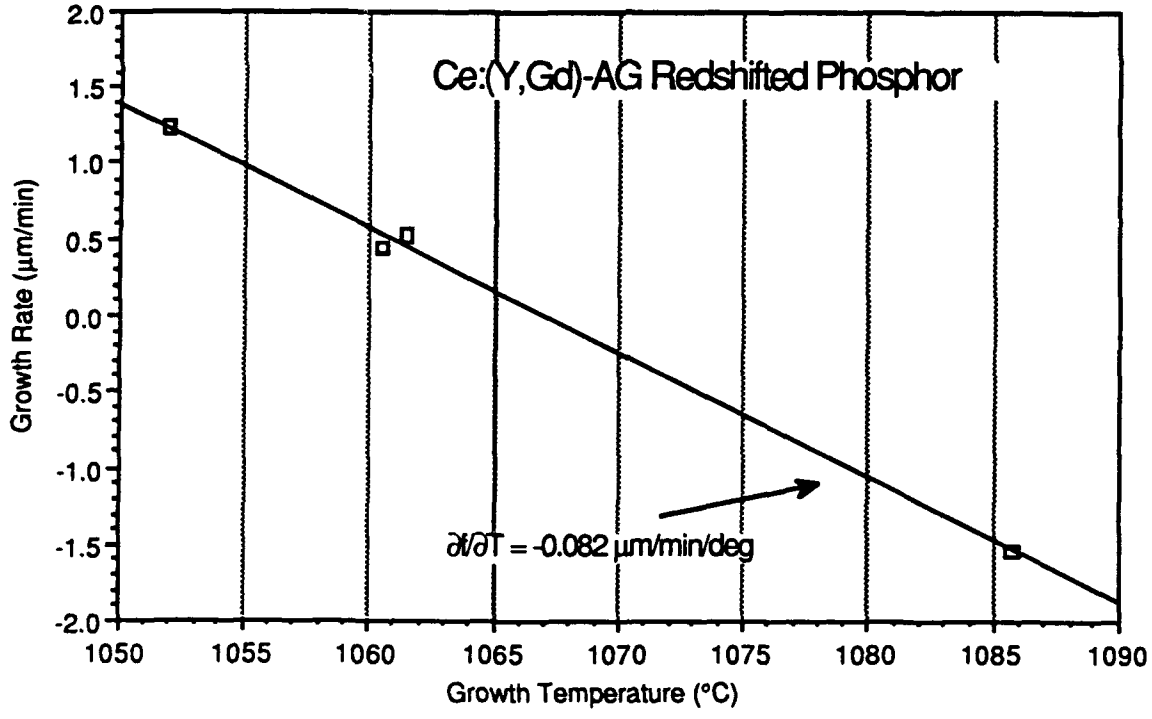

Fig. 17. Growth rate dependence on temperature for Ce:$Y_2Gd_1Al_5O_{12}$ phosphor layers grown on YAG substrates.

Cathodoluminescence measurements (figs. 18-19) showed a red-shift of 20 nm, and, most importantly, almost a two-fold increase in the luminance at the red wavelength of 650 nm. The light output at 650 nm was 31% of the spectral peak for this composition, as compared to 19% for Ce:YAG. The cerium emission in the fully substituted garnet, $Gd_3Al_5O_{12}$, would exhibit a larger red-shift, but it cannot be grown as an epitaxial layer on YAG. Epitaxial layers of Ce:$Gd_3Al_5O_{12}$ could be grown on $Gd_3Al_5O_{12}$, and they would be good red faceplates in color projection systems since they would have a red-shift of about 50 nm.

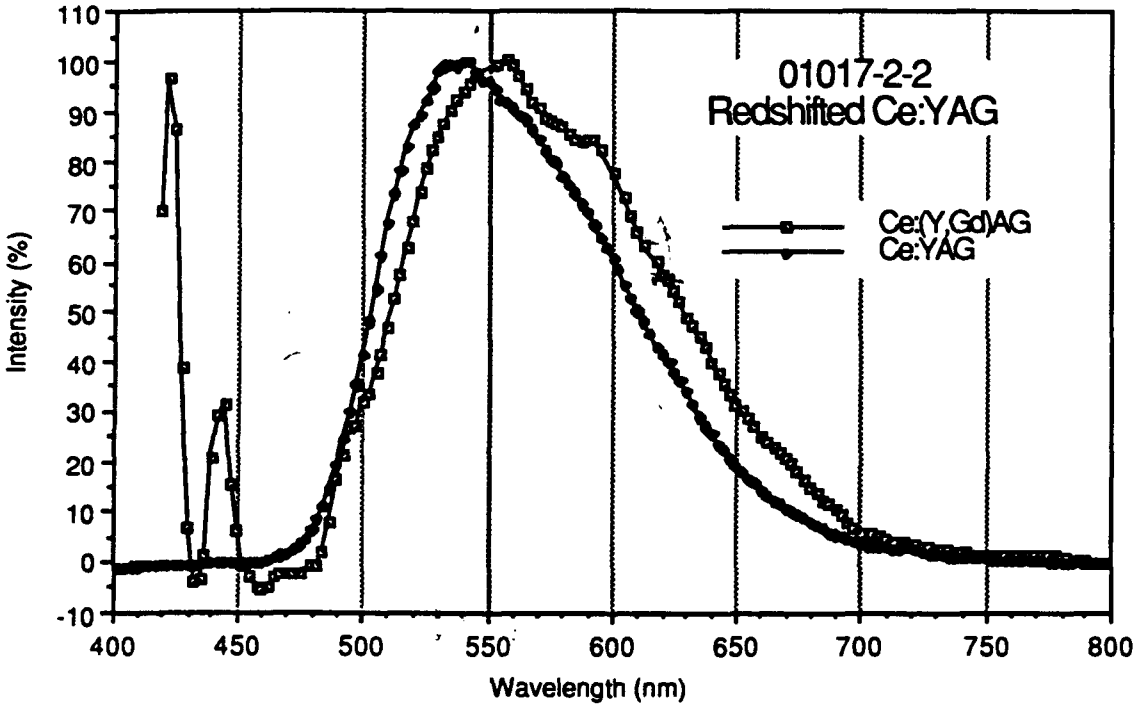

Fig. 18. Cathodoluminescent spectrum of a Ce:$Y_2Gd_1Al_5O_{12}$ phosphor layer grown on a YAG substrate.

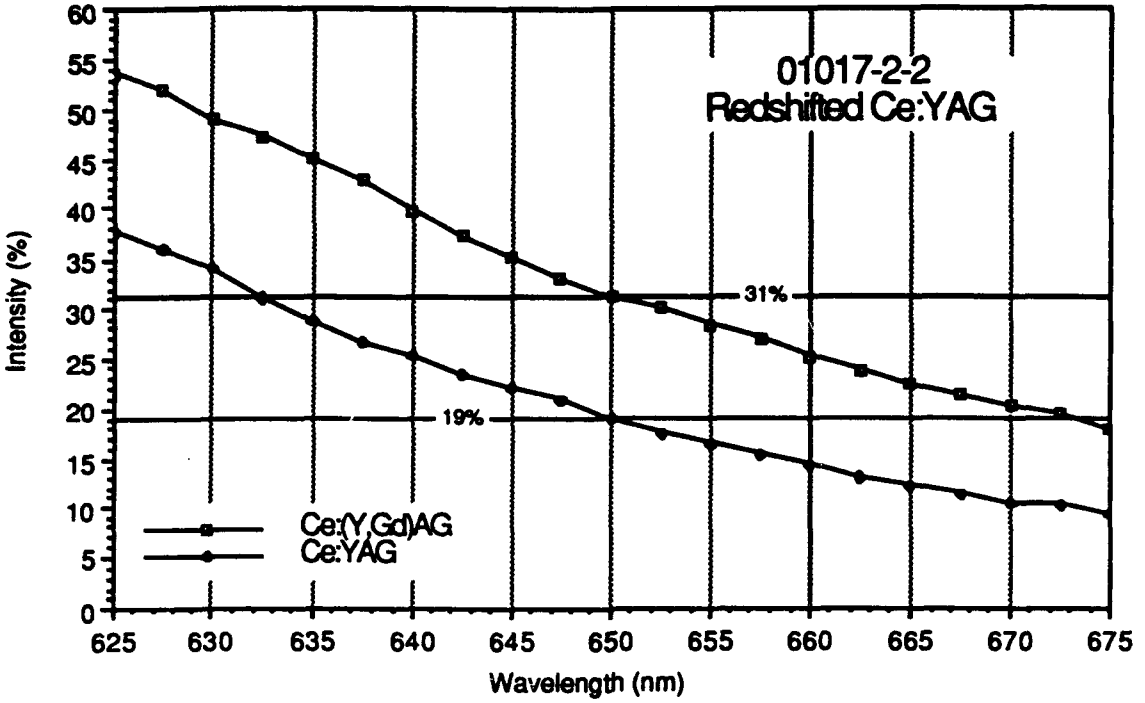

Fig. 19. Cathodoluminescent spectrum (detail) of a Ce:$Y_2Gd_1Al_5O_{12}$ phosphor layer grown on a YAG substrate.

2.7 Data on Delivered Items

A description of the first deliverable item, four non-reticulated Ce:YAG epitaxial phosphor faceplates of one-inch diameter, appears as Table IV.

Table IV. The first deliverable item, four one-inch diameter non-reticulated Ce:YAG epitaxial phosphor faceplates.

Specimen Number	Phosphor Layer Thickness (μm)
00319-2-1	7.0
00320-2-1	17.6
00320-2-2	19.2
00320-2-3	17.1

The second deliverable item consisted of two 2-inch diameter Ce:YAG faceplates (00606-1-1 and 00608-1-1). Thomas Electronics prepared cathode ray tubes for Trident International from these 2-inch Ce:YAG faceplates which were prepared with a facet texture. Their tests at 25 kV anode potential show a line resolution of 0.003 inch at 2.5 watt/in^2 and 0.007 inch at 25 watt/in^2. The resolution is limited by the electron gun rather than the epitaxial faceplate. The measured efficiency at 3.9 watt/cm^2 is 2.7 lumens/watt. This efficiency is higher than what we have measured in our laboratory, and this might be due to the higher beam writing speed (a factor of 2.5) used in the tests at Thomas. Since the Thomas writing speed is closer to the actual operating condition, we may have higher efficiencies than anticipated for our reticulated faceplates.

Trident International has measured the light output of these tubes at anode potentials up to 40 kV. Table V below summarizes their results and extrapolates the performance of three-inch tubes of the same quality. Fig. 20 shows cathodoluminescence data taken by Trident International on a two-inch faceplate.

Table V. Performance data for Ce:YAG faceplates at 40 kV anode potential.

	Demonstrated (2")	Predicted (3")
Faceplate Luminance, fL	62,700	86,750
Faceplate Efficiency, L/W	4.84	4.84
Raster Size, in^2 (cm^2)	1 (6.45)	3.63 (23.4)
Beam Power, W	90	413
Beam Power Density, W/cm^2	14	18
Faceplate Output, L	435	2000

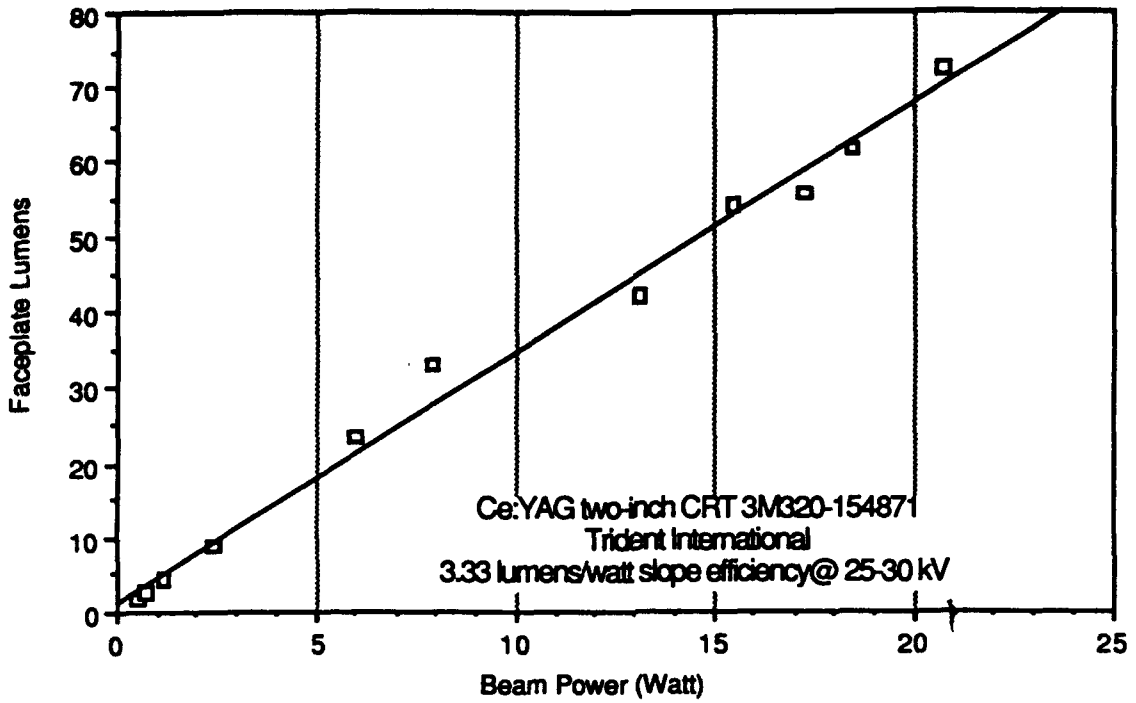

Fig. 20. Cathodoluminescent data for a facet-textured two-inch Ce:$Y_3Al_5O_{12}$ epitaxial phosphor faceplate.

Six reticulated 3-inch epitaxial phosphor faceplates of Ce:YAG were shipped to the NTSC to satisfy the remainder of the deliverable items. One of these faceplates broke in transit, and it was replaced. Table VI lists the shipped faceplates, and figs. 21-34 show the properties of these faceplates.

Table VI. The final deliverable item, six 3-inch diameter reticulated Ce:YAG epitaxial phosphor faceplates. Data for seven faceplates are shown.

Specimen Number	Phosphor Layer Thickness (μm)	
01214-1-1	25	
10109-1-2	17	
10122-1-2	16	
10123-1-1	11	
10122-1-3	15	(damaged)
10212-1-2	17	
10214-1-1	12	

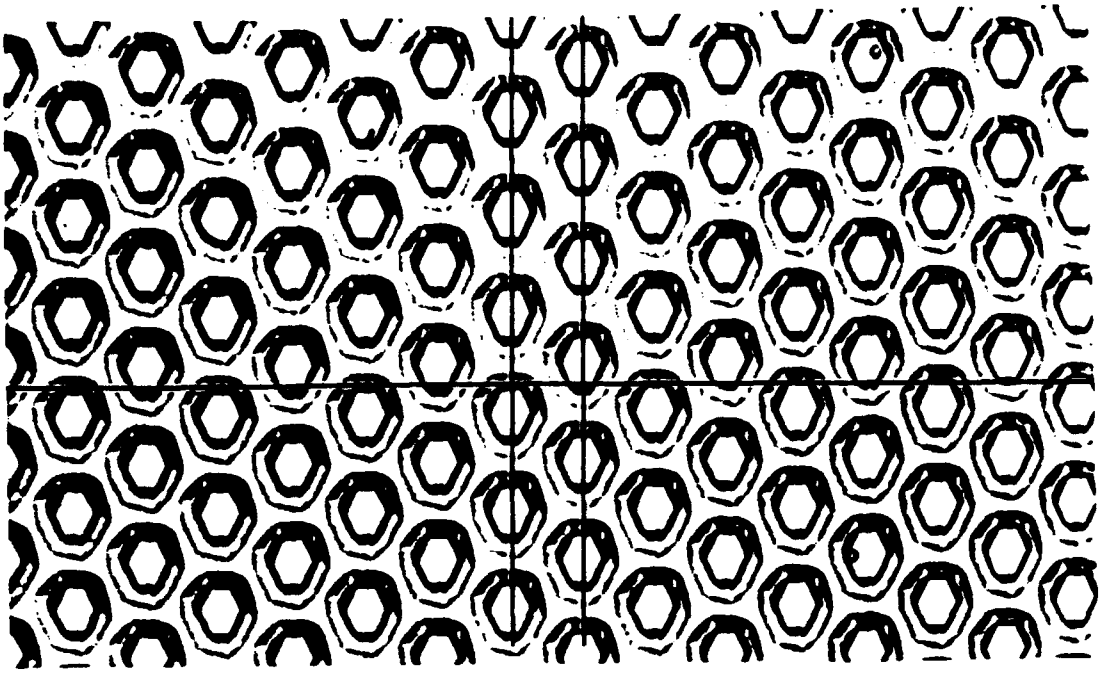

Fig. 21. Reticulated surface of the three-inch Ce:$Y_3Al_5O_{12}$ epitaxial phosphor faceplate number 01214-1-1.

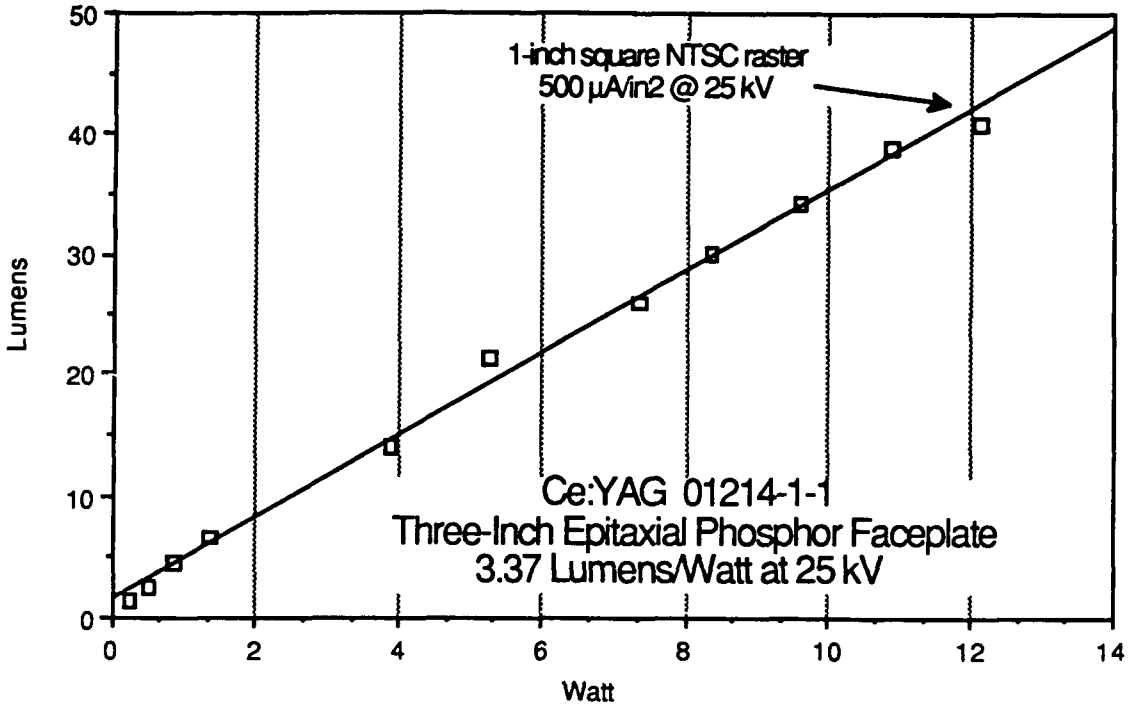

Fig. 22. Cathodoluminescence efficiency at 25 kV for the three-inch Ce:$Y_3Al_5O_{12}$ epitaxial phosphor faceplate number 01214-1-1.

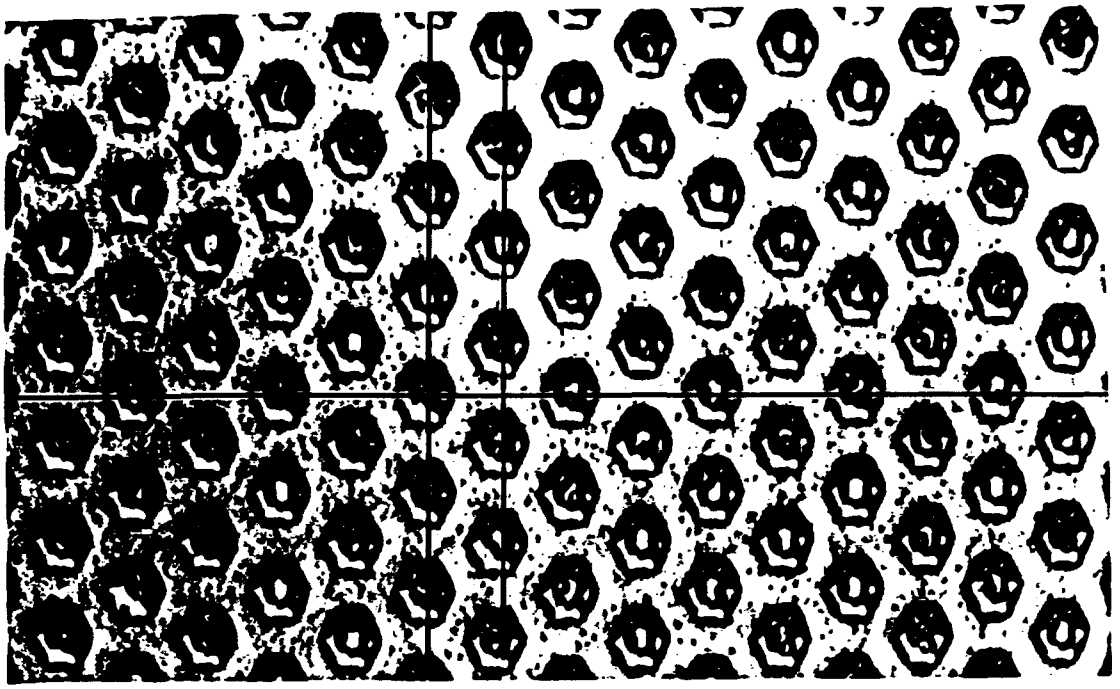

Fig. 23. Reticulated surface of the three-inch Ce:$Y_3Al_5O_{12}$ epitaxial phosphor faceplate number 10109-1-2.

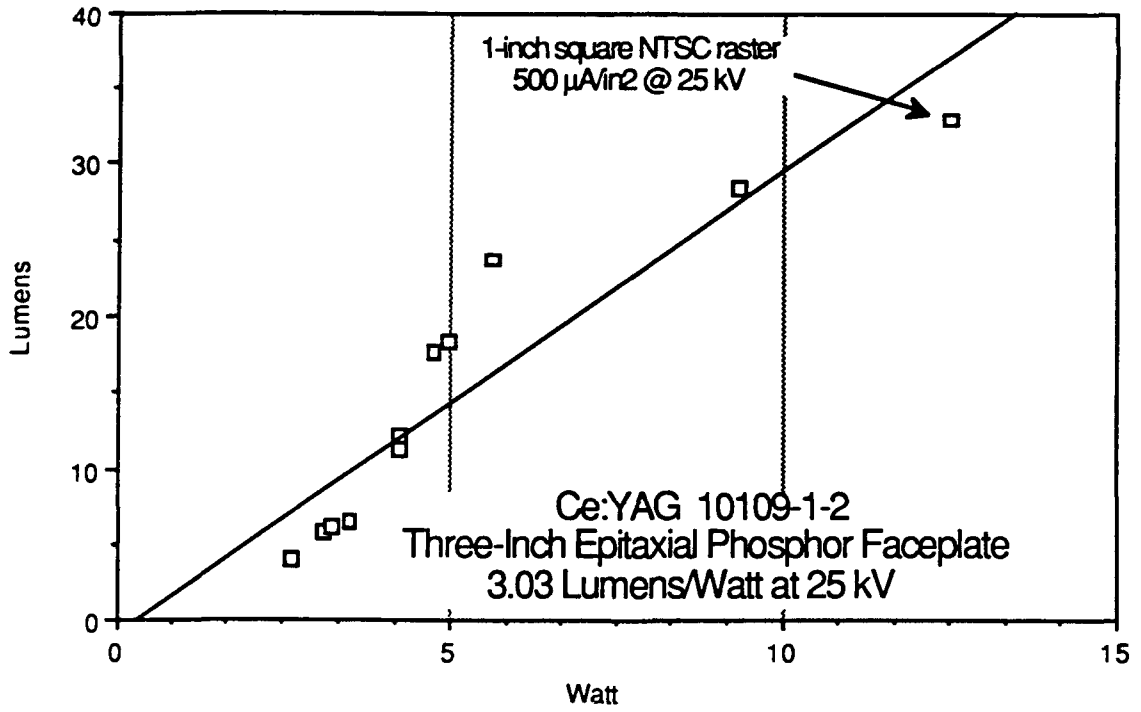

Fig. 24. Cathodoluminescence efficiency at 25 kV for the three-inch Ce:$Y_3Al_5O_{12}$ epitaxial phosphor faceplate number 10109-1-2.

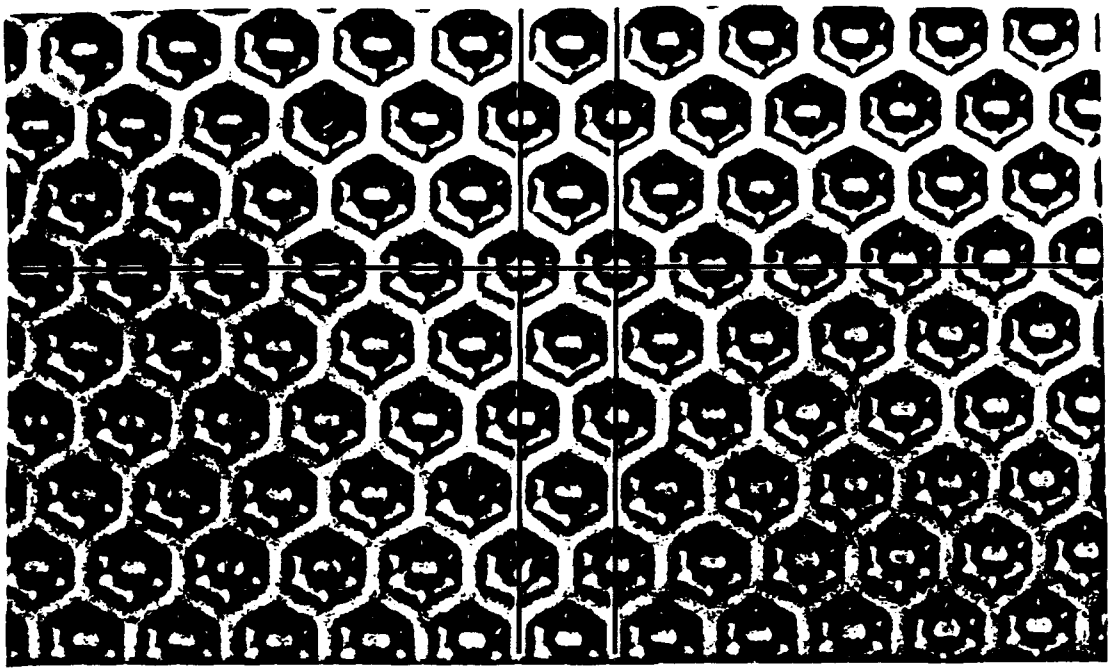

Fig. 25. Reticulated surface of the three-inch Ce:$Y_3Al_5O_{12}$ epitaxial phosphor faceplate number 10122-1-2.

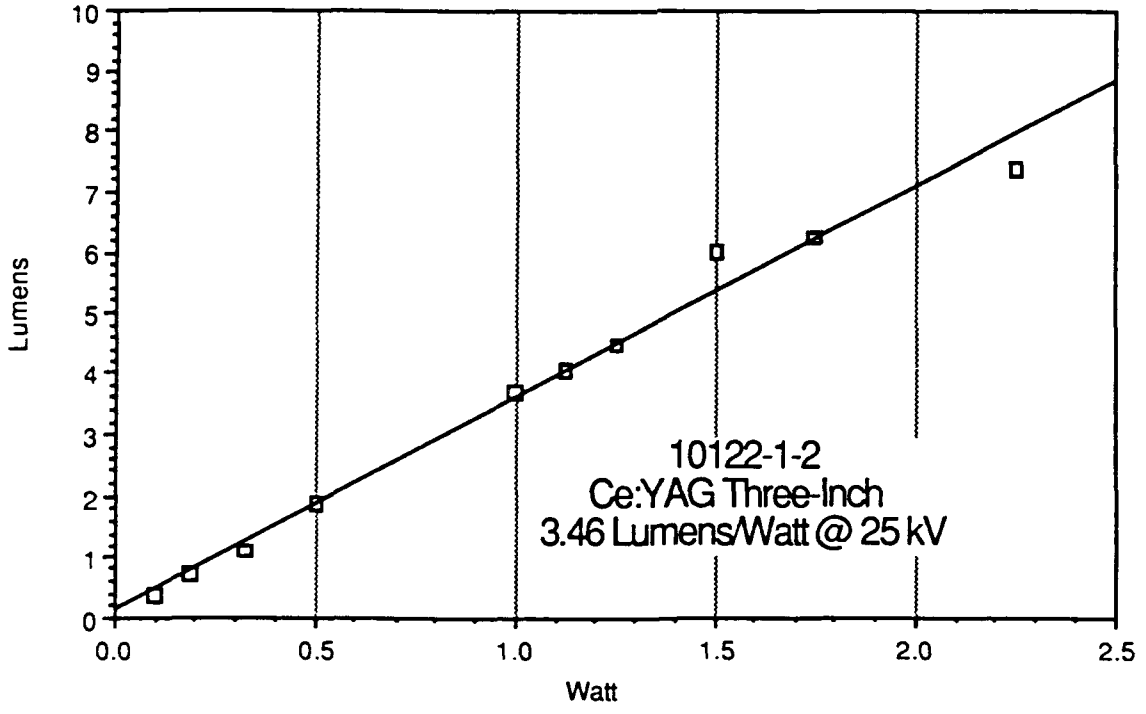

Fig. 26. Cathodoluminescence efficiency at 25 kV for the three-inch Ce:$Y_3Al_5O_{12}$ epitaxial phosphor faceplate number 10122-1-2.

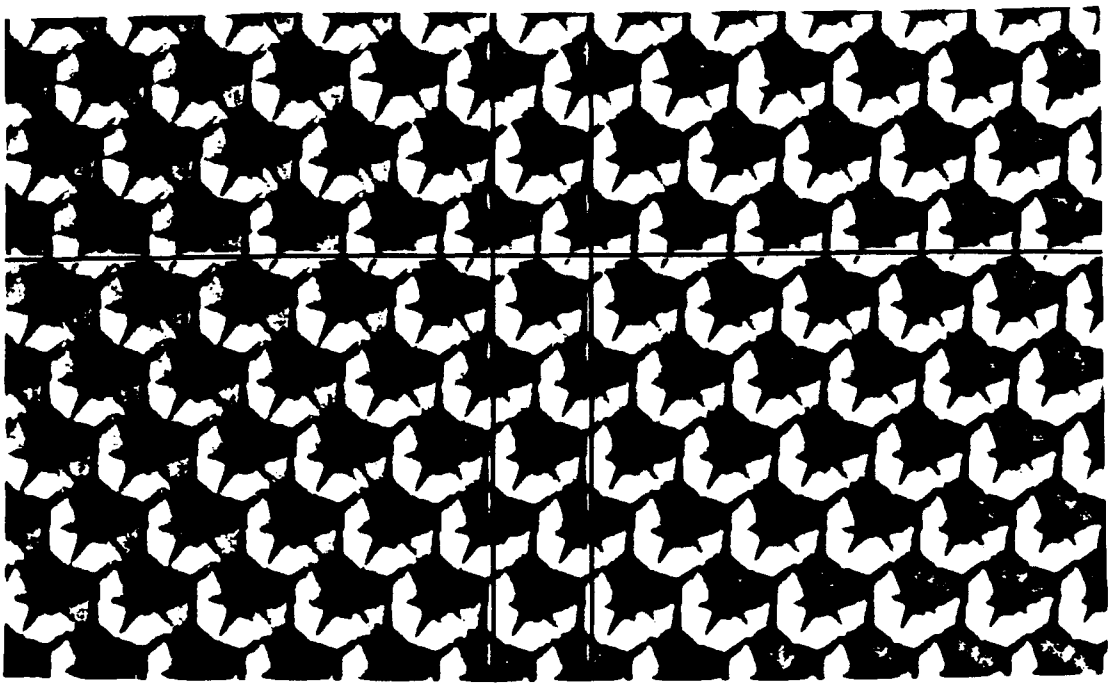

Fig. 27. Reticulated surface of the three-inch Ce:$Y_3Al_5O_{12}$ epitaxial phosphor faceplate number 10123-1-1.

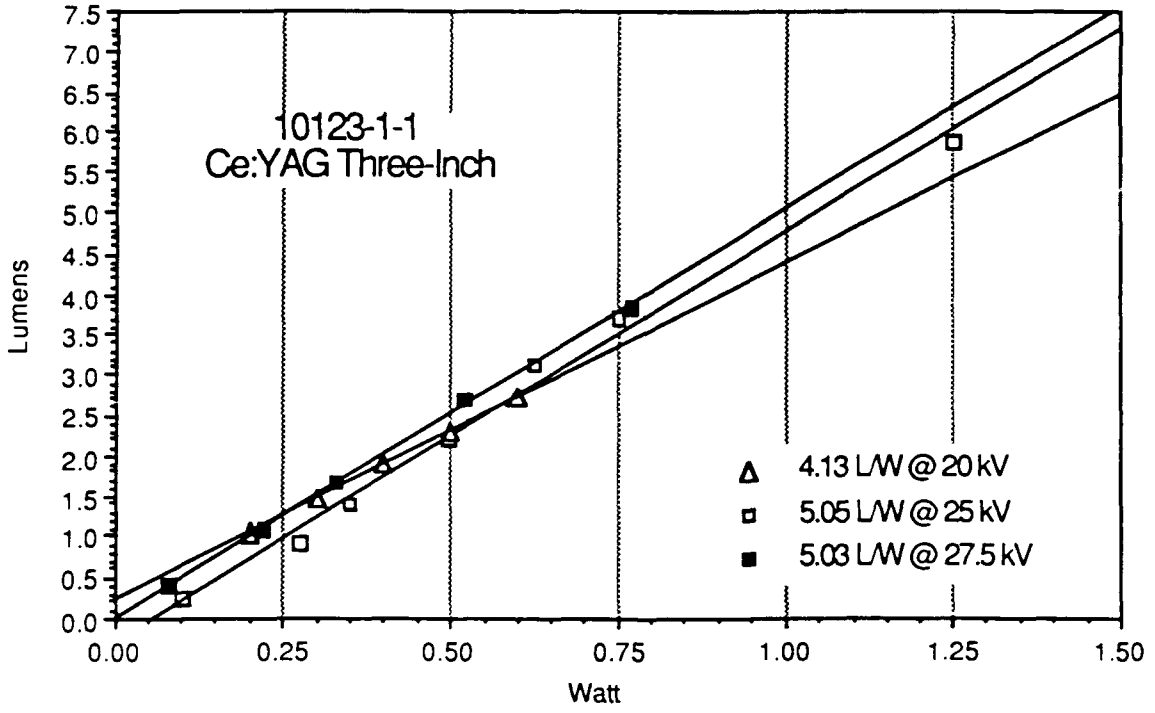

Fig. 28. Cathodoluminescence efficiency at 25 kV for the three-inch Ce:$Y_3Al_5O_{12}$ epitaxial phosphor faceplate number 10123-1-1.

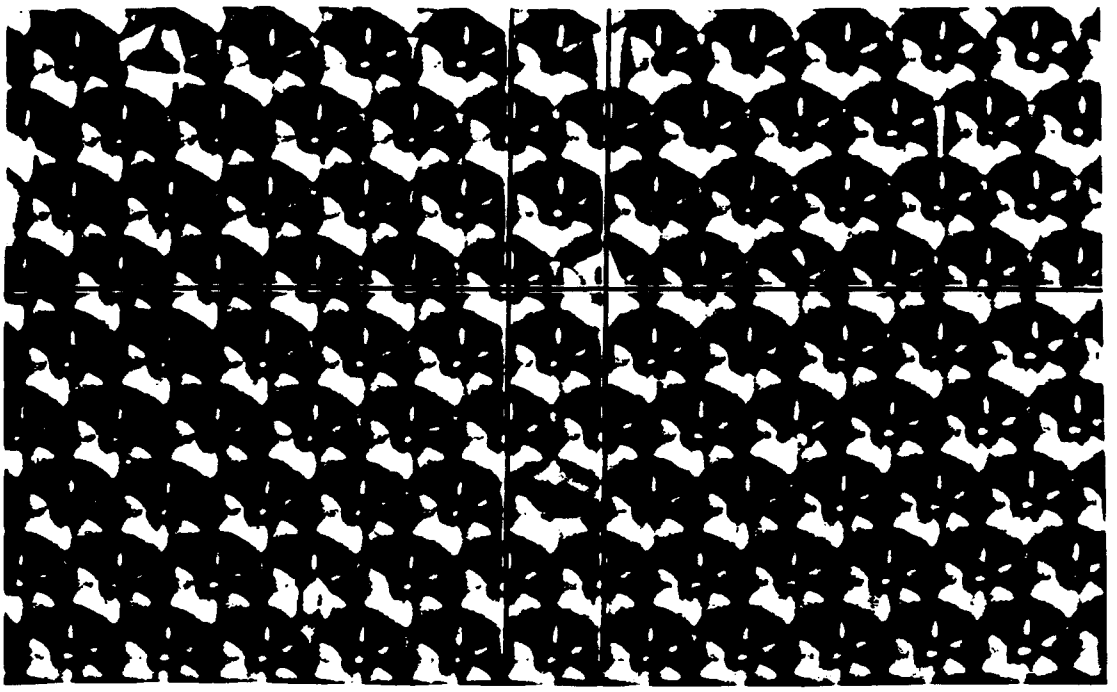

Fig. 29. Reticulated surface of the three-inch Ce:$Y_3Al_5O_{12}$ epitaxial phosphor faceplate number 10122-1-3.

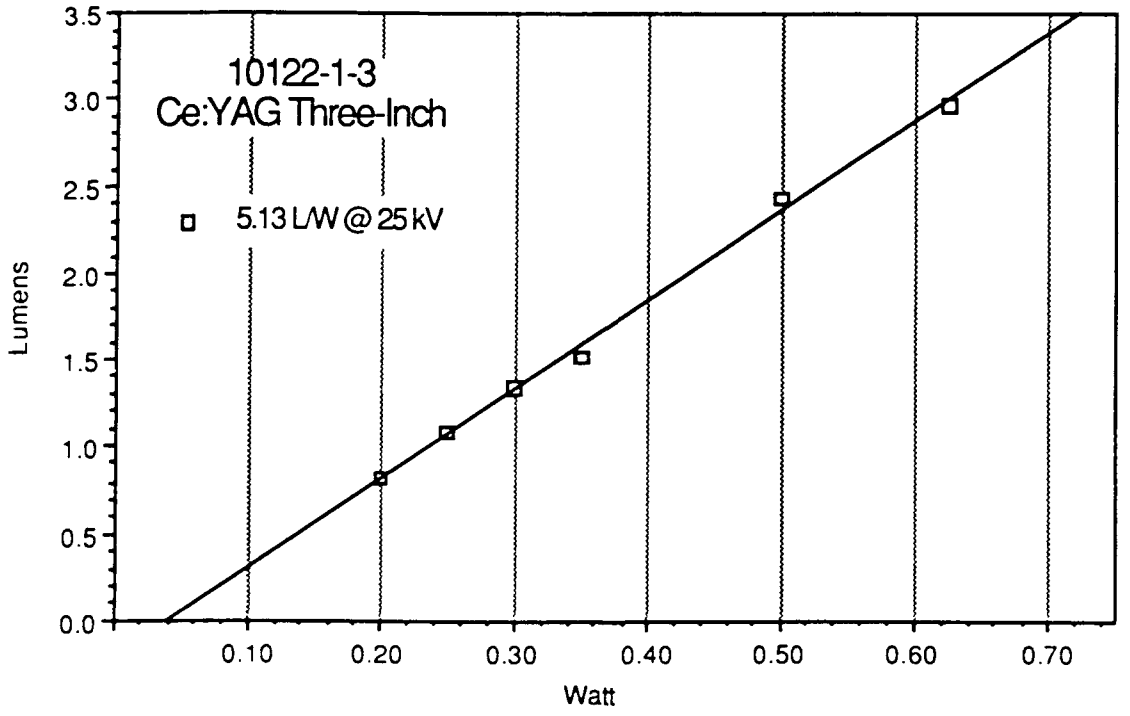

Fig. 30. Cathodoluminescence efficiency at 25 kV for the three-inch Ce:$Y_3Al_5O_{12}$ epitaxial phosphor faceplate number 10122-1-3.

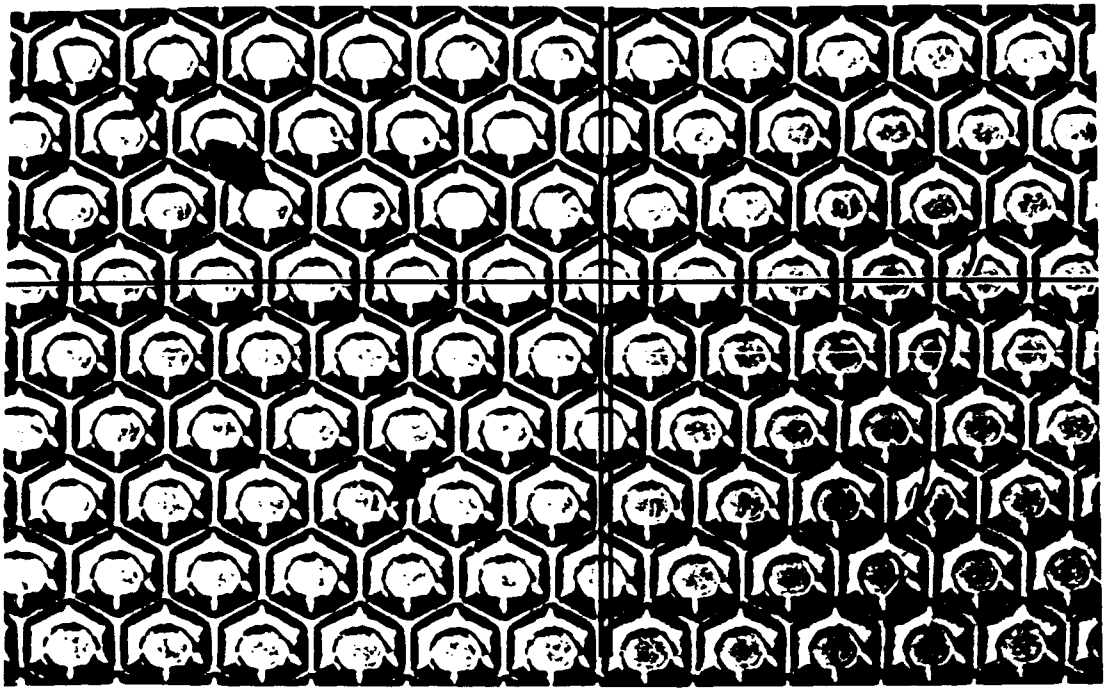

Fig. 31. Reticulated surface of the three-inch Ce:$Y_3Al_5O_{12}$ epitaxial phosphor faceplate number 10212-1-2.

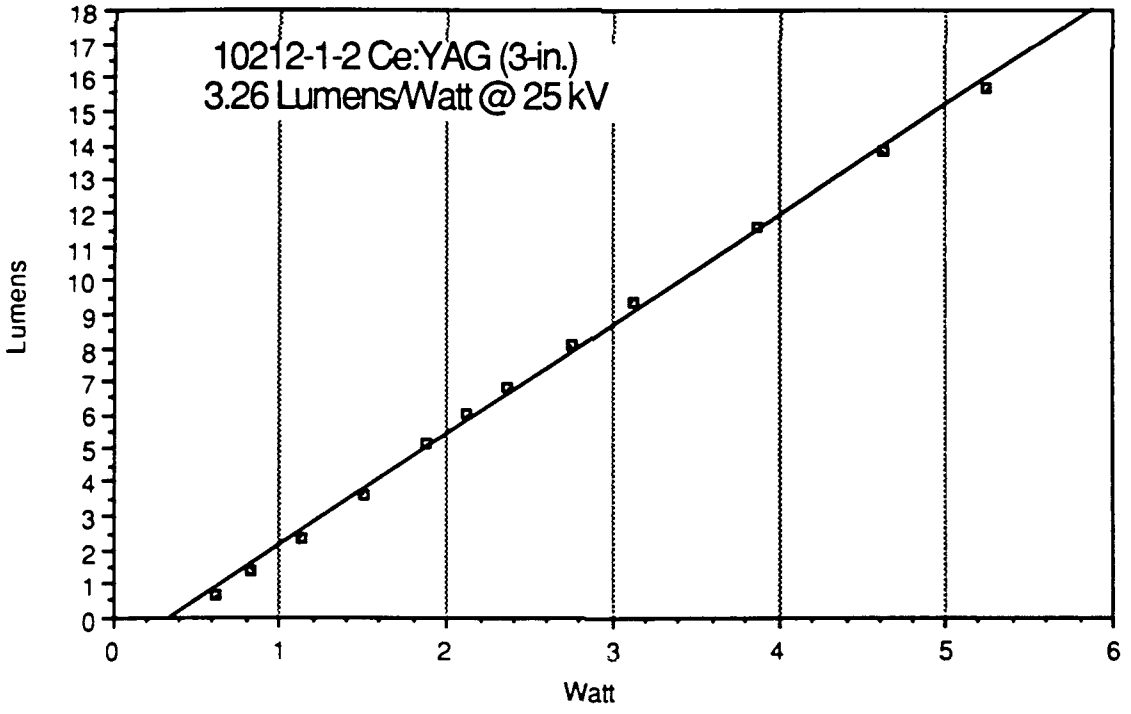

Fig. 32. Cathodoluminescence efficiency at 25 kV for the three-inch Ce:$Y_3Al_5O_{12}$ epitaxial phosphor faceplate number 10212-1-2.

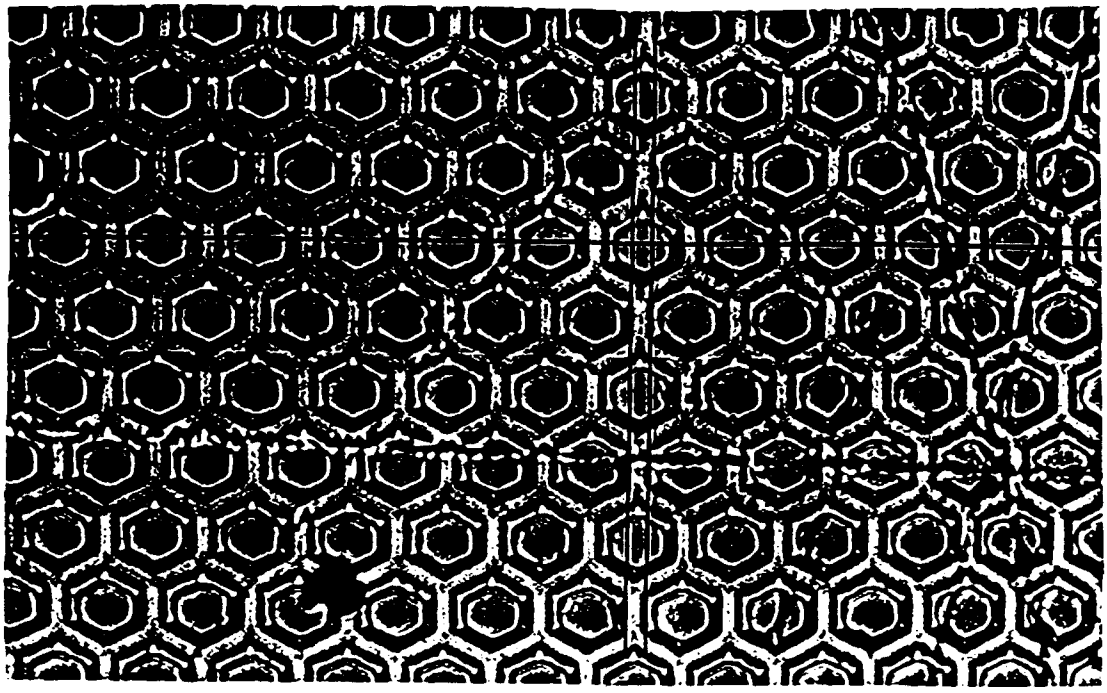

Fig. 33. Reticulated surface of the three-inch Ce:$Y_3Al_5O_{12}$ epitaxial phosphor faceplate number 10214-1-1.

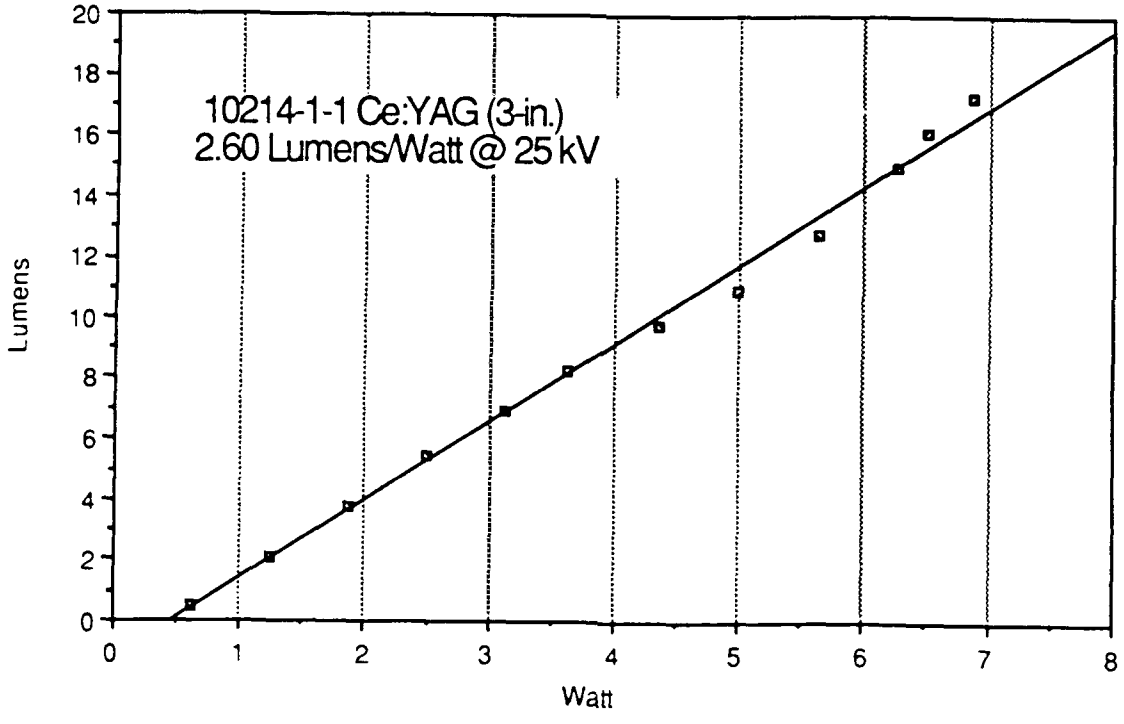

Fig. 34. Cathodoluminescence efficiency at 25 kV for the three-inch Ce:$Y_3Al_5O_{12}$ epitaxial phosphor faceplate number 10214-1-1.

An analysis of cathodoluminescent efficiency of reticulated faceplates (fig. 35) shows that reticulation is most effective when there is a minimum in the ratio of the mesa top to bottom area. This ratio is one for an unreticulated faceplate, and zero for a reticulation which is a pointed pyramid, as for specimen 10122-1-3. This pointed reticulation, however, gives "ghost" images of the raster in the six-fold symmetry of the reticulation, so that there appears to be a trade-off between efficiency and contrast in the final images. This "ghosting" effect must still be quantified.

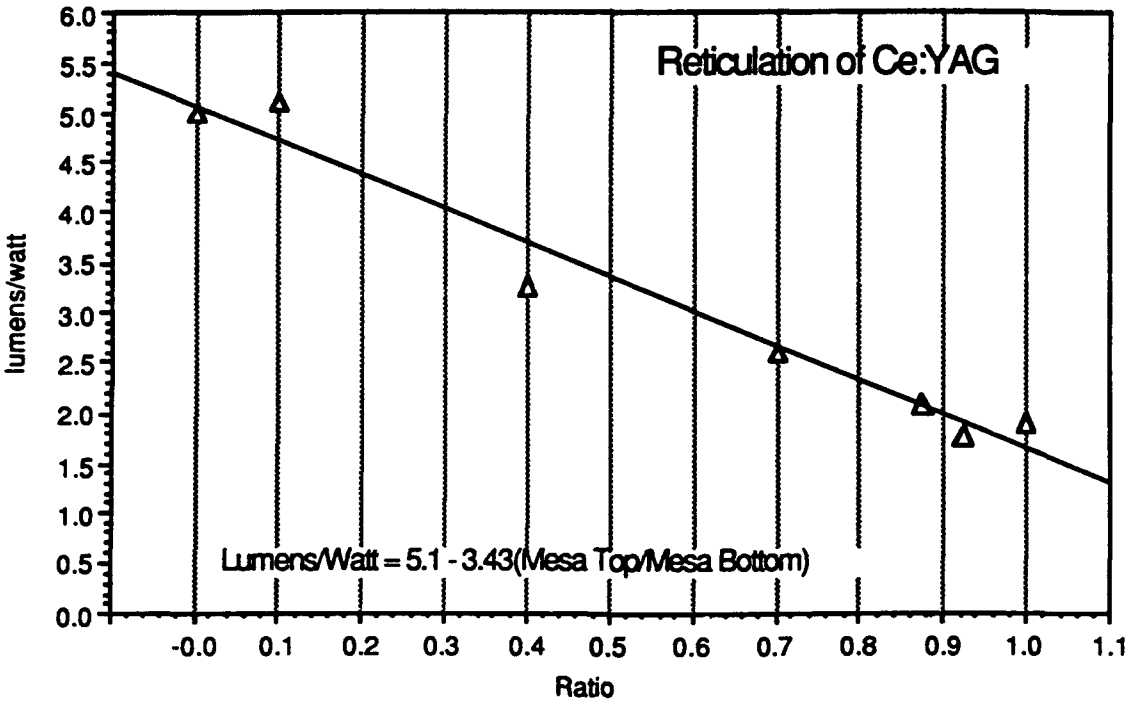

Fig. 35. Cathodoluminescence efficiency at 25 kV for the three-inch Ce:$Y_3Al_5O_{12}$ epitaxial phosphor faceplates as a function of reticulation depth.

3. RECOMMENDATIONS FOR FURTHER WORK.

3.1 High Luminance Reticulated Faceplates

Ce:YAG epitaxial phosphor faceplates are capable of 2000 lumens light output in either their reticulated or facet-textured form in a 2.75-inch diagonal raster. Higher light outputs can be obtained from larger diameter faceplates, but the largest avialable YAG crystals are presently three-inches in diameter. Thus, crystal growth of four-inch YAG and epitaxy on these crystals would be suitable areas for research.

Wafer flatness is a requirement for photolithographic reticulation over a large diameter faceplate. Epitaxty requires a surface which is free of even the smallest scratch or defect. Thus, polishing of YAG wafers to higher flatness and perfection would be a suitable area for research.

The reticulation process used for this study involved etching in hot phosphoric acid. A rapid etching rate had to be used to effect the reticulation before the etching mask was dissolved. This technique was marginally successful, and defects were introduced into the faceplate as the mask was undercut in some areas. Further research on alternative masking materials and etching methods would be fruitful.

Reticulation is most effective when there is a minimum in the ratio of the mesa top to bottom area, but this pointed reticulation gives "ghost" images of the raster in the six-fold symmetry of the reticulation. This "ghosting" effect must still be quantified.

3.2 Red/Green/Blue Phosphors.

Ce:$Gd_3Al_5O_{12}$ (Ce:GdAG, red), Ce:$Y_3Al_5O_{12}$ (Ce:YAG, green), and Ce:$La_2Be_2O_5$ (Ce:BEL, blue), appear to be an appropriate trio of epitaxial phosphors for a high intensity color projection display. Ce:BEL has not as yet been bonded to a CRT neck assembly, so that its suitability as a faceplate material is still unknown. Research on such bonding would be appropriate.

The growth of large crystals of $Gd_3Al_5O_{12}$ as substrates for epitaxial red phosphor faceplates would be a suitable area for research.

3.3 Summary Recommendations.

Crystal growth of four-inch diameter YAG, polishing of these YAG wafers to higher flatness and perfection, and epitaxy on these wafers would be suitable areas for research. Further research on alternative masking materials and etching methods, and quantification of the reticulation "ghosting effect, is also required.

Ce:$Gd_3Al_5O_{12}$ (Ce:GdAG, red), Ce:$Y_3Al_5O_{12}$ (Ce:YAG, green), and Ce:$La_2Be_2O_5$ (Ce:BEL, blue), appear to be an appropriate trio of epitaxial phosphors for a high intensity color projection display. The growth of large crystals of $Gd_3Al_5O_{12}$ as substrates for epitaxial red phosphor faceplates would be a suitable area for research.

4.0 ACKNOWLEDGEMENTS

Much of the epitaxial processing and acid etching was done by E.M. Porbansky. The photolithography was performed by K.K. Wong and M. Long. A. Ribaudo prepared the scanning electron micrographs. Rhenium deposition was by G. West. J. Fleming fabricated the large diameter YAG wafers. The Ce:BEL crystal was grown by M. Long.

5.0 REFERENCES.

1. M.W. van Tol and J. van Esdonk, IEEE Trans. Electron Devices **ED-30**, 193 (1983).

2. J.M. Robertson and M.W. van Tol, Appl. Phys. Lett. **37**, 471 (1980).

3. W.F. van der Weg and M.W. van Tol, Appl. Phys. Lett. **38**, 705 (1981).

4. J.M. Robertson and M.W. van Tol, Phys. Stat. Sol. (a) **63**, K59 (1981).

5. G.W. Berkstresser, et al., J. Elctrochem. Soc. **135**, 1302 (1988).

6. U. Levy and H.H. Yaffe, SID International Symposium Digest, 1984, p. 336 ff.

7. H.J. Levinstein, et al., Appl. Phys. Lett. **19**, 486 (1971).

8. D.M. Gualtieri, J. Appl. Phys. **50**, 2170 (1979).

9. D.M. Gualtieri, P.F. Tumelty, and M.A. Gilleo, J. Appl. Phys. **52**, 2335 (1981).

10. D.M. Gualtieri and P.F. Tumelty, J. Appl. Phys. **53**, 2489 (1982).

11. J.A. Burton, R.C. Prim, and W.P. Slichter, J. Chem. Phys. **21**, 1987 (1953).

12. P.F. Bongers, et al., U.S. Patent No. 4,298,820 (1981).

13. D.M. Gualtieri, et al., U.S. Patent No. 4,728,178 (1988).

14. D.T.C. Huo and T.W. Hou, J. Electrochem. Soc. **133**, 1492 (1986).

15. B. Strocka, J. Appl. Phys. **60**, 2977 (1986).

16. C.F. Cline and R.C. Morris, U.S. Patent No. 3,866,142 (1975).

6.0 APPENDICES

6.1 Paper Prepared for 1991 International Display Research Conference (San Diego, October 16, 1991).

The following pages contain the paper, High Luminance Monochrome Faceplates for Compact Projection Dispalys, by D.M. Gualtieri, H. van de Vaart, T. St. John, and R. C. Hebb, which will be presented at the 1991 International Display Research Conference in San Diego CA, on October 16, 1991.

HIGH LUMINANCE MONOCHROME FACEPLATES FOR COMPACT PROJECTION DISPLAYS

D.M. Gualtieri and H. van de Vaart
Allied-Signal Inc., Research and Technology
P.O. Box 1021, Morristown, NJ 07962-1021

T. St. John
Trident International, Inc., Central Florida Research Park
3290 Progress Drive, Suite 155, Orlando, Florida 32826

R. C. Hebb
Code 253, Naval Training Systems Center
12350 Research Parkway, Orlando, Florida 32826-3224

Summary

Epitaxial phosphor faceplates of cerium activated yttrium aluminum garnet (YAG) phosphor (P-46) have been prepared on single crystal YAG faceplates up to three inches in diameter. Photolithographic reticulation of the faceplates was performed to increase the external efficiency of the epitaxial phosphor. A 1 x 1 inch raster on a two-inch diameter faceplate has produced a faceplate luminance of 62,700 fL with a 40 kV excitation at an efficiency of 4.84 lumens/watt. This is 435 lumens from a one square-inch raster at 90 W/in^2 excitation. Extrapolated performance of 2000 lumens is expected from three inch diameter (2.75 inch diagonal raster) faceplates.

Introduction.

Epitaxial phosphors of Ce:YAG (P-46) on single crystal faceplates of YAG have properties which are suitable for projection CRTs. The cathodoluminescent efficiency of Ce:YAG, about 2 Lumens/Watt in a single crystal faceplate at 25 kV excitation, is low compared with other phosphors, but the luminance of Ce:YAG is linearly proportional to excitation power and does not saturate. M.W. van Tol and J. van Esdonk [1] operated epitaxial phosphor faceplates at power levels of 10 W/cm^2. J.M. Robertson and M.W. van Tol [2] tested epitaxial phosphor faceplates of Ce:YAG, Tb:YAG, and Eu:YAG at power levels to 10^4 W/cm^2. They found that Ce:YAG is linear to the highest power levels, but that the light output of Tb:YAG and Eu:YAG saturates at power levels above 1 W/cm^2. Thus, Ce:YAG is preferred as a high intensity monochrome phosphor. This saturation arises from excited state absorption and cross-relaxation processes [3], and it is a general feature of many phosphors, for example Mn:$BaAl_{12}O_{19}$ [4]. AT&T Bell Laboratories has developed a modified terbium phosphor composition, $Tb_{0.2}Y_{0.1}Lu_{2.7}Al_3Ga_2O_{12}$, with improved saturation characteristic [5]. This phosphor has shown a brightness of 4,800 fL in a standard 60 Hz, 525-line, 2:1 interlace 2.5-inch by 1.7-inch raster excited with a 25 kV, 2 mA beam. This is 140 lumens at 50 watts excitation, or 2.8 Lumens/Watt at an excitation power density of 1.82 W/cm^2.

Robertson and van Tol [2] have investigated the growth of epitaxial phosphors on various crystal faces of YAG. They found that (111)-oriented substrates give phosphors of the highest efficiency, and that (110)-, (211)-, and (100)-orientations yield phosphors of slightly lower efficiency.

Levy and Yaffe [6] have shown that the thermal quenching temperature of Ce:YAG is about 400 °C, and that a decrease in light output is first evident at 200 °C. They determined that it is safe to operate a single crystal Ce:YAG faceplate at thermal gradients up to 150 °C/inch, and that a three inch diameter epitaxial phosphor faceplate could be operated at 25 watts excitation with no cooling. Since the thermal conductivity of YAG is high, forced-air cooling is very effective at high excitation levels. Forced-air cooling can extract about 60% of the heat, radiation can dissipate about 20% of the heat, and conduction down the neck can dissipate the remaining 20%. In the present study, however, a liquid coolant lens cell was used for faceplate power dissipation. Coulombic degradation does not occur in epitaxial phosphor faceplates, whereas 0.5 W/cm^2 is the conventional limit for projection CRTs. For example, operation of P53 at 0.5 W/cm^2 results in an extremely short lifetime.

The major factor limiting the external efficiency of Ce:YAG phosphors is the high refractive index of the YAG substrate (1.84), which allows only rays less than a critical angle of 33° to be emitted from the faceplate. The remaining rays are waveguided to the edges, so that only 16% of the cathodoluminescence is emitted from the faceplate. Reticulation, that is patterning the phosphor into shapes which reflect more rays into the critical cone, can significantly increase the external efficiency of epitaxial phosphor faceplates. Fig. 1 schematically illustrates the waveguiding effect, and fig. 2 illustrates the role of the reticulation in reflecting a greater fraction of the cathodoluminescence into the critical cone.

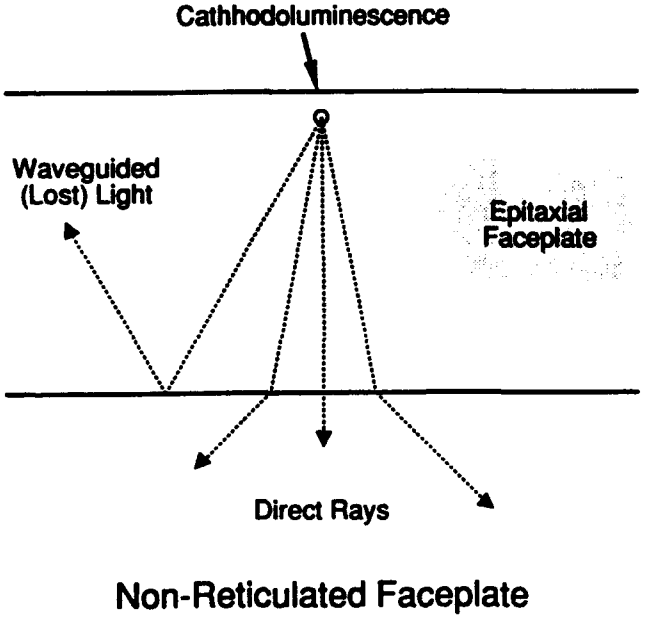

Fig. 1. Schematic illustration of waveguiding effect in single crystal epitaxial phosphor faceplates.

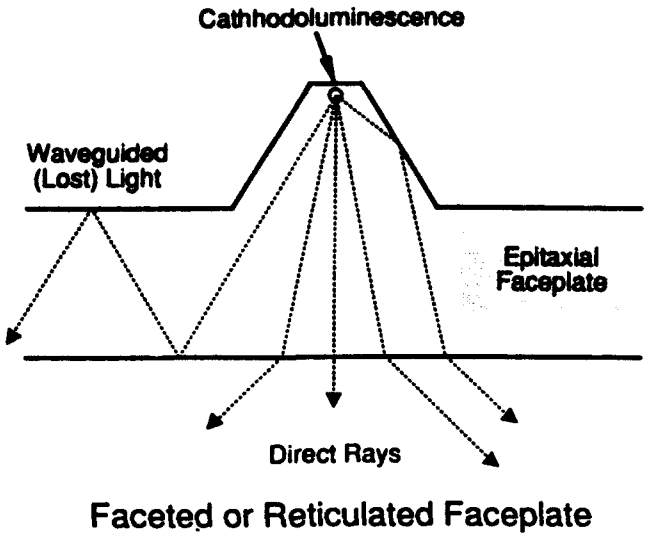

Fig. 2. Schematic illustration of the role of reticulation in reflecting a greater fraction of the cathodoluminescence into the critical cone of 33° half-angle in YAG faceplates.

P.F. Bongers, et al. [7], have etched grooves in the phosphor to increase the external efficiency. D.M. Gualtieri, et al. [8] have used a faceted epitaxial layer for the same purpose. D.T.C. Huo and T.W. Hou [9], have used photolithographic techniques to pattern a Ce:YAG epitaxial phosphor faceplate with an array of rectangular mesas. They were able to increase the external efficiency by a factor of three. A truncated cone geometry can increase the external efficiency by a factor of 5.5, if such a shape can be formed in the phosphor layer. Such reticulation will not limit the faceplate resolution if a small mesa size is used.

Epitaxial Phosphor Deposition.

A procedure for the epitaxial growth of YAG by liquid phase epitaxy is contained in ref.[10]. A summary of this process as applied to the epitaxial deposition of Ce:YAG phosphor on YAG faceplates follows.

A single crystal wafer of YAG is prepared from a cylindrical crystal boule by slicing, lapping, and polishing. Polishing proceeds through finer grit, and a final polish is done with a colloidal silica mixture, as is common for the polish of garnet crystal wafers. The wafer is carefully cleaned and mounted in a substrate holder which allows rotation and translation. Epitaxy is achieved by dipping the substrate into a platinum crucible holding the molten constituent oxides of the Ce:YAG composition in the proportions listed in Table I. The melt composition of Table I can be specified by the parametric convention established by Blank, *et al.* [11], as follows:

$R_1 = Al_2O_3/Y_2O_3 = 3.8$
$R_3 = PbO/2B_2O_3 = 6.0$
$R_4 = (Y_2O_3 + Al_2O_3)/(Y_2O_3 + Al_2O_3 + B_2O_3 + 1/2PbO) = 0.04.$

These powders are heated to 1050 °C, a temperature well above the melting point of the mixture, and allowed to "soak" for 24 hours. The melt is stirred for one hour at 1050 °C and 200 rev/min just before each layer growth. After stirring, the melt is cooled to the growth temperature of about 980°C in 45 minutes (melt saturation occurs at about 990°C).

Table I. Melt for the growth of epitaxial layers of Ce:YAG on YAG substrates at 980 °C. Note that cerium oxide, the dopant, is not included in the mole fraction calculation.

Oxide	Mole Fraction	Moles	Grams
PbO	0.90282	3.44684	769.299
Al_2O_3	0.01737	0.06632	6.762
B_2O_3	0.07524	0.28724	19.998
Y_2O_3	0.00457	0.01745	3.941
CeO_2		0.00581	1.000
	1.00000	3.82367	801.000

The YAG faceplate wafers, 2- or 3-inch in diameter by 0.100 inch thickness, are thermally equilibrated above the melt surface for ten minutes, dipped to the melt surface, and rotated at 200 rev/min. for about ten minutes. The Ce:YAG epitaxial phosphor layer grows at a rate of about 1.5 μm/min. After growth, the substrate with the epitaxial layer is raised above the melt, and the residual flux is spun-off by rapid rotation of 500 rev/min. Removal of the faceplate from the furnace to room temperature proceeds over the course of 90 minutes. This slow exit rate prevents thermal shock and cracking of the wafers. This entire process is done in a class 100 laminar flow hood. Remaining traces of solidified growth solution on the wafers are removed in a 40% solution of nitric acid at 90 °C. Layer thickness is measured by weight, using a density of 4.565 g/cc, the density of pure $Y_3Al_5O_{12}$. Optical thickness measurement is not possible since there is no refractive index difference between the layer and the substrate.

Faceplate Reticulation.

Reticulation, or patterning of the phosphor layer, allows a greater fraction of rays to enter the critical cone of 33° and exit the faceplate. Fig. 1 is a photograph of a portion of the surface of a photolithographically reticulated three-inch faceplate showing the hexagonal reticulation used and the facets of the etched YAG crystal which form the surface of the reticulation structure. Reticulation is accomplished by photolithographically producing an hexagonal pattern of gold, which acts as an acid resist, on the faceplate surface, and then etching in a 3:1 by volume mixture of phosphoric and sulfuric acid at 210 °C. The hexagonal pattern is aligned with the <1 1 2> direction in the plane of the <1 1 1> wafer, and etching exposes the (211) facets of the garnet crystal which produce the six-fold tent structure shown in fig. 3.

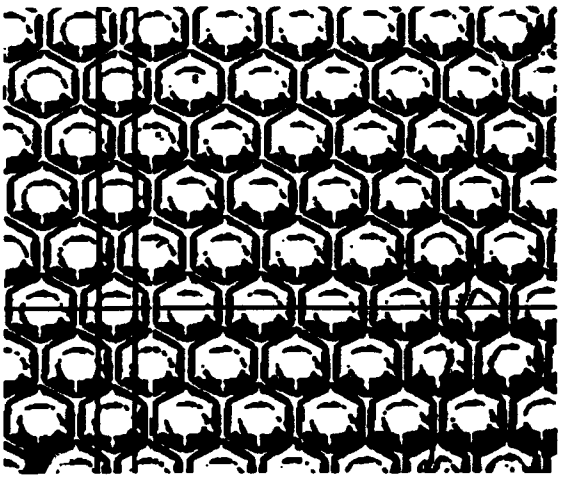

Fig. 3. Photograph of the reticulation pattern for Ce:YAG faceplates. The reticulation is an array of truncated six-fold pyramids formed from the (211) facets of the YAG crystal.

Faceplate Characterization.

Table II and fig. 4 illustrate the cathodoluminescent efficiency at 36.4 - 36.9 kV anode potential for a 2-inch Ce:YAG single crystal faceplate sealed to a projection neck assembly by Thomas Electronics [12]. This Ce:YAG faceplate was not reticulated; instead, it was produced with a slight facet texture [8] which allows an enhanced efficiency intermediate between a non-reticulated and a reticulated phosphor. The lack of saturation to high power density is evident up to the tested limit of 84 Watt/in^2 (13 Watt/cm^2). One measurement at an anode potential of 40 kV and 90 Watt/in^2 (13.95 Watt/cm^2) gave an efficiency of 4.84 Lumens/Watt and 435 Lumens light output from the one-inch square NTSC raster used in these tests. All our measurements have shown increasing efficiency with increasing anode potential.

Table II. Cathodoluminescence of an unreticulated 2-inch Ce:YAG faceplate with a slight facet texture, as excited by a one-inch square NTSC raster.

kV	mA	Watt	fL	Lumens	L/W
36.30	0.023	0.853	594	4.12	4.836
36.40	0.053	1.929	1365	9.48	4.914
36.40	0.082	2.988	2104	14.61	4.890
36.40	0.127	4.616	3267	22.69	4.915
36.50	0.184	6.705	4785	33.23	4.956
36.50	0.255	9.318	6501	45.15	4.845
36.50	0.330	12.038	8602	59.74	4.962
36.60	0.443	16.221	11308	78.53	4.841
36.60	0.585	21.415	14806	102.82	4.801
36.60	0.780	28.552	19558	135.82	4.757
36.60	1.000	36.600	25300	175.69	4.800
36.70	1.418	52.055	36080	250.56	4.813
36.70	1.507	55.307	37620	261.25	4.724
36.80	1.631	60.021	39050	271.18	4.518
36.80	1.791	65.898	42570	295.62	4.486
36.80	1.862	68.511	44000	305.56	4.460
36.80	1.950	71.760	45650	317.01	4.418
36.90	2.039	75.239	47190	327.71	4.356
36.90	2.216	81.770	52250	362.85	4.437
36.90	2.283	84.243	52800	366.67	4.353

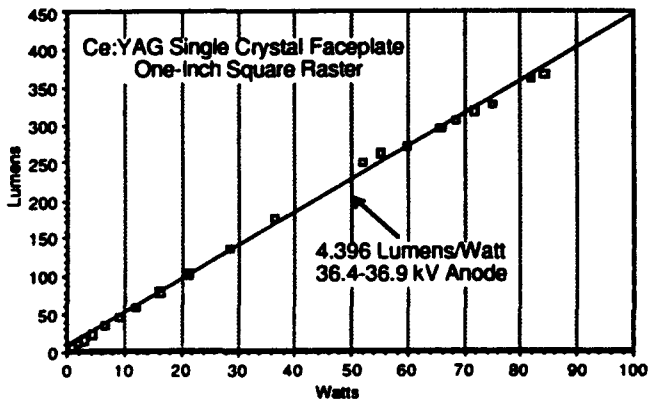

Fig. 4. Lumens/Watt data of Table II. Note the linear performance to high power density (13 W/in^2).

Fig. 5 illustrates the efficiency of a one-inch diameter faceplate with the reticulation pattern of fig. 3, as measured in a demountable faceplate apparatus. The measured efficiency at 25 kV for unreticulated faceplates is in the range 1.9-2.0 L/W. Measurements of 3-inch faceplates are now underway.

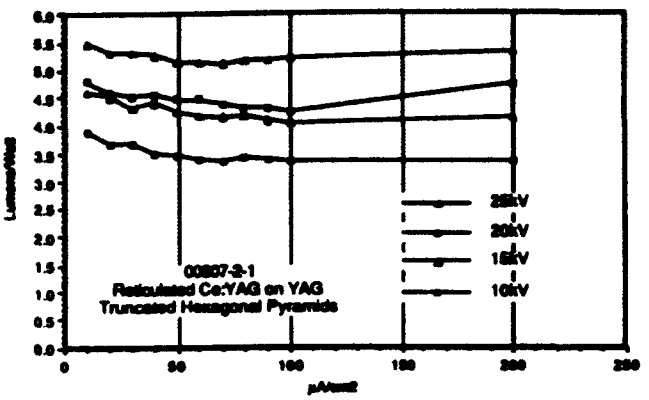

Fig. 5. Efficiency data for truncated six-fold pyramid reticulation on Ce:YAG. Efficiency of an unreticulated faceplate at 25 kV is about 2.0 Lumens/Watt.

Conclusions.

Single crystal faceplates of Ce:YAG phosphor (P-46), epitaxially grown on YAG, show high internal efficiencies at high anode potentials. Reticulation can increase the external efficiency to the point at which a monochrome 2000 Lumen projection CRT can be achieved for a three-inch faceplate, as shown in Table III. Equivalent red and blue single crystal faceplates must be identified to complement this green phosphor to produce a compact color projection system.

Table III. Performance data for Ce:YAG faceplates.

	Demonstrated (2")	Predicted (3")
Faceplate Luminance, fL	62,700	86,750
Faceplate Efficiency, L/W	4.84	4.84
Raster Size, in^2 (cm^2)	1 (6.45)	3.63 (23.4)
Beam Power, W	90	413
Beam Power Density, W/cm^2	14	18
Faceplate Output, L	435	2000

Acknowledgements.

This research was supported at Allied-Signal by contract N61339-90-C-046 of the Naval Training Systems Center; and at Trident International by contract N61339-90-C-047 of the Naval Training Systems Center. This support of the U.S. Navy is gratefully acknowledged.

References.

1. M.W. van Tol and J. van Esdonk, IEEE Trans. Electron Devices ED-30, 193 (1983).

2. J.M. Robertson and M.W. van Tol, Appl. Phys. Lett. 37, 471 (1980).

3. W.F. van der Weg and M.W. van Tol, Appl. Phys. Lett. 38, 705 (1981).

4. J.M. Robertson and M.W. van Tol, Phys. Stat. Sol. (a) 63, K59 (1981).

5. G.W. Berkstresser, et al., J. Electrochem. Soc. 135, 1302 (1988).

6. U. Levy and H.H. Yaffe, SID International Symposium Digest, 1984, p. 336 ff..

7. P.F. Bongers, et al., U.S. Patent No. 4,298,820 (1981).

8. D.M. Gualtieri, et al. U.S. Patent No. 4,713,577 (1987); U.S. Patent No. 4,728,178 (1988).

9. D.T.C. Huo and T.W. Hou, J. Electrochem. Soc. 133, 1492 (1986).

10. D.M. Gualtieri, Appl. Phys, Lett. 59, 650 (1991).

11. S.L. Blank, W.A. Biolsi and J.W. Nielsen, IEEE Trans. Magnetics MAG-13, 1095 (1977).

12. Thomas Electronics, Inc., 100 Riverview Drive, Wayne, NJ 07470, Tel. (201)-696-5200.

ENCLOSURE 11.2

FINAL REPORT

SINGLE CRYSTAL PHOSPHOR FACEPLATES FOR HIGH RESOLUTION, HIGH INTENSITY CATHODE RAY TUBES

FEBRUARY 1992

Final Report

SINGLE CRYSTAL PHOSPHOR FACEPLATES FOR HIGH RESOLUTION, HIGH INTENSITY CATHODE RAY TUBES

Purchase Order No. 9166

Submitted By

Applied Physics Laboratory
ALLIED-SIGNAL INC.
Research and Technology
P.O. Box 1021
Morristown, New Jersey 07962-1021

Submitted To:
Trident International Inc.
Central Florida Research Park
3290 Progress Drive Suite 155
Orlando, Florida 32826

Allied Signal

Single Crystal Phosphor Faceplates for High Resolution High Intensity Cathode Ray Tubes

a study for

Trident International, Inc.
Central Florida Research Park
3290 Progress Drive, Suite 155
Orlando, Florida 32826

by

D.M. Gualtieri
Allied-Signal, Inc.
Research and Technology
P.O. Box 1021
Morristown, NJ 07962-1021

February 1992

TABLE OF CONTENTS

Single Crystal Phosphor Faceplates for High Resolution High Intensity Cathode Ray Tubes

a study for

Trident International, Inc.
Central Florida Research Park
3290 Progress Drive, Suite 155
Orlando, Florida 32826

by

D.M. Gualtieri
Allied-Signal, Inc.
Research and Technology
P.O. Box 1021
Morristown, NJ 07962-1021

February 1992

1.0.0 INTRODUCTION

Conventional CRT faceplates are formed by the deposition of phosphor powder on the inside of a glass envelope of limited thermal conductivity. The image resolution and power capabilities of these faceplates are limited, and many applications now require CRT performance at the limits of phosphor faceplate technology. For example, sunlight-readable head-up displays (HUDs) for aircraft require a brightness of 10,000 foot-lamberts, a performance just achieved by conventional CRTs in stroke mode, and a factor of ten beyond that achieved in raster mode. The resolution of conventional faceplates is limited by phosphor particle size to twenty micrometers. High intensity operation is limited by a decomposition threshold of about 1 watt/cm^2. The phosphor particles will actually melt at about 5 watts/cm^2. High intensity operation also limits phosphor lifetime by a process called coulombic degradation. This failure mode reduces the intensity of P53, a standard phosphor, to 50% of its initial value after an electron dosage of 140 coulombs/cm^2. This leads to a CRT lifetime in a high luminance application of about 1000 hours under the best conditions.

Garnets are crystalline materials with many technologically useful properties. Garnets are oxides of the general composition $R_3T_5O_{12}$ (R and T are large and small metal or metalloid elements) which are resistant to chemical attack and high temperatures. There is much diversity in garnet composition since R and T can be combinations of one or several elements cohabiting a crystal sublattice, and R and T range over much of the Periodic Table. As an example, the yttrium in $Y_3Al_5O_{12}$ (YAG) can be partially replaced with neodymium to form the useful laser crystal Nd-YAG. YAG is used not only as a laser material, but as a substrate for the deposition of other garnet compositions. In particular, YAG doped with rare-earth elements, when grown as epitaxial layers on YAG substrates, is a cathodoluminescent material. Such layers can be used as phosphor faceplates in cathode ray tubes with significant advantages over standard, powder phosphor, faceplates. The single crystal nature of such epitaxial faceplates allows a higher resolution, and the intimate thermal contact between the epitaxial phosphor and the thermally conductive substrate allows operation of cathode ray tubes at power levels which would destroy a conventional powder phosphor.

Epitaxial phosphors are fluorescent crystalline layers which are grown on crystalline substrates. The usual case is homoepitaxial growth, in which a fluorescent ion is substituted for another ion in a host composition epitaxially grown onto a substrate of the host composition. An example is Ce:YAG epitaxially grown on YAG substrates, where cerium is incorporated into the layer on yttrium sites. The more unusual case is heteroepitaxy, in which a layer is grown on a substrate of different crystal structure; for example, zinc sulphide deposited on sapphire. Since electrons penetrate only a few microns into epitaxial phosphors, the epitaxial layer need not be very thick, 5-20 microns are usually sufficient. Epitaxial layers can be grown on top of other epitaxial layers to form penetration phosphors, in which different colors are excited at different anode potentials.

Epitaxial phosphor faceplates (EPF) have several significant advantages, which are summarized below:

1) *Ultra-High Resolution.* Resolution is limited only by electron beam size.

2) *Fast Decay Time.* Fluorescence decay of Ce:YAG (10 nsec), a standard epitaxial phosphor, is an order of magnitude faster than conventional powder phosphors.

3) *High Power Operation.* Epitaxial phosphors will not decompose at high power levels. There is no "burn". Thermal quench temperature is much higher than for powder phosphors.

4) *Superior Ageing Characteristics.* No coulombic degradation.

5) *Superior Mechanical Properties.* Single crystals have high strength. Faceplates resist scratching.

Since epitaxial phosphors are single crystals with no granulation, resolution is limited only by the dimension of the electron beam. Prof. Albert Crewe of the Fermi Institute, University of Chicago, has tested a Ce:YAG epitaxial phosphor faceplate fabricated by Allied-Signal, Inc. in a high resolution electron microscope and found no granulation to 0.1 μm spot size. This Ce:YAG epitaxial phosphor faceplate was further tested to a current density of 1000 A/cm^2 at 5 kV without permanent damage. M.W. van Tol and J. van Esdonk operated epitaxial phosphor faceplates at power levels of 10 W/cm^2 [1]. J.M. Robertson and M.W. van Tol tested epitaxial phosphor faceplates of Ce:YAG,

Tb:YAG, and Eu:YAG at power levels to 10^4 W/cm^2 [2]. They found that Ce:YAG is linear to the highest power levels, but that the light output of Tb:YAG and Eu:YAG saturates at power levels above 1 W/cm^2. Thus, Ce:YAG is preferred as a high intensity monochrome phosphor. The saturation in Tb:YAG arises from excited state absorption and cross-relaxation processes and it is a general feature of many phosphors, for example Mn:$BaAl_{12}O_{19}$ [3,4]. AT&T Bell Laboratories has developed a modified terbium composition, $Tb_{0.2}Y_{0.1}Lu_{2.7}Al_3Ga_2O_{12}$, with improved saturation characteristic [5]. Such a phosphor has shown a peak line brightness of 28,000 fL at a 25,000 inch/sec writing speed when excited with a 25 kV, 2 mA beam. This is equivalent to 594 lumens in a 2.75 inch diagonal raster.

Levy and Yaffe have shown that the thermal quenching temperature of Ce:YAG is about 400°C, and that a decrease in light output is first evident at 200°C [6]. They determined that it is safe to operate an EFP at thermal gradients up to 150°C/inch, and that a three inch diameter epitaxial phosphor faceplate can be operated at 25 watts excitation with no cooling. Since the thermal conductivity of YAG is high, forced-air cooling is very effective at higher excitation levels. Forced-air cooling can extract about 60% of the heat, radiation can dissipate about 20% of the heat, and conduction down the neck can dissipate the remaining 20%. Coulombic degradation does not occur in epitaxial phosphor faceplates, whereas 0.5 W/cm^2 is the conventional limit for projection CRTs. Operation of P53 at 0.5 W/cm^2 results in an extremely short lifetime.

The fluorescent spectrum of cerium in garnet crystals is a function of the atomic spacing in the crystal which is reflected in the lattice constant. It is possible to red-shift the green emission of Ce:YAG by incorporation of gadolinium. In the extreme case, $Ce:Gd_3Al_5O_{12}$ can be grown as the analog of $Ce:Y_3Al_5O_{12}$, and the spectral peak is shifted almost 50 nm towards the red. A blue-shift is possible, by using a small rare-earth ion in place of yttrium, but the magnitude of such a blue-shift is not sufficient to produce much energy at blue wavelengths suitable for color CRTs. Although other activators in YAG, notably thulium, are blue emitters, cerium seems to be the only activator which will not saturate at high power levels. Two blue cerium emitters, $Ce:La_2Be_2O_5$ (Ce:BEL) and $Ce:Y_2SiO_5$ (cerium orthosilicate), are candidates for blue faceplates. $Ce:Y_2SiO_5$ has emission extending below blue, so that much of its light output is not visible. Its performance in CRTs has been investigated by AT&T Bell Laboratories and elsewhere, and saturation has been observed in this phosphor. Ce:BEL, however, emits prominently in the blue, and does not appear to saturate. Thus, $Ce:Gd_3Al_5O_{12}$ (Ce:GdAG, red), $Ce:Y_3Al_5O_{12}$ (Ce:YAG, green), and $Ce:La_2Be_2O_5$ (Ce:BEL, blue), appear to be an appropriate trio of epitaxial phosphors for a high intensity color projection display. Figure 1.0.0.1 shows the spectra of these phosphors.

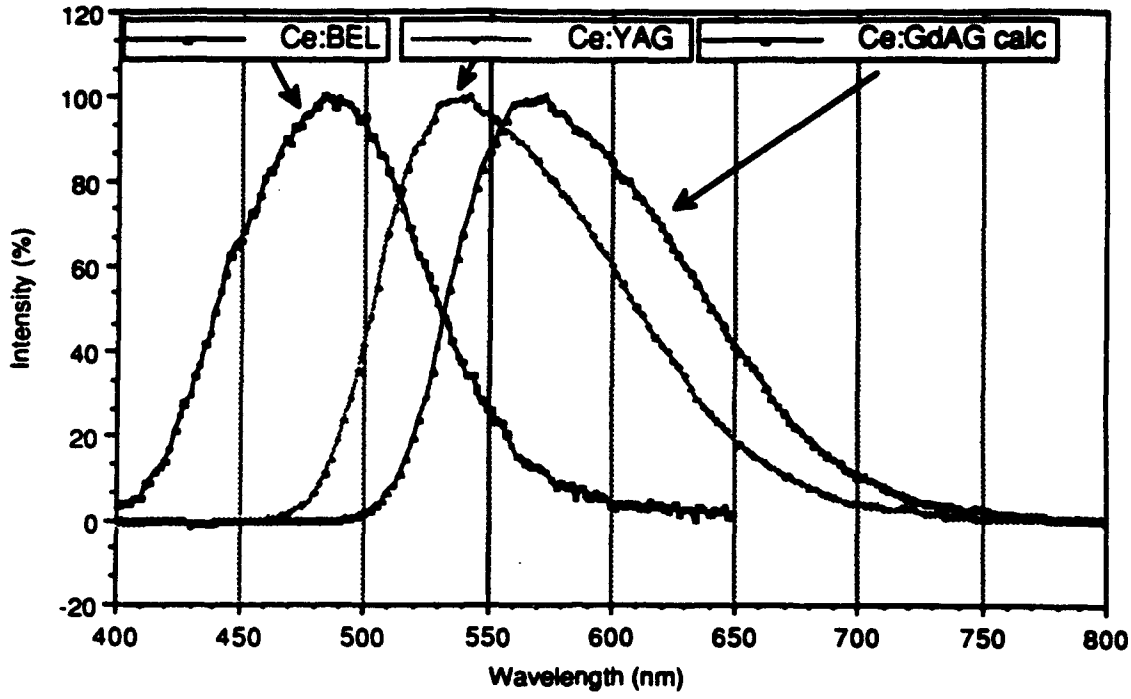

Fig. 1.0.0.1 Spectra of Ce:BEL (blue), Ce:YAG (green) and Ce:GdAG (red) phosphors.

2.0.0 PROCESS

Table 2.0.0.1 shows the major stages of the process for the production of epitaxial phosphor faceplates.

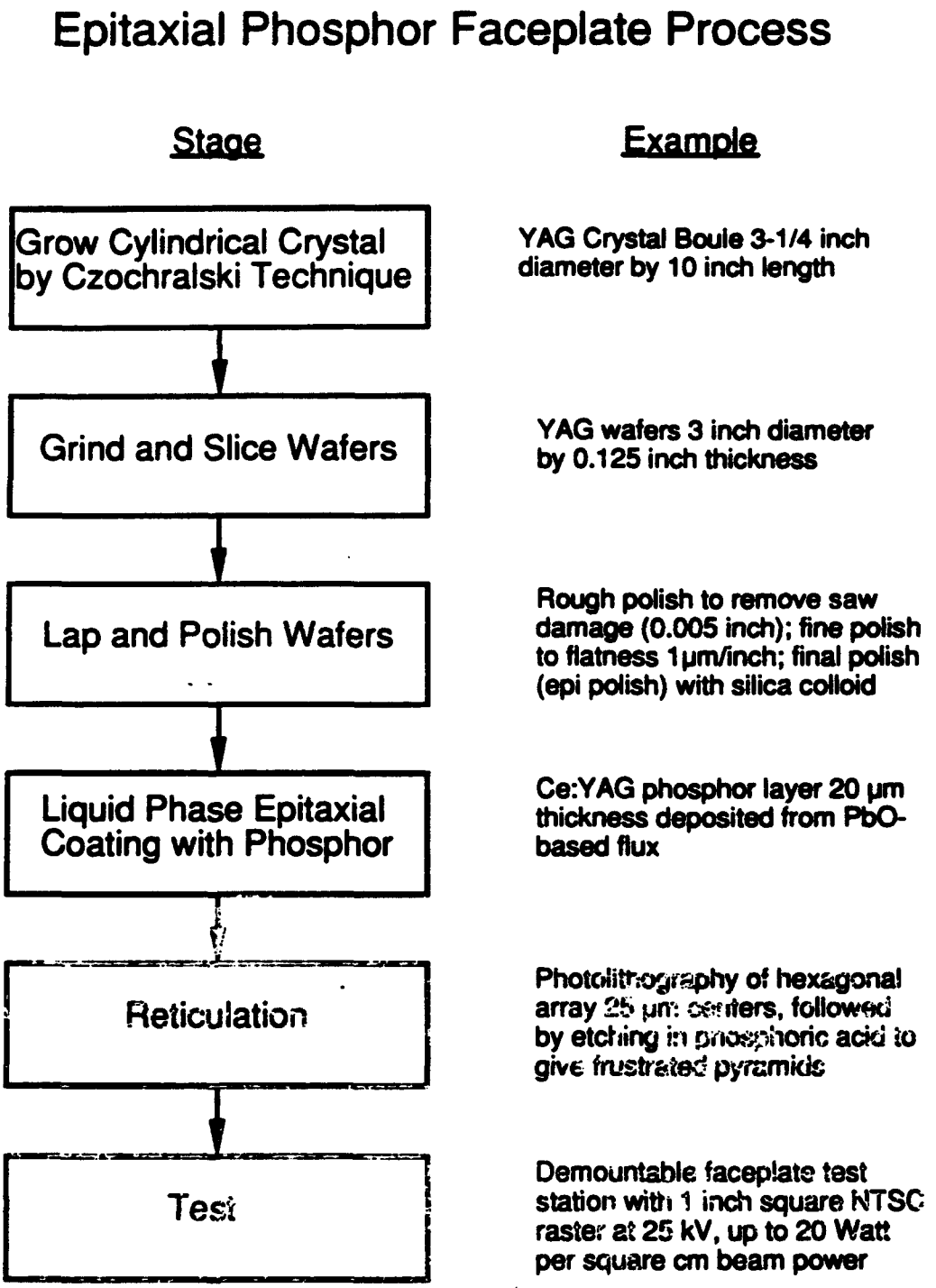

Table 2.0.0.1. Major stages of the process for the production of epitaxial phosphor faceplates.

2.1.0 Crystal Growth Process of Substrate Wafers

There are presently two processes which are suitable for the growth of the substrate wafers used in epitaxial phosphor faceplates. These are the Czochralski method, which has produced large single crystals of YAG up to three inches in diameter; and the Heat Exchanger Method. The Heat Exchanger Method (HEM™) is being used for the commercial production of 10-inch diameter sapphire crystals of very high quality. It is possible to grow sapphire by HEM free of scattering centers for stringent optical applications. HEM is used also for commercial production of multi-crystalline silicon ingots for photovoltaic and optical applications. Titanium-doped sapphire (Ti:Sapphire) boules are grown routinely for cw and pulsed laser applications. A number of mixed oxides, fluorides and compound semiconductors has also been grown by HEM.

2.1.1 Undoped Crystal Boule

Substrate wafer crystal for epitaxial phosphor faceplates of YAG have been produced up to three inches in diameter by the Czochralski process. In the Czochralski process, a melt is produced in a crucible by induction heating. A "seed" crystal is dipped into the melt and withdrawn with rotation at a slow rate as the melt is cooled. This produces solidified crystal on the seed with the same crystallographic orientation as the seed. Usually crystal weight is used as a process variable to control the growth in a feedback loop.

There are difficulties involved in the growth of large diameter Czochralski crystals. The crystal is in contact with the liquid melt, and in the case of YAG it is actually immersed in liquid. This leads to considerable thermal stress on the crystal which can cause cracking. Also, scale-up from one diameter to a larger diameter is troublesome, since the exact parameters for stable crystal growth depend critically on the thermal environment of the crystal. There is a steep "learning curve."

In the HEM method, he crucible with the seed positioned at the bottom is loaded with a material charge and placed on top of a heat exchanger. After evacuation, heat is supplied by the graphite heater and the material charge is melted. The seed is prevented from melting by forcing gaseous helium through the heat exchanger.Growth is started after sufficient meltback of the seed is achieved by increasing the flow of helium and thereby decreasing the heat exchanger temperature. The liquid temperature gradients are controlled by the furnace temperature, while the temperature gradient in the solid is controlled by the heat exchanger temperature. Crystal growth is achieved by controlling the heat input as well as the heat extraction. After solidification is complete, the gas flow through the heat exchanger is decreased to equilibrate the temperature throughout the crystal during the annealing and cooldown stage.

HEM is the only crystal growth process in which both the heat input and heat extraction are controlled. The heat flow is set up such that the heat input is from the sides and top of the crucible and the heat extraction is primarily through the heat exchanger at the bottom of the crucible. Under these conditions a convex solid-liquid interface is set up so that core-free crystals can be grown. The convexity of the solid-liquid interface can be controlled by changing the ratio of heat input and heat extraction. The independent liquid and solid temperature gradients are achieved without movement of the crucible, heat zone or crystal. After the crystal is grown, it is still in the heat zone and can be cooled at a controlled rate to relieve solidification stresses. This unique capability allows the growth of

sapphire up to 32 cm diameter and weighing about 50 kg without cracking due to thermal stresses associated with such large sizes.

A distinguishing feature of HEM, as compared with the Czochralski, top-seeded process, is that the solid-liquid interface is submerged beneath the surface and is surrounded by the melt. Under these conditions the thermal and mechanical perturbations are damped out by the surrounding molten mass before reaching the interface. This results in uniform temperature gradients at the interface. In the Czochralski process, growth occurs at the melt surface where the local gradients vary sufficiently to cause solidification and remelting of the crystal. Precise control of the furnace and heat exchanger temperatures, combined with minimized thermal perturbations resulting from the submerged interface, gives HEM an advantage over the Czochralski techniques for growing high-quality crystals.

In HEM growth, after the crystal is grown, the temperature of the furnace is reduced to just below the solidification temperature and the helium flow is reduced at a desired rate. The whole crystal can, therefore, be brought to high temperatures to anneal the solidification stresses, followed by uniform cooling at a controlled rate to room temperature. Because *in situ* annealing is part of the solidification cycle, HEM can reduce the defect density. Further the last and most impure material to solidify is along the crucible walls, where it can be removed. These features of HEM produce uniform, growth and the only sapphire free of light scatter. In the case of sapphire and silicon, it has been demonstrated that once crystal growth parameters are established, large crystals can be grown. The HEM has been adapted for the growth of Ti:Al_2O_3. HEM is cost competitive with Czochralski. The furnace is uncomplicated, automated, and well insulated, which results in low equipment, labor and energy costs.

2.1.2 Doped Crystal Boule

Single crystal boule may be produced with the activator ion grown into the crystal. There are both advantages and disadvantages to this technique. The principal advantage is that the subsequent deposition of the phosphor by liquid phase epitaxy is not required. The disadvantages relate to the difficulty in achieving as high an activator concentration as desired, maintaining the proper charge state of the activator, and the usually lower growth rate required for doped crystals.

One of the problems with doped crystals is the segregation coefficient of dopant in the host crystal. The segregation coefficient is the ratio of the concentration of a species in the crystal to that in the melt. If the segregation coefficient is low, there is a gradation in dopant concentration along the length of the crystal and it is necessary to grow crystals at low growth rates in order to maintain high quality. These problems are minimized as the segregation coefficient is higher and essentially there are minimal problems when the segregation coefficient is unity. For example, the segregation coefficient of Ti in Al_2O_3 and Nd in YAG is rather low, approximately 0.16. The growth of Nd-doped YAG for laser applications proceeds at about one-fifth the rate as for undoped YAG.

Ce-doped BEL has been produced in boule form, so that subsequent epitaxy of a phosphor layer is not required, but an anneal in a hydrogen atmosphere is required to bring the cerium into its reduced Ce^{3+} charge state. Likewise, the blue phosphor Ce:Y_2SiO_5 has been produced by AT&T Bell Laboratories as doped boule one-inch in diameter.

Researchers from Hitachi Chemical Co. [17] have reported growth of the similar crystal $Ce:Gd_2SiO_5$ in diameters to two-inch.

2.1.3 Current Size Limitations

The Czochralski method has produced YAG crystal up to three inches in diameter. Experience indicates that four inch crystal is a possibility, but only by a flat interface technique pioneered at Allied-Signal. However, a considerable development effort would be required to attain a process for the Czochralski growth of four inch YAG.

The Heat Exchanger Method (HEM™) is being used for the commercial production of 10-inch diameter sapphire crystals of very high quality. The growth of YAG crystal to this diameter appears possible. These melting point of YAG (1950°C) is lower than that for Al_2O_3 (2040°C): therefore, current HEM™ furnaces are adequate for growing this crystal. In the case of sapphire (Al_2O_3) crystals grown by HEM™, the processing is carried out under vacuum; however, it is expected that even though the host phosphor materials may be stable under vacuum, it may be necessary to control the atmosphere during growth of doped crystals. The candidate phosphor materials are compatible with using a molybdenum crucible and graphite resistance heat zone of the HEM™ furnace so that these crystals can be grown with existing HEM™ furnaces. In the case of BEL, it would be necessary to set up additional safety procedures for handling BeO raw material and BEL crystals because of their toxic nature.

2.2.0 Optical Fabrication of Wafer Faceplates

Fabrication of wafer faceplates from crystal boule is accomplished by standard techniques available in most optical shops. This involves centerless grinding of the crystal boule to diameter, xray orientation, wafer slicing with an ID saw, lapping and polishing. The requirement of the final polish is severe. This "epi" grade polish involves the use of a chemical-mechanical colloidal silica polish on a soft pad to produce a surface free of defects which would interfere with the subsequent epitaxial phosphor growth stage.

2.2.1 Grind and Slice Wafers

The crystal boule is first ground to the required diameter using a centerless grinding technique. After alignment of the crystal by xray diffraction, wafers are sliced by the type of saw ("ID" saw) used in processing of semiconductor wafers.

2.2.2 Lap and Polish

The sliced wafers are polished using finer grit until the saw damage has been removed (about 0.005 inch in the case of YAG) and the required flatness of about 1 μm/inch has been achieved. A final polish ("epi" polish) is done with a colloidal silica suspension to achieve a polish beyond an optical polish into the regime of a polish on an atomic scale.

2.2.3 Current Size Limitations

Since the semiconductor industry is now fabricating wafers up to ten and twelve inches in diameter, it is concluded that wafer fabrication will not constrain the development of large diameter single crystal faceplates.

2.3.0 Liquid Phase Epitaxy Process

The following is a general procedure for the growth of epitaxial layers of Ce:YAG on YAG substrates. A YAG wafer, prepared by the processes in the previous sections, is carefully cleaned and mounted in a substrate holder which allows rotation and translation. Epitaxy is achieved by dipping the substrate into a platinum crucible holding the molten constituent oxides of the Ce:YAG composition in the proportions listed in Table 2.3.0.1.

Table 2.3.0.1. Melt for the growth of epitaxial layers of Ce:YAG on YAG substrates at 980 °C. Note that cerium oxide, the dopant, is not included in the mole fraction calculation.

Oxide	Mole Fraction	Moles	Grams
PbO	0.90282	3.44684	769.299
Al_2O_3	0.01737	0.06632	6.762
B_2O_3	0.07524	0.28724	19.998
Y_2O_3	0.00457	0.01745	3.941
CeO_2		0.00581	1.000
	1.00000	3.82367	801.000

The platinum crucible, 3-inches high by 2.25-inch diameter for epitaxial growth on one-inch diameter wafers, is placed in a vertical furnace. These powders are heated to 1050 °C, a temperature well above the melting point of the mixture, and allowed to "soak" for 24 hours. The melt is stirred for one hour at 1050 °C and 200 rev/min just before each layer growth. After stirring, the melt is cooled to the growth temperature of about 980°C in 45 minutes (melt saturation occurs at about 990°C).

The YAG faceplate wafers are thermally equilibrated above the melt surface for ten minutes, dipped to the melt surface, and rotated at 200 rev/min. for about ten minutes. The Ce:YAG epitaxial phosphor layer grows at a rate of about 1.5 μm/min. After growth, the substrate with the epitaxial layer is raised above the melt, and the residual flux is spun-off by rapid rotation of 500 rev/min. Removal of the faceplate from the furnace to room temperature proceeds over the course of 90 minutes. This slow exit rate prevents thermal shock and cracking of the wafers. This entire process is done in a class 100 laminar flow hood. Remaining traces of solidified growth solution on the wafers are removed in a 40% solution of nitric acid at 90 °C. Layer thickness is measured by weight, using a density of 4.565 g/cc, the density of pure $Y_3Al_5O_{12}$. Optical thickness measurement is not possible since there is no refractive index difference between the layer and the substrate.

2.3.1 Equipment

Fig. 2.3.1.1 shows the equipment involved in the liquid phase epitaxy process. There are motor assemblies to "dip" and rotate the wafers in the solution, but the major

piece of equipment is the large-bore vertical tube furnace which heats and maintains the solution at about 1100°C ± 1°C.

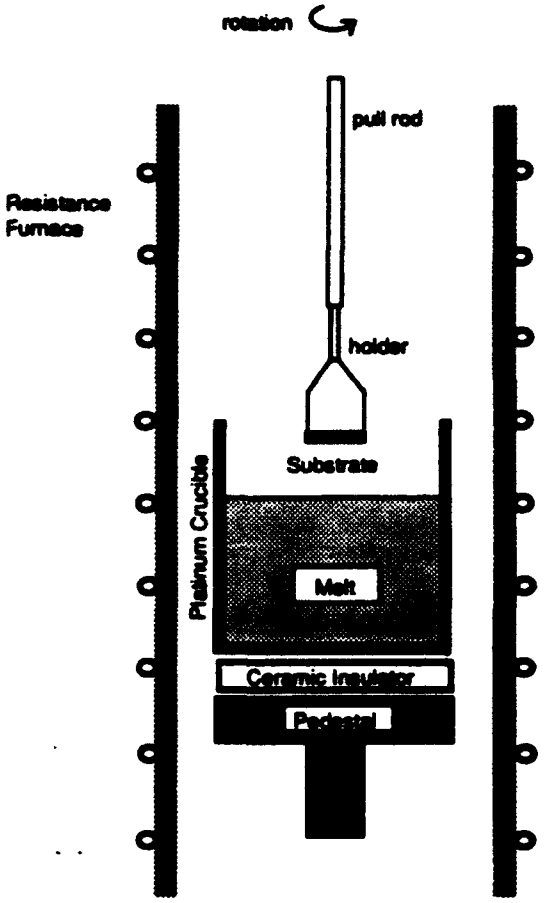

Fig. 2.3.1.1. Schematic diagram of system for liquid phase epitaxial growth of single crystal phosphors of Ce-YAG on YAG substrates.

2.3.2 Current Size Limitations

Liquid phase epitaxy is routinely carried out for wafers up to three inches in diameter in the preparation of magneto-optical materials. These wafers, however, are thin (0.020 inch) compared with YAG faceplate wafers (0.125 inch). Generally, a slower withdrawal rate from the epitaxy furnace is required for these thick wafers. Liquid phase epitaxy has been demonstrated on four-inch diameter by 0.020 inch thick wafers. There appears to be no fundamental size limitation for the liquid phase epitaxy process.

2.4.0 Photoreticulation

The major factor limiting the external efficiency of Ce:YAG phosphors is the high refractive index of the YAG substrate (1.84), which allows only rays less than a critical angle of 33° to be emitted from the faceplate. The remaining rays are waveguided to the

edges, so that only 16% of the cathodoluminescence is emitted from the faceplate. Higher external efficiencies can be expected from Ce:YAG through reticulation, a texturing of the epitaxial phosphor into structures which will focus the cathodoluminescence towards the observer. Non-reticulated epitaxial phosphors have low external efficiencies, since the cathodoluminescence is waveguided by the high refractive index of YAG to the edge of the faceplate.

P.F. Bongers, et al., [12] have etched grooves in the phosphor to increase the external efficiency. D.M. Gualtieri, et al. [13] have used a faceted epitaxial layer for the same purpose. D.T.C. Huo and T.W. Hou [14], have used photolithographic techniques to pattern a Ce:YAG epitaxial phosphor faceplate with an array of rectangular mesas. They were able to increase the external efficiency by a factor of three. A truncated cone geometry can increase the external efficiency by a factor of 5.5, if such a shape can be formed in the phosphor layer. Such reticulation will not limit the faceplate resolution if a small mesa size is used. The reticulation concept is shown schematically in fig. 2.4.0.1

Non-reticulated faceplates of Ce:YAG have an NTSC raster efficiency at 25 kV of 1.9 - 2.0 lumens/watt, when measured in our characterization station, so that at a beam power of 10 watts/cm^2 an NTSC raster of 2.75-inch diagonal on a *non-reticulated* Ce:YAG faceplate will have a luminance of 450 lumens. The best *reticulated* faceplate was found to give 5.38 lumens/watt at a beam power of 5 watt/cm^2. A beam power of 16 watt/cm^2 will be required for 2000 lumen output at such an efficiency. Fig. 2.4.0.2 shows the results of cathodoluminescent measurements on a reticulated faceplate.

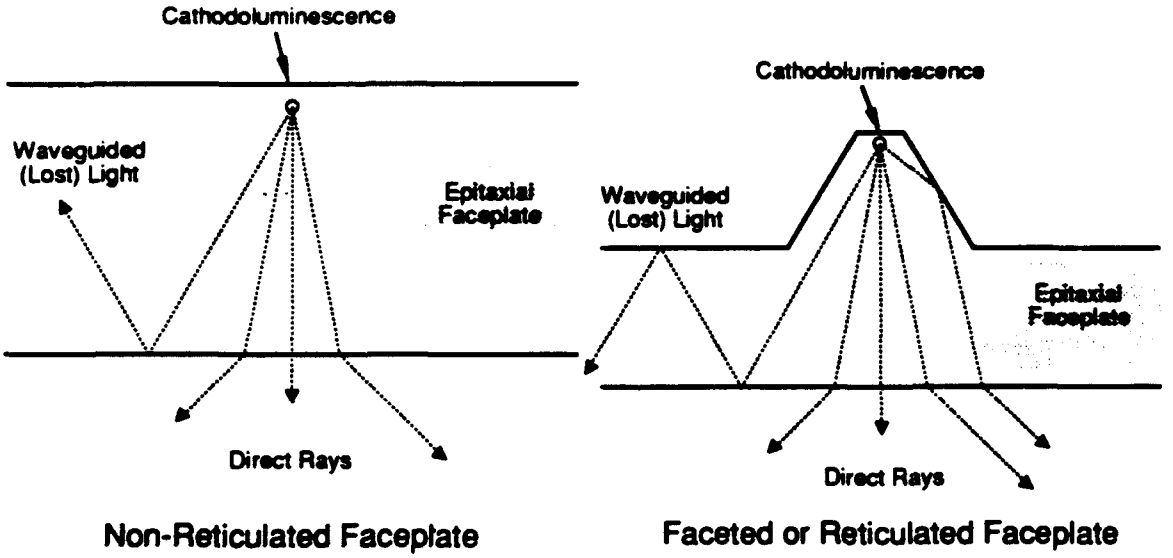

Fig. 2.4.0.1. Schematic illustration of waveguiding effect in epitaxial faceplates, and the role of reticulation in directing light into the critical cone.

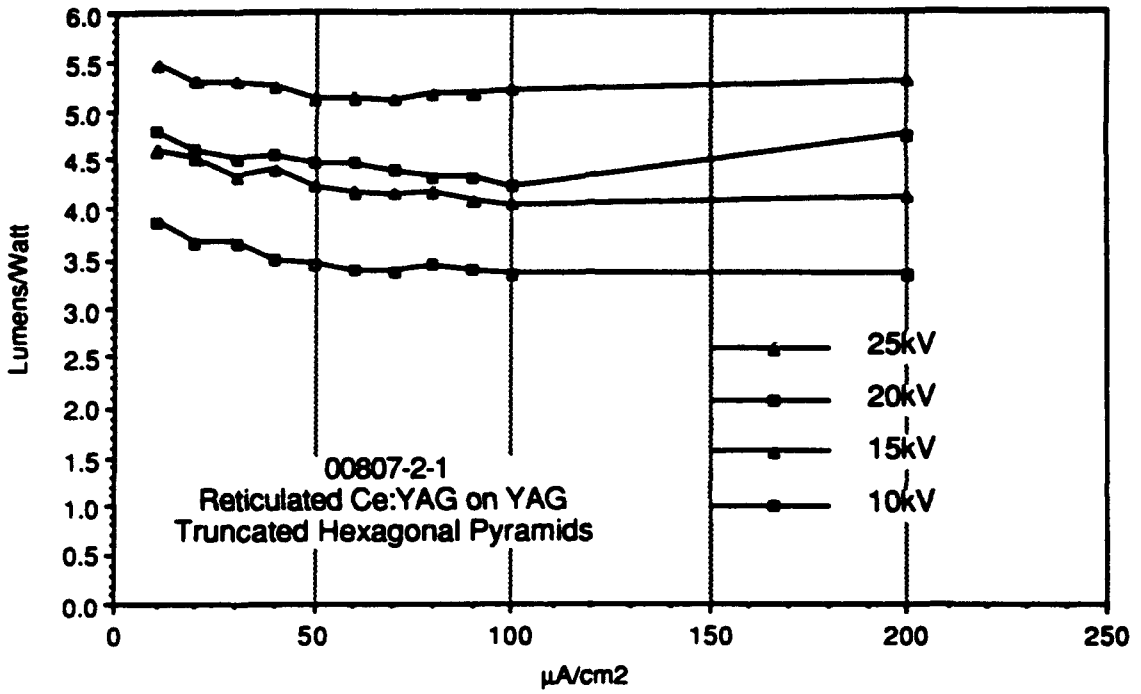

Fig. 2.4.0.2. Cathodoluminescent measurements on a reticulated faceplate.

2.4.1 Equipment

Photoreticulation is done by techniques common to fabrication of semiconductor devices. A mask aligner of micron resolution is required, typically a contact printer as distinct from a projector. A typical resist coater/developer/stripper line is required. Either a metallizer, such as an electron beam evaporator, or a plasma reactor for silica deposition are required to coat the wafers with an acid resisting mask for the etching stage. A phosphoric acid etcher is required. All this equipment must be sited in a class 100 clean room.

2.4.2 Current Size Limitations

Since the semiconductor industry is now fabricating wafers up to ten and twelve inches in diameter, it is concluded that this processing step will not constrain the development of large diameter single crystal faceplates.

3.0.0 FACEPLATE AND PHOSPHOR MATERIALS

3.1.0 Cerium Activators

Cerium seems to be the only activator which will not saturate at high power levels. Two blue cerium emitters, Ce:$La_2Be_2O_5$ (Ce:BEL) and Ce:Y_2SiO_5 (cerium orthosilicate), are candidates for blue faceplates. Ce:Y_2SiO_5 has emission extending below blue, peaking at about 390 nm, so that much of its light output is not visible. A similar phosphor Ce:Gd_2SiO_5 has a better spectral overlap with the visible, peaking at 430 nm. The performance of Ce:Y_2SiO_5 has been investigated by AT&T Bell Laboratories and elsewhere, and saturation has been observed in this phosphor. Ce:BEL, however, emits prominently in the blue, and does not appear to saturate. Thus, Ce:$Gd_3Al_5O_{12}$ (Ce:GdAG, red), Ce:$Y_3Al_5O_{12}$ (Ce:YAG, green), and Ce:$La_2Be_2O_5$ (Ce:BEL, blue), appear to be an appropriate trio of epitaxial phosphors for a high intensity color projection display.

3.2.0 Red Phosphors

3.2.1 Ce:(Y,Gd)AG on YAG

It is possible to epitaxially grow a red-shifted garnet composition on YAG wafer substrates. This garnet composition, Ce:$Y_2Gd_1Al_5O_{12}$, is strained with respect to the YAG wafer, and its red-shift is only about a third as large as that of Ce:$Gd_3Al_5O_{12}$. This composition has a lattice constant (measured perpendicularly at the (444) reflection) about 0.4% greater than YAG, which is just under the typical facet limit of 0.5%. Figs. 3.2.1.1 and 3.2.1.2 show cathodoluminescence measurements for this composition. There is a red-shift of 20 nm, and, most importantly, almost a two-fold increase in the luminance at the red wavelength of 650 nm. The light output at 650 nm was 31% of the spectral peak for this composition, as compared to 19% for Ce:YAG. The cerium emission in the fully substituted garnet, $Gd_3Al_5O_{12}$, would exhibit a larger red-shift, but it cannot be grown as an epitaxial layer on YAG.

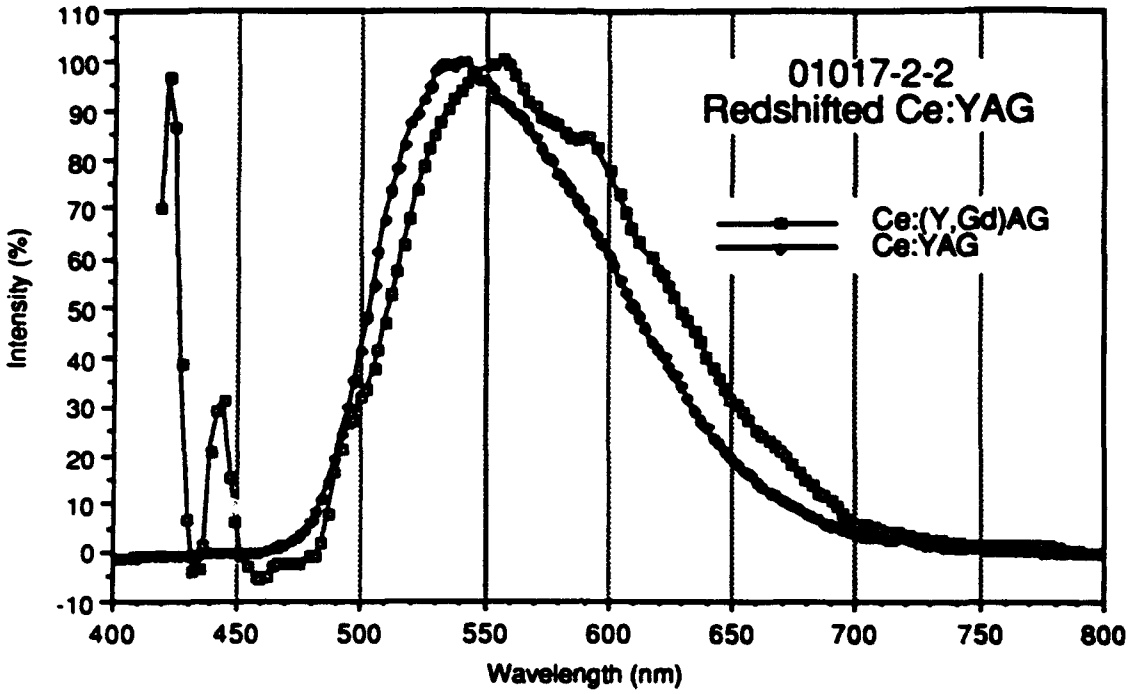

Fig. 3.2.1.1 Cathodoluminescent spectrum of a Ce:$Y_2Gd_1Al_5O_{12}$ phosphor layer grown on a YAG substrate.

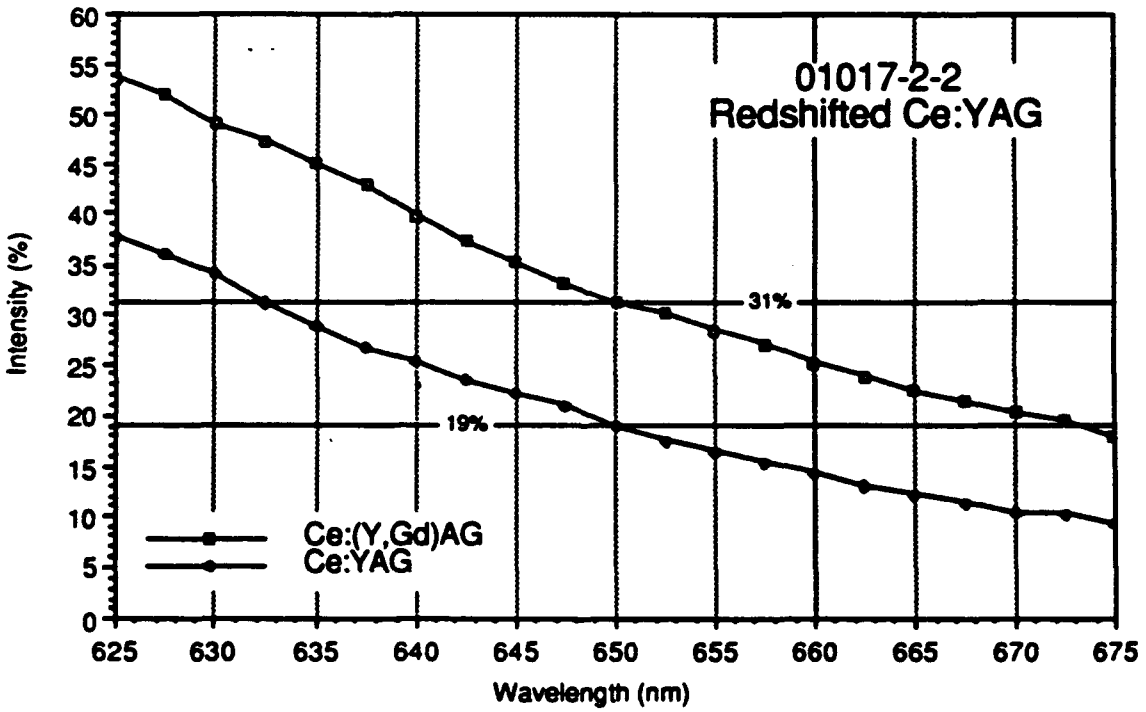

Fig. 3.2.1.2. Cathodoluminescent spectrum (detail) of a Ce:$Y_2Gd_1Al_5O_{12}$ phosphor layer grown on a YAG substrate.

3.2.2 Ce:GdAG on GdAG

Epitaxial layers of Ce:$Gd_3Al_5O_{12}$ could be grown on $Gd_3Al_5O_{12}$, and they would be good red faceplates in color projection systems since they would have a red-shift of about 50 nm.

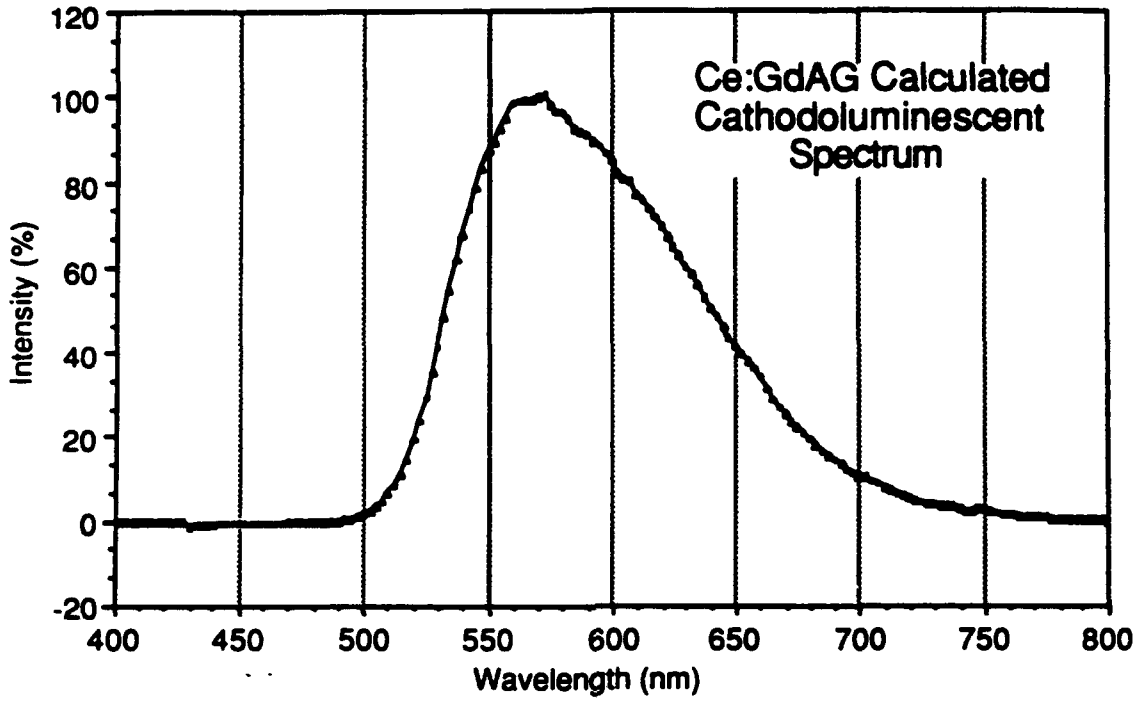

Fig. 3.2.2.1. Calculated spectrum of Ce:$Gd_3Al_5O_{12}$.

3.3.0 Green Phosphors

3.3.1 Ce:YAG

Cerium YAG is the material of choice for green epitaxial phosphors. Its cathodoluminescent spectrum appears as fig. 3.3.1.1.

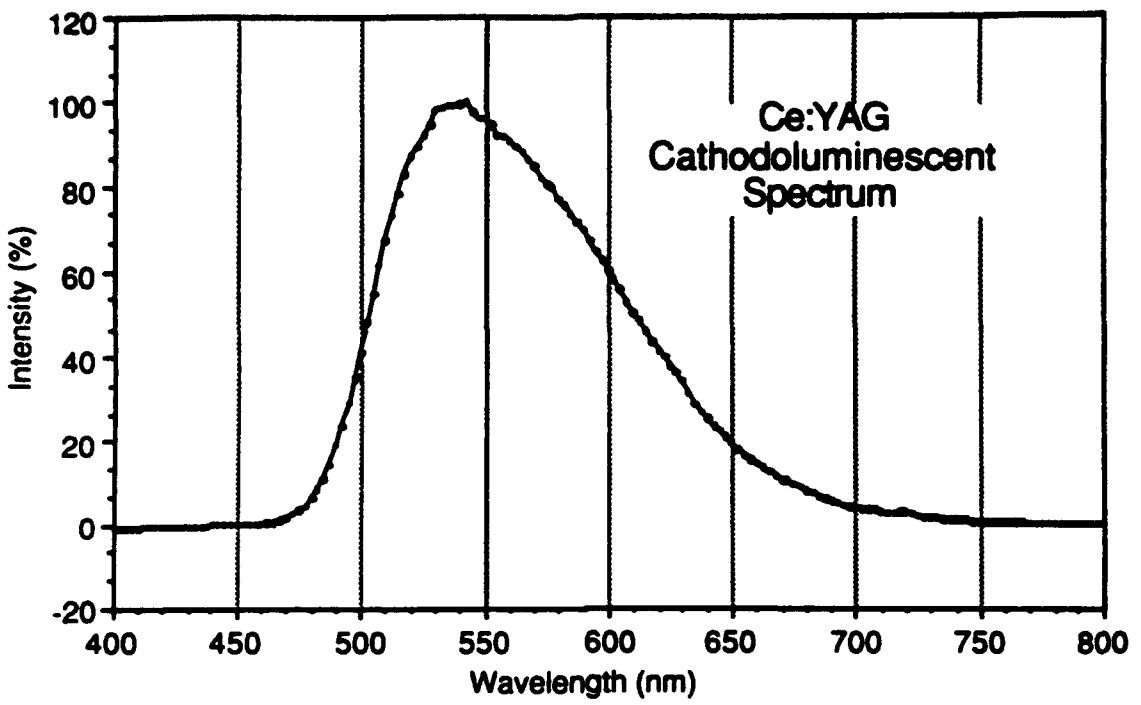

Fig. 3.3.1.1. Spectrum of Ce:$Y_3Al_5O_{12}$.

Non-reticulated faceplates of Ce:YAG have an NTSC raster efficiency at 25 kV of 1.9 - 2.0 lumens/watt, when measured in our characterization station, so that at a beam power of 10 watts/cm^2 an NTSC raster of 2.75-inch diagonal on a *non-reticulated* Ce:YAG faceplate will have a luminance of 450 lumens. The best *reticulated* faceplate was found to give 5.38 lumens/watt at a beam power of 5 watt/cm^2. A beam power of 16 watt/cm^2 will be required for 2000 lumen output at such an efficiency.

3.4.0 Blue Phosphors

3.4.1 Ce:BEL

The cathodoluminescence of Ce:BEL was characterized in a thin wafer of a Czochralski boule prepared from a melt of 0.5% cerium content [16]. Ce:BEL proved to be an excellent blue phosphor with a peak fluorescence at 485 nm and a fluorescence bandwidth (FWHM) of 80 nm (fig. 3.4.1.1). Thus, there is significant light energy at the extremely blue wavelength 445 nm. The measured cathodoluminescent efficiency of the available, as-grown Czochralkski crystal was 0.1 lumen/watt, weighted according to the C.I.E. photoptic curve. It was found that annealing at 1150 °C in a reducing atmosphere of 10% hydrogen in argon doubles the efficiency of Ce:BEL to 0.2 lumens/watt (fig. 3.4.1.2). Annealing also changes the appearance of the crystals from an orange color to transparent. It was also found that the light output of Ce:BEL does not saturate up to an electron beam power of 19 watt/cm^2.

Mass spectroscopy of the Ce:BEL crystal revealed a cerium content of 3.9×10^{18} atoms/cc, as compared with 23×10^{18} atoms/cc for YAG. If the cerium content of Ce:BEL can be increased to the level of cerium in YAG, this six-fold increase in concentration could increase the C.I.E. weighted efficiency of Ce:BEL to 1.2 lumens/watt. Since the refractive indices of Ce:BEL are about the same value as the refractive index of YAG, reticulation will yield the same increase in external efficiency.

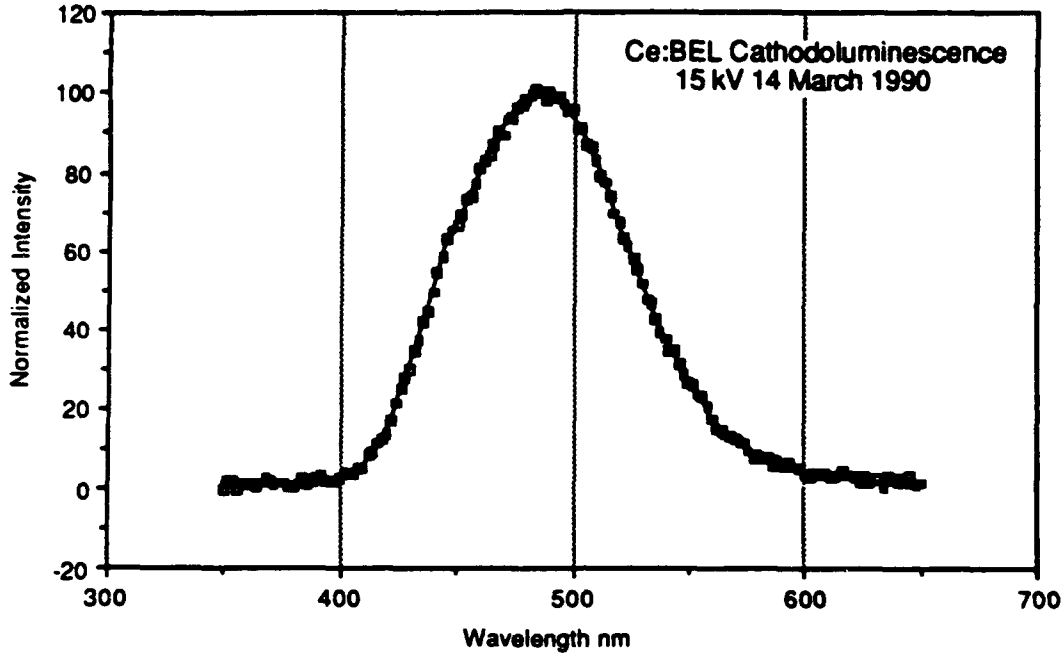

Fig. 3.4.1.1. Cathodoluminescence spectrum of Ce:BEL.

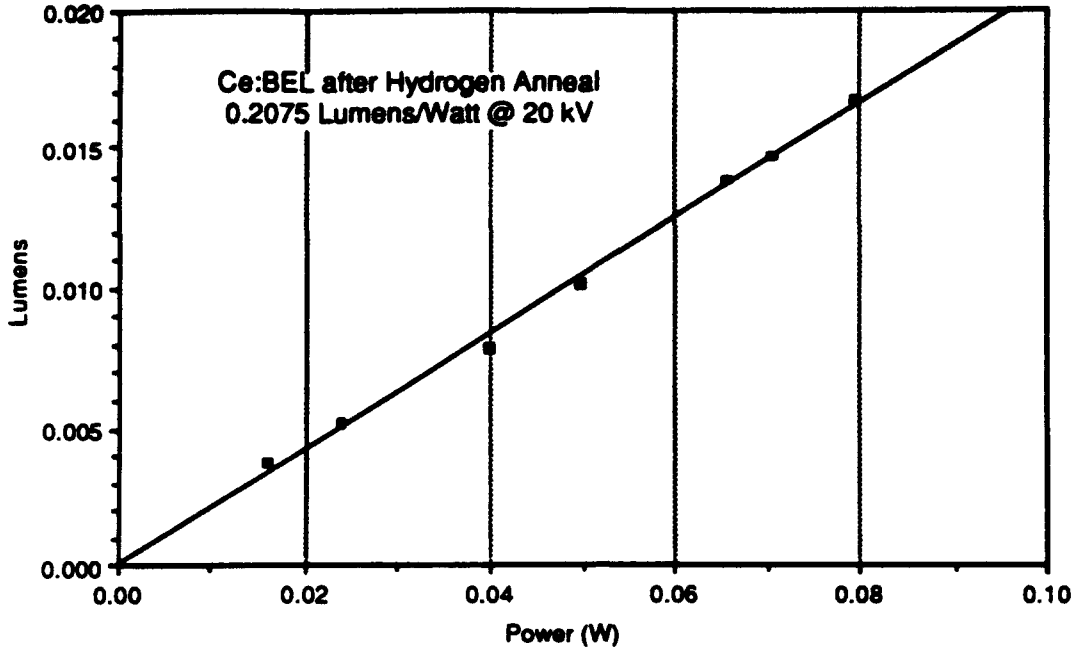

Fig. 3.4.1.2. Cathodoluminescent efficiency of Ce:BEL after hydrogen anneal.

3.4.2 Ce:Y_2SiO_5 and Ce:Gd_2SiO_5

Fig. 3.4.2.1 shows the cathodoluminescent spectrum of the blue emitting cerium activated phosphor Ce:Y_2SiO_5. Since the spectrum of Ce:Y_2SiO_5 peaks at about 390 nm, much of its light output is not visible, reducing its efficiency. The similar phosphor Ce:Gd_2SiO_5 has a spectrum which peaks at 430 nm.

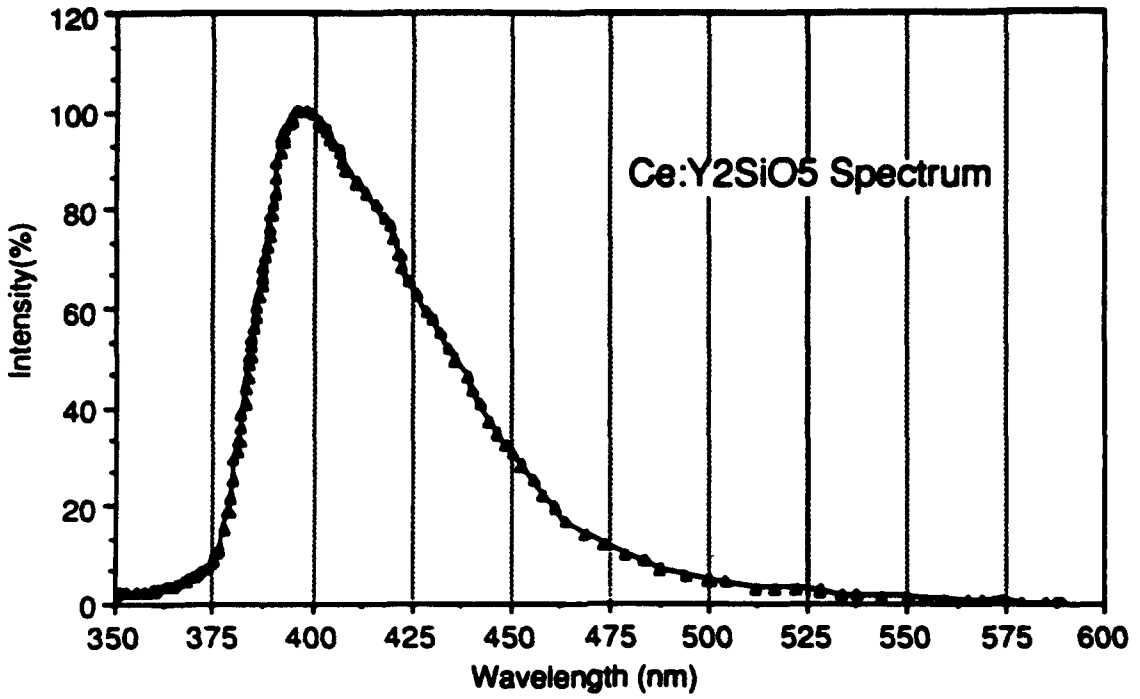

Fig. 3.4.2.1. Cathodoluminescent spectrum of the blue emitting cerium activated phosphor Ce:Y_2SiO_5.

4.0.0 SCALE-UP CONSIDERATIONS

Table 4.0.0.1 summarizes the actual performance of two inch Ce:YAG faceplates and the predicted performance of three and four inch faceplates.

Table 4.0.0.1. Performance data for Ce:YAG faceplates.

	Demonstrated (2")	Predicted (3")	Predicted (4")
Faceplate Luminance, fL	62,700	86,750	86,750
Faceplate Efficiency, L/W	4.84	4.84	4.84
Raster Size, in^2 (cm^2)	1 (6.45)	3.63 (23.4)	5.88 (37.9)
Beam Power, W	90	413	413
Beam Power Density, W/cm^2	14	18	10.9
Faceplate Output, L	435	2000	2000

4.1.0 Crystal Growth Process of Substrate Wafers

The Czochralski method has produced YAG crystal up to three inches in diameter. Experience indicates that four inch crystal is a possibility, but only by a flat interface technique pioneered at Allied-Signal. However, a considerable development effort would be required to attain a process for the Czochralski growth of four inch YAG.

The Heat Exchanger Method (HEM™) is being used for the commercial production of 10" diameter sapphire crystals of very high quality. The growth of YAG crystal to this diameter appears possible. These melting point of YAG (1950°C) is lower than that for Al_2O_3 (2040°C): therefore, current HEM™ furnaces are adequate for growing this crystal. In the case of sapphire (Al_2O_3) crystals grown by HEM™, the processing is carried out under vacuum; however, it is expected that even though the host phosphor materials may be stable under vacuum, it may be necessary to control the atmosphere during growth of doped crystals. The candidate phosphor materials are compatible with using a moybdenum crucible and graphite resistance heat zone of the HEM™ furnace so that these crystals can be grown with existing HEM™ furnaces. In the case of BEL, it would be necessary to set up additional safety procedures for handling BeO raw material and BEL crystals because of their toxic nature.

Crystal Systems Inc. (Dr. Chandra P. Khattak, 27 Congress Street, Salem, MA 01970, Telephone (508)-744-5059) is proposing a program for development of the HEM™ method for crystal growth of candidate phosphor materials. The first phase is a feasibility phase followed by the development phase. During the feasibility stage it is intended to develop procedures so that the growth characteristics of these materials can be established. Crucibles approximately two inches in diameter would be utilized for this effort. It is expected that single crystal material samples would be available for testing for high resolution, high brightness video projection CRT applications. Close cooperation would be maintained with the user so that optimization of this material for the application can be achieved. The problems involved with growth of larger crystals would also be identified during this phase. The development phase will be undertaken depending upon the results of the feasibility phase.

Crystal Systems Inc. expects that the feasibility phase could be completed in approximately a six-month time frame. The cost of their effort would be $50,000 per candidate phosphor material. This cost does not include the raw materials, installation of additional safety features required for beryllium crystal growth, or crystal characterization.

4.2.0 Optical Fabrication

Since the semiconductor industry is now fabricating wafers up to ten and twelve inches in diameter, it is concluded that wafer fabrication will not constrain the development of large diameter single crystal faceplates.

4.3.0 Liquid Phase Epitaxy

Liquid phase epitaxy is routinely carried out for wafers up to three inches in diameter in the preparation of magneto-optical materials. These wafers, however, are thin (0.020 inch) compared with YAG faceplate wafers (0.125 inch). Generally, a slower withdrawal rate from the epitaxy furnace is required for these thick wafers. Liquid phase epitaxy has been demonstrated on four-inch diameter by 0.020 inch thick wafers. There appears to be no fundamental size limitation for the liquid phase epitaxy process.

4.4.0 Photoreticulation

Since the semiconductor industry is now fabricating wafers up to ten and twelve inches in diameter, it is concluded that this processing step will not constrain the development of large diameter single crystal faceplates.

5.0.0 COST ESTIMATES

The following cost estimates for the production of 100 and 200 faceplates per year are calculated on the basis of minimal dedicated facilities being constructed to accomplish each step necessary for the production of faceplates at these quantities. At the 100 and 200 faceplate per year levels, such minimal facilities would still be significantly under-utilized, and the cost per faceplate is high. Section 5.5.0 below contains estimates of faceplate cost with the assumption of 100% utilization of facilities. These costs for 100% utilization will be lower that those which can be anticipated from tolling these steps to outside vendors, perhaps by as much as 25%.

5.1.0 Crystal Growth Process of Substrate Wafers

The following table is an estimate of cost per wafer of substrate wafer growth for three inch and four inch diameter wafers at a 100 and 200 wafer per year production level. Note that the facility is not fully utilized at even the 200/year level.

Cost of YAG Substrate Wafer Crystal Growth at 100% and 80% Yield for Dedicated Facility (maximum facility utilization at 400 faceplates/year)

	Three-Inch Wafers		**Four-Inch Wafers**	
	100/year	**200/year**	**100/year**	**200/year**
Capital Equipment (5 yr. amort.)	500	250	700	350
Laboratory Facility	600	300	600	300
Materials	150	150	300	300
Fabrication & Maintenance	35	35	50	50
Labor & Employee Overhead	175	175	225	225
Electrical Power	25	25	30	30
Environmental/Toxic Disposal	20	20	30	30
Cost per Wafer at 100% Yield	1505	955	1935	1285
Cost per Wafer at 80% Yield	**1881.25**	**1193.75**	**2418.75**	**1606.25**

5.2.0 Fabrication

The following table is an estimate of cost per wafer of substrate wafer polishing for three inch and four inch diameter wafers at a 100 and 200 wafer per year production level. Note that the facility is not fully utilized at even the 200/year level.

Cost of Wafer Polishing at 100% and 80% Yield for Dedicated Facility (maximum facility utilization at 800 faceplates/year)

	Three-Inch Wafers		Four-Inch Wafers	
	100/year	200/year	100/year	200/year
Capital Equipment (5 yr. amort.)	400	200	450	225
Laboratory Facility	600	300	600	300
Supplies	20	20	25	25
Maintenance	5	5	5	5
Labor & Employee Overhead	50	50	50	50
Environmental/Toxic Disposal	10	10	15	15
Cost per Wafer at 100% Yield	1085	585	1145	620
Cost per Wafer at 80% Yield	**1356.25**	**731.25**	**1431.25**	**775**

5.3.0 Liquid Phase Epitaxy

The following table is an estimate of cost per wafer of phosphor epitaxy for three inch and four inch diameter wafers at a 100 and 200 wafer per year production level.

Cost of Unreticulated Epitaxial Phosphor Faceplates at 100% and 50% Yield for Dedicated Facility (maximum facility utilization at 200 faceplates/year)

	Three-Inch Wafers		Four-Inch Wafers	
	100/year	200/year	100/year	200/year
Capital Equipment (5 yr. amort.)	600	300	750	375
Laboratory Facility	600	300	600	300
Materials (less substrate wafer)	160	180	220	245
Fabrication & Maintenance	15	15	20	20
Substrate Wafer	1115	1115	1485	1485
Labor & Employee Overhead	175	175	225	225
Electrical Power	40	20	60	30
Environmental/Toxic Disposal	20	15	25	20
Cost per Wafer at 100% Yield	2725	2120	3385	2700
Cost per Wafer at 50% Yield	**5450**	**4240**	**6770**	**5400**

5.4.0 Photoreticulation

The following table is an estimate of cost per wafer of wafer reticulation for three inch and four inch diameter wafers at a 100 and 200 wafer per year production level. Note that the facility is not fully utilized at even the 200/year level.

Cost of Faceplate Reticulation at 100% and 80% Yield for Dedicated Facility (maximum facility utilization at 1000 faceplates/year)

	Three-Inch Wafers		Four-Inch Wafers	
	100/year	200/year	100/year	200/year
Capital Equipment (5 yr. amort.)	1150	575	1150	575
Laboratory Facility	800	400	800	400
Supplies (Chemicals, Photomasks)	400	200	450	225
Labor & Employee Overhead	60	60	75	75
Environmental/Toxic Disposal	20	15	25	20
Cost per Wafer at 100% Yield	2430	1250	2500	1295
Cost per Wafer at 80% Yield	**3037.5**	**1562.5**	**3125**	**1618.75**

5.5.0 Cost Summary

The following table is an estimate of cost per wafer of fully processed faceplates of three inch and four inch diameter at a 100 and 200 wafer per year production level. Note that these cost include idle equipment/workspace expenses at even the 200/year level.

Summary Costs of Epitaxial Phosphor Faceplates for Dedicated Facility

	Three-Inch Wafers		Four-Inch Wafers	
	100/year	200/year	100/year	200/year
Cost per Unreticulated Faceplate	**5450**	**4240**	**6770**	**5400**
Cost of Reticulation	3037.5	1562.5	3125	1618.75
Cost per Reticulated Faceplate	**8487.5**	**5802.5**	**9895**	**7018.75**

The following table is an estimate of cost per wafer of fully processed faceplates of three inch and four inch diameter at a 100% utilization of facilities.

Summary Costs of Epitaxial Phosphor Faceplates for 100% Facility Utilization

	Three Inch	Four Inch
YAG Wafer Crystal Growth	850	1200
YAG Wafer Polishing	265	285
Bare YAG Wafer Ready for Epitaxy	1115	1485
Epitaxial Phosphor Faceplate (Unreticulated)	4240	5400
Photoreticulation	600	650
Reticulated Epitaxial Phosphor Faceplate	4840	6050

6.0.0 RECOMMENDATIONS AND CONCLUSIONS

Ce:YAG epitaxial phosphor faceplates are capable of 2000 lumens light output in either their reticulated or facet-textured form in a 2.75-inch diagonal raster. Higher light outputs can be obtained from larger diameter faceplates, but the largest available YAG crystals are presently three-inches in diameter. Single crystals of YAG greater than three inches in diameter can be obtained only after a further development of either the Czochralski or HEM™ techniques.

Wafer flatness is a requirement for photolithographic reticulation over a large diameter faceplate. Epitaxy requires a surface which is free of even the smallest scratch or defect. Thus, polishing of YAG wafers to higher flatness and perfection would be a suitable area for research.

The reticulation process involves etching in hot phosphoric acid. A rapid etching rate has to be used to effect the reticulation before the etching mask is dissolved. This technique is marginally successful, and defects are introduced into the faceplate as the mask is undercut in some areas. Further research on alternative masking materials and etching methods is necessary.

Reticulation is most effective when there is a minimum in the ratio of the mesa top to bottom area, but this pointed reticulation gives "ghost" images of the raster in the six-fold symmetry of the reticulation. This "ghosting" effect must still be quantified.

Ce:$Gd_3Al_5O_{12}$ (Ce:GdAG, red), Ce:$Y_3Al_5O_{12}$ (Ce:YAG, green), and Ce:$La_2Be_2O_5$ (Ce:BEL, blue), appear to be an appropriate trio of epitaxial phosphors for a high intensity color projection display. Ce:BEL has not as yet been bonded to a CRT neck assembly, so that its suitability as a faceplate material is still unknown. Research on such bonding would be appropriate.

The growth of large crystals of $Gd_3Al_5O_{12}$ as substrates for epitaxial red phosphor faceplates would be a suitable area for research.

Further research on alternative masking materials and etching methods, and quantification of the reticulation "ghosting effect, is also required.

Ce:$Gd_3Al_5O_{12}$ (Ce:GdAG, red), Ce:$Y_3Al_5O_{12}$ (Ce:YAG, green), and Ce:$La_2Be_2O_5$ (Ce:BEL, blue), appear to be an appropriate trio of epitaxial phosphors for a high intensity color projection display. The growth of large crystals of $Gd_3Al_5O_{12}$ as substrates for epitaxial red phosphor faceplates would be a suitable area for research.

The HEM™ method seems to be the most appropriate path to large diameter crystals. This would require further development, as proposed by Crystal Systems, Inc.

7.0.0 REFERENCES.

1. M.W. van Tol and J. van Esdonk, IEEE Trans. Electron Devices **ED-30**, 193 (1983).
2. J.M. Robertson and M.W. van Tol, Appl. Phys. Lett. **37**, 471 (1980).
3. W.F. van der Weg and M.W. van Tol, Appl. Phys. Lett. **38**, 705 (1981).
4. J.M. Robertson and M.W. van Tol, Phys. Stat. Sol. (a) **63**, K59 (1981).
5. G.W. Berkstresser, et al., J. Elctrochem. Soc. **135**, 1302 (1988).
6. U. Levy and H.H. Yaffe, SID International Symposium Digest, 1984, p. 336 ff.
7. H.J. Levinstein, et al., Appl. Phys. Lett. **19**, 486 (1971).
8. D.M. Gualtieri, J. Appl. Phys. **50**, 2170 (1979).
9. D.M. Gualtieri, P.F. Tumelty, and M.A. Gilleo, J. Appl. Phys. **52**, 2335 (1981).
10. D.M. Gualtieri and P.F. Tumelty, J. Appl. Phys. **53**, 2489 (1982).
11. J.A. Burton, R.C. Prim, and W.P. Slichter, J. Chem. Phys. **21**, 1987 (1953).
12. P.F. Bongers, et al., U.S. Patent No. 4,298,820 (1981).
13. D.M. Gualtieri, et al., U.S. Patent No. 4,728,178 (1988).
14. D.T.C. Huo and T.W. Hou, J. Electrochem. Soc. **133**, 1492 (1986).
15. B. Strocka, J. Appl. Phys. **60**, 2977 (1986).
16. C.F. Cline and R.C. Morris, U.S. Patent No. 3,866,142 (1975).
15. T. Utsu and S. Akiyama, Eighth American Conference on Crystal Growth (Vail, Colorado, July 1990), Abstract No. 81a.

[redacted]

By: [redacted]

SEPTEMBER 24, 1990

September 26, 1990

TEST DATA

3M320 YAG S/N 154871

YAG: 00606-1-1 1

ANODE: 25KV G2 = 1000V G1 = 106.7V

1" X 1" RASTER SIZE

IB2	EMOD[4]	H. SCAN[2]	Brightness[3]
10μA	28.1V	.0026	176 fL.
100μA	44.6V	.0028	1,506 fL.
250μA	56.6V	.0034	3,300 fL.
500μA	68.8V	.0064	5,500 fL.
1000μA	83.8V	.0093	9,600 fL.

Breakdown: Good

Leakage: Good

1. The cutoff voltage is the Grid No. 1 to Cathode voltage required for visual extinction of an undeflected focused spot. This is accomplished by adjusting the Grid 1 control.

2. The line width is measured at the center of the CRT, using the method slit scan.

3. Area brightness of a raster having the size indicated and the measurement taken with a photometer with a photometric response curve. The photometer shall have a photometric response curve and an acceptance area is sufficiently large to measure several adjacent scan lines. The raster is generated using a horizontal frequency of 15,750Hz and a vertical frequency of 60Hz. (Initial brightness without filter shall be 1,000 Ft.L.)

4. Is the difference between the recorded cutoff voltage and the voltage at the indicated conditions.

September 26, 1990

TEST DATA

3M320 YAG S/N 154988

YAG: 00608-1-1 1

ANODE: 25KV G2 = 1000V G1 = 96.9V

1" X 1" RASTER SIZE

IB2	EMOD[4]	H. SCAN[2]	Brightness[3]
10µA	17.5V	.0023	144 fL.
100µA	37.3V	.0030	1,430 fL.
250µA	56.9V	.0040	3,660 fL.
500µA	75.1V	.0059	6,720 fL.
1000µA	91.4V	.0070	10,600 fL.

Breakdown: Good

Leakage: Good

19808/SS S.N.S-1668 Date: 9/21/90 Photo Research Mod VI Multiplot

File #	Description (one line)	Date	Max.	Min.	F1	F2
27	3M320YAG-154871 @25KV-25UA (1"X1" SIZE)	9/21/90	3.730e-02	1.001e-04	0	3.720e-04

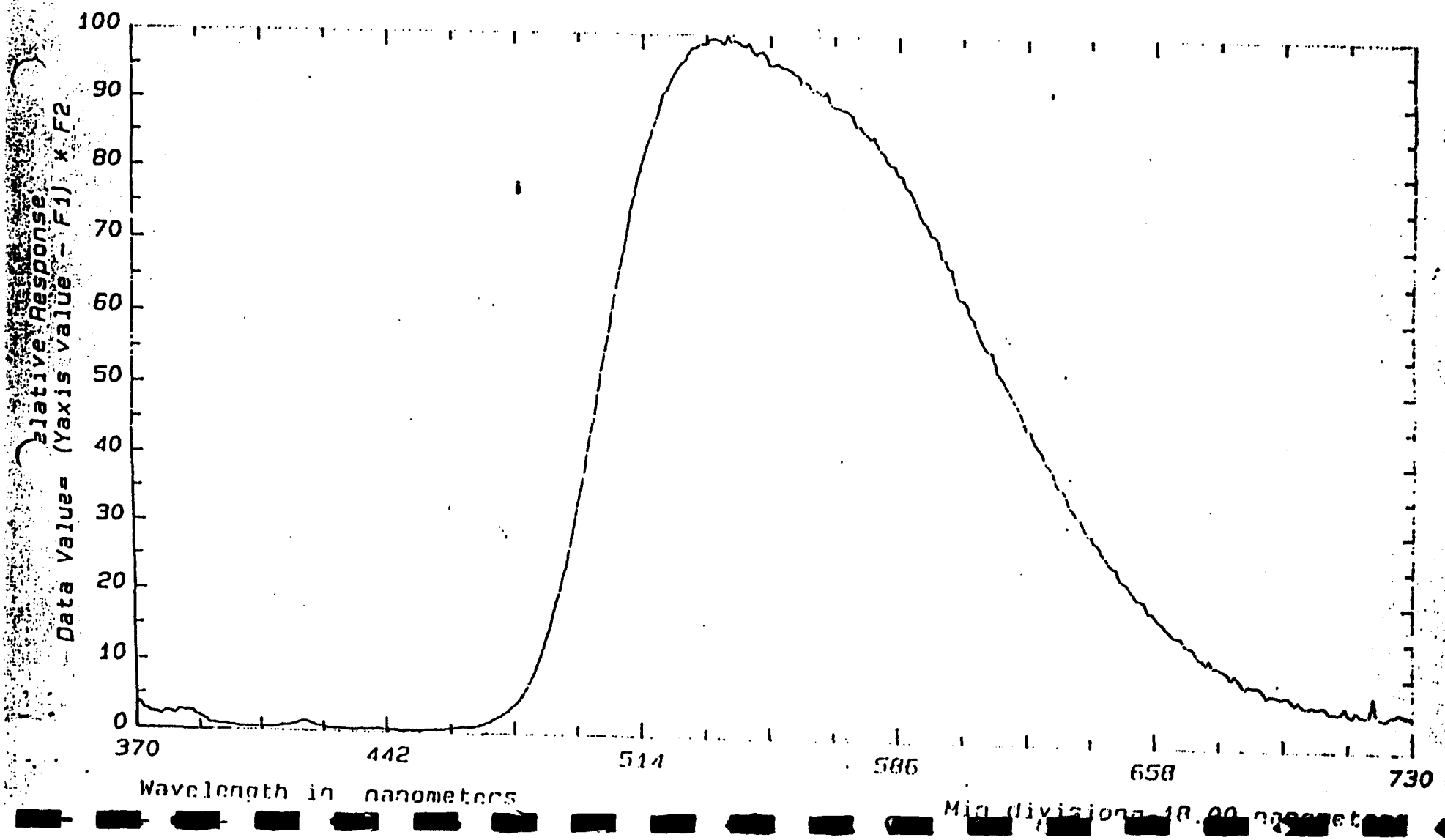

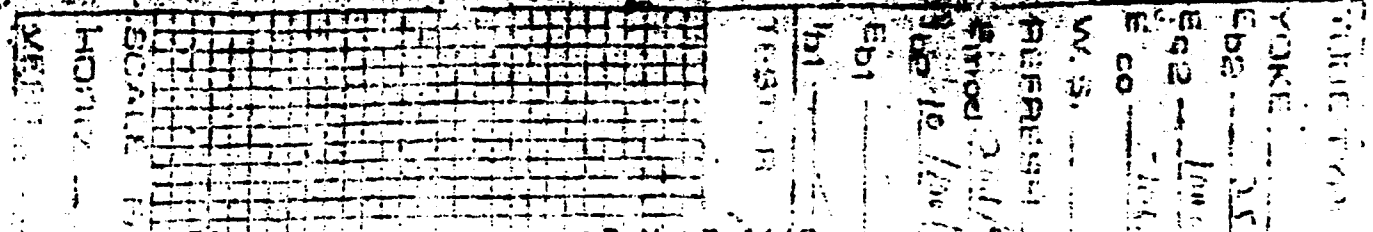

Date: 9/21/90 S.N. S-1668
Measurement description:
MS20Y8G-154871 @25KV-25UA (1"X1" SIZE)

Data type:	Radiance.
Lens/Acces. used:	OL-7
Measuring field:	20 minutes
Front Filter:	OPEN
Rear Filter:	OPEN
Lower Wavelength:	370 nm
Upper Wavelength:	730 nm
Wavelength Interval:	1 nm
Spectral Bandwidth:	1 nm
Scan speed/mode:	Fast

R A D I O M E T R I C D A T A :

(370 to 730-nm)

Integrated Radiance= 4.4364E 00 Watts/Ster*m^2

Photon Radiance= 1.2826E 19 Photons/Ster*m^2*s

Luminous Efficiency= 4.5934E 02 Lumens/Watt

P H O T O M E T R I C D A T A :

Luminance= 6.0150E 02 FootLamberts, or,
2.0609E-03 Cd/m^2

C H R O M A T I C I T Y D A T A :

CIE 1931: X= 1.5011E-03 x= 0.4049
Y= 2.0609E-03 y= 0.5559
Z= 1.4516E-02 z= 0.0392

CIE/UCS 1960: u = 0.1828 v = 0.3764

CIE/UCS 1976: u' = 0.1828 v' = 0.5646

Correlated Color Temperature is out of range

THOMAS ELECTRONICS

CRT ELECTRON BEAM ENERGY DISTRIBUTION PROFILE Center - L/R

TUBE TYPE 3M32G YAG · S/N 13481 DATE 9/20/90

YOKE _____

E_{b2} 25 KDC

E_{c2} 1000 vDC

E_{co} -106.7 vDC

W. S. _____ in/sec

REFRESH _____ Hz

Emod 28.1/44.6/56.6 vDC

I_{b2} 10/100/250 µA

E_{b1} _____ vDC

I_{b1} _____ µA

TESTER B.A

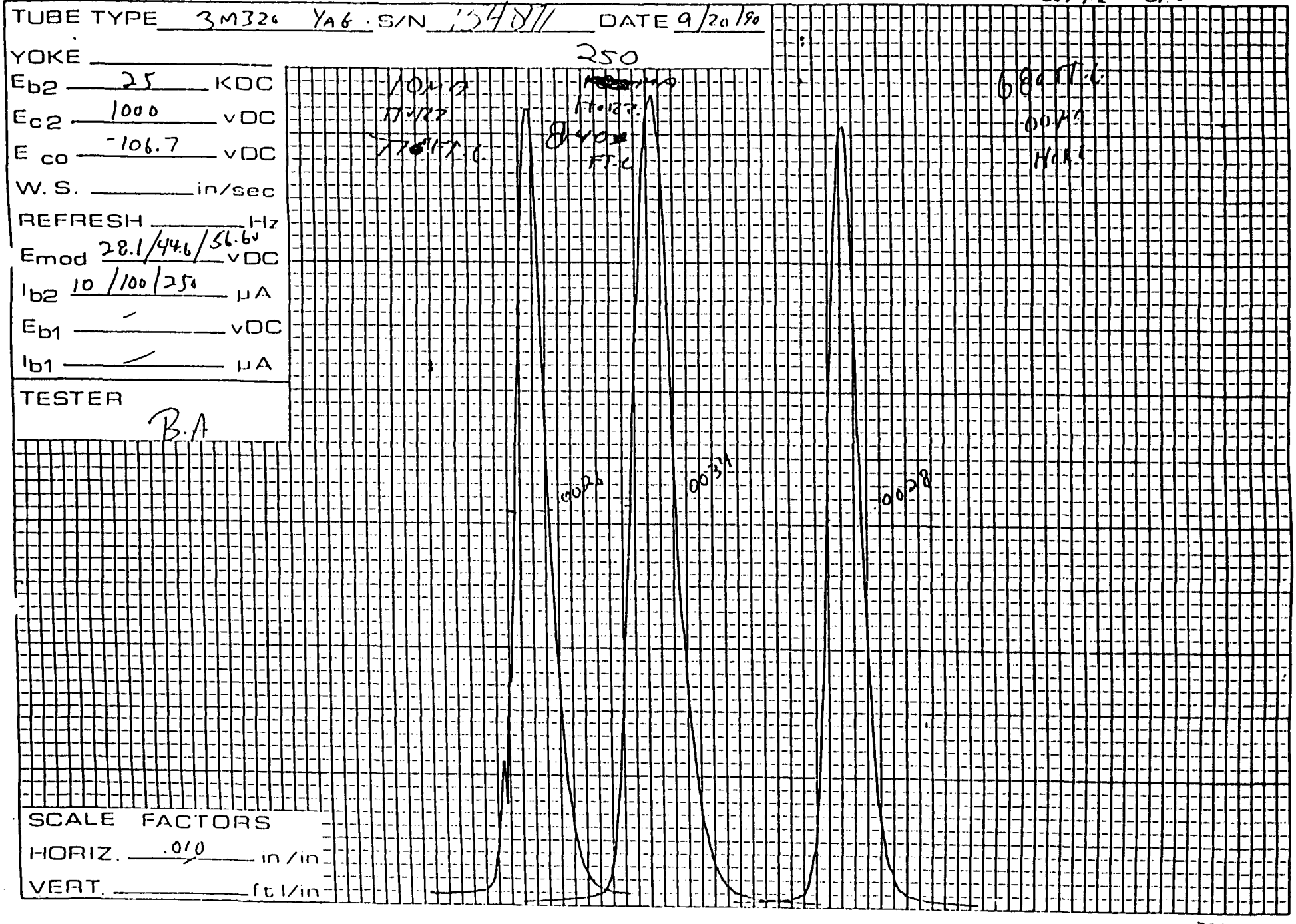

SCALE FACTORS

HORIZ. .010 in/in

VERT. _____ ft l/in

701-2035

CRT ELECTRON BEAM ENERGY DISTRIBUTION PROFILE center - c/c

TUBE TYPE 3M32o YA6 S/N 15487 DATE 9/20/90

YOKE _____

E_{b2} 25 KDC

E_{c2} 1000 vDC

E_{co} -106.7 vDC

W. S. _____ in/sec

REFRESH _____ Hz

Emod 68.8/83.8 vDC

I_{b2} 500/1000 µA

E_{b1} _____ vDC

I_{b1} _____ µA

TESTER R.A.

SCALE FACTORS

HORIZ. .010 in/in

VERT. _____ ft.l/in

19808/SS S.N.S-1668 Date: 9/21/90 Photo Research Mod VI Multiplot

File #	Description (one line)	Date	Max.	Min.	F1	F2
26	3M320YAG -154988 @25KV--(25UA) 1"X1" SIZE	9/21/90	2.748e-02	7.595e-05	0	2.748e-04

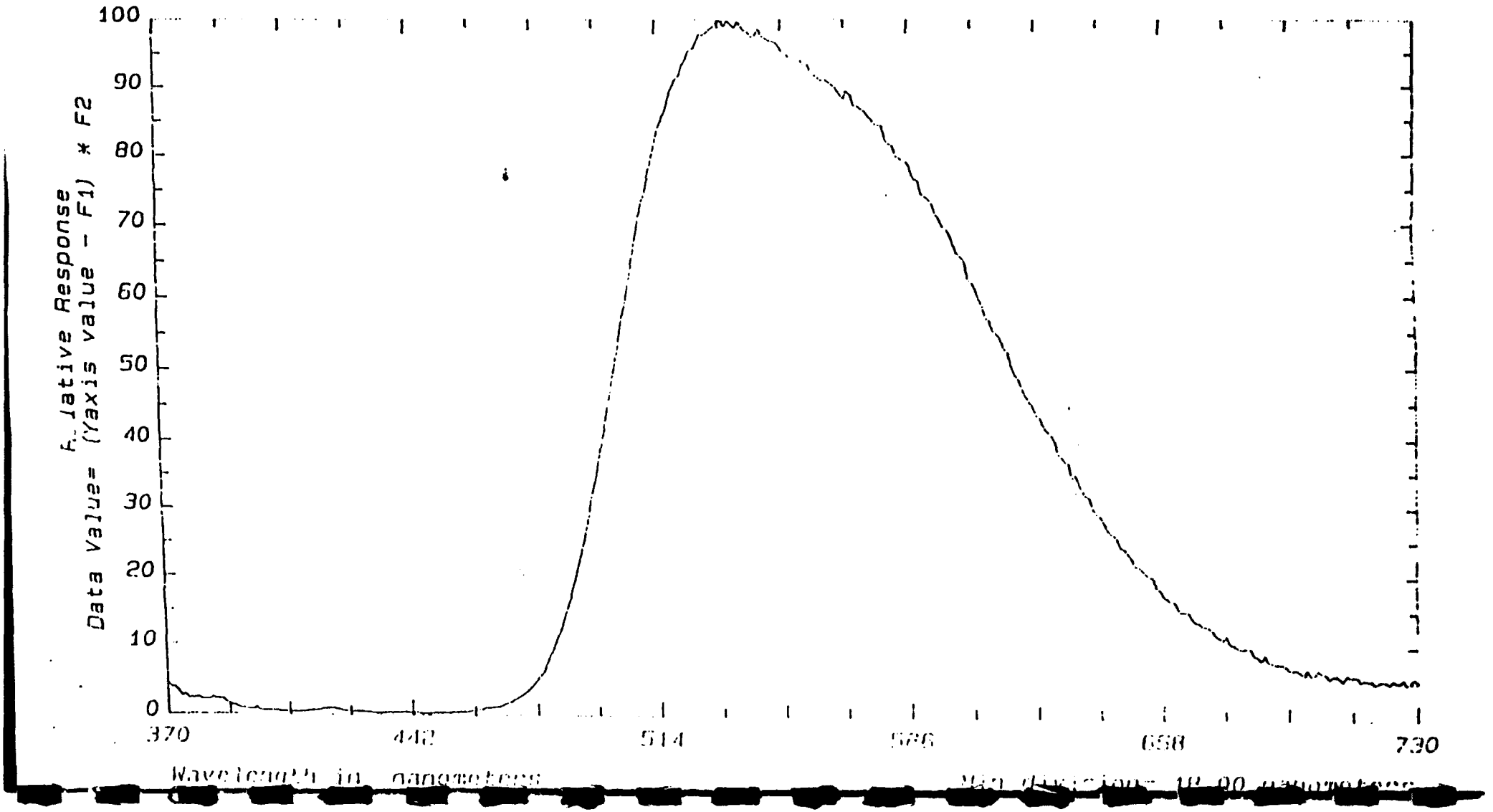

Date: 9/21/90 S.N. S-1668

Instrument description:
R820/AG - 154983 @25KV-(200A) 1"X1" SIZE

Data type: Radiance.
Lens/Acces. used: CL-7
Measuring field: 20 minutes
Front Filter: OPEN
Rear Filter: OPEN
Lower Wavelength: 370 nm
Upper Wavelength: 730 nm
Wavelength Interval: 1 nm
Spectral Bandwidth: 1 nm
Scan speed/mode: Fast

RADIOMETRIC DATA

380 to 780 nm

Integrated Radiance= [illegible] Watts/Ster*m^2

Photon Radiance= [illegible] Photons/Ster*m^2*s

Luminous Eff. [illegible] Lumens/Watt

PHOTOMETRIC DATA

Luminance= [illegible] footLamberts, or [illegible] Cd/m^2

COLORIMETRIC DATA

CIE 1931: X= [illegible] x= 0.1621
Y= [illegible] y= 0.2564
Z= [illegible] z= 0.[illegible]

CIE/UCS 1960: u = 0.1[illegible] v = 0.3753

CIE/UCS 1976: u'= 0.1212 v'= 0.5641

Correlated Color Temperature is out of range

CRT ELECTRON BEAM ENERGY DISTRIBUTION PROFILE center - c/w

TUBE TYPE 3M32D YA6 S/N 154 988 DATE 9/20/91

YOKE _____

E_{b2} 25 KDC

E_{c2} 1000 vDC

E_{co} -96.9 vDC

W. S. _____ in/sec

REFRESH _____ Hz

E_{mod} 17.5 / 37.3 / 56.9 vDC

I_{b2} 10 / 100 / 250 µA

E_{b1} _____ vDC

I_{b1} _____ µA

TESTER B.A.

SCALE FACTORS

HORIZ. .010 in / in.

VERT. 11.1/in.

701-2031

CRT ELECTRON BEAM ENERGY DISTRIBUTION PROFILE

TUBE TYPE 3M320 Y16 S/N 154988 DATE 9/20/90

YOKE

E_{b2} 25 KDC

E_{c2} 1000 vDC

E_{co} -96.9 vDC

W. S. in/sec

REFRESH Hz

Emod 75.1 / 91.1 vDC

I_{b2} 500 / 1000 µA

E_{b1} vDC

I_{b1} µA

TESTER

SCALE FACTORS

HORIZ. in/in.

VERT. µA/in

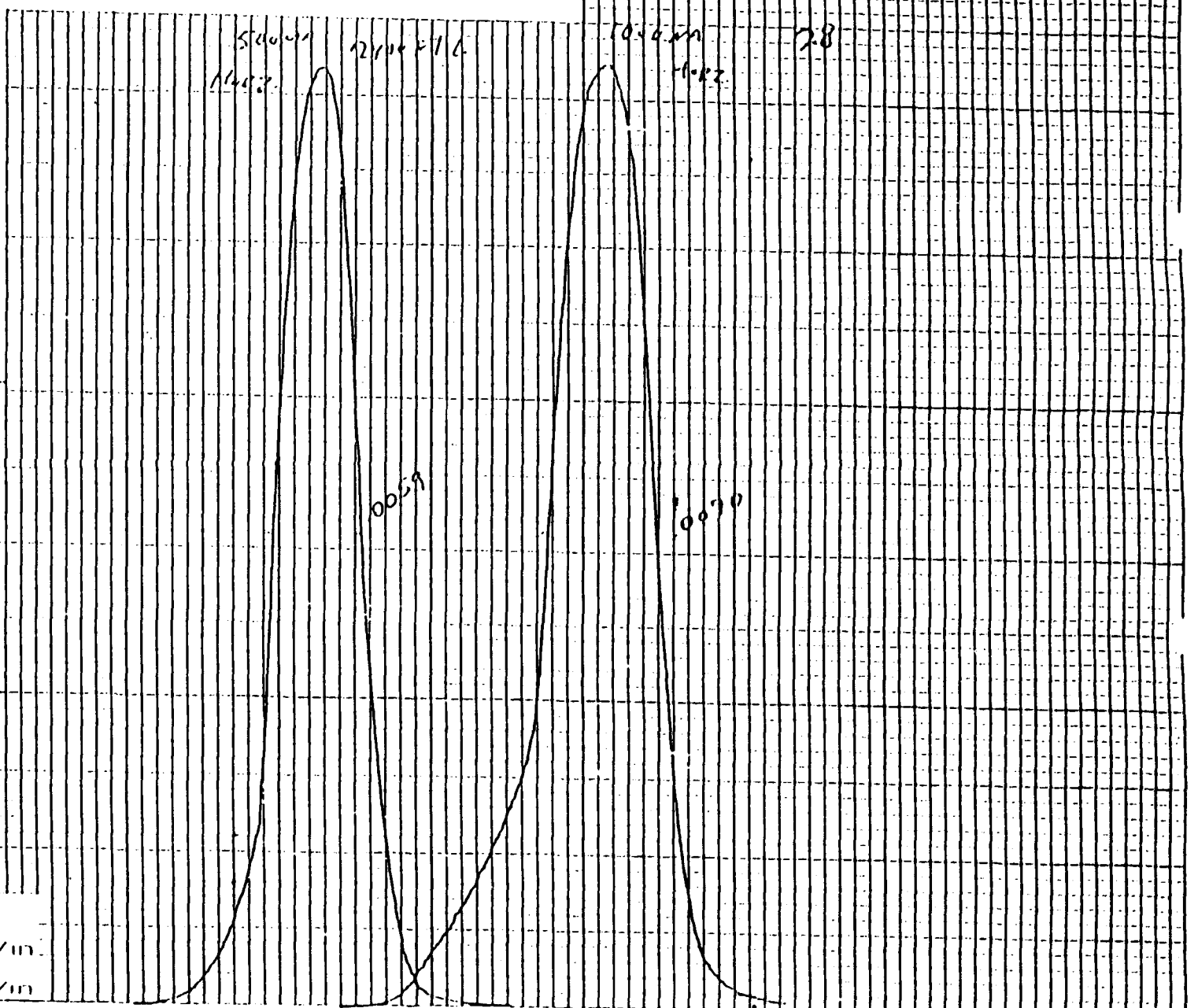

701-203C

ENCLOSURE 1(3)

CRT COOLING ANALYSIS

BY: TRIDENT INTERNATIONAL, INC.

HEAT EXCHANGER
150 CFM AIR

CRT HEAT LOSS CALCULATION
SINGLE CRYSTAL FACE PLATE CRT

COOLING GEOMETRY CONSIST OF THE FOLLOWING:
A.) FIN HEAT EXCHANGER
B.) CRT MOUNT, CHASSIS
C.) CYLINDER BODY OF EXCHANGER
D.) INSULATED WINDOW AREA

FLUID TEMPERATURE CHARACTERISTIC Tf

EXCHANGER ROOT TEMP	70 C	ESTIMATED FOR ITERATION
AIR TEMP.	24 C	
Tf =(75+24)/2 + 273	320 DEG K	

KINEMATIC VISCOSITY	v	17.72 E-6 m^2/s
Ceff CONDUST.	k	0.0278W/m C
PRANDEL NO.	Pr	0.704

AIR AVALIABLE FOR COOLING:
THREE FANS EACH PRODUCING 200 CFM OF AIR.
OF THIS AIR 450 CFM WILL BE DELIVERED TO THREE CRTS.
THEREFORE EACH CRT WILL HAVE 150CFM FOR COOLING

150 CFM = 4320 IN^3/SEC
DUCT COOLING AREA 6 X 6 INCHES
VELOCITY OF AIR IN DUST 120 IN/SE = 3.06 m/s = u

FREE STREAM VELOCITY *u*
CHARACTERISTIC LENGTH x

		FIN EXCHANGER	CHASSIS MOUNT	CYLINDER	
CHRT LENGTH	R2-R1	.0533 m	DEPTH .152m	DIA	.094m
RENOLDS NO.		9213	26325		16233
NUSSELT NO. Nu		39.68	65.39		NA
Nu =.453(Re)^.5(Pr)^.33					
CONVECTION Ceff h		40.28 W/m^2 C	23.86W/m^2 C		22.18W/m^2 C
h=(2)Nu k/x				FIG 2.3	38=h*D/k
FIN EFF. Neff		93%	65%		NA
REFERENCE		FIG 2.1	FIG 2.2		
Lc=		.0265m	.206m		
R2c=		.0735m			
Am=		60.68E-6 m^2	.00131 m^2		
Ff=		0.192	0.887		

CONVECTION AREA
FIN EXCH.=5(2(PI)((R2c)^2-(R1)^2) CYL AREA=PI * DIA*LG
CHASSIS=2((2)LENGTH*DEPTH)

	.1005m^2	.0336m^2	6.75E-3m^2

Q=Neff*Area*h*(To-Tu)
Q=(1/R) * (To-Tu)

1/R =	3.805 W/C	1.92W/C	.150W/C

Qt= (3.805+1.92+.150)*(To-Tu)
Qt=350
Tu= 24 C

CAL: To= 83.6 C

TABLE ; 1

CRT WALL TEMPERATURE
HEAT EXCHANGER

HEAT LOSS OF CRT TO HEAT EXCHANGER
SINGLE CRYSTAL FACEPLATE

COOLING GEOMETRY CONSIST OF THE FOLLOWING
A.) CRT IS SITTING HORIZONTAL
B.) THE SPACE BETWEEN CRT AND EXCHANGER IS ALL FLUID. d=.25 INCH
C.) STEADY STATE CONDITION IS PRESENT.
D.) FLUID PROPERTIES ARE EQUIVALENT TO ETHYLENE GLYCOL

FLUID TEMPERATURE CHARACTERISTIC Tf.

EXCHANGER ROOT TEMPERATURE.	83.6 C	
CRT GLASS TEMPERATURE.	117 C	ESTIMATED FOR ITERATION
Tf=(117+83.6)/2	100 C	

PROPERTIES

KINEMATIC VISCOSITY	v	2.03 E-6 m^2/s
Ceff CONDUST.	k	0.263W/m C
PRANDEL NO.	Pr	22.4
EXPANSION Ceff	B	.65E-3/C

GRADHOF NO.
Gr=9.8* B*(T1-T2)*d^3/v^2 Gr= 19804

THERMAL CONDUTIVITY
ke=k*(C (Gr Pr)^n * (L/d)^m ke= 1.42 W/m C
FOR CONSTANT SEE TABLE 2-3
HORIZONTAL ANNULUS

HEAT LOSS Q=PI*DIA*LG(ke/d)(T1-T2) Q=(T1-T2) (1/R)
d= GAP = .25 in
DIA= ID of HEAT EXCHANGER = 3.50 in
LG= LENGTH OF ALUMINUM MATERIAL IN CONTACT WITH LIQUID
LG= 1.95 in
1/R= 3.09
HEAT LOSS NEEDED
Q=350 Watts
THEREFORE TEMPERATURE AT CRT WALL
T1=197 C

CRT CALCULATED TEMP.

HEAT LOSS	TEMPERATURE
180 W	128 C
250W	170 C
350W	197C

TABLE 2

TABLE 3

Table 7-3 Summary of empirical relations for free convection in enclosures in the form of Eq. (7-60), correlation constants adjusted by Holman [74]

Fluid	*Geometry*	$Gr_\delta Pr$	Pr	$\frac{L}{\delta}$	C	n	m	*Ref(s).*
Gas	Vertical plate, isothermal	< 2000	$k_f/k = 1.0$					6, 7, 55, 59
		6000–200,000	0.5–2	11–42	0.197	$\frac{1}{4}$	$\frac{1}{4}$	
		200,000–1.1×10^7	0.5–2	11–42	0.073	$\frac{1}{3}$	$\frac{1}{3}$	
	Horizontal plate, isothermal, heated from below	< 1700	$k_f/k = 1.0$					
		1700–7000	0.5–2	—	0.059	0.4	0	6, 7, 55, 59, 62, 63,
		7000–3.2×10^5	0.5–2	—	0.212	$\frac{1}{4}$	0	66
		$> 3.2 \times 10^5$	0.5–2	—	0.061	$\frac{1}{3}$	0	
Liquid	Vertical plate, constant heat flux or isothermal	10^4–10^7	1–20,000	10–40	Eq. (7-50)	—	—	18, 61
		10^6–10^9	1–20	1–40	0.046	$\frac{1}{3}$	0	
	Horizontal plate, isothermal, heated from below	< 1700	$k_f/k = 1.0$					7, 8, 58, 63, 66
		1700–6000	1–5000	—	0.012	0.6	0	
		6000–37,000	1–5000		0.375	0.2	0	
		37,000–10^8	1–20		0.13	0.3	0	
		$> 10^8$	1–20		0.057	$\frac{1}{3}$	0	
Gas or liquid	Vertical annulus	Same as vertical plates						
	Horizontal annulus, isothermal	6000–10^5	1–5000	—	0.11	0.29	0	56, 57, 60
		10^5–10^8	1–5000	—	0.40	0.20	0	
	Spherical annulus	120–1.1×10^9	0.7–4000		0.228	0.226	0	43
						—	—	

CRT HEAT LOSS
SINGLE CRYSTAL FACEPLATE

EXCHANGER ROOT TEMP FOR FORCED CONVECTION

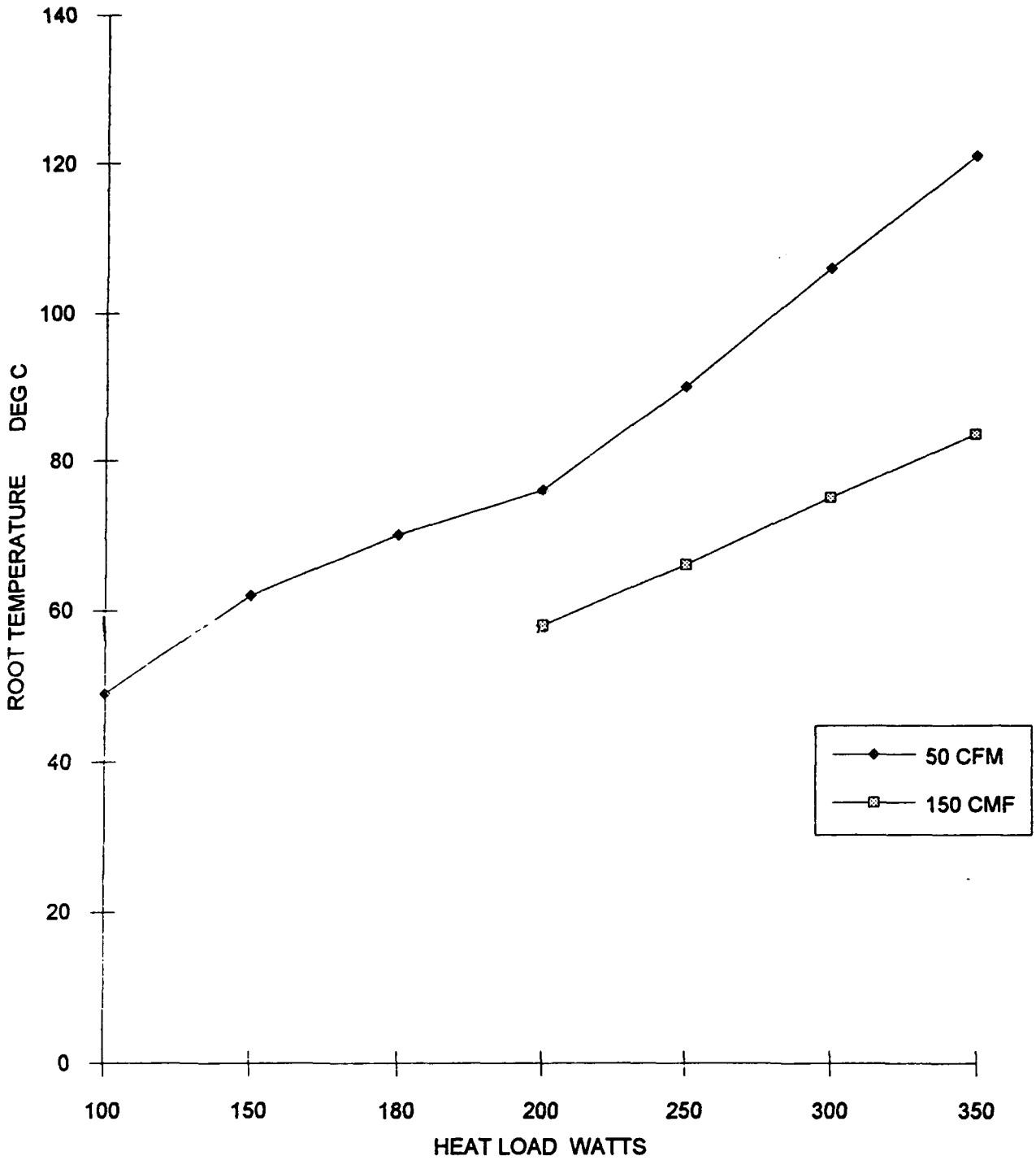

Fig. 2.1 Efficiencies of circumferential fins of rectangular profile, according to Ref. 3.

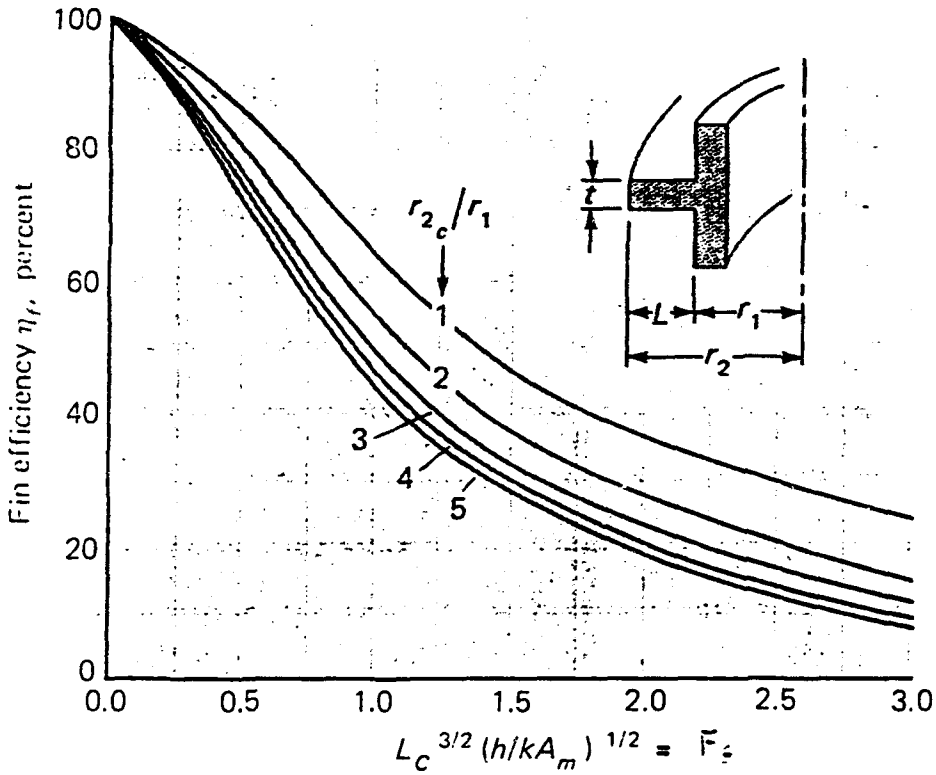

$L_c = L + \frac{t}{2}$

$r_{2c} = r_1 + L_c$

$A_m = t(r_{2c} - r_1)$

Fig. 2.2 Efficiencies of rectangular and triangular fins.

$$L_c = \begin{cases} L + \frac{t}{2} & \text{rectangular fin} \\ L & \text{triangular fin} \end{cases}$$

$$A_m = \begin{cases} tL_c & \text{rectangular fin} \\ \frac{t}{2}L & \text{triangular fin} \end{cases}$$

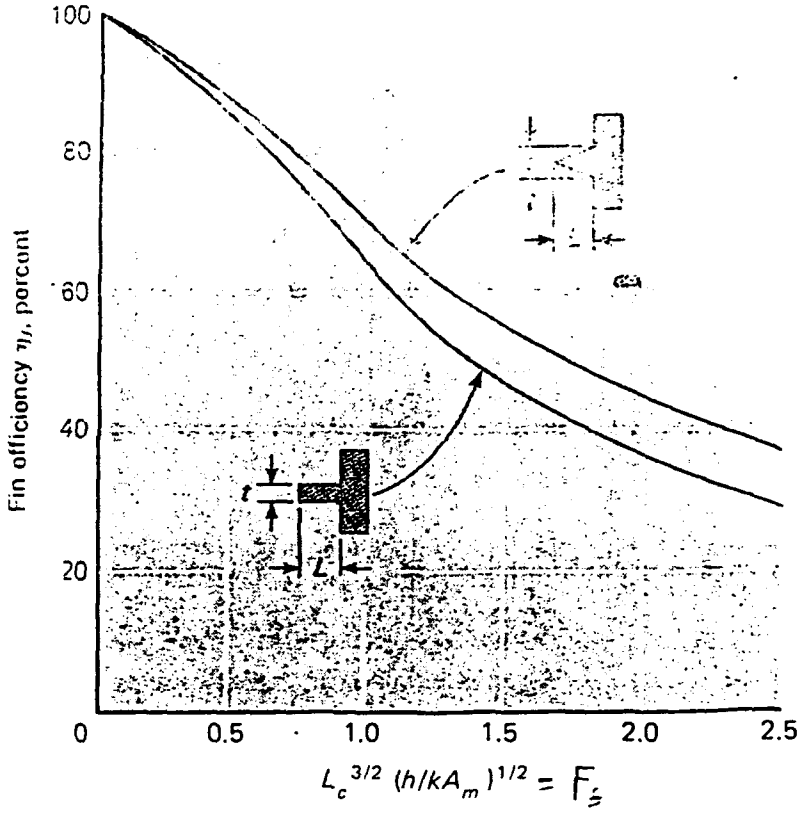

Fig. 2.3 Data for heating and cooling of air flowing normal to single cylinders, from Ref. 10.

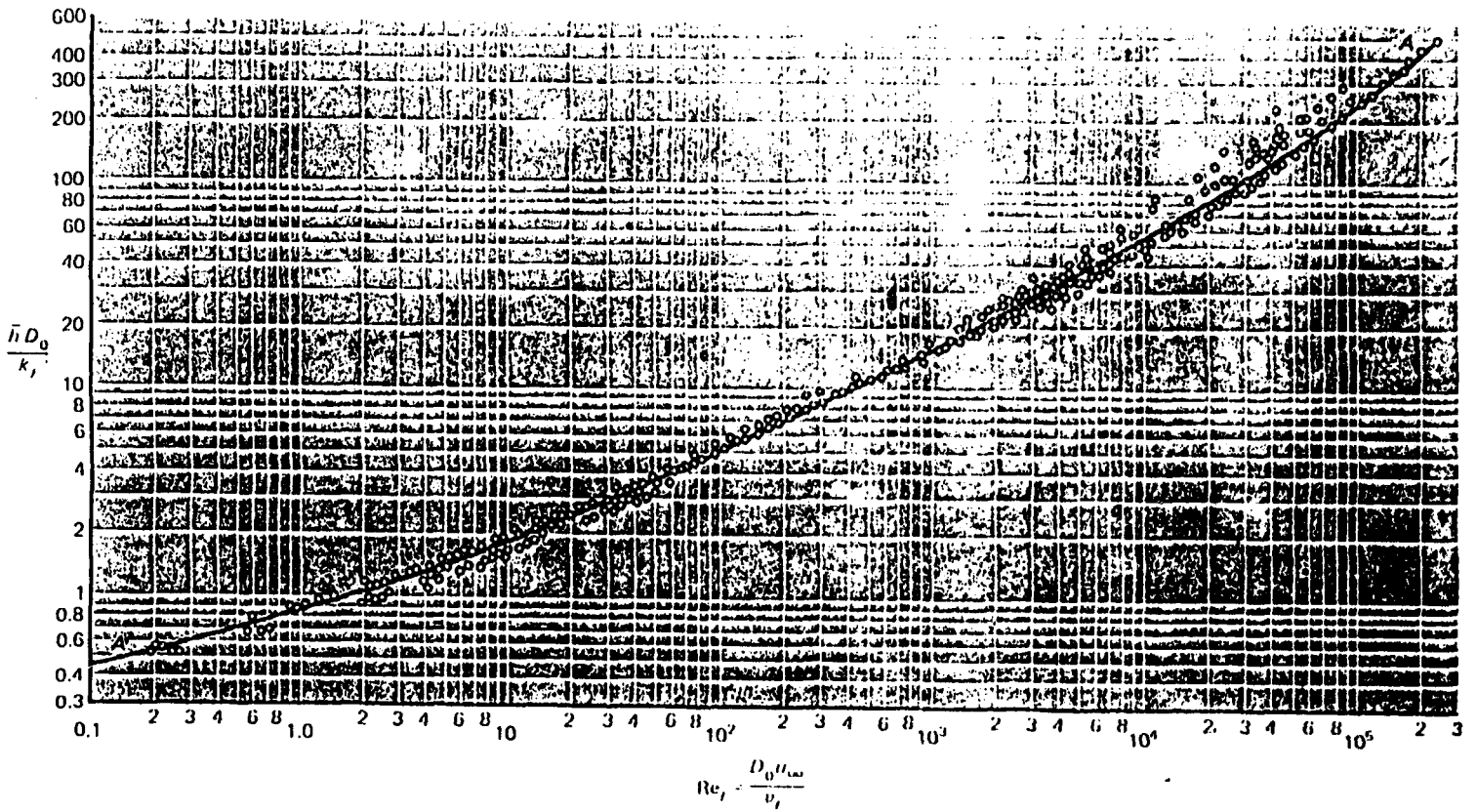

ENCLOSURE 11.5

FINAL REPORT

THE STUDY OF THE PERFORMANCE OF A YAG FACEPLATE

FEBRUARY 3, 1992

Prepared for:

TRIDENT INTERNATIONAL, INC.
Orlando, Florida

Final Report

THE STUDY OF THE PERFORMANCE OF A YAG FACEPLATE

February 3, 1992

Prepared by:

Eric H. Ford

OPTICAL RESEARCH ASSOCIATES
550 N. Rosemead Boulevard
Pasadena, California 91107
(818) 795-9101

1.0 BACKGROUND

Trident International, Inc (TII) has funded Optical Research Associates (ORA) to undertake a study to determine the effects on the performance of a CRT of a change in faceplate material from a relatively low index of refraction glass (Nd = 1.537) to Yttrium Aluminum Garnet (YAG) crystal with relatively high index (1.832). The two primary goals of the study are to (1) evaluate the effect of anti-reflection coatings in reducing reflection losses at the glass boundaries and halation effects and (2) to determine the optimum index matching fluid and analyze its effectiveness in producing an optically coupled system. Since ORA's primary area of expertise is optical design and optical system engineering, and not coating design, ORA sub-contracted the services of Bruce Reinbolt of Santa Barbara Applied Optics (SBAO) to perform the coating portion of the study.

2.0 PROJECTION SYSTEM CHARACTERISTICS

Since the phosphor is deposited or grown directly on the faceplate material, it is in optical contact with the faceplate, eliminating most of the losses in injecting the emitted energy into the faceplate material. However, since the phosphor emits over a wide angular range, a significant portion of the energy can fall outside of the critical angle of the faceplate material. For the older faceplate materials (index = 1.537), the critical angle is 40.6° into air. Energy at angles greater than 40.6° is "waveguided" (totally internally reflected through multiple bounces) radially out to the edge of the faceplate and lost to the system.

CRT projection systems commonly are designed for *f* numbers approaching F/1.0, and possibly faster. In addition, due to the geometry of typical projection systems, the required field of view is often 25° -30° half-angle, with an aperture stop location central to the projection lens to reduce distortion and aid field correction. As a result, chief ray angles (the "central" ray of the optical bundle) are often steep at the focal plane (phosphor surface). It is normal for the chief ray angle at the faceplate to exceed the object field chief ray angle for air-coupled systems, and for optically coupled systems, for the chief ray angle to be nearly twice as steep as the object field chief ray angle. Thus, for CRT projection systems with a half field projection angle of 25°, the chief ray angle at the phosphor would be greater than 50°, if it were in air, and is reduced to between 30° and 40° in the faceplate material. To this must be added the angle due to the *f* number of the lens system, bringing the steepest ray angle to greater than 70° equivalent in air or nearly 40° in the faceplate glass.

From this quick analysis, it can be seen that the CRT projection system works at very steep angles, and that air-glass boundaries can have a profound effect on the system performance. It also indicates the reason why optically coupled or fluid coupled systems are in use for projection systems. Fluids are often used to cool the CRT faceplate when very high luminous output is required. In order to reduce the angles at which rays enter the faceplate-coolant-window assembly, the strongly negative, rearmost field lens is used as the window of the coolant chamber. The steepest bundles from the edge of the field are incident upon the curved front surface of the field lens at an incidence angle much closer to normal than is the case with a flat coolant window. This benefits the transfer of energy, as the fluid then reduces the index difference between the faceplate and the adjacent lens (no glass to air boundary).

Several effects take place at the boundary of the faceplate and coolant fluid which affect system performance. These are all related to the reflection and scattering losses at the interface. Energy scattered or reflected at the faceplate/coolant boundary are manifested as halation of the image or as contrast decrease due to broad angle scattering. Halation is probably due to the first reflection from the boundary to the phosphor surface and back to the boundary, where it is mostly transmitted as a defocused image of the source. Optimization of the characteristics of this boundary is discussed in section 5.0.

3.0 OPTICAL EFFECTS OF YAG FACEPLATES

When the index of the faceplate is increased from the original 1.537 to that of YAG (1.832), the critical angle becomes approximately 33°. This would imply that a YAG faceplate in air would tend to put out significantly less power than a lower index faceplate, since the angular distribution of the energy inside the faceplate is similar, but the part which can pass through into the air is limited to 33° instead of the 40°+ of the lower index faceplate. Stating it differently, for the same *f* number optical system, the solid angle in the faceplate is smaller for the higher index material, and therefore, a smaller cone of the emitted energy is injected into the optical system. The magnitude of this decrease in screen irradiance is $N1^2/N_2^2 \approx 0.70$, or a drop of 30%.

This would only hold true if the source in both faceplates were perfectly matched to the faceplate index, so that no boundary was encountered in passing from the phosphor into the faceplate. However, if a boundary (differential index) exists, then the difference in screen irradiance would not be seen, as the source output characteristics would be modified equivalently to the lens *f* number, cancelling the effect.

It would seem that this effect is independent of whether the lens system is optically coupled or not and this would indicate that the optimum faceplate material is the one with the lowest possible index, in order to maximize the collected energy.

The effectiveness of fluids in coupling the faceplate to the optical system is also dependent on the faceplate index, with higher index fluids required to efficiently couple higher index faceplates. This will be discussed in more depth later in this report.

4.0 PROJECTION LENS SYSTEMS

In order to evaluate the effects of the high index faceplate material on the optical system, ORA requested that TII supply a typical lens system from an existing projection system to use for the analysis. TII forwarded a patent supplied by US Precision Lens Corporation to be used for this purpose. TII expressed interest primarily in optically coupled systems, in which the CRT faceplate is coupled to the lens system through the use of a index matching fluid.

ORA used the patent (U.S. Patent 4,900,139, included as Appendix A) to generate models of lens systems for analysis. Two different configuration were modeled: one with an air gap between the field lens and the flat faceplate/coolant assembly, and the other with the field lens in optical contact (through a fluid) with the faceplate. Both lenses from the patent were poorly corrected from the patent data, but were reoptimized by releasing the aspheric coefficients and several variable airspaces to hold first order properties (focus and magnification).

Figure 1 shows the optically coupled model and Figure 2 shows a projection lens with a flat window on the coolant chamber and an air gap to the field lens. Correction is significantly better with the second, air-spaced design due to the fact that it has three aspheric, plastic elements and an additional degree of freedom in the bending of the field lens. However, both are representative of types of lenses used in fast CRT projection systems. Ray angles are steeper in the faceplate for the optically coupled system, but incidence angles are shallower at the coolant window interface. These designs are used in the analysis which follows.

5.0 ANALYSIS OF YAG FACEPLATE PERFORMANCE

In order to reduce reflection loss at the YAG faceplate fluid interface, two approaches were investigated. This involved (1) varying the refractive index of the coolant fluid, or (2) coating the faceplate with a matching layer. It will be seen that either adding a matching

layer or increasing the index of the cooling fluid can reduce the reflection losses to that of the current 1.537 index faceplate systems or better.

The spectral performance of the original faceplates are calculated, as well as the performance of the YAG faceplates with various index fluids and coatings. The nomenclature used is as shown below:

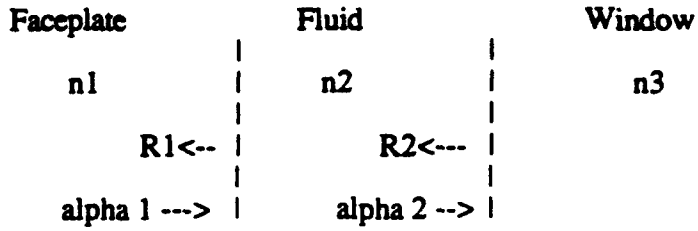

where R1 is the reflection at the faceplate/fluid boundary, and
R2 is the reflection at the fluid/window boundary.

The index of the current phosphor faceplate is 1.537 used with a fluid of index 1.41 and a front panel of 1.572. The reflections at the interfaces for this system are R1 = 0.2% and R2 = 0.3%. Changing the faceplate to YAG increases the index to about 1.83, which results in an R1 = 1.6%. By changing the index of the fluid, the value of R1 can be reduced as shown in Figure 3. An index of at least 1.6 would be required to restore the R1 values of the current system. The reflection losses for the YAG system become worse with angle as shown in Figure 4, but again can be improved with increasing fluid index. An alpha 1 of 33° was used as the incidence angle at the faceplate fluid interface based on information from Trident.

Since it may be difficult to attain an appropriate fluid with the proper index, the other option is to coat the faceplate with a single layer matching film. A film of index nf would be positioned as shown below:

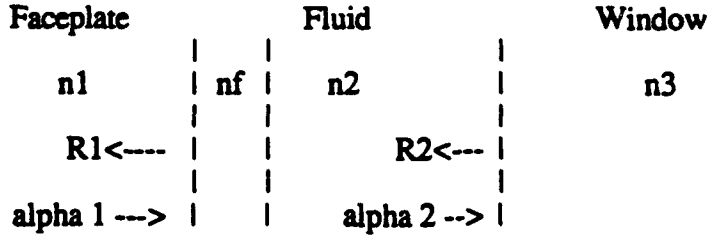

where nf is the matching single layer coating.

Choosing an index of approximately 1.6 will reduce the reflection at one wavelength as shown in Figure 5 and 6. The performance of a thin film interference coating varies as a function of wavelength, which is shown in Figure 7 for nf = 1.6 at 0 and 33° incidence on the YAG/film interface. A film of this type is normally deposited at temperatures of 200°C to 300°C to improve its durability. It would be more efficient to deposit this film prior to bonding the faceplate if processing conditions are not hostile to the coating. A possible candidate for the film would be Al203. There are other materials between 1.5 and 1.7 which may also be possibilities. For instance, the performance of SiO, which has an index of 1.7 and is very durable, is shown in Figure 8. This material may be even more appropriate for the optically coupled systems with steeper angles than those modeled here.

6.0 CHROMATIC FILTERS

An additional question was raised as to whether thin film spectral filters could be used to modify the performance of the YAG faceplate, shown in Figure 9 (provided by Trident via fax on 10/09/91), to an F-53 (green) or a P-22 (red). Figure 10 shows the spectral distribution of the the current, lower index faceplate, also provided by Trident (fax, 10/11/91).

It is possible to produce distributions similar to the P-23 (blue) in Figure 10 for the red and green filters. This would require that the spectral range performance for the green and red filters be defined with wavelength and transmittance tolerances for system-to-system variation. Filter glasses would, however, be the best choice for this application, as they would not suffer from the angular dependence of thin film filters. They would also be measurably less expensive to produce in the required 4 inch diameters than their thin film counterparts.

Using optical thin film filters, it is possible to divide and/or isolate certain portions of the YAG spectral response. Shown as sketched lines on the Figure 9 YAG spectral distribution curve are two edge filters. These are simple thin film designs, but they have several drawbacks in this application. The incidence angles on filters with current designs will range over at least 30°. The cut-off edge of any thin film filter shifts toward shorter wavelength as the angle increases, resulting in a color variation of the output. This phenomenon does not occur with filter glass.

The surface to be coated would be at least 4 inches in diameter, and if a narrow spectral spike is required, such as that shown in Figure 10 for the P-22 (red) band, with rigid spectral requirements, it would result in a low volume, low yield (expensive) part.

To reduce non-uniformity in the coating thickness, it is desirable that the filter be coated on a flat surface. If the optical design requires that the coating be placed on a strongly curved surface, cost can be expected to increase. Coating yields for multilayer filters are are typically lower than those for anti-reflection coatings.

7.0 CONCLUSIONS

ORA, with the help of Bruce Reinbolt of SBAO, has analyzed the characteristics of CRT faceplates to evaluate the effects of using a high index YAG material. Uncoated and with poorly index-matched fluids, reflection losses at the faceplate/fluid interface are nearly an order of magnitude greater than for current, low index faceplates.

From an optical performance viewpoint, low index faceplates may perform better than high index faceplates in energy collection, if the phosphor is index matched to the faceplate.

The halation effects that were seen in the original test plates were probably caused by the high reflection losses at the YAG/fluid (or YAG/air, if observed) interface. Reduction of this reflection can be accomplished by increasing the fluid index from 1.41 to between 1.58 and 1.75. It can also be improved by using the existing fluid if a film of index 1.5 to 1.7 is placed on the YAG faceplate. Implementing either of these solutions will increase the efficiency of the system to some degree by reducing reflection losses and decreasing halation effects.

Chromatic filtering of the spectral output of the phosphor is probably accomplished most effectively by filter glass materials, which are much less angularly sensitive than thin film filters.

FIGURE 1

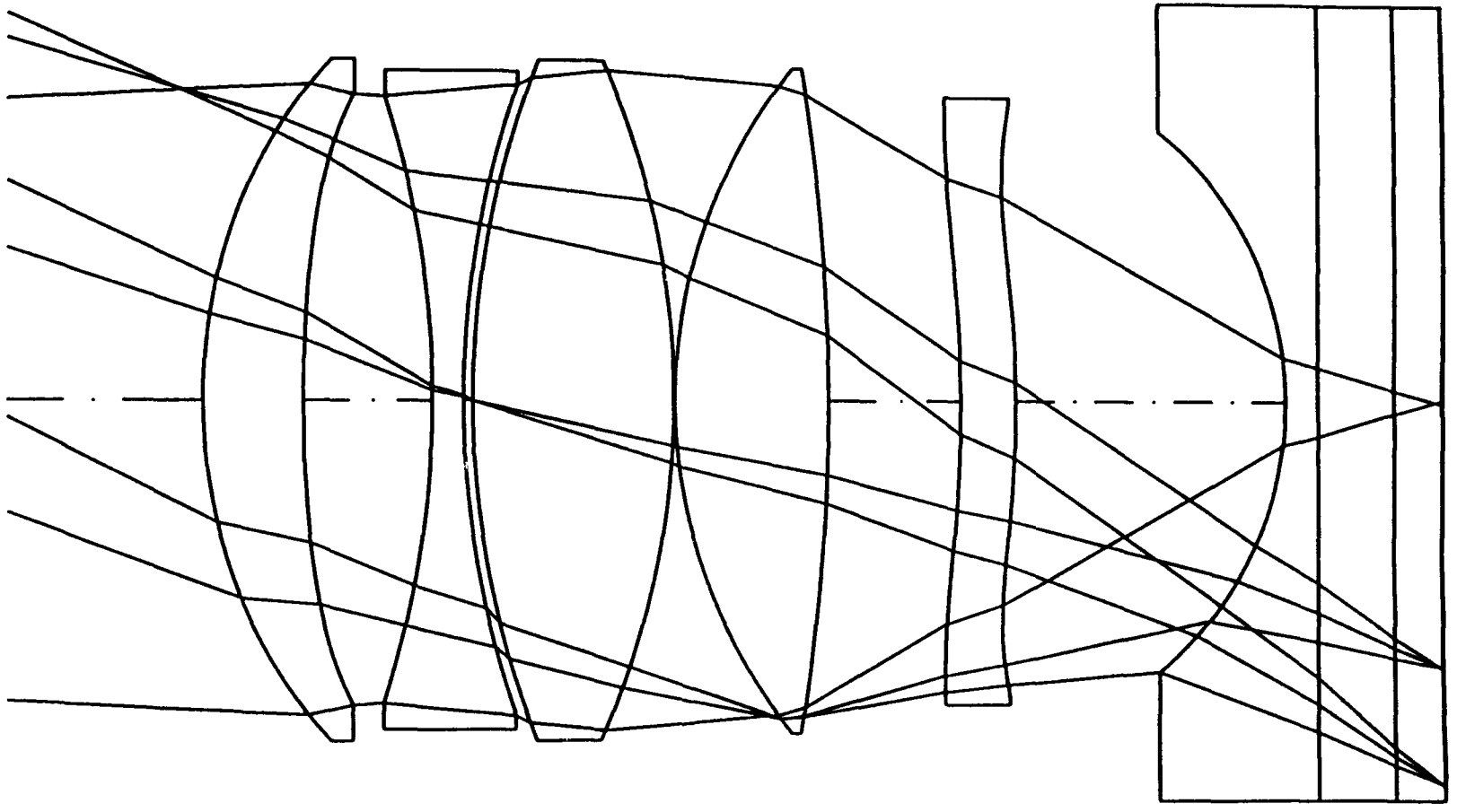

27.78 MM

Optically Coupled CRT Projection Lens

Position: 1
Scale: 0.90

ORA 3-Feb-92

FIGURE 2

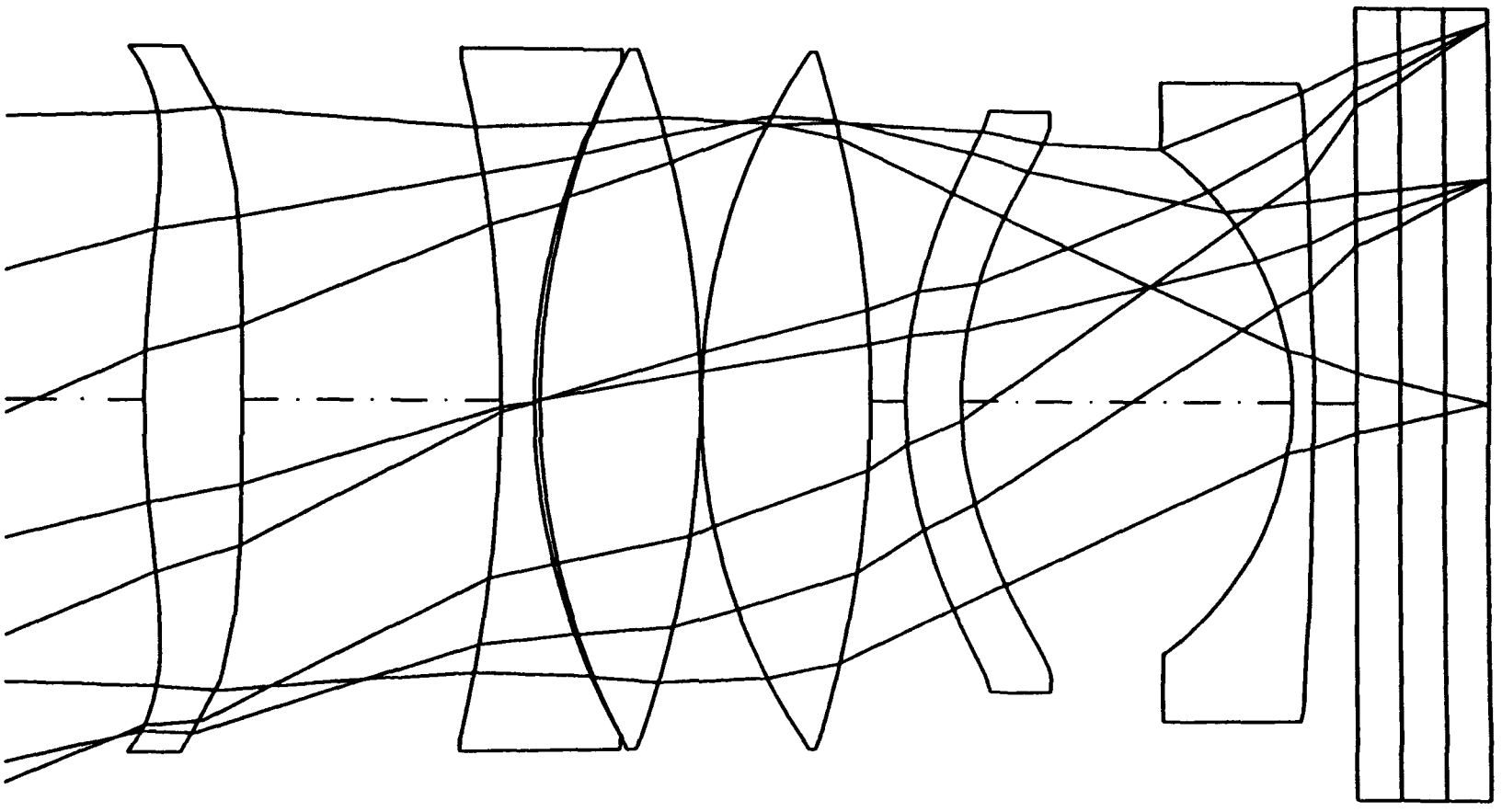

31.25 MM

Air Spaced CRT Projection Lens

Position: 1
Scale: 0.80 ORA 3-Feb-92

FIGURE 3

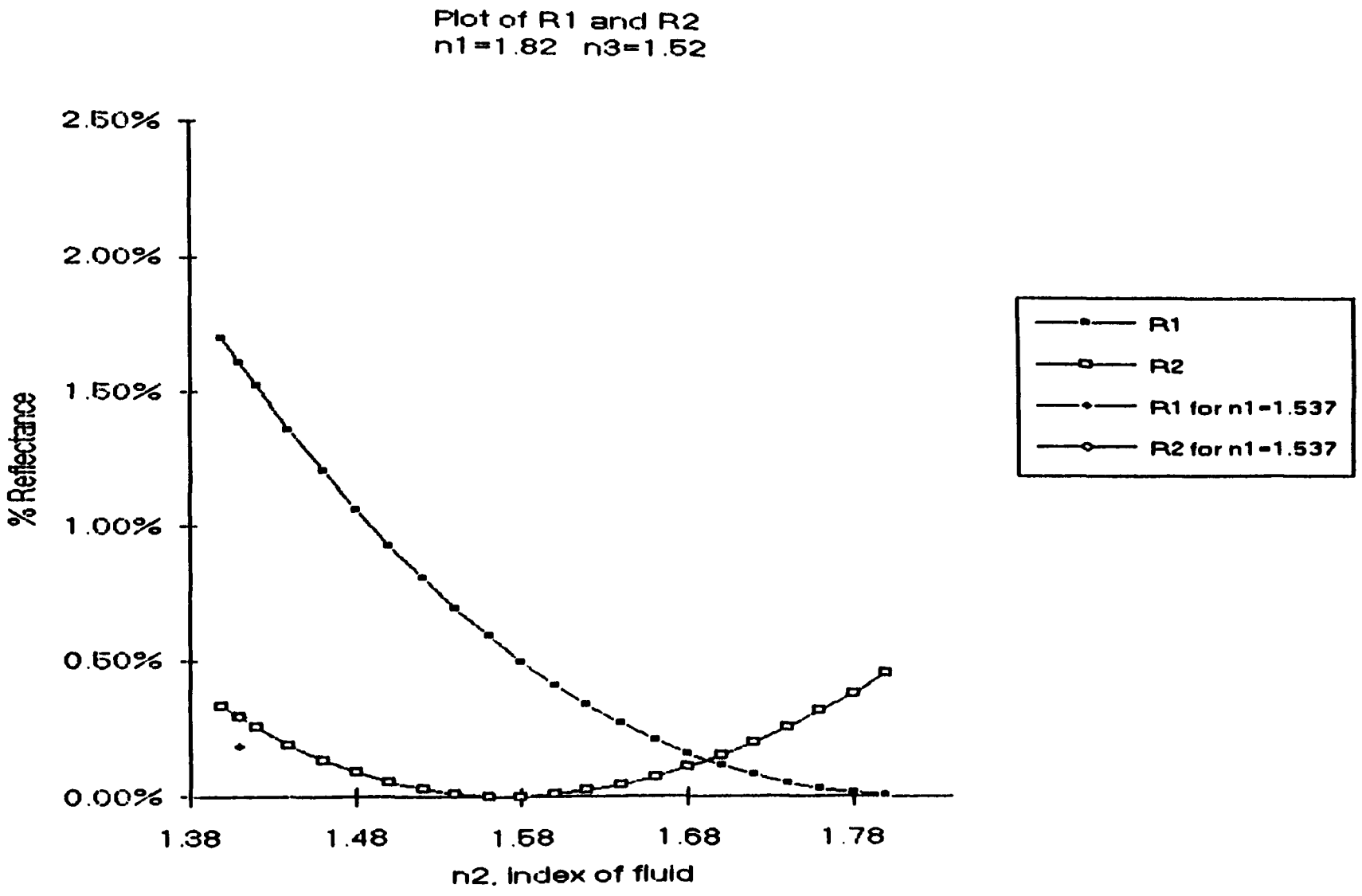
Plot of R1 and R2
n1=1.82 n3=1.52
2.50%
2.00%
1.50%
1.00%
0.50%
0.00%
% Reflectance
1.38
1.48
1.58
1.68
1.78
n2, index of fluid
R1
R2
R1 for n1=1.537
R2 for n1=1.537

FIGURE 4

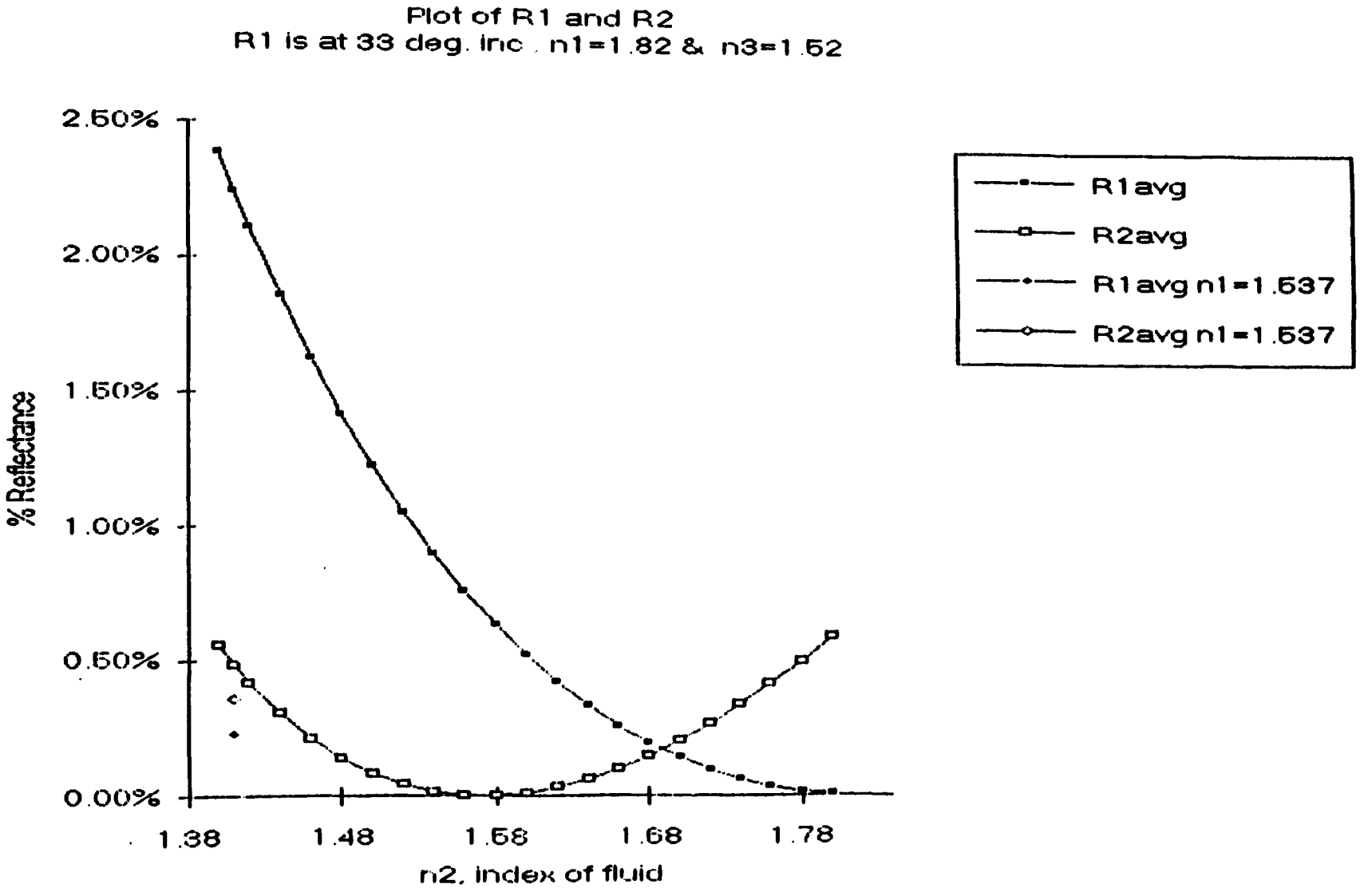
Plot of R1 and R2
R1 is at 33 deg. inc . n1=1.82 & n3=1.52
2.50%
2.00%
1.50%
1.00%
0.50%
0.00%
% Reflectance
1.38
1.48
1.58
1.68
1.78
n2, index of fluid
R1avg
R2avg
R1avg n1=1.537
R2avg n1=1.537

FIGURE 5

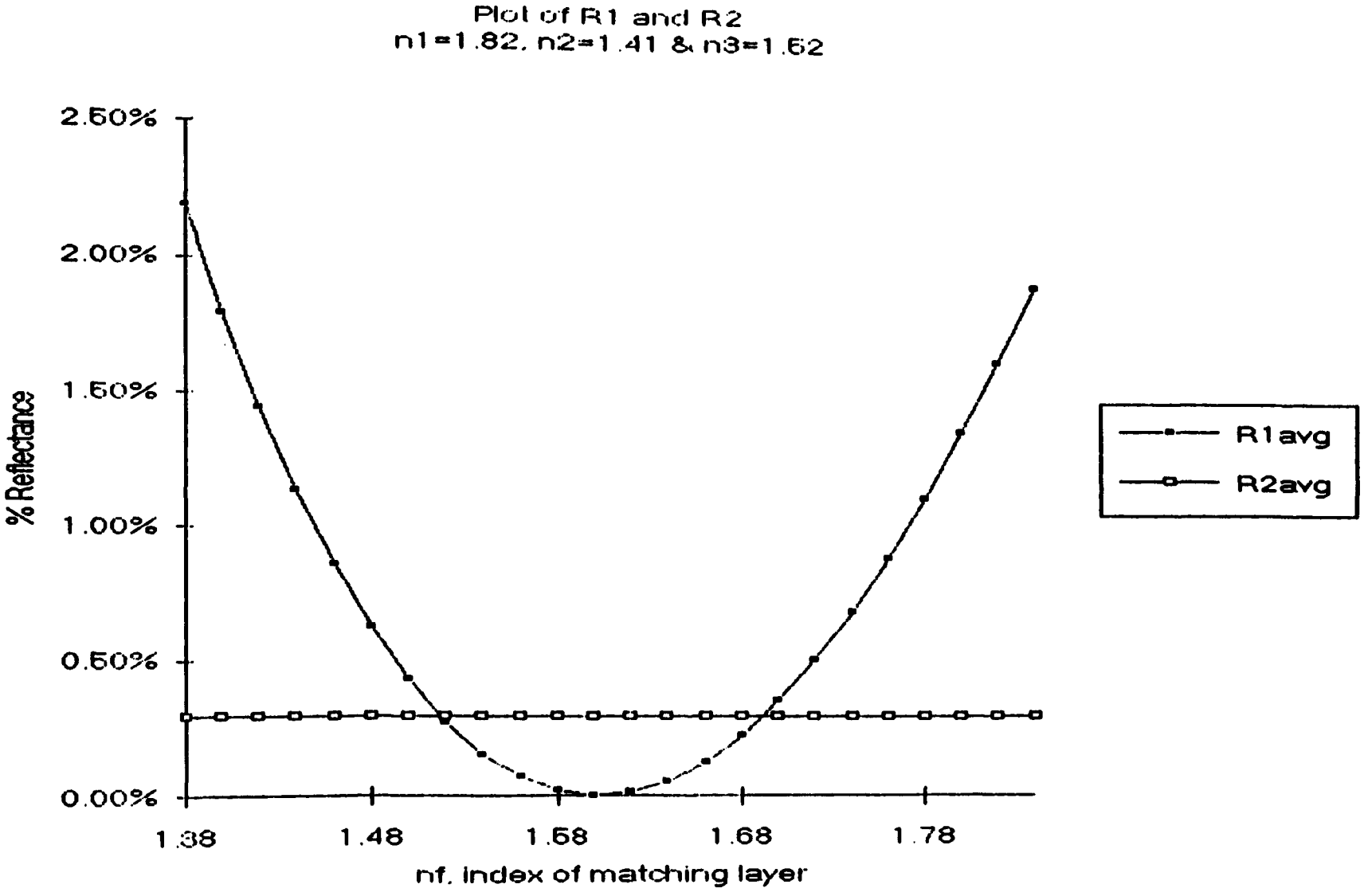
Plot of R1 and R2
n1=1.82, n2=1.41 & n3=1.62
2.50%
2.00%
1.50%
1.00%
0.50%
0.00%
% Reflectance
1.38
1.48
1.58
1.68
1.78
nf, index of matching layer
R1avg
R2avg

FIGURE 6

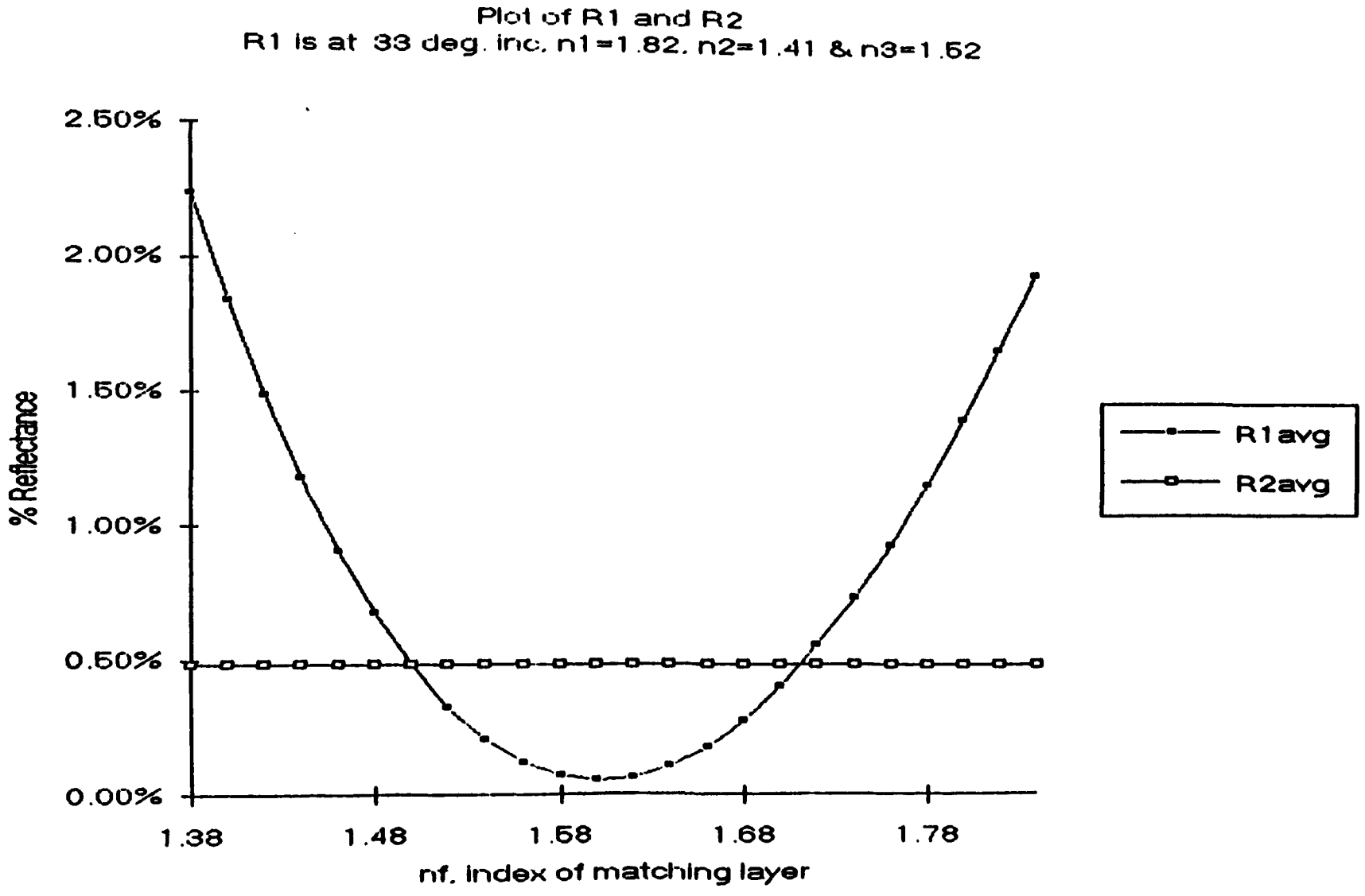
Plot of R1 and R2
R1 is at 33 deg. inc. n1=1.82, n2=1.41 & n3=1.52
2.50%
2.00%
1.50%
1.00%
0.50%
0.00%
% Reflectance
1.38
1.48
1.58
1.68
1.78
nf, index of matching layer
R1avg
R2avg

FIGURE 7

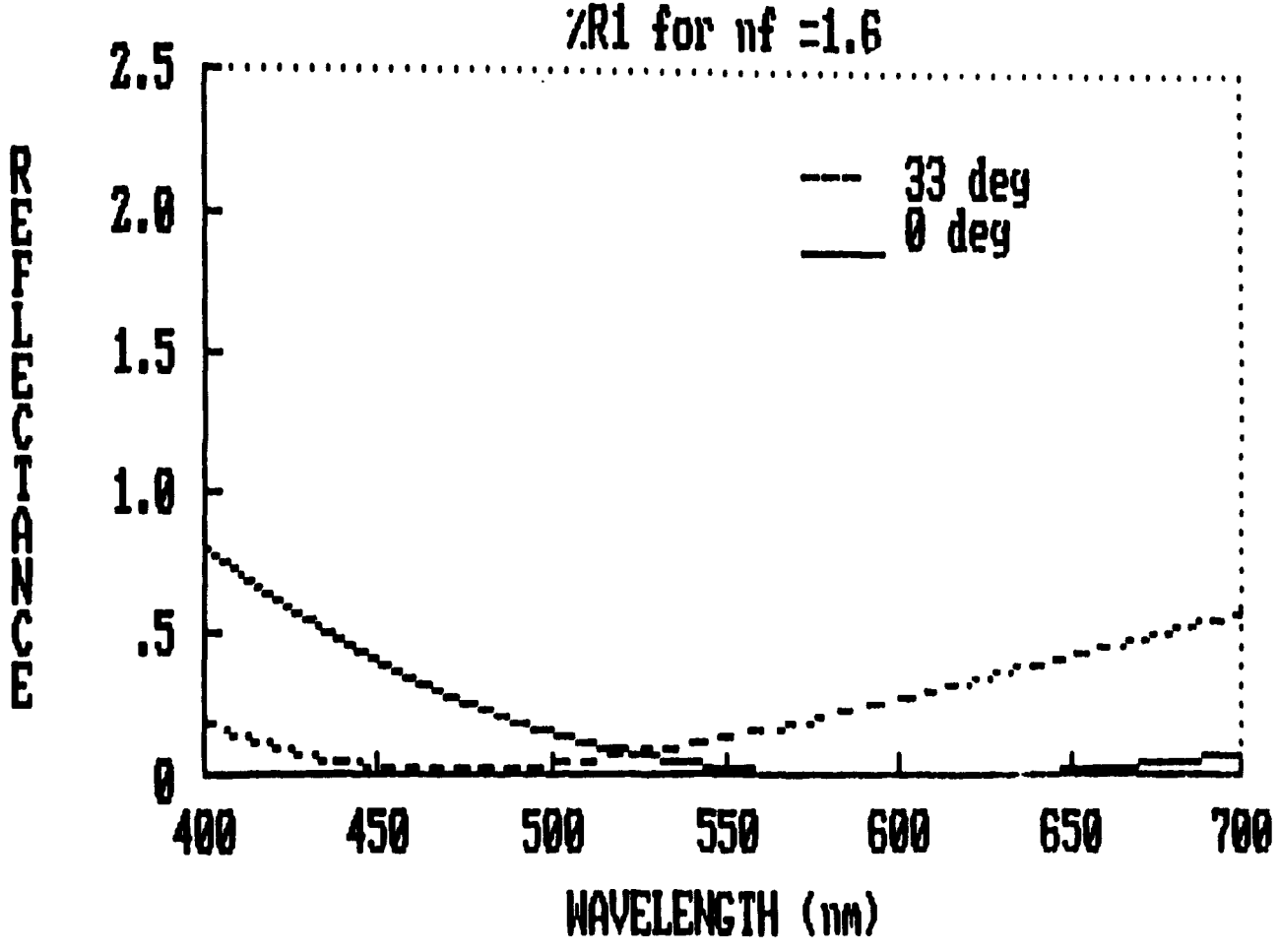
%R1 for nf =1.6
2.5
2.0
1.5
1.0
.5
0
REFLECTANCE
33 deg
0 deg
400
450
500
550
600
650
700
WAVELENGTH (nm)

FIGURE 8

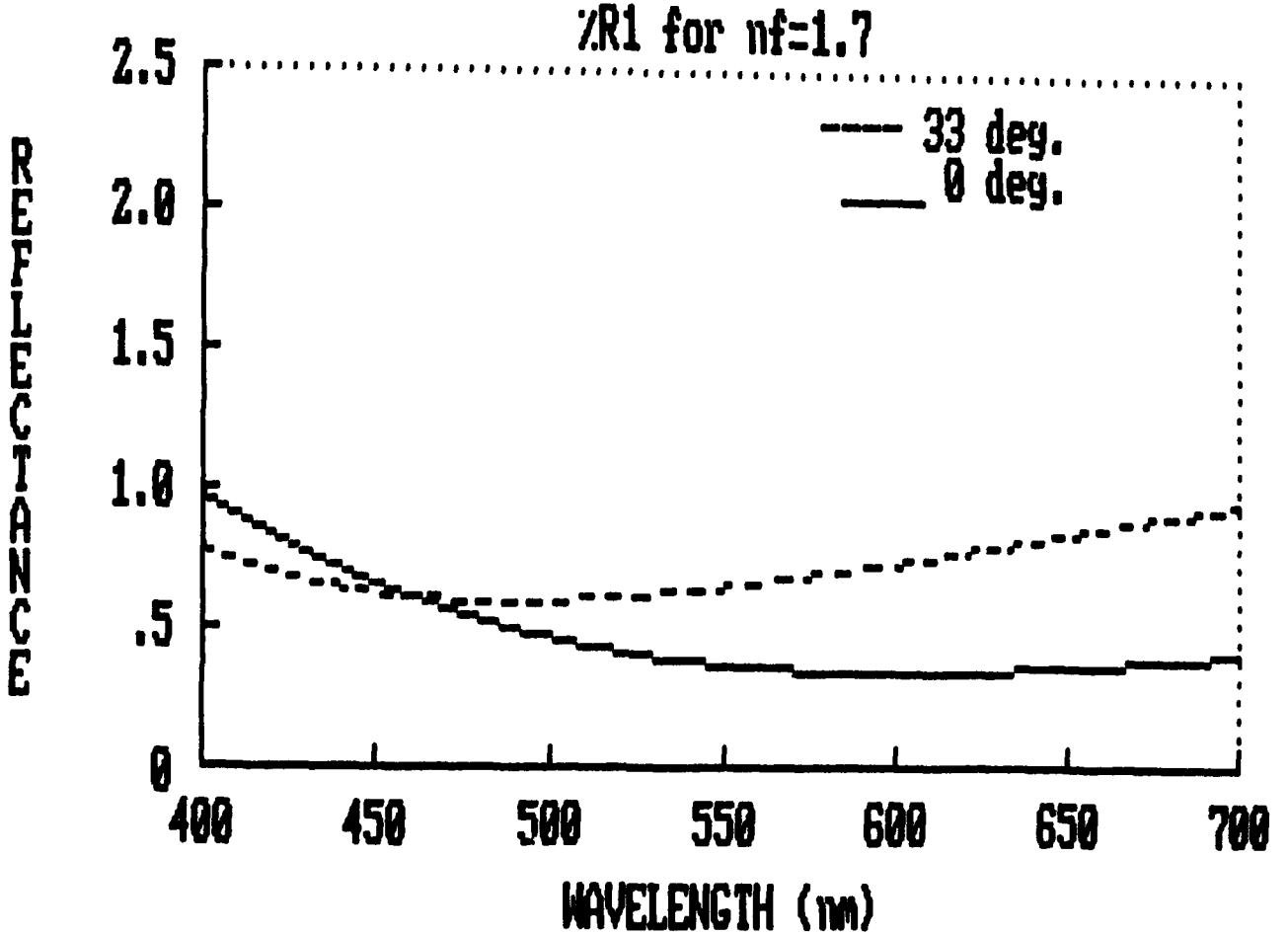
%R1 for nf=1.7
33 deg.
0 deg.
REFLECTANCE
2.5
2.0
1.5
1.0
.5
0
400
450
500
550
600
650
700
WAVELENGTH (nm)

01-D

164

Maximum Useful Screen H (mm)	Maximum Useful Screen V (mm)	Maximum Useful Screen D (mm)	Focus Type	Cathode	Screen Panel t (mm) (Nd=1.537)	Liquid t (mm) (Nd=1.41)	Front Panel t (mm) (Nd=1.572)
82	64	104	Electro Static	Oxide	4.0		
112	87	141.8	Electro Static	Oxide	5.75		
112	87	141.8	Electro Static	Oxide	5.75		
156	116	194.4	Electro Static	Oxide	7.0		
156	116	194.4	Magnetic	Impregnated	7.0		
82	64	104	Electro Static	Oxide	4.0	3.2	4.0
112	87	141.8	Electro Static	Oxide	5.75	5.0	5.75
112	87	141.8	Electro Static	Oxide	5.75	5.0	5.75
156	116	194.4	Electro Static	Oxide	7.0	4.3	7.0
156	116	194.4	Magnetic	Impregnated	7.0	4.3	7.0
82	64	104	Electro Static	Oxide	4.0	For 36" & 41" system	
112	87	141.8	Electro Static	Oxide	5.75	For 41" & 46" system	
112	87	141.8	Electro Static	Oxide	5.75	For 46" system	

Spectral Energy Distribution Curves

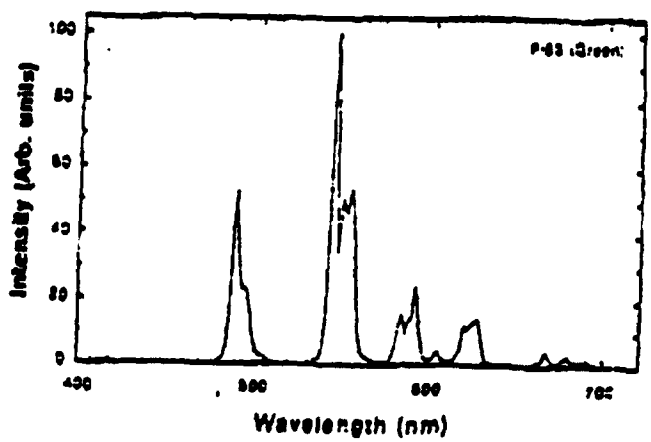

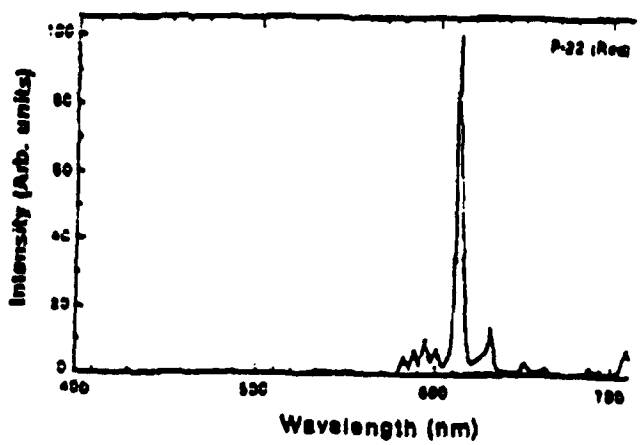

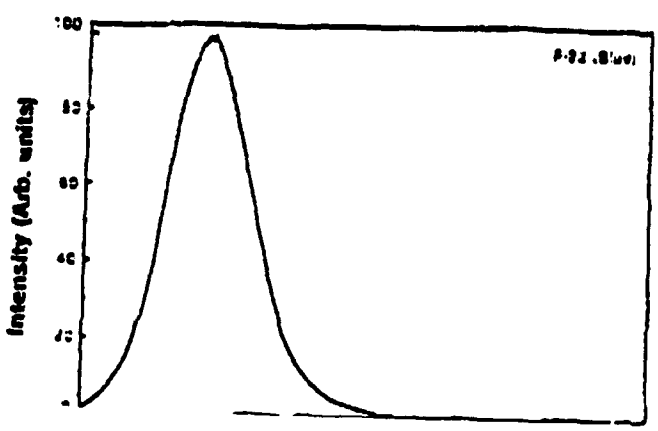

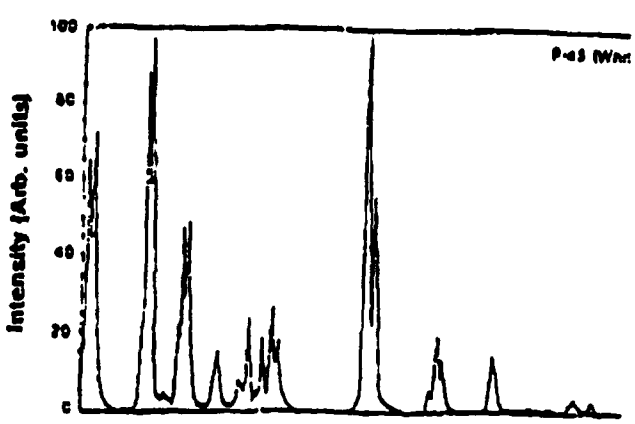

FIGURE 10

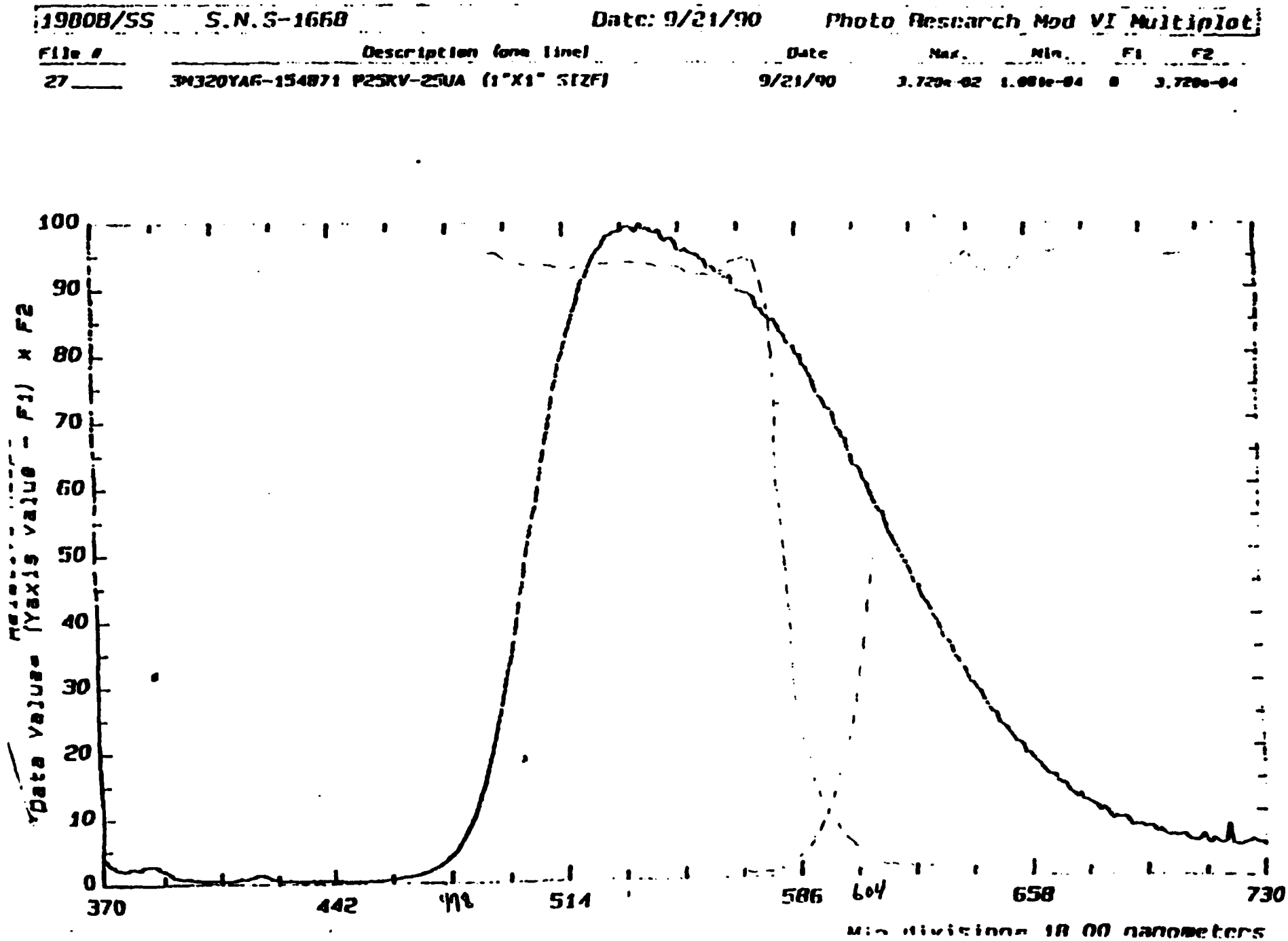
19808/SS S.N.S-1668 Date: 9/21/90 Photo Research Mod VI Multiplot
File # Description (one line) Date Max. Min. F1 F2
27 3M320YAG-154871 P25KV-25UA (1"X1" SIZE) 9/21/90 3.720e-02 1.081e-04 0 3.720e-04
100
90
80
70
60
50
40
30
20
10
0
(Data value (Yaxis value - F1) x F2
370
442
478
514
586
604
658
730
Min divisions 10.00 nanometers

APPENDIX A

Projection Lens Patent

United States Patent [19]

Kreitzer

[11] **Patent Number: 4,900,139**

[45] **Date of Patent: Feb. 13, 1990**

[54] **COLOR CORRECTED PROJECTION LENS**

[75] Inventor: Melvyn H. Kreitzer, Cincinnati, Ohio

[73] Assignee: U. S. Precision Lens, Inc., Cincinnati, Ohio

[21] Appl. No.: 266,234

[22] Filed: Oct. 28, 1988

Related U.S. Application Data

[63] Continuation of Ser. No. 48,026, May 11, 1987, abandoned.

[51] Int. Cl.[4] G02B 13/18; G02B 9/00; G02B 3/00

[52] U.S. Cl. 350/432; 350/463; 350/412

[58] Field of Search 350/412, 432, 463, 465

[56] **References Cited**

U.S. PATENT DOCUMENTS

3,446,547	5/1969	Jeffree	350/465
4,620,773	11/1986	Fukuda	350/432
4,682,862	7/1987	Moskovich	350/432
4,776,681	10/1988	Moskovich	350/432
4,810,075	3/1989	Fukuda	350/432
4,824,224	4/1989	Fukuda et al.	350/432

FOREIGN PATENT DOCUMENTS

0198016	11/1983	Japan	350/432

Primary Examiner—Bruce Y. Arnold
Assistant Examiner—Ronald M. Kachmarik
Attorney, Agent, or Firm—Robert H. Montgomery

[57] **ABSTRACT**

A lens comprising from the image side a first lens unit which is a positive element with at least one aspheric surface; a three element lens unit consisting of a biconcave element, a biconvex element and another positive component, in that order; a third lens unit having a strongly concave image side surface and which serves as a field flattener and to correct the Petzval sum of the lens.

59 Claims, 2 Drawing Sheets

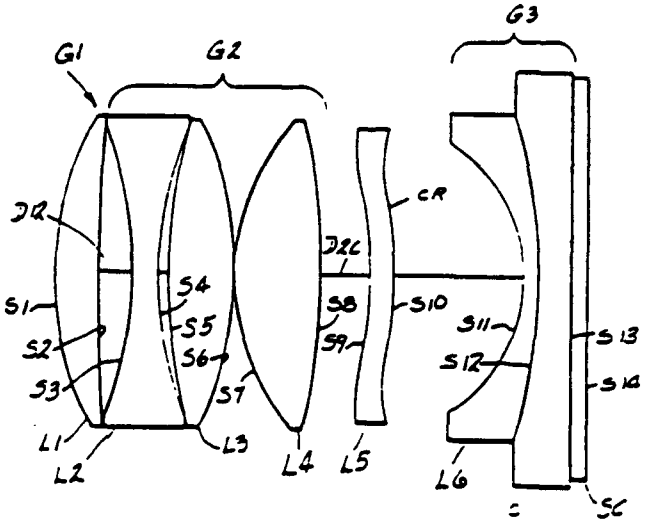

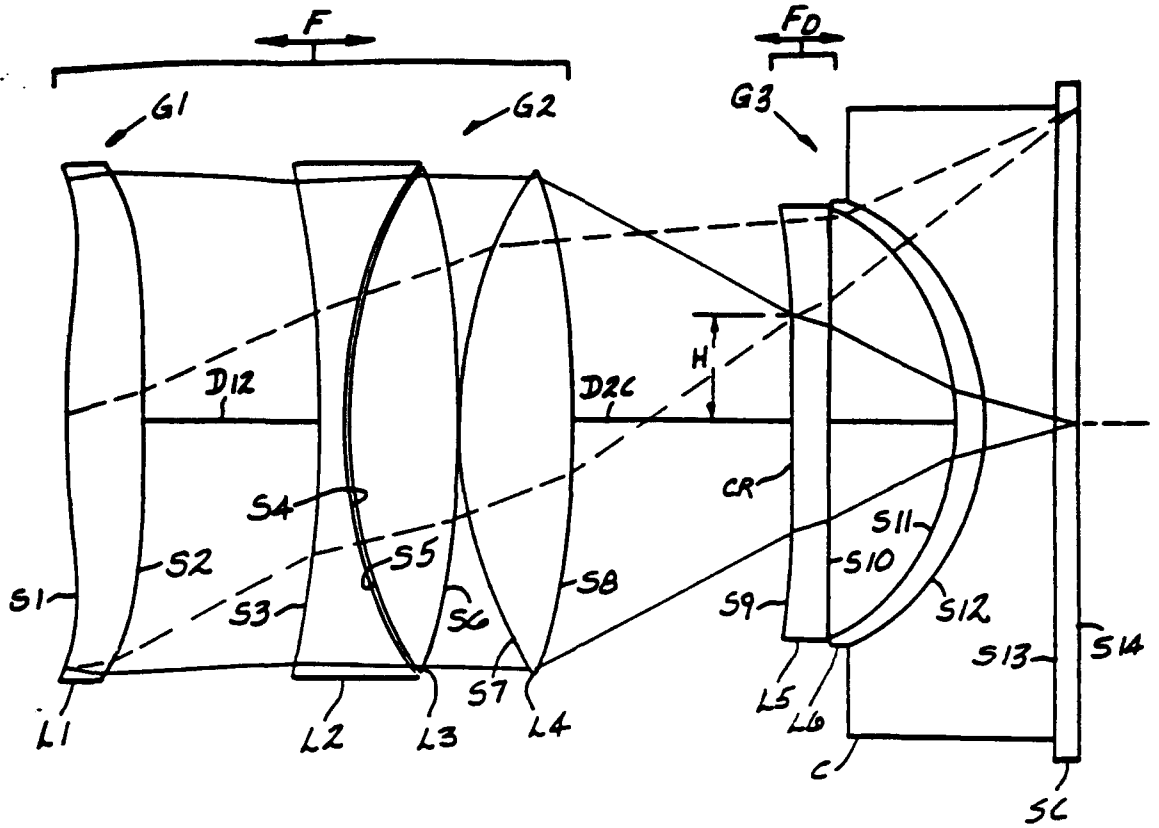
F
FD
G1
G2
G3
D12
D2C
H
CR
S1
S2
S3
S4
S5
S6
S7
S8
S9
S10
S11
S12
S13
S14
L1
L2
L3
L4
L5
L6
C
SC

FIG-1

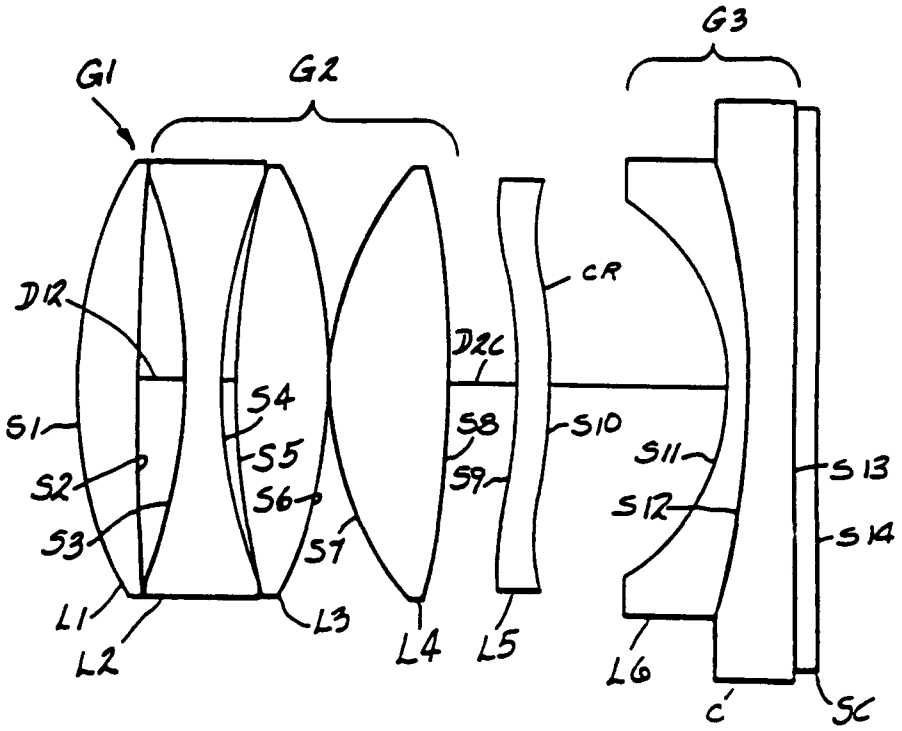
G1
G2
G3
D12
D2C
CR
S1
S2
S3
S4
S5
S6
S7
S8
S9
S10
S11
S12
S13
S14
L1
L2
L3
L4
L5
L6
C'
SC

FIG-2

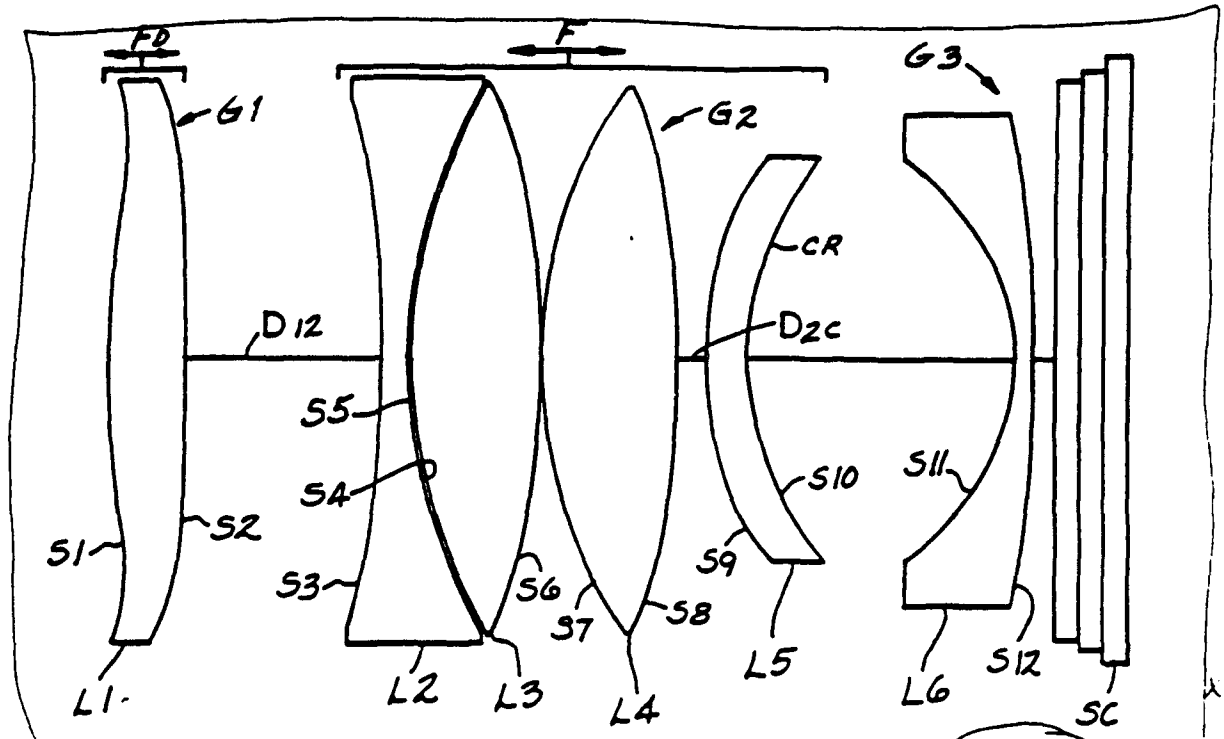
FD
F
G1
G2
G3
CR
D12
D2C
S1
S2
S3
S4
S5
S6
S7
S8
S9
S10
S11
S12
L1
L2
L3
L4
L5
L6
SC

FIG-3

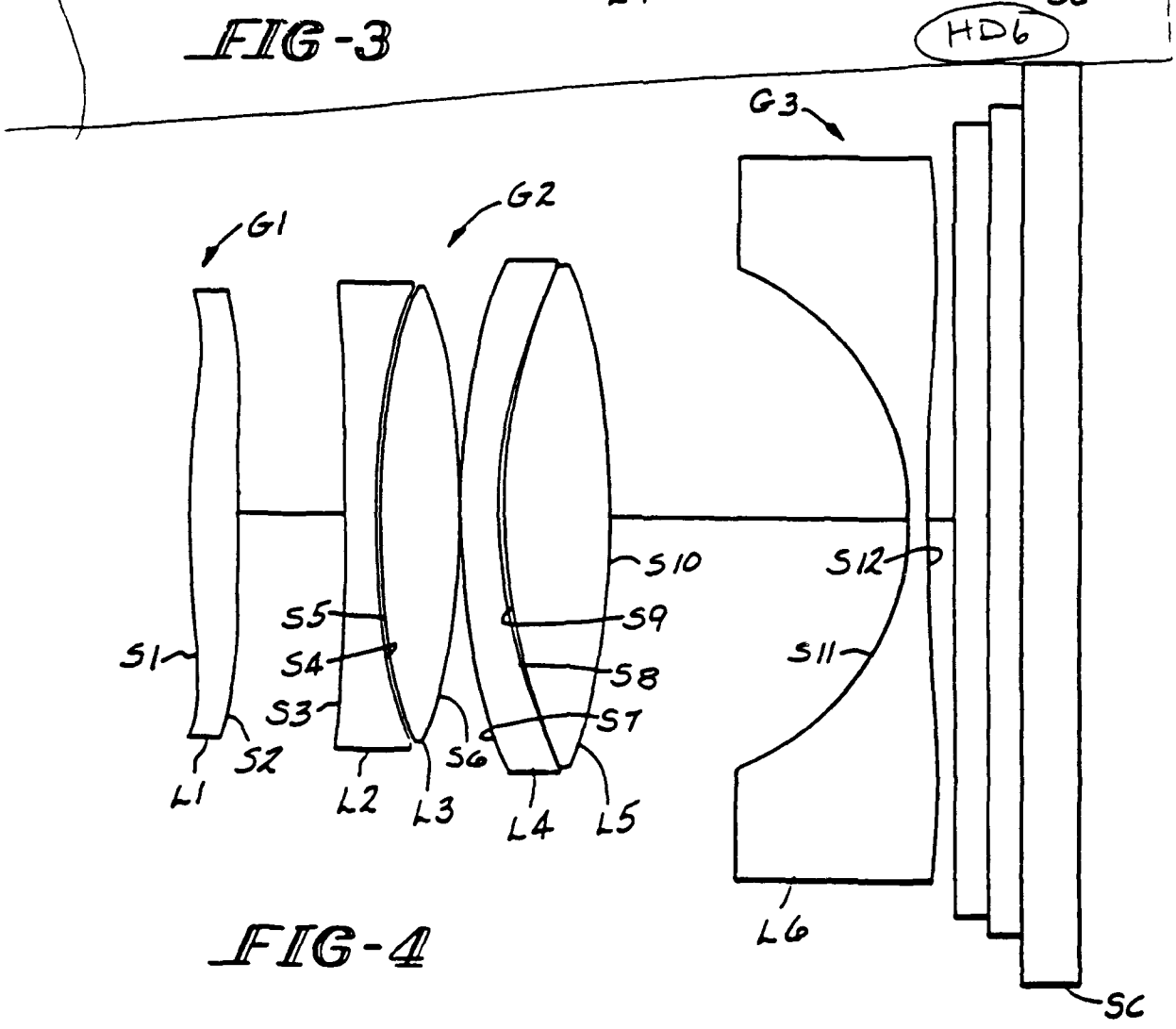
HD6
G1
G2
G3
S1
S2
S3
S4
S5
S6
S7
S8
S9
S10
S11
S12
L1
L2
L3
L4
L5
L6
SC

FIG-4

COLOR CORRECTED PROJECTION LENS

RELATED APPLICATION

This is a continuation of application Ser. No. 07/048,026 filed May 11, 1987 now abandoned.

FIELD OF THE INVENTION

This invention relates to projection lenses for cathode ray tubes and, more particularly, relates to such lenses which are color corrected.

BACKGROUND OF THE INVENTION

In projection television systems, it is common practice to utilize three cathode ray tubes (CRT's) of different colors, namely, red, blue and green. Utilizing three monochromatic CRT's does not require a color corrected lens for normal usage. Examples of such lenses are shown in U.S. Pat. Nos. 4,300,817, 4,348,081 and 4,526,442.

In practice, the phosphors of the three differently colored CRT's emit polychromatically with the green phosphor having significant side bands in blue and red. This chromatic spread can effect the image quality, particularly in situations where high resolution is of prime concern. Where there is to be a data display or large magnification, this color spread manifests itself as lowered image contrast and visible color fringing.

The degree of color correction required in the lenses for these applications depends on the intended application of the lenses.

In general, for lower resolution systems, such as for the projection of typical broadcast television, good color optical performance out to three cycles per millimeter as measured by the modulation transfer function (MTF) is adequate. In these cases, partial color correction may be adequate. For data display via red, green and blue inputs (RGB), and for high definition television, good performance out to ten cycles per millimeter, as measured by the MTF, may be required, and total color correction then becomes necessary.

The requirement for partial or total color correction always complicates an optical design problem. In projection television, it is of vital concern not to alleviate this difficulty by relaxing important system specification, such as field coverage, lens speed, and relative illumination. Additionally, it is often desirable that the lenses be capable of high performance over a significant range of magnifications. A typical front projection requirement might be from a magnification of 10× to 60×. This further complicates the optical design.

Accordingly, the present invention provides a new and improved projection lens for a cathode ray tube of high definition while maintaining a wide field angle and large relative aperture. The invention also provides a CRT projection lens that maintains a high level of image quality over a wide range of magnifications, for example, 10× to 60× or greater.

SUMMARY OF THE INVENTION

Briefly stated, a lens embodying the invention in one form thereof consists from the image side a first lens unit which is a positive element with at least one aspheric surface; a three element lens unit consisting of a biconcave element, a biconvex element and another positive component, in that order; a third lens unit having a strongly concave image side surface and which serves as a field flattener and to correct the Petzval sum of the lens; and a weak power corrector lens element having at least one aspheric surface that significantly improves the higher order sagittal flare aberration is positioned between the second and third lens units.

The first two elements of the second lens unit form a color correcting doublet of overall menicus shape concave to the image side.

An object of this invention is to provide a new and improved color corrected lens for cathode ray tube projection which provides enhanced image quality while maintaining a large relative aperture and wide field.

Another object of this invention is to provide a new and improved color corrected lens for cathode ray tube projection which maintains enhanced image quality thoughout a wide range of magnifications.

The features of the invention which are believed to be novel are particularly pointed out and distinctly claimed in the concluding portion of the specification. The invention, however, together with further objects and advantages thereof, may best be appreciated by reference to the following detailed description taken in conjunction with the drawings.

BRIEF DESCRIPTION OF THE DRAWINGS

FIGS. 1–4 are schematic side elevations of lenses which may embody the invention.

DETAILED DESCRIPTION OF PREFERRED EMBODIMENTS OF THE INVENTION

Different projection lenses embodying the invention are set forth in Tables I–X and exemplified in the drawings.

In the drawings, the lens units are identified by the reference G followed by successive arabic numerals, except that a corrector lens unit is designated by the reference CR; lens elements are identified by the reference L followed by successive arabic numerals from the image to the object end. Surfaces of the lens elements are identified by the reference S followed by successive arabic numerals from the image to the object end. The reference SC denotes the screen of a cathode ray tube, while the reference C denotes a liquid optical coupler between the screen SC and the overall lens. In the embodiments of FIGS. 1 and 2, the coupler C contributes optical power as hereinafter explained.

In all disclosed embodiments of the invention, the first lens unit G1 comprises an element L1 of positive power and has at least one aspheric surface defined by the equation:

$$x = \frac{Cy^2}{1 + [1 - (1 + K)C^2y^2]^{\frac{1}{2}}} + Dy^4 + Ey^6 + Fy^8 + Gy^{10} + Hy^{12} + Iy^{14}$$

where x is the surface sag at a semi-aperture distance y from the axis A of the lens. C is the curvature of a lens surface at the optical axis A equal to the reciprocal of the radius at the optical axis. K is a conic constant and D, E, F, G, H and I are aspheric coefficients of correspondingly fourth through fourteenth order.

Reference is now made to FIG. 1, which discloses a lens embodying the invention. The lens of FIG. 1 comprises three lens units, G1, G2, and G3, as seen from the image side or the projection screen (not shown). Lens unit G1 consists of a single element L1 having two

aspheric surfaces. Lens unit G2 consists of a color correcting doublet L2 and L3 of weak total optical power which is closely spaced to a biconvex element L4. Lens unit G3 comprises an element having a concave image side surface, and a liquid coupler which optically couples the lens to the faceplate CS of a cathode ray tube. The construction of the coupler is disclosed and claimed in co-pending U.S. application Ser. No. 820,266 filed Jan. 17, 1986. The coupler C comprises a housing which defines a peripheral wall which is sealed against CRT faceplate CS. The housing has a window at the other side which is closed by a meniscus element L6 having a strongly concave image side surface. Lens unit G3 provides correction for field curvature and contributes to reduction of Petzval sum. Coupler C is filled with a liquid having an index of refraction close to the index of refraction of element L6 and the CRT faceplate. Thus, surface S12 of element L6 does not have to be highly finished. The material of element L6 may be a plastic material such as acrylic or, as specified in Table 1, may be glass having spherical surfaces. Element L5 is a corrector, which is positioned between lens units G2 and G3 and as exemplified in Table 1, has two aspheric surfaces.

Corrector element L5 is positioned with respect to lens unit G2 such that the marginal axial rays OA intersect surface S9 thereof at a height substantially less than the clear aperture of the lens, while allowing the dimension above the height H to be configured to correct for aberrations due to off-axis rays. In FIG. 1, the marginal axial rays AR are indicated in full line, while the off-axis rays OA are indicated in short broken line. The corrector element L5 is configured and spaced from lens unit G2 to permit the central portion thereof up to the height H to be utilized to aid in correction of aperture dependent aberrations and for this reason, L5 should be within a distance D_{2C}/F_0 where D_{2C} is the axial spacing between lens unit G2 and corrector element L5, and F_0 is the equivalent focal length (EFL) of the lens.

In all cases, The corrector lens unit CR where used is shaped to contribute to correction of spherical aberration in the center and to contribute to correction of off-axis aberrations toward the ends. These off-axis aberrations are sagittal oblique spherical, coma and astigmatism.

Lenses as shown in FIG. 1 are described in the prescriptions of Tables I and II. The lens of Table III has the same form but is not optically coupled to the CRT screen SC.

Lenses as shown in FIG. 2 are described in the prescriptions of Tables IV, V, VI, VII and VIII. In the lenses of Tables VI and VII the coupler C has no optical power.

Lenses as shown in FIG. 3 are described in the prescriptions of Tables IX and X. These lenses are air spaced from the CRT screen SC. The screen SC is shown as comprising two outer plates with a coolant therebetween.

A lens as shown in FIG. 4 is described in the prescription of Table XI. Here, there is no corrector CR, and the second biconvex element of the second lens unit is split into two elements.

In the following tables, the lens elements are identified from the image end to the object end by the reference L followed successively by an arabic numeral. Lens surfaces are identified by the reference S followed by an arabic numeral successively from the image to the object end. The index of refraction of each lens element is given under the heading N_D. The dispersion of each lens element as measured by its Abbe number is given by V_D. EFL is the equivalent focal length of the lens and the semi-field angle is set forth. F/No. is the relative aperture of the lens, and the aperture stop is indicated in relation to a surface. The aspheric surfaces of the lens elements are in accordance with the coefficients set forth in the foregoing aspheric equation

The following Tables also set forth the magnification (M) of the image as an inverse function of the object, and the diagonal of the CRT for which the lens is designed. The dimension for the diagonal is for the phosphor raster of the CRT screen. The raster may vary for different CRT's having a nominal diagonal

TABLE I

LENS	SURFACE	RADII (mm)	AXIAL DISTANCE BETWEEN SURFACES (mm)	N_D	V_D
	S1	283.871			
L1			21.700	1.491	57.2
	S2	−1056.263			
			49.800		
	S3	−329.768			
L2			7.400	1.689	31.17
	S4	137.720			
			0.750		
	S5	142.596			
L3			30.000	1.491	57.25
	S6	−222.552			
			0.250		
	S7	133.119			
L4			32.400	1.517	64.17
	S8	−253.947			
			62.100		
	S9	−1569.033			
L5			10.000	1.491	57.2
	S10	3665.023			
			36.420		
	S11	−69.434			
L6			8.000	1.517	64.17
	S12	−70.013			
C			18.000	1.410	55.0
	S13	Plano			

f/No = 1.2 CRT Diagonal = 161 mm
EFL = 169.0 mm Magnification = −0.0619
Semi-field = 24° Aperture stop is 6.00 mm after S5
Aspheric Surfaces S1, S2, S9, S10

	S1	S2	S9
D	-0.2310×10^{-6}	-0.1901×10^{-6}	-0.2135×10^{-7}
E	-0.3115×10^{-10}	-0.2372×10^{-10}	-0.3129×10^{-11}
F	0.1117×10^{-14}	0.1940×10^{-14}	-0.1604×10^{-15}
G	-0.4454×10^{-18}	-0.3978×10^{-18}	0.2514×10^{-19}
H	0.7641×10^{-22}	0.6081×10^{-22}	0.2123×10^{-20}
I	-0.3878×10^{-26}	-0.3494×10^{-26}	-0.2904×10^{-24}

	S10
D	0.1728×10^{-6}
E	-0.6890×10^{-10}
F	0.1558×10^{-14}
G	0.1647×10^{-17}
H	0.1056×10^{-20}
I	-0.1015×10^{-24}

TABLE II

LENS	SURFACE	RADII (mm)	AXIAL DISTANCE BETWEEN SURFACE (mm)	N_d	V_d
	S1	195.212			
L1			17.300	1.491	57.2
	S2	−1341.860			
			43.340		
	S3	−255.343			
L2			5.890	1.689	31.16

TABLE II-continued

	S4	123.557				
			1.030			
	S5	131.041				
L3			28.840	1.589	61.25	
	S6	−177.940				
			0.200			
	S7	109.648				
L4			30.280	1.517	64.20	
	S8	−205.352				
			D8			
	S9	−127.299				
L5			7.961	1.491	57.2	
	S10	−211.498				
			D10			
	S11	−58.675				
L6			6.000	1.526	60.03	
	S12	−60.201				
C			7.000			
	S13	Plano				

f/No = 1.1 CRT Diagonal = 124 mm
EFL = 135.0 mm Aperture stop is 0.00 mm after S5
Semi-field = 23°
Aspheric Surfaces S1, S2, S9, S10

	S1	S2	S9
D	-0.3078×10^{-9}	-0.2154×10^{-9}	0.1118×10^{-9}
E	-0.8541×10^{-13}	-0.7388×10^{-13}	-0.2040×10^{-13}
F	0.4895×10^{-14}	0.8120×10^{-14}	-0.1373×10^{-13}
G	-0.4086×10^{-17}	-0.3506×10^{-17}	0.4412×10^{-17}
H	0.8618×10^{-21}	0.7248×10^{-21}	0.1932×10^{-20}
I	-0.6304×10^{-25}	-0.5796×10^{-25}	-0.7326×10^{-25}

	S10	Focusing Data EFL (mm)	D8 (mm)	D10 (mm)	M
D	0.1483×10^{-5}				
E	-0.3031×10^{-9}	130.3	44.87	39.69	−.0992
F	-0.8927×10^{-14}	135.0	48.22	30.09	−.0500
G	-0.3316×10^{-16}	138.2	51.78	22.12	−.0165
H	0.3663×10^{-19}				
I	-0.8052×10^{-23}				

TABLE III

LENS		SURFACE RADII (mm)	AXIAL DISTANCE BETWEEN SURFACES (mm)	N_d	V_d
	S1	258.727			
L1			21.700	1.491	57.2
	S2	−1207.846			
			47.750		
	S3	−329.768			
L2			7.400	1.673	32.17
	S4	137.720			
			0.740		
	S5	142.596			
L3			30.000	1.589	61.26
	S6	−277.752			
			0.250		
	S7	133.119			
L4			32.400	1.517	64.20
	S8	−253.948			
			57.490		
	S9	396.343			
L5			10.00	1.491	57.2
	S10	479.403			
			31.400		
	S11	−69.734			
L6			4.760	1.491	57.2
	S12	Plano			

f/No. = 1.2 CRT Diagonal = 131.8 mm
EFL = 168. mm Magnification = −.0314
Semi-field = 24° Aperture stop is 22.5 mm after S5
Aspheric Surfaces S1, S2, S9, S10

	S1	S2	S9
D	-0.2401×10^{-9}	-0.1956×10^{-9}	0.2561×10^{-9}
E	-0.2852×10^{-10}	-0.2302×10^{-10}	-0.4838×10^{-10}
F	-0.8694×10^{-15}	0.1560×10^{-14}	0.4407×10^{-15}

TABLE III-continued

G	-0.1983×10^{-17}	-0.8864×10^{-17}	0.2810×10^{-17}
H	0.4700×10^{-22}	0.1246×10^{-21}	0.1976×10^{-21}
I	-0.3071×10^{-25}	-0.8422×10^{-25}	-0.5596×10^{-25}

S7

D	0.4413×10^{-7}
E	-0.1366×10^{-11}
F	0.1180×10^{-15}
G	-0.6114×10^{-20}
H	0.2027×10^{-24}
I	-0.2456×10^{-29}

TABLE IV

LENS		SURFACE RADII (mm)	AXIAL DISTANCE BETWEEN SURFACES (mm)	N_d	V_d
	S1	64.117			
L1			10.000	1.491	57.2
	S2	454.506			
			7.933		
	S3	−88.724			
L2			6.000	1.620	36.3
	S4	88.724			
			2.290		
	S5	133.595			
L3			15.000	1.517	64.2
	S6	−61.130			
			0.100		
	S7	52.655			
L4			20.000	1.517	64.2
	S8	−145.278			
			11.189		
	S9	−81.110			
L5			6.000	1.491	57.20
	S10	−65.972			
			29.963		
	L11	−35.209			
L6			3.200	1.620	36.30
	S12	−125.000			
C			7.530	1.410	60.00
	S13	Plano			

f/No = 1.0 CRT Diagonal = 30.5 mm
EFL = 67.5 mm Aperture stop is 11.25 mm after S5
Semi-field = 29°
Aspheric Surfaces S1, S9, S10

	S1	S9	S10
D	-0.1074×10^{-5}	0.1299×10^{-5}	0.2701×10^{-5}
E	-0.1105×10^{-8}	0.1361×10^{-8}	0.2393×10^{-8}
F	0.8360×10^{-12}	0.1851×10^{-11}	0.1398×10^{-11}
G	-0.1195×10^{-14}	0.6225×10^{-15}	0.9554×10^{-15}
H	0.6780×10^{-18}	-0.3643×10^{-17}	-0.2834×10^{-17}
I	-0.2118×10^{-21}	0.1561×10^{-20}	0.1139×10^{-20}

Focusing Data EFL (mm)	D10 (mm)	M
67.94	29.55	−.0831
67.46	29.96	−.0935

TABLE V

LENS		SURFACE RADII (mm)	AXIAL DISTANCE BETWEEN SURFACES (mm)	N_d	V_d
	S1	76.197			
L1			13.000	1.491	57.2
	S2	−472.688			
			10.334		
	S3	−81.639			
L2			4.000	1.620	36.30
	S4	90.843			
			0.066		
	S5	91.468			
L3			21.100	1.517	64.17
	S6	−91.468			

TABLE V-continued

			0.150		
	S7	84.109			
L4			19.200	1.569	61.27
	S8	−120.724			
			12.366		
	S9	−80.743			
L5			6.140	1.491	57.2
	S10	−105.033			
			D10		
	S11	−40.819			
L6			4.000	1.491	57.2
	S12	−44.000			
C			3.000	1.443	50.0
	S13	Plano			

f/No = 1.0 CRT Diagonal = 121.6
EFL = 77.2 mm Aperture stop is 6.33 mm after S5
Semi-field = 33°
Aspheric Surfaces S1, S2, S9, S10, S11

	S1	S2	S9
D	-0.6915×10^{-6}	-0.3031×10^{-6}	0.3387×10^{-6}
E	-0.3240×10^{-9}	-0.1899×10^{-9}	-0.1011×10^{-9}
F	-0.1245×10^{-12}	0.0000×10^{-10}	-0.1141×10^{-12}
G	-0.3111×10^{-16}	0.0000×10^{-10}	0.1345×10^{-15}
H	0.4997×10^{-19}	0.0000×10^{-0}	-0.2782×10^{-19}
I	-0.2346×10^{-22}	0.0000×10^{-0}	0.9852×10^{-22}

	S10	S11
D	0.3964×10^{-6}	-0.6488×10^{-6}
E	0.4331×10^{-9}	0.1265×10^{-9}
F	-0.5884×10^{-13}	0.1142×10^{-12}
G	0.3546×10^{-16}	0.2181×10^{-16}
H	-0.7876×10^{-19}	0.2972×10^{-19}
I	-0.6164×10^{-22}	-0.1388×10^{-22}

Focusing Data		
EFL(mm)	D10 (mm)	M
78.25	34.06	−.0944
77.16	25.29	−.1170
77.95	34.40	−.1000

TABLE VI

LENS		SURFACE RADII (mm)	AXIAL DISTANCE BETWEEN SURFACES (mm)	N_d	V_d
	S1	89.851			
L1			16.000	1.491	57.2
	S2	452.287			
			15.205		
	S3	−141.472			
L2			5.000	1.620	36.30
	S4	111.221			
			1.200		
	S5	113.348			
L3			32.500	1.517	64.20
	S6	−113.348			
			0.200		
	S7	84.350			
L4			25.000	1.517	64.20
	S8	−1933.295			
			21.747		
	S9	−205.505			
L5			9.000	1.491	57.2
	S10	−112.793			
			D10		
	S11	−57.034			
L6			5.500	1.620	36.30
	S12	plano			

f/No. = 1.0
EFL = 105.0
Semi-field = 30°
Aperture stop is 6.50 mm after S5
Aspheric Surfaces S1, S2, S9, S10

	S1	S2	S9
D	-0.1719×10^{-9}	0.2117×10^{-9}	0.2250×10^{-9}
E	-0.2179×10^{-9}	-0.4171×10^{-10}	0.4005×10^{-9}

TABLE VI-continued

F	0.1418×10^{-12}	0.4446×10^{-12}	-0.5722×10^{-13}
G	-0.6256×10^{-16}	0.1553×10^{-16}	0.6671×10^{-16}
H	0.1324×10^{-19}	-0.1450×10^{-19}	-0.1316×10^{-19}
I	-0.9909×10^{-24}	0.3482×10^{-23}	-0.1631×10^{-23}

		Focusing Data		
	S10	EFL(mm)	D10(mm)	M
D	0.7114×10^{-9}			
E	0.4129×10^{-9}	105.1	40.52	−.1334
F	0.6282×10^{-14}	106.3	39.53	−.1200
G	0.1164×10^{-16}	107.2	38.83	−.1076
H	0.3025×10^{-19}			
I	-0.9300×10^{-23}			

TABLE VII

LENS		SURFACE RADII (mm)	AXIAL DISTANCE BETWEEN SURFACES (mm)	N_d	V_d
	S1	90.401			
L1			17.000	1.491	57.2
	S2	551.710			
			15.615		
	S3	−148.320			
L2			6.000	1.620	36.4
	S4	100.940			
			0.300		
	S5	102.822			
L3			30.000	1.517	64.2
	S6	−134.365			
			0.200		
	S7	85.055			
L4			24.500	1.517	64.2
	S8	−309.659			
			25.369		
	S9	−155.451			
L5			9.000	1.491	57.2
	S10	−112.107			
			D10		
	S11	−57.391			
L6			4.000	1.620	36.4
	S12	plano			

f/No = 1.2 CRT Deagonal = 122 mm
EFL = 104.7 mm Aperture stop is 9.90 mm after S5
Semi-field = 28°
Aspheric Surfaces S1, S2, S9, S10

	S1	S2	S9
D	-0.2255×10^{-9}	0.1469×10^{-9}	0.2639×10^{-9}
E	-0.1505×10^{-9}	-0.1695×10^{-10}	0.4973×10^{-9}
F	0.7536×10^{-13}	0.3153×10^{-13}	-0.8870×10^{-13}
G	-0.3857×10^{-16}	0.5873×10^{-17}	0.4468×10^{-16}
H	0.9174×10^{-20}	-0.7355×10^{-20}	-0.1095×10^{-19}
I	-0.1059×10^{-23}	0.1920×10^{-23}	-0.1734×10^{-23}
K	1.326		

		Focusing Data		
	S10	EFL (mm)	D10 (mm)	M
D	0.8827×10^{-9}			
E	0.4826×10^{-9}	104.8	36.40	−.1161
F	0.6637×10^{-14}	105.7	35.55	−.0987
G	-0.8763×10^{-17}	103.6	37.30	−.1233
H	0.2104×10^{-19}			
I	-0.6838×10^{-23}			

TABLE VIII

LENS		SURFACE RADII (mm)	AXIAL DISTANCE BETWEEN SURFACES (mm)	N_d	V_d
	S1	79.527			
L1			14.000	1.491	57.2
	S2	380.482			
			14.450		
	S3	−116.430			
L2			4.500	1.620	36.4

TABLE VIII-continued

	S4	93.704				
			0.10			
	S5	93.126				
L3			31.000	1.517	64.2	
	S6	−93.126				
			0.200			
	S7	73.005				
L4			20.000	1.517	64.2	
	S8	−206.286				
			16.870			
	S9	−94.045				
L5			8.000	1.491	57.2	
	S10	−83.071				
			D10			
	S11	−53.241				
L6			5.75	1.620	36.4	
	S12	−130.000				
C			8.000	1.435	50.0	
	S13	plano				

f/No. = 1.2 CRT Diagonal = 12a.e mm
EFL = 9e.9 Aperture stop is e.20 mm after S5
Semi-field = 29°
Aspheric Surfaces S1. S2. S9. S10

	S1	S2	S9
D	−0.2013 × 10⁻⁹	0.2863 × 10⁻⁹	0.9194 × 10⁻⁹
E	−0.4457 × 10⁻¹³	−0.1806 × 10⁻¹³	0.9549 × 10⁻¹³
F	0.3147 × 10⁻¹⁸	0.1593 × 10⁻¹⁸	−0.2721 × 10⁻¹⁸
G	−0.1513 × 10⁻²³	0.4444 × 10⁻²³	0.1107 × 10⁻²³
H	0.3487 × 10⁻²⁸	−0.6001 × 10⁻²⁸	−0.4843 × 10⁻²⁸
I	−0.2575 × 10⁻³³	0.1777 × 10⁻³³	0.5510 × 10⁻³³
K	1.326		

	S10	Focusing Data EFL (mm)	D10 (mm)	M
D	0.1532 × 10⁻⁵			
E	0.8778 × 10⁻⁹	96.87	45.21	−.109
F	0.3840 × 10⁻¹⁴	95.96	46.12	−.123
G	−0.9903 × 10⁻¹⁹	98.07	44.05	−.092
H	0.6608 × 10⁻²⁴			
I	−0.1801 × 10⁻²⁹			

TABLE IX

LENS		SURFACE RADII (mm)	AXIAL DISTANCE BETWEEN SURFACES (mm)	N_d	V_d
	S1	178.554			
L1			13.000	1.491	57.2
	S2	2078.521			
			D2		
	S3	−255.343			
L2			5.890	1.689	31.2
	S4	123.551			
			1.030		
	S5	131.041			
L3			28.640	1.589	61.3
	S6	−177.989			
			0.200		
	S7	109.648			
L4			30.280	1.517	64.2
	S8	−205.352			
			0.210		
	S9	100.488			
L5			8.830	1.491	57.2
	S10	92.312			
			70.634		
	S11	−50.216			
L6			4.000	1.491	57.2
	S12	−368.024			
			D12		
	S13	Plano			

f/No. = 1.1 CRT Diagonal = 124 mm
EFL = 134.3 mm Aperture stop is 0.00 mm after S5
Semi-field = 23°
Aspheric Surfaces S1. S2. S9. S10. S11. S12

	S1	S2	S9
D	−0.1394 × 10⁻⁷	0.6554 × 10⁻⁷	0.8[illegible]
E	0.2185 × 10⁻¹¹	−0.3830 × 10⁻¹¹	0.120[illegible]
F	−0.9562 × 10⁻¹⁶	−0.1[illegible]	−0.62[illegible]
G	−0.3269 × 10⁻²¹	−0.3621 × 10⁻²¹	0.3[illegible]
H	−0.1475 × 10⁻²⁶	−0.4355 × 10⁻²⁶	−0.[illegible]
I	0.2055 × 10⁻³¹	0.[illegible] × 10⁻³¹	0.[illegible]

	S10	S11	S12
D	0.4[illegible] × 10⁻⁷	0.1151 × 10⁻⁷	0.[illegible]
E	−0.1594 × 10⁻¹¹	0.6[illegible] × 10⁻¹¹	−0.1e21 × 10⁻¹¹
F	0.1[illegible] × 10⁻¹⁶	0.4[illegible] × 10⁻¹⁶	0.[illegible]
G	−0.1501 × 10⁻²¹	0.[illegible] × 10⁻²¹	−0.[illegible]
H	0.6239 × 10⁻²⁶	−0.4504 × 10⁻²⁶	0.[illegible]
I	−0.1204 × 10⁻³¹	0.[illegible] × 10⁻³¹	−0.[illegible]

Focusing Data EFL (mm)	D2 (mm)	D12 (mm)	M
135.05	50.[illegible]	[illegible]	−.[illegible]
134.33	46.[illegible]	4.[illegible]	−.05[illegible]
133.[illegible]	43.[illegible]	[illegible]	−.[illegible]

TABLE X

LENS		SURFACE RADII (mm)	AXIAL DISTANCE BETWEEN DISTANCES (mm)	N	V
	S1	164.313			
L1			17.3[illegible]	1.49[illegible]	57.2
	S2	−4893.612			
			D2		
	S3	−255.343			
L2			5.89[illegible]	1.68[illegible]	31.[illegible]
	S4	123.551			
			1.030		
	S5	131.041			
L3			28.64[illegible]	1.58[illegible]	61.25
	S6	−177.989			
			0.20[illegible]		
	S7	109.648			
L4			30.280	1.517	64.2
	S8	−205.352			
			0.26[illegible]		
	S9	78.134			
L5			10.0[illegible]	1.491	57.2
	S10	67.389			
			e0.21[illegible]		
	S11	−48.559			
Lo			4.000	1.491	57.2
	S12	−252.989			
			1.302		
	S13	Plano			
			D12		

f/No. = 1.1 CRT Diagonal = 124 mm
EFL = 135.7 mm Aperture stop is 0.00 mm after S5
Semi-field = 23°
Aspheric Surfaces S1. S2. S9. S10. S11. S12

	S1	S2	S9
D	−0.2911 × 10⁻⁹	−0.1945 × 10⁻⁹	−0.3015 × 10⁻⁹
E	−0.7792 × 10⁻¹⁰	−0.5934 × 10⁻¹⁰	0.8356 × 10⁻¹⁰
F	0.7366 × 10⁻¹⁴	0.7111 × 10⁻¹⁴	−0.1079 × 10⁻¹³
G	−0.4384 × 10⁻¹⁷	−0.3414 × 10⁻¹⁷	0.4778 × 10⁻¹⁸
H	0.7916 × 10⁻²¹	0.7097 × 10⁻²¹	−0.1167 × 10⁻¹⁰
I	−0.3500 × 10⁻²⁵	−0.4415 × 10⁻²⁵	−0.8726 × 10⁻²⁵

	S10	S11	S12
D	0.2618 × 10⁻⁷	0.1161 × 10⁻⁷	0.7559 × 10⁻⁹
E	−0.3268 × 10⁻¹⁰	−0.6628 × 10⁻¹⁰	−0.5860 × 10⁻¹⁰
F	0.9906 × 10⁻¹³	0.4292 × 10⁻¹³	0.2597 × 10⁻¹³
G	−0.1459 × 10⁻¹⁵	0.9961 × 10⁻¹⁷	−0.4923 × 10⁻¹⁷
H	0.7475 × 10⁻¹⁹	−0.5969 × 10⁻¹⁹	0.1168 × 10⁻²⁰
I	−0.1894 × 10⁻²²	0.1511 × 10⁻²²	0.6336 × 10⁻²⁴

Focusing Data EFL (mm)	D2 (mm)	D12 (mm)	M
135.71	48.71	11.73	−.1000
134.97	44.80	5.42	−.0500

TABLE X-continued

	134.36	41.5	1.50	−.016

TABLE XI

LENS		SURFACE RADII (mm)	AXIAL DISTANCE BETWEEN SURFACES (mm)	N_d	V_d
	S1	100.333			
L1			9.000	1.491	57.2
	S2	−143.21.009			
			20.1000		
	S3	−600.536			
L2			6.000	1.785	25.7
	S4	132.672			
			0.080		
	S5	134.262			
L3			15.350	1.589	61.3
	S6	−132.733			
			0.200		
	S7	171.218			
L4			7.000	1.491	57.2
	S8	100.514			
			1.200		
	S9	111.209			
L5			19.450	1.589	61.3
	S10	−142.661			
			55.750		
	S11	−68.468			
L6			4.000	1.491	57.2
	S12	269.671			

f/No = 1.4 CRT Diagonal = 125.8 mm
EFL = 111.6 Magnification = .0263
Semi-field = 34° Aperture stop is 5.05 mm after S5
Aspheric Surfaces S1, S2, S7, S8, S11, S12

	S1	S2	S7
D	-0.9964×10^{-6}	-0.3034×10^{-6}	0.6027×10^{-6}
E	-0.4344×10^{-9}	-0.3497×10^{-9}	-0.1651×10^{-10}
F	-0.1037×10^{-12}	-0.3718×10^{-13}	0.5166×10^{-14}
G	0.1695×10^{-16}	-0.1261×10^{-16}	-0.6497×10^{-17}
H	0.1831×10^{-19}	0.2801×10^{-19}	0.6405×10^{-21}
I	0.2021×10^{-23}	-0.1241×10^{-23}	-0.7613×10^{-24}

	S8	S11	S12
D	0.1130×10^{-6}	-0.3187×10^{-5}	-0.8632×10^{-6}
E	0.3713×10^{-12}	0.2489×10^{-9}	0.1616×10^{-9}
F	-0.1677×10^{-15}	-0.2606×10^{-12}	-0.1755×10^{-13}
G	-0.8127×10^{-18}	0.1321×10^{-15}	0.2955×10^{-17}
H	0.6405×10^{-21}	0.7036×10^{-19}	0.1630×10^{-21}
I	-0.9106×10^{-24}	-0.4831×10^{-22}	-0.1388×10^{-24}

Table XII sets forth the powers K_{G1}, K_{G2}, K_{G3}, and K_{CR} of the lens units of each of the examples as a ratio of the power of the overall lens.

TABLE XII

TABLE	K_{G1}/K_O	K_{G2}/K_O	K_{G3}/K_O	K_{CR}/K_O
I	.373	.949	−1.032	−.068
II	.392	1.000	−1.149	−.203
III	.387	.948	−1.189	.124
IV	.452	.838	−1.021	−.011
V	.574	.838	−.838	−.108
VI	.479	.755	−.838	−.212
VII	.488	.803	−1.080	.139
VIII	.478	.789	−.975	.083
IX	.340	1.000	−1.149	−.004
X	.377	.947	−1.099	−.095
XI	.355	1.009	−1.013	— —

It will be seen that the corrector element CR has little optical power. Its primary purpose is to provide aspheric surfaces for correction of aberrations.

In all embodiments, except that of Table XI, all elements of lens unit G2 are glass with spherical surfaces, and thus avoid focus drift with temperature.

In the examples of Tables IV-VIII the optical power of the first lens unit K_1/K_O is greater than 0.4. This is permissable in view of the spacing D_{12}/F_O which is less than 0.2. Thus the spacing D_{12}/F_O will be a function of the axial optical power of the first lens unit. The lesser the optical power of the first lens unit, the greater the spacing D_{12}/F_O may be.

The optical power of the doublet consisting of L2 and L3 is all embodiments is very weak.

The axial spacing between L3 and the power element L4 is very small, less than one tenth of one per cent of the EFL of the lens.

The power of the corrector element CR as a ratio to the power of the lens is weak and

$$0.1 > K_{CR}/K_O > 0.3$$

Thus any change in index of refraction of the corrector element due to temperature does not adversly affect the focus of the lens.

Table XIII sets forth the spacing of element L1 and L2, D_{12}/F_O, and also the spacing of the corrector element from the second lens unit D_{2C}/F_O, together with the ratio of the powers of L2 and L3 to the power of the lens.

TABLE XIII

TABLE	D_{12}/F	D_{2C}/F	K_2/K	K_3/K
I	264	245	−1.19[illegible]	[illegible]
II	314	36[illegible]	−1.15[illegible]	[illegible]
III	284	342	−1.180	[illegible]
IV	11[illegible]	166	−.96[illegible]	[illegible]
V	134	160	−.96[illegible]	0[illegible]
VI	148	20[illegible]	−.99[illegible]	.96[illegible]
VII	151	242	−1.031	[illegible]
VIII	14[illegible]	1[illegible]	1.12[illegible]	[illegible]
IX	321	— —	−1.12[illegible]	1.01[illegible]
X	302	050	−1.13[illegible]	1.02[illegible]
XI	181	−.13	−.81[illegible]	[illegible]

The color correcting doublet of the second lens unit is designed to provide the necessary color correction without introducing uncorrectable aberrations. The lenses of Tables I, II, III, VII and VIII provide modulation transfer functions of ten cycles/millimeter over most of the field. In these examples, the absolute optical power of the biconcave element L2 and the first biconvex element L3 are greater than the optical power of the overall lens.

The lens of Table XI provides an MTF of 6.3 cycles/millimeter and the embodiments of Tables IV-VIII provide 5.0 cycles/millimeter.

The lens of Table XI and FIG. 4 utilizes a two element power component L4 and L5 where L4 is acrylic and has two aspheric surfaces, and has an axial power which is about 21% of L5. The EFL's of the lenses as set forth in the prescriptions may vary as the lens is focused for various projection distances and magnifications.

The lenses of Tables I and III are designed for front projection at predetermined distances and provide image/object magnifications of 16.4× and 31.5× respectively.

The lens of Table II is also designed for front projection and has a range of magnifications 10× to 60×. To focus for varying image distances elements L1-L5 move in the same direction with the corrector L5 moving differentially to correct for aberrations introduced by movement of lens units G1 and G2. In FIG. 1, the focusing movement of elements L1-L4 is shown by the

arrow F and the focusing movement of element L5 is shown by the arrow F_D.

The lenses of Tables IX and X are also designed and have magnifications of 10× to 60×. Here elements L1-L5 move axially for focusing with L1 moving differentially at a lesser rate. This differential movement corrects for aberrations introduced by the focusing movement of elements L1-L5. In FIG. 3, the focusing movement of elements L2-L5 is shown by the arrow F while the differential movement of element L1 is shown by the arrow F_D.

The lenses of Table IV-VIII are designed for rear projection and in some cases are provided with focusing capability dependent on the magnification required for the size of the viewing screen. That is, the same lens may be used for a forty or fifty inch diagonal viewing screen.

The lens of Table XI does not use a corrector element CR as shown in the other embodiments, but does include a weak meniscus L4 having two aspheric surfaces as a part of the second lens unit G2.

It may thus be seen that the objects of the invention set forth as well as those made apparent from the foregoing description are efficiently attained. While preferred embodiments of the invention have been set forth for purposes of disclosure, modification of the disclosed embodiments of the invention as well as other embodiments thereof may occur to those skilled in the art. Accordingly, the appended claims are intended to cover all of the embodiments of the invention and modifications to the disclosed embodiments which do not depart from the spirit and scope of the invention.

Having described the invention, what is claimed is:

1. A projection lens for use in combination with a cathode ray tube where the projection lens is closely coupled to the cathode ray tube, said lens comprising from the image end a first lens unit of positive optical power having at least one aspheric surface and contributing to correction of aperture dependent aberrations, a second lens unit providing a majority of the positive power of said lens, and a third lens unit having a strongly concave image side surface which provides correction for field curvature and Petzval sum of other units of said lens, said second lens unit consisting from the image end of a biconcave element, a biconvex element and a positive component, said biconcave element and said biconvex element forming a color correcting doublet and being of overall meniscus shape concave to the image end, said color correcting doublet being axially spaced from said positive component a distance less than 0.01 of the equivalent focal length of said lens.

2. The lens of claim 1 where said doublet is axially spaced from said first lens unit at least 0.1 of the equivalent focal length of said lens.

3. The lens of claim 1 further including a corrector lens unit of weak optical power having two aspheric surfaces positioned between said second and third lens units, said corrector lens unit being axially spaced from said second lens unit a distance

$$0.4 > D_{2C}/F_O > 0.15$$

where D_{2C} is the axial spacing distance between said second lens unit and said corrector element and F_O is the equivalent focal length of said lens.

4. The lens of claim 3 where said lens has a variable magnification, said first and said second lens units move axially in fixed relation to focus said lens and said corrector lens unit moves axially in the same direction but at a differential rate.

5. The lens of claim 3 where said element of said first lens unit has two aspheric surfaces.

6. The lens of claim 3 where the axial marginal rays traced from the long conjugate intersect a surface of said corrector lens unit substantially below the clear aperture of said image side surface.

7. The lens of claim 1 where said element of said first lens unit has two aspheric surfaces.

8. The lens of claim 1 where said first and second lens units move axially in the same direction at differential rates to vary the focus of said lens.

9. The lens of claim 8 where the axial spacing between said first lens unit and said second lens unit is

$$0.4 > D_{12}/F_O > 0.1$$

where D_{12} is the distance between the first and second lens units and F_O is the equivalent focal length of said lens.

10. The lens of claim 1 where said positive lens component is also biconvex.

11. The lens of claim 1 where all elements of said second lens unit have spherical surfaces.

12. The lens of claim 1 wherein said corrector lens has two aspheric surfaces, said corrector lens unit being axially spaced from said second lens unit a distance

$$0.4 > D_{2C}/F_O > 0.15$$

where D_{2C} is the axial distance between said biconvex element and said biconvex lens and F_O is the equivalent foal length of said lens.

13. A projection lens for use in combination with a cathode ray tube where the projection lens is closely coupled to the cathode ray tube, said lens comprising from the image end a first lens unit of positive optical power having at least one aspheric surface and contributing to correction of aperture dependent aberrations, a second lens unit providing a majority of the positive power of said lens, and a third lens unit having a strongly concave image side surface which provides correction for field curvature and Petzval sum of other units of said lens, said second lens unit consisting from the image end of a biconcave element, a biconvex element and a positive component, said biconcave element and said first biconvex element forming a color correcting doublet and being of overall meniscus shape concave to the image end, said positive component comprising two elements, one of said elements of said positive component having two aspheric surfaces and being of meniscus shape.

14. The lens of claim 13 where said doublet is spaced from said first lens unit at least 0.1 of the focal length of said lens.

15. A projection lens for use in combination with a cathode ray tube where the projection lens is closely coupled to the cathode ray tube, said lens comprising from the image end a first lens unit of positive optical power having at least one aspheric surface and contributing to correction of aperture dependent aberrations, said first lens unit consisting of a single element, a second lens unit providing a majority of the positive power of said lens, and a third lens unit having a strongly concave image side surface which provides correction for field curvature and Petzval sum of other units of said lens, said second lens unit comprising from the image

end a biconcave element, a biconvex element and a positive element, said biconcave element and said biconvex element forming a color correcting doublet and being of overall meniscus shape concave to the image end, and a corrector lens unit of weak optical power having at least one aspheric surface positioned between said second and third lens units, said corrector lens unit being axially spaced from said second lens unit a distance

$$0.4 > D_{2C}/F_0 > 0.15$$

where D_{2C} is the axial spacing distance between said second lens unit and said corrector element and F0 is the equivalent focal length of said lens.

16. The lens of claim 15 where said element of said first lens unit has two aspheric surfaces.

17. The lens of claim 15 where said lens has a variable magnification, said first and said second lens units move axially in fixed relation to focus said lens and said corrector lens element moves axially in the same direction but at a differential rate.

18. The lens of claim 15 where said first and second lens units move axially in the same direction at differential rates to vary the focus of said lens.

19. The lens of claim 15 where said positive element is also biconvex.

20. The lens of claim 15 where all elements of said second lens unit have spherical surfaces.

21. The lens of claim 15 where the axial marginal rays traced from the long conjugate intersect the image side surface of said corrector lens unit substantially below the clear aperture of said image side surface.

22. A projection lens for use in combination with a cathode ray tube where the projection lens is closely coupled to the cathode ray tube, said lens comprising from the image end a first lens unit of postive optical power having at least one aspheric surface and contributing to correction of aperture dependent aberrations, a second lens unit providing a majority of the positive power of said lens, and a third lens unit having a strongly concave image side surface which provides correction for field curvature and Petzval sum of the other units of said lens, said second lens unit comprising from the image end a biconcave element, a biconvex element and a positive lens element, said biconcave element and said biconvex element forming a color correcting doublet and being of overall meniscus shape concave to the image end, a corrector lens unit positioned between said second and third lens units, said lens having a variable focus and said first lens unit, said second lens unit, and said corrector lens unit being movable axially in the same direction to change the focus of said lens, one of said first lens unit and said corrector lens unit moving differentially with respect to the other movable lens units.

23. The lens of claim 22 where said biconcave element has an absolute optical power greater than the power of said lens.

24. The lens of claim 22 where said first lens unit consists of a single element having two aspheric surfaces.

25. The lens of claim 22 where the axial spacing between said first lens unit and said second lens unit is

$$0.4 > D_{12}/F_0 > 0.1$$

where D_{12} is the distance between the first and second lens units and Fo is the equivalent focal length of said lens.

26. The lens of claim 22 where said positive component is also biconvex.

27. The lens of claim 22 where all elements of said second lens unit have spherical surfaces.

28. The lens of claim 22 where said first lens unit moves differentially.

29. The lens of claim 22 where said corrector lens unit moves differentially.

30. A projection lens for use in combination with a cathode ray tube where the projection lens is closely coupled to the cathode ray tube, said lens comprising from the image end a first lens unit of positive optical power having at least one aspheric surface and contributing to correction of aperture dependent aberrations, a second lens unit providing a majority of the positive power of said lens, and a third lens unit having a strongly concave image side surface which provides correction for field curvature and Petzval sum of other units of said lens, said second lens unit comprising from the image end a biconcave element, a biconvex element and a positive element, said biconcave element and said biconvex element forming a color correcting doublet and being of overall meniscus shape concave to the image end, and a corrector lens unit of weak optical power having at least one aspheric surface positioned between said second and third lens units, said corrector lens unit being axially spaced from said second lens unit a distance

$$0.4 > D_{2C}/F_0 > 0.15$$

where D_{2C} is the axial spacing distance between said second lens unit and said corrector element and F0 is the equivalent focal length of said lens.

31. The lens of claim 30 where said first lens unit consists of a single element having two aspheric surfaces.

32. The lens of claim 30 where said positive element is also biconvex.

33. The lens of claim 30 where all elements of said second lens unit have spherical surfaces.

34. A projection lens for use in combination with a cathode ray tube where the projection lens is closely coupled to the cathode ray tube, said lens comprising from the image end a first lens unit of weak optical power having at least one aspheric surface and contributing to correction of aperture dependent aberrations, a second lens unit providing a majority of the positive power of said lens, said second lens unit being spaced from said first lens unit at least 0.1 of the equivalent focal length of the lens, and a third lens unit having a strongly concave image side surface which provides correction for field curvature and Petzval sum of other units of said lens, said second lens unit comprising from the image end a biconcave element, a biconvex element and a positive element, said biconcave element and said biconvex element forming a color correcting doublet and being of overall meniscus shape concave to the image end, and a corrector lens unit of weak optical power positioned between said second and third lens, said corrector lens unit having at least one aspheric surface, the configuration and the positioning of said corrector lens element from said second lens unit being such that the axial marginal rays from said second lens unit as traced from the long conjugate intersect a sur-

face of said corrector lens unit at a height H from the optical axis of said lens that is less than the clear aperture of said surface of said corrector lens unit, said corrector lens surface being configured to contribute to correction of aperture dependent aberrations within said height H, said surface of said corrector lens beyond said height H being configured to contribute to correction of aberrations due to off-axis rays

35. The lens of claim 34 wherein said positive element of said second lens unit is biconvex.

36. The lens of claim 34 where said corrector lens unit consists of a single element.

37. The lens of claim 34 where all elements of said second lens unit have spherical surfaces.

38. A projection lens for use in combination with a cathode ray tube where the projection lens is closely coupled to the cathode ray tube, said lens comprising from the image end a first lens unit of positive optical power having at least one aspheric surface and contributing to correction of aperture dependent aberrations, said first lens unit comprising a front meniscus element convex toward the image end, a second lens unit providing a majority of the positive power of said lens, said second lens unit being spaced from said meniscus element at least 0.1 of the equivalent focal length of the lens, and a third lens unit having a strongly concave image side surface which provides correction for field curvature and Petzval sum of other units of said lens, said second lens unit consisting from the image end of a biconcave element, a biconvex element and a positive element, said biconcave element and said biconvex element forming a color correcting doublet and being of overall meniscus shape concave to the image end, and a corrector lens unit of weak optical power positioned between said second and third lens, the configuration and the positioning of said corrector lens element from said second lens unit being such that the axial marginal rays from said second lens unit as traced from the long conjugate intersect a surface of said corrector lens unit at a height H from the optical axis of said lens that is less than the clear aperture of said surface of said corrector lens unit, said corrector lens surface being configured to contribute to correction of aperture dependent aberrations within said height H, said surface of said corrector lens beyond said height H being configured to contribute to correction of aberrations due to off-axis rays.

39. The lens of claim 38 wherein said positive element of said second lens unit is biconvex.

40. The lens of claim 38 where said corrector lens unit consists of a single element.

41. A projection lens for use in combination with a cathode ray tube where the projection lens is closely coupled to the cathode ray tube, said lens comprising from the image end a first lens unit of weak positive optical power having at least one aspheric surface and contributing to correction of aperture dependent aberrations, a second lens unit providing a majority of the positive power of said lens, and a third lens unit having a strongly concave image side surface which provides correction for field curvature and Petzval sum of other units of said lens, said second lens unit comprising from the image end a biconcave element, a biconvex element and a positive element, said biconcave element and said biconvex element forming a color correcting doublet and being of overall meniscus shape concave to the image end, and a corrector lens unit of weak optical power positioned between said second and third lens, the configuration and the positioning of said corrector lens unit from said second lens unit being such that the axial marginal rays from said second lens unit as traced from the long conjugate intersect a surface of said corrector lens unit at a height H from the optical axis of said lens that is less than the clear aperture of said surface of said corrector lens unit, said corrector lens surface being configured to contribute to correction of aperture dependent aberrations within said height H, said surface of said corrector lens beyond said height H being configured to contribute to correction of aberrations due to off-axis rays

42. The lens of claim 41 wherein said positive element of said second lens unit is biconvex.

43. The lens of claim 41 where said corrector lens unit consists of a single element.

44. The lens of claim 41 where said biconcave element has an absolute optical power greater than the power of said lens and said biconvex element has an optical power greater than the optical power of said lens.

45. The lens of claim 41 where said biconcave element has an absolute optical power greater than the power of said lens.

46. The lens of claim 41 where all elements of said second lens unit have spherical surfaces

47. The lens of claim 41 where said color correcting doublet is of weak negative optical power

48. The lens of claim 41 where the absolute optical power of said biconcave element is greater than the optical power of said biconvex element

49. The lens of claim 41 where said lens has a variable magnification, said first and said second lens units move axially in fixed relation to focus said lens and said corrector lens element moves axially in the same direction but at a differential rate.

50. The lens of claim 41 where said first and second lens units move axially in the same direction at differential rates to vary the focus of said lens.

51. A projection lens system for use in combination with a cathode ray tube comprising:

(a) a first lens at the image end of said lens system wherein the surface of said first lens on the image side is convex to the image on the axis of said first lens and is concave to the image at and near the clear aperture of said first lens and the other surface of said first lens is concave to the image.

(b) a second lens adapted to be closely coupled to a cathode ray tube, said second lens having a concave image side surface;

(c) a color correcting doublet located between said first and second lenses, said color correcting doublet being comprised of a biconcave lens and a biconvex lens;

(d) a biconvex lens located between said color correcting doublet and said second lens; and

(e) a corrector lens located between said biconvex lens and said second lens, said corrector lens being shaped and positioned to contribute to correction of spherical aberrations in the central portion thereof and to contribute to the correction of aberrations due to off axis rays beyond said central portion.

52. The lens of claim 51 where both elements of said color correcting doublet and said biconvex lens are glass having spheric surfaces.

53. The lens of claim 51 where said color correcting doublet is of weak negative optical power.

54. The lens of claim 51 where said doublet is spaced from said first lens unit at least 0.1 of the equivalent focal length of said lens.

55. The lens of claim 51 where said first lens has two aspheric surfaces.

56. The lens of claim 51 where said color correcting doublet is axially spaced from said biconvex element no more than 0.01 of the equivalent focal length of said lens.

57. The lens of claim 51 where said doublet is concave to the images.

58. A projection lens system for use in combination with a cathode ray tube comprising

(a) a first lens at the image end of said lens system wherein the surface of said first lens on the image side is convex to the image on the axis of said first lens and is concave to the image at and near the clear aperture of said first lens and the other surface of said first lens is concave to the image;

(b) a second lens adapted to be closely coupled to the cathode ray tube, said second lens having a concave image side aspheric surface;

(c) a color correcting doublet located between said first and second lenses, the color correcting doublet being comprised of a biconcave lens and a biconvex lens;

(d) a biconvex lens located between said color correcting doublet and said biconvex lens; and

(e) a meniscus lens convex to the image located between said doublet and said biconvex lens.

59. The lens system of claim 58 wherein both surfaces of said second lens are aspheric.

* * * * *

ENCLOSURE 11.6

TEST BED PROJECTOR
OPERATORS MANUAL

OPERATOR'S MANUAL

Manufactured by:
TRIDENT INTERNATIONAL, INC.
Central Florida Research Park
3290 Progress Drive, Ste. 155
Orlando, FL 32826
305-282-3344
407

TABLE OF CONTENTS

SECTION 1.0 INTRODUCTION

We are proud to present the Trident T-100, a highly sophisticated video/data large screen projector.

The T-100's performance capabilities are satisfying the needs of professionals in a variety of applications in the fields of training, education, industry, entertainment and communications.

This manual will introduce you to the T-100 and explain it's operating procedures.

SECTION 2.0 THE T-100 PROJECTOR

The T-100 is an advanced, user-friendly, microprocessor controlled video/data projector. The T-100 differs from other products in the market in that the unit is electronically configured to adapt to various input signals.

These configurations are stored in a non-volatile memory that stores all operating parameters such as height, width, colorimetry, registration and RGB configurations. Thus, when a power failure occurs, or the projector is shut off, the memory will retain the data required to have the unit resume operation once power is restored. When in the RGB mode, the user may store and recall up to eight different configurations, eliminating the need for interface boxes in many applications.

Standard with the T-100 projector is a Remote Control which features a 24 key keypad and an eight character alpha-numeric LED display. For ease of use in low light environments an optional backlit keypad is available.

From the Remote Control the user can access an on-line reference HELP menu system that acts as a reminder of the various steps and numerical codes critical to the proper set up of the unit.

OPTIONAL EQUIPMENT- Many optional items are manufactured specifically for the Trident T-100. For a complete listing of these contact your Trident representative.

Note: The T-100 can also be controlled via any device communicating through an RS232-ASCII port.

2.1 FEATURES

- Simplified sweep reversal for front or rear projection
- On-line Reference (HELP) menu
- Access and Control of an internal diagnostics program monitoring sweep operation
- Test pattern generator featuring
- Crosshair for centering
- Crosshatch for registration
- Crosshatch for sweep direction
- Individual CRT cut-off
- Video source selection
- RGB selection and interface control
- Programmed inversion of analog horz and vert syncs
- Selection of analog RGB sync formats: composite, separate H & V, or sync on green
- Store and Recall of up to eight RGB configurations
- Switcher channel select
- Switcher configuration
- Capable of ceiling or floor mounting with automatic position sensing and sweep reversal
- Registration:
  4 master controls
  10 full picture controls
  42 fine tuning precision controls
- Optionalbacklit registration controls for ease of operation in dark environment
- Integral NTSC comb filter for improved resolution
- Wide band pass video amps
- Internal automatic EGA/CGA interface
- Switch mode power supply
- No external controls
- Quick change tube assemblies
- Easily accessible modular assemblies
- Quiet operation
- Rugged construction
- Aluminum chassis acts as heat-sink
- Electrostatic arcing protection through slow high voltage turn on
- Differential video amplifier inputs on all analog RGB, sync and video
- Safe operation - high voltage components not exposed
- Security bit - prevents inadvertent changing of input device operating parameters
- Initialize RAM - allows logic return to factory set basic operating parameters

2.2 SYSTEM CONFIGURATION CONTROLS

REMOTE CONTROL:

The Remote Control features an optional backlit keypad and alpha-numeric light emitting diode (LED) display for ease of operation in darkened environments. It is attached to the projector via a commercially available four wire modular telephone cable.

ADJUSTMENTS:

- Color
- Picture (contrast)
- Brightness
- Detail
- Tint (hue)
- Red H & V position
- Green H & V position
- Blue H & V position
- Height
- Width

CONFIGURATION CONTROLS:

- RGB selection and interface control
- Inversion of RGB analog sync
- Selection of sync formats:
- separate H & V
- composite H & V
- sync on green
- Storage and recall of up to eight RGB configuration parameters
- Selection of 2 RGB (one analog and one TTL) and 2 composite multi-standard video channels
- Optional switcher with multiple composite video, RGB and audio inputs
- Aspect ratio control 1:1 to 2:1

2.3 SPECIFICATIONS

LIGHT OUTPUT:

- 450 lumens (650 lumens peak white)

RESOLUTION:

- 1024 x 1280 pixels (up to 1400 scan lines)
- 32 MHz bandwidth
- 475 lines in NTSC

SCANNING RATES:

- Horizontal: auto locking from 14 to 42 KHz
- Vertical: auto locking from 45 to 120 Hz
- Retrace time: less than 5 microseconds
- Interlaced or non-interlaced sync
- Adjustable aspect ratios from 1:1 to 2:1

COMPOSITE VIDEO INPUTS:

- Two selectable multi-standard channels with switchable 75 ohm terminations. One channel has loop through capability, while the second allows the signal to be inverted under program control. The second channel also doubles as vertical sync input for analog RGB operation. These channels accept 1 V P-P composite video with negative sync and automatic decoding for sensing and locking in PAL, SECAM and NTSC.
- Standard BNC coaxial connectors
- The optional switching unit will enable the use of up to twenty composite video channels. In addition, there are ten audio stereo channels available.

RGB INPUTS:

- Analog: .5 V to 2.5 V P-P switchable 75 ohm terminated differential inputs
- RGB may be inverted under program control
- Sync input may be inverted under program control, for use with composite sync or horizontal and sync on green when in the separate sync mode of operation
- TTL input is IBM PC/XT/AT CGA/EGA compatible
- Connectors: RGB analog and sync (BNC)
  RGB/TTL (9 pin female sub-miniature "D")
- The optional switching unit makes available ten RGB channels

CATHODE RAY TUBES:

- 5.5" CRT
- Liquid cooled
- Color filtering for enhanced color purity
- Bright phosphor screen
- Larger diameter electronic gun for increased resolution
- Electrostatically focused
- Non-browning strontium-filled glass

INPUT LINE VOLTAGE:

- Automatic internal sensing and switch over circuitry (117 or 240 V AC +/- 15%)
- Frequency 48 to 62 Hz

HIGH VOLTAGE:

- 35KV

POWER CONSUMPTION:

- 350 watts

KEYSTONE CORRECTION:

- +/- 25 degrees

TEMPERATURE:

- Minus 10 C to + 45 C
- Minus 25 C to + 75 C (storage)

HUMIDITY:

- Operational up to 90% non-condensing

LENSES:

- F1.0 (130 mm) improved acrylic coated lenses
- Separate dual focus adjustments for each lens yielding crisper images (one for the center image area and one for the edges)
- Optional high resolution glass lenses also available. See 2.0 'Optional equipment'.

SCREEN APPLICATION AND SET-UP:

- Flat or curved screen, front or rear projection, ceiling or floor mounting

PICTURE SIZE:

- From 30 in. x 40 in. to 15 ft. x 20 ft.
- From .76 m x 1.01 m to 4.5 m x 6.1 m

DIMENSIONS:

- Length - 33.00 in. (83 cm)
- Width - 22.00 in. (55 cm)
- Height - 9.25 in. (23 cm)

WEIGHT:

- 74.00 lbs.
- 33.60 kg.

SHIPPING WEIGHT:

- 125 lbs.
- 45.5 kg. (approx.)

THROW DISTANCE:

- 1.5 times image width

2.4 SERVICE AND MAINTENANCE

Trident projectors are highly reliable systems with minimal service and maintenance required other than an occasional wiping of the lenses using a non-abrasive cloth and ordinary glass cleaner. The design of the T-100 system is modular. If service is required, it is simply and inexpensively accomplished through the replacement of a module.

2.5 LOGISTICS SUPPORT

Trident's Logistics Support Policy covers in-warranty and out-of-warranty situations.

- In Warranty. Trident will replace or repair, or have replaced or repaired free of charge, defects in any unit subassembly or component which has failed as a result of workmanship or normal usage for the period described in 2.6, Limited Warranty. Shipment of replacement material that has a known defect will be made within forty-eight (48) hours of receipt of the defective material at Trident, Orlando, Florida. The shipping address for all materials is:

Trident International, Inc.
3290 Progress Drive
Suite 155
Orlando, FL 32826
Attn: Logistics Support Coordinator

- Out-of-Warranty. Trident will replace or repair, at the Dealer's/End-User's expense, any failed parts or assemblies which cannot otherwise be repaired by the Dealer, and which are qualified as product related defects (not operator error, ect.). In situations where the cause of failure is known, Trident will perform work for the fee prescribed in our repairs price list and in the time frame prescribed in that document. In situations where Trident must troubleshoot to determine cause(s) of failure , Trident will charge a fixed fee to evaluate said failure, will quote repair cost, and should customer release us to do the repair, credit the evaluation fee. The shipping address for all materials is:

Trident International, Inc.
3290 Progress Drive
Suite 155
Orlando, FL 32826
Attn: Logistics Support Coordinator

2.6 LIMITED WARRANTY

Trident International, Inc. warrants this product to be free from defects in material and workmanship, under normal use, subject to the limitations provided below.

2.7 LIMITATIONS

- WARRANTY PERIOD. For one year after the date of purchase by the customer. During this period, Trident will repair or replace any defective part without charge for labor or material. This Limited Warranty applies only to parts supplied or designed by Trident.

- DATE OF PURCHASE. To establish the date of purchase and invoke this Limited Warranty, the Trident Warranty Registration Card must be completed, signed and returned to Trident, postmarked no later than ten (10) days from the date of purchase. If the Trident Warranty Registration Card is not returned within such time, Trident will not honor warranty claims.

- ORIGINAL PURCHASER. This Limited Warranty is limited to the original purchaser (end-user) of this product from either Trident or Trident's authorized dealer, distributor, or authorized agent.

- WARRANTY SERVICE. For repairs under this Limited Warranty, this product must be presented to Trident, an authorized Trident service center, or the authorized Trident selling dealer. A copy of Trident's Product Logistic Support Policy and Implementation is shipped with each projector.

- SHIPPING. Prior to shipping this product or any subassembly to Trident, a Return Authorization Number must be obtained from Trident's Service Department. This product must be shipped in the manufacturer's original shipping carton or other Trident-approved packaging. All freight and shipping charges to and from Trident must be prepaid by the purchaser. This product must be shipped by air or delivered by purchaser or his representative. Damage resulting from abuse in shipment of this product is not covered by this Limited Warranty. Trident-approved shipping cartons are available from Trident at a nominal charge.

- ENVIRONMENTAL DAMAGE. This Limited Warranty does not cover damage or repairs that are necessary due to floods, winds, fires, lightning, accidents, corrosive atmosphere, excessive exposure to water (moisture) or heat, or any other conditions beyond the control of Trident.

- SERIAL NUMBER DEFACEMENT. This Limited Warranty is void for this product if the serial number has been changed, removed or defaced.

- MISUSE. This Limited Warranty does not cover repairs that are necessary due to:

  (a) incorrect installation;

  (b) incorrect voltage conditions, blown fuses, open circuit breakers, or any other inadequacy or interruption of electrical service;

  (c) misapplication, abuse, improper servicing or any other improper operation, including misadjustment of any control;

  (d) defects in or caused by associated equipment; or

  (e) repair and/or modification attempted by anyone other than Trident, a Trident service center or the Trident authorized dealer.

***** NOTE ***** NOTE ***** NOTE ***** NOTE ***** NOTE *****

- TRIDENT MAKES NO WARRANTY OF ANY KIND, EXPRESS OR IMPLIED, IN CONNECTION WITH THIS PRODUCT AS HEREINABOVE PROVIDED. IMPLIED WARRANTIES OF MERCHANTABILITY OR FITNESS FOR A PARTICULAR PURPOSE OR ARISING FROM A COURSE OF DEALING OR USAGE OR TRADE ARE SPECIFICALLY EXCLUDED. SHOULD THIS PRODUCT PROVE TO BE DEFECTIVE IN MATERIAL OR WORKMANSHIP, THE PURCHASER'S SOLE REMEDY SHALL BE SUCH REPAIR OR REPLACEMENT AS HEREINABOVE EXPRESSLY PROVIDED AND UNDER NO CIRCUMSTANCES SHALL TRIDENT BE LIABLE FOR ANY LOSS OR DAMAGE, DIRECT, INCIDENTAL OR CONSEQUENTIAL, INCLUDING LOSS OF PROFITS OR BUSINESS OPPORTUNITIES RESULTING FROM INABILITY TO USE THIS PRODUCT. TRIDENT SHALL NOT BE LIABLE FOR ANY DAMAGES RESULTING FROM DEALER OR DISTRIBUTOR INSTALLATION OR SERVICES.

***** NOTE ***** NOTE ***** NOTE ***** NOTE ***** NOTE *****

SECTION 3.0 INSTALLATION/SERVICING

3.1 FACILITY PLANNING CONSIDERATIONS

Each installation will be unique in some way. There are several considerations, that must be included in the planning for every viewing area.

Lighting is critical to good viewing. Too much ambient light causes the image to look faded, washed out and weak. Strong light sources, such as windows, can cause reflections which are irritating to the viewer, lessening the impact of the video message.

Room traffic patterns are also important. Will late comers disrupt the audience? If speakers are using the projectors, can they reach the controls? Is there enough room for multiple video input devices, e.g. videodisc and computer?

3.2 IMAGE SIZE

The projector is preset for an image six feet high by eight feet wide (6'x 8'). That means that the distance from the center of the screen to the center of the GREEN lens on the projector must be twelve feet (12'). This is called the throw distance and is calculated at 1.5 times the image width.

Changing the image size means changing the throw distance, i.e. moving the projector, and readjusting lenses focus and registration (section 5).

3.3 PROJECTION MODES

The T-100 projector can be mounted for front or rear projection, floor or ceiling mounts.

On axis projection means that the plane of the lens face parallels the plane of the screen and the center of the GREEN lens is aligned with the center of the screen. This is impractical for most installations but any other positioning causes a distortion known as the keystone effect (which is defined and discussed in paragraph 5.6).

The T-100 projector has a built in correction to counter most of this effect. The lenses are mounted at a twelve degree angle to compensate for floor and ceiling mounts.

The keystone effect occurs in the horizontal as well as the vertical plane. Aligning the projector to the center of the screen with its face parallel to the screen will minimize the need for corrections.

3.4 UNPACKING

The projector has been carefully packed at the factory to prevent damage in transit. Before removing unit from the carton/crate, check for any obvious damage. If damage is visible, notify Trident and the carrier at once.

CAUTION -- Two people are required to safely lift and carry the projector.

NOTE - The T-100 has been tested and adjusted at the factory to project a 6' x 8' picture. It is recommended that a Performance Check be made before permanent installation to ensure the projector was not damaged during shipment. If the projector is moved often, periodic performance checks will ensure optimum performance.

3.5 MOUNTING

When setting up the projector be sure the mounting platform, floor or ceiling mount, is level and as closely aligned with the center of the screen as possible. This will reduce the magnitude of any focus and alignment corrections.

The T-100 projector can be attached to the ceiling using the mounting bracket assembly (Trident part # 200011). The mounting bracket is secured to a customer supplied 1 1/2" diameter pipe, externally threaded.

(See figure 2 'Mounting Bracket Assembly') Securely attach support angles (items 1 & 2) to bottom of projector using 5/16 18 x 5/8 hex head screws with 5/16 lockwashers (items 6 & 7) ensuring that the slotted angle adjust holes are positioned towards the rear of the projector.

Loosely fasten the travel limiter brackets (items 3 & 4) to support angles using two 7/16 - 14 x 1 1/4" hex head screws (item 8) with 7/16 lock washer and 7/16 nut (items 10 & 9). Screw the hand knobs into the limiter angles and tighten, ensuring the support angles and limiter angles are parallel. Tighten the two 7/16" screws and re-tighten the hand knobs.

Screw the limiter brackets (mounted to the projector) <u>over</u> the hanging cross plate and align the four cross plate mounting holes with the holes on the bracket. Insert the four 1/4 20 x 3/4" screws (item 13) through the limiter bracket and crossplate and tighten with 1/4 20 lockwashers (item 15) and 1/4 20 nuts (item 14). After projector is in place ensure that all mounting hardware is secured.

NOTE: For ceiling mounts, it is suggested that initial focus, alignment and registration be done on a table under the mounting fixture. The controls are much more accessible. Small adjustments will still be required after mounting. Vertical sweep reversal is automatic for Trident projectors.

3.6 LEAKAGE TEST

(See figure 3 'Leakeage Test Procedure') Connect a 1500 ohm 10 watt resistor, parallel by a 0.15 mfd AC-type capacitor between a known good earth ground (water pipe, conduit, etc.) and a clear metal portion of the cabinet, as shown in the sketch. Measure the AC voltage across the combination 1500 resistor and 0.15 mfd capacitor with power OFF and again with power ON. Reverse the AC plug on the set and repeat the AC voltage measurements. Voltage measured must not exceed .3 volts RMS. This corresponds to 0.5 milliamp AC. Any value exceeding this limit constitutes a potential shock hazard and must be corrected immediately.

3.7 WARNINGS AND PRECAUTIONS

X-RADIATION - During the operation of any solid state video system, the picture tube is a primary source of x-radiation. The projector system has been designed to prohibit the leakage of x-rays. Radiation absorbing materials are permanently bonded to the CRT glass so that the shielding may not be inadvertently left off. It complies with all U.S. Dept. of Health, Education and Welfare rules governing the emission of x-radiation. FOR CONTINUED X-RADIATION PROTECTION, YOU SHOULD NEVER ATTEMPT TO REPLACE THE LENSES, PROJECTION TUBES OR OTHER ELECTRONIC COMPONENTS in the system yourself. Instead, all service to the system should be performed by a Trident trained authorized service technician.

HIGH VOLTAGE - The projector system contains HIGH VOLTAGE derived from power supplies capable of delivering LETHAL quantities of energy. TO AVOID SERIOUS INJURY NEVER ATTEMPT TO REMOVE THE TOP COVER OF THE PROJECTION UNIT. There are no user-serviced parts in the Projection unit. All parts replacement should be performed by a qualified technician.

EXPOSURE TO RAIN OR MOISTURE - To reduce fire or shock hazard, NEVER EXPOSE THE PROJECTOR SYSTEM TO RAIN OR MOISTURE. If this happens inadvertently, do not use the system until it has been inspected and/or serviced by a qualified technician.

PROJECTION TUBES - The projection tubes inside the projection unit enclose a high vacuum. Care must be taken to ensure that the projector is not dropped or otherwise subjected to violent blows.

The tubes may be damaged if the projection unit is operated at brightness levels beyond its designed capabilities. Operating brightness at maximum output for extended periods of time, puts undue stress and extremely heavy duty cycles on CRT's (cathode ray tubes) which decreases tube longevity.

******* WARNING *******

Attempts to alter the factory-set internal controls or to change other control settings not specifically discussed in this manual can lead to permanent damage to the unit and cancellation of the Warranty.

SECTION 4.0 OPERATING THE T-100 PROJECTOR

4.1 GENERAL INFORMATION

This section of the Operator's Manual deals with how to operate the system in the NTSC, PAL or SECAM modes. It includes system activation and turn-off, image adjustments, alignments and any change in projector configuration, i.e. image size, rear projection, projection angle or RGB operation. Any changes that need to be made to suit your needs will require a few simple adjustments.

The Trident projectors are pre-set at the factory with a 6' x 8' picture.

4.2 THROW DISTANCE

(See figure 4 'Throw Distance Example')The formula to compute the throw distance for a desired image width is 1.5 times image width, measured from the center of the screen to the center of the green lens as shown in the drawing. Following the above instruction, position the projector accordingly. The T-100 units are capable of projecting an image as small as 40 inches or as large as 20 feet wide. If an image size other than 6' x 8' is desired, it will be necessary to make two mechanical adjustments: lateral lens adjustment and lens focus which are explained in paragraphs 5.3 and 5.4.

4.3 *PROJECTION MODES*

All Trident projectors have the ability to project in either front, rear, ceiling, and floor/table projection modes.

4.4 ON AXIS PROJECTION

On axis projection is projecting an image with the projector's lenses perpendicular to the screen. Projecting at any angle other than perpendicular to the center of the screen will cause some keystone distortion.

4.5 THE BACK PANEL

The back panel of the T-100 contains seven BNC connectors, six termination switches, two modular phone jacks, a nine pin sub-min d connector, the power ON/OFF switch, the AC input for 110/220 V, and the fuse box.

From left to right, the first four BNC connectors are analog inputs for RGB and external sync. The fifth and sixth (marked "2" and "1") accept composite video inputs. The seventh is the feedthru for the video 1 channel.

4.6 OPERATING INSTRUCTIONS

4.6.1 THE REMOTE CONTROL

The Remote Control features a keypad, with a back-lighting option, and an 8 character alpha-numeric LED display for ease of operation in darkened environments. It is attached to the projector via a commercially available four wire modular telephone cable.

The Remote Control has the following capabilities:

- Source selection and set-up
- 8 character display provides meaningful feedback on projector operation
- uses RS232, 7 bit, even parity, 1200 baud 3 wire link so that the projector can be controlled directly by a computer serial port

See paragraph 4.7 for FUNCTION COMMANDS/CODES listing

The Remote Control socket is located on the back panel of the projector. It is labeled Remote Control.

Code entries should be made deliberately. Inaccurate entries will result in an "INVALID" prompt. Should this occur, reenter the correct code. With the power switch on the rear panel ON all operations are performed using the Remote Control.

4.6.2 APPLYING POWER

The ON/OFF power switch located next to the AC power socket in the rear panel of the projector, controls the supply of AC power to the system. Depressing the upper portion of this switch places it in the ON position applying power to the system. Depressing the lower portion cuts OFF power to the system. Once the projector power switch is ON, all further controlling may be done using the Remote Control.

There is a secondary ON/OFF power switch on the registration controls panel. It is for use when the Remote Control is not connected and replaces the Remote Control function of controlling power to the CRTs.

When power is first applied to the projector, either through the switch on the back of the projector or the ON/OFF key on the Remote Control, the projector goes through a warm up test cycle before it is ready to accept commands. The display read outs will cycle through BATT OK or BATT BAD (battery state), and READY. Now power may be applied to the CRTs.

NOTE - Be sure to turn the projector power switch OFF when moving the projector or changing power supplies.

***** WARNING *****

-- Potentially LETHAL voltages exist within the projector even with the ON/OFF power switch in the OFF position. Do not remove covers which expose high voltage components.

***** WARNING *****

4.6.3 COMPOSITE VIDEO (NTSC/PAL/SECAM)

There are two composite video channels, 1 and 2. Channel selection is determined by the input jack the equipment is plugged into.

To enter the composite video 1 or 2 modes, use the Remote Control. When power has been turned ON and the projector is ready to operate, the display will read READY. Press the ON/OFF key, the projector will come up in the operating mode it was shut down in. If it comes up in other than the desired mode:

- Composite video channel 1 VIDEO 1 VID1 SB

Press the [VIDEO] key. When the prompt 'VIDEO' appears, press digit key [1].

- Composite video channel 2 VIDEO 2 VID2 SB

Press the [VIDEO] key. When the prompt 'VIDEO' appears, press digit key [2].

4.6.3.1 NTSC/PAL/SECAM BLANKING

The NTSC/PAL/SECAM operation input does not use the maximum viewing area possible within the transmission facility standards. Trident projectors offer blanking for the top, left edge, and right edge of the picture, while in video only. No blanking is required in RGB.

4.6.4 RGB OPERATING INSTRUCTIONS

Operation of the RGB mode in the T-100 is different from NTSC/PAL/SECAM operation only in how video information is processed. Instead of a composite video signal, RGB requires separate RED, GREEN and BLUE signals and, in some cases, one or two separate sync lines depending on the computer being used. The four modes of RGB operation are ..

DIGITAL - This mode of operation uses the 9 pin 'd' connector on the back panel as an input, and is compatable with the IBM CGA and EGA adapters. An internal interface will automatically sense which adapter is in use and adjust the projectors operating frequency, along with the way the RGB signals are decoded.

ANALOG SYNC ON GREEN - In this mode the sync signals are contained within the green channel of the RGB. Only three cables are required to connect the projector to the source.

ANALOG COMPOSITE SYNC - In this mode the horizontal and vertical sync signals are combined into a composite signal which connects to the sync terminal on the back panel. Four cables are required for this type of installation.

ANALOG SEPARATE SYNC - In this mode the sync signals are provided separately, and five cables are required to make the connection. The horizontal sync is connected to the sync input while the vertical sync is connected to the video 2 input. While the projector is cabled for this mode, only the video 1 channel is available for normmal composite video input.

The T-100 has built in logic to allow operation in all four of these RGB modes.

4.6.4.1 RGB OPERATION AND MEMORY

The projector, in the RGB mode of operation, has the ability to store and retrieve eight possible configurations. These are kept in a non-volitile memory, one whose contents are not lost when there is no power, and contain the following ..

brightness setting
contrast setting
picture width setting
picture highth setting
mode of RGB (DIGITAL, SYNC ON GREEN, COMPOSITE, SEPARATE)
sync polarities

4.6.4.2 SELECTING A RGB CONFIGURATION

a. Select [RGB] on the Remote Control. The prompt RGB will appear on the display.

b. Enter a digit from 1 to 8 to select the desired RGB configuration. After the system has been initialized the eight RGB memories default to

1 - RGB Sync on Green
2 - RGB Composite Sync
3 - RGB Seperate Sync
4 - RGB TTL Sync
5 - RGB TTL Sync
6 - RGB TTL Sync
7 - RGB TTL Sync
8 - RGB TTL Sync

a. Select RGB and a non-volatile memory file (1 - 8).

b. Determine which of the RGB modes the input computer operates in.

c. Select the operating mode (see paragraph 4.6.4.6).

d. When the operating mode is displayed on the Remote Control, the projector will accept inputs from the computer.

e. Using the projected image and the codes from the RGB operating codes listing, operating parameters of the file data may be changed to match those of a "compatible".

f. When the operating parameters are set, the image can be changed using the controls on the top half of the Remote Control (see section 6.0).

g. Parameter changes made are now stored in the non-volatile file and may be recalled.

4.6.4.3 RGB OPERATING MODES (TTL AND ANALOG)

TTL RGB RGB DIG RGBD SB

Press the [RGB] key. The prompt RGB will appear. Then press a single digit key in the range 1 to 8 to select the RGB parameter table to use. At this time the display will show the current mode. If it is in an analog RGB mode, do the following:

- Press,

[4][0] [ENTER]

to get into RGB TTL mode.

ANALOG RGB WITH COMPOSITE H & V SYNC RGB CS RGBC SB

Press the [RGB] key. The prompt RGB will appear. Then press a single digit key in the range 1 to 8 to select the RGB parameter table to use. At this time the display will show the current mode. If it is not the desired mode, do the following:

- Press,

[4][3] [ENTER]

to get into RGB composite sync mode.

ANALOG RGB WITH SEPARATE H & V SYNC RGB SS RGBS SB

cPress the [RGB] key, the prompt RGB will appear. Then press a single digit key in the range [1] thru [8] to select the RGB parameter table to use. At this time the display will show the current mode. If it is not the desired mode, do the following:

- Press,

[4][4] [ENTER]

to get into RGB ANALOG separate sync mode.

ANALOG RGB WITH SYNC ON GREEN RGB SOG RGBG SB

Press the [RGB] key. The prompt RGB will appear. Then press a single digit key in the range [1] thru [8] to select the RGB parameter table to use. At this time the display will show the current mode. If it is not the desired mode, do the following:

- Press,

[4][5] [ENTER]

to get into an RGB ANALOG SYNC ON GREEN mode.

4.6.5 "TEST" OPERATING MODE

CODE [1][1] [ENTER]

Internal crosshair/crosshatch generator TEST TESTSB

Press,

[1][1] [ENTER].

The prompt TEST will appear. At this time a crosshair should be projected. Upon entering this mode the keypad is automatically put into the second level mode of operation. In this mode certain of

the digit keys have functions mapped into them.

- [1] - Exit test mode to previous mode
- [2] - Step through the test patterns available
- [3] - Leave the second level mode of keypad operation
- [4] - Toggle the RED CRT ON/OFF
- [5] - Toggle the GREEN CRT ON/OFF
- [6] - Toggle the BLUE CRT ON/OFF
- [8] - Toggle REGISTRATION ON/OFF
- [7] - Enter the RED CRT centering adjust mode
- [9] - Enter the BLUE CRT centering adjust mode

Detailed instructions will be found in section 5.0.

4.6.6 "HELP" OPERATING MODE

Press,

[1][0] [ENTER]

INTERNAL TEXT GENERATOR HELP HELP SB

Press,

[1][0] [ENTER]

The following display will be shown on the screen,

T-100 HELP MENU

1 = COMMAND SUMMARY
2 = SETUP PROJECTOR
3 = REGISTRATION
4 = SOURCE SELECTION
5 = RGB STORE/RECALL
6 = SWITCHER SUPPORT
7 = DIAGNOSTICS

TO VIEW THE DESIRED HEADING
PRESS THE APPROPRIATE NUMBER
KEY.

When in the HELP mode, the following commands apply.

NOTE: Applicable commands are included on each page of directions. Whenever the main menu is displayed and until a topic key [1] thru [9] is selected the down arrow key is the only active key on the Remote Control. It returns to previous video mode when pressed.

- Topic selection requires only a single digit entry
- While in the topic area, the left and right arrow keys control forward and back paging
- The up arrow will always return to the main

- The image controls, TINT, DETAIL, etc. are useable in the HELP mode. When image adjustments are complete, [ENTER] must be pressed to return arrow key control to the HELP mode

4.6.7 DIAGNOSTICS

There are six (6) diagnostic messages which can appear on the remote display, to give a warning of improper operation. These are prioritized in the order of their severity.

'NO XXXX' were XXXX is one of the following abbrieviations VID1,VID2,HELP,TEST,RGBS,RGBD,RGBS,RGBG, representing one of the possible sources. This indicates that no valid input has been detected.

'H FAIL' indicates that the horizontal deflection circuit has failed.

'V FAIL' indicates that the vertical deflection circuit has failed.

'H LOCK' indicates that the horizontal auto-lock circuit can not syncronize with the input signal.

'MUTE' indicates that although the horizontal circuit is in a state of lock, the input signal is no longer in sync.

'L BLANK' indicated that the picture is being blanked out by the lock circuit.

The status of these six items can be checked by pressing

[4][8] [ENTER].

This displays an eight bit binary value, where a bit value of one indicates a failure determined by the bit position. After viewing the display press the ENTER key to clear the display back to the normal status prompt, ignoring the momentary INVALID message.

It is primarily for use by repair technicians and may give readouts confusing to the operator.

Operator troubleshooting procedures can be found in section 7.0.

4.6.8 SWITCHER OPERATION (Optional)

An optional switcher unit is available for the T-100 projector. It allows the user to access one of ten possible channels of input, each of which can contain 2 composite video signals, an RGB input, and a stereo audio input.

NOTE: When using the switcher, channel 8 in the RGB non-volatile memory files should be left empty. That is the channel the switcher loads to.

4.7 FUNCTION COMMANDS/CODES

The following functions are all accomplished using the Remote Control. Several features have been programmed into the logic to simplify operation and prevent inadvertent changes to operating data. This paragraph discusses those features, describes the available code functions and lists the display readouts associated with each code.

4.7.1 FIRST AND SECOND LEVELS OF CONTROL

Press,

[2][3] [ENTER]

The controlling logic for the T-100 projector has been structured at two levels. The first level requires code entries of two digits plus pressing the [ENTER] key to activate a command. The requirement for multiple key activation reduces the possibility of accidental parameter changes during normal operation. Level 1 is the normal operating level in the VIDEO and RGB modes.

The second level of operation requires only single key entries to activate a function. It is for use when the operator is concentrating on picture adjustments, focusing, alignment or registration. For that reason, the TEST mode always is called up in the second level of operation.

To enter the second level mode of operation press,

[2][3] [ENTER]

When the command is entered, the display on the Remote Control will show the level entered and then return to the current mode of operation display. To exit the second level, simply press key [3].

NOTE: In the TEST mode, accidentally pressing key [3] will place the logic commands at level 1, requiring 2 digit plus [ENTER] entries thus using level 1 codes. If single key commands do not appear to be working, select code [2][3] [ENTER] to insure that the logic is in level 2.

Level 2 control keys and their functions are:

- [1] - TEST MODE:
  Exits to last operating mode (VIDEO or RGB).
  Exits second level (single digit) mode.
  - VIDEO or RGB modes:
    Exits to TEST mode.

- [2] - Step through the test patterns available
- [3] - Leave the second level mode of keypad operation
- [4] - Toggle the RED CRT ON/OFF
- [5] - Toggle the GREEN CRT ON/OFF
- [6] - Toggle the BLUE CRT ON/OFF
- [7] - Enter the RED CRT centering adjust mode
- [8] - Toggles the registration amplifiers on /off
- [9] - Enter the BLUE CRT centering adjust mode

NOTE: Code [2] (step through the test patterns available) is not operational in video and RGB modes.

4.7.2 SECURITY BIT OPERATION

Press,

[2][8] [ENTER] and [2][9] [ENTER]

The T-100 has the capability of setting and storing the operating logic data for 24 separate RGB input devices. Each data file can To prevent inadvertent loss or changing of the data files, a security system has been built into the logic. The entry code listings have been structured so that all normally required codes are numbered [1]-[2][7] and the less used and more critical codes are numbered [3][0] and above.

To prevent access to codes [3][0] and above select [2][8] ENTER. The Remote Control display will show SECURE. Anytime a protected code is selected, the display will read SECURE. To gain access to the protected codes, select [2][9] ENTER. The term INSECURE will be displayed on the Remote Control.

Trident recommends that the projector be operated with the security bit activated. Inadvertent commands while in the VIDEO and RGB modes could cause changes in the stored operating parameters, with disastrous effect on image quality.

4.7.3 INITIALIZE DATA STRUCTURE IN RAM

There may be times when the projector logic hangs-up, either through computer or operator error. If that should happen, initializing the data structure will reset certain parameters to factory loaded values. The procedure is to press,

[5][3] [ENTER]

on the Remote Control. The display will read YOU SURE. Press the [0] key for 'YES', any other key for 'NO'. When you select 'YES' [0], the following occurs:

- The RGB channels are set up to default as described above.
- If a switcher is installed, all channels are set to VIDEO A. The current switcher channel goes to zero.
- All heights and widths are set to maximum.

- All brightness (BRIGHT) and contrast (PICTURE) levels are set to 75%.
- All centering is set to 50% (nominal null point)
- COLOR and TINT are set at 50% (nominal null point)
- DETAIL is set at 75%.
- Blanking is set at approximately 100%.

Should you initialize the data structure, a complete alignment and registration procedure is recommended.

4.7.4 EXTERNAL TEST PATTERN GENERATORS

The internal test pattern generator in the T-100 may not have enough high resolution capability to adequately adjust some very high resolution inputs. To allow centering and image adjustments using an external test pattern generator, the internal TEST mode functions in second level have been duplicated in first level operation. Codes [1][3], [1][4] and [1][5] control the CRTs power and [2][0], [2][1] and [2][2] control image centering. The image adjustment controls function the same in both 1 and 2 levels. By entering [2][3] [ENTER] single key controls are the same as in the TEST mode.

4.7.5 CODE LISTING

Those commands followed by an asterisk require the use of directional arrows.

ENTRY CODE	FUNCTION TO BE PERFORMED	DISPLAY READOUT
[ON/OFF]	Unit ready to turn on	READY
	Battery check - OK (power applied)	BATT OK
	Battery to be replaced	BATT BAD
	Unit turned OFF - wait 20 seconds prior to turning ON again	WAIT
	Main power ON - automatic turn ON	AUTO ON
	Command entered with unit OFF	NOT ON
[STANDBY]	States message followed by SB	MSG+SB
[DETAIL]*	Adjustment	DETAIL
[PICTURE]*	Adjustment	PICT
[TINT]*	Adjustment	TINT
[BRIGHT]*	Adjustment	BRITE
[VIDEO]	Composite video channel A mode	VIDEO 1
	Composite video channel A & Standby	VID1 SB
	Composite video channel B mode	VIDEO 2
	Composite video channel B & Standby	VID2 SB
	Video mode waiting for digit 1-2 entry	VIDEO
	Any other digit than 1-2	INVALID
[COLOR]*	Adjustment	COLOR
[RGB] (1-8)	Digital RGB mode	RGB DIG
	Digital RGB & Standby	RGBD SB
	RGB waiting for digit 1-8 entry	RGB
	Any other digit than 1-8	INVALID

ENTRY CODE	FUNCTION TO BE PERFORMED	DISPLAY READOUT
[1][0]	Help menu	HELP
	Help & Standby	HELP SB
[1][1]	Test mode - Test generator - crosshair	TEST
	Test mode & Standby	TEST SB
[2]	Used in conjunction with code 11. This is a step up command. By pulsing 2 a crosshatch will appear. By pulsing it a second time a crosshatch with sweep indicator will appear. Pulsing 2 a third time will take the test generator back to crosshair.	
[1][3]	Toggle red CRT ON	RED ON
	Toggle red CRT OFF	RED OFF
[1][4]	Toggle green CRT ON	GRN ON
	Toggle green CRT OFF	GRN OFF
[1][5]	Toggle blue CRT ON	BLUE ON
	Toggle blue CRT OFF	BLUE OFF
[2][0]*	Red CRT shift for image centering and registration	RCENTER
[2][1]*	Green CRT shift for image centering and registration	G CENTER
[2][2]*	Blue CRT shift for image centering and registration	B CENTER
[2][3]	Enters & exits second level of operation 2ND ON In VIDEO & RGB modes it allows same single key control of functions as the test mode. By pulsing 23 a second time 2ND OFF	
[2][8]	Set security bit -- locks entry to codes [3][0] and higher	SECURE
[2][9]	Clear security bit. Enables entry to higher number codes.	INSECURE
[3][0]*	Selects horizontal width adjust mode	H SIZE
[3][1]*	Selects vertical [illegible] adjust mode	V SIZE
[3][2]*	Selects top blanking adjust mode	BLANK
[3][3]	Horizontal sweep polarity select	SWEEP
[3][4]	Analog RGB sync polarity select for ceiling mounted units	ANA SYNC
[3][5]	Enter dac adjust mode	ADJ MODE
[3][6]	Enter dac set mode	SET MODE
[3][7]	Store swicher channel configuration	STORE
[3][8]	Select switcher channel	SELECT
[3][9]	Analog RGB invert	ARGB INV
[4][0]	Digital (TTL) sync mode	RGB DIG
	Digital (TTL) sync mode and standby	RGBD SB
[4][3]	Analog RGB composite sync mode.	RGB CS
	Analog composite sync mode and standby	RGBC SB
[4][4]	Analog RGB separate sync mode	RGB SS
	Analog RGB separate sync and standby	RGBS SB

ENTRY CODE	FUNCTION TO BE PERFORMED	DISPLAY READOUT
[4][5]	Analog sync on green mode	RGB SOG
	Analog sync on green and standby	RGBG SB
[4][6]	Video clamp select toggle	SYNC TIP
		BK PORCH
[4][7]	Terminal recall	TERM
[4][8]	Display diagnostic byte where "X" is either an one or a zero and an one indicates an error condition	XXXXXXXX
[4][9]	Auto lock enable toggle	AUTO ON
		AUTO OFF
[5][0]	VCR switch enable toggle	VCRS ON
		VCRS OFF
[5][1]	Registration enable toggle	REG ON
		REG OFF
[5][2]	Display software version level	VER X.XX
[5][3]	Initialize the data structures	INITIAL
[5][4]	Select the dac adjust step size	STEP
Transmission error - required Re-Enter command		RESEND
Illegal command entered		INVALID

SECTION 5.0 ADJUSTMENT AND REGISTRATION PROCEDURES

Alignment and registration may be done using either internal or external test pattern generators.

NOTE: For external pattern generators, select level two operation of the Remote Control [2][3] [ENTER]. Commands are now identical to the internal test program with the exception of key [2], which selects the internal patterns.

5.1 PERFORMANCE CHECK

This procedure is accomplished to verify projector registration. It is a confidence check for the operator, assuring that the projector is ready to perform.

The check should be performed before each use.

a. Check power cord connections
b. Check Remote Control connections
c. Check video source connections
d. Turn the projector ON/OFF switch to ON.
   - Allow a fifteen minute warm up period.
e. Turn on power at the Remote Control when READY is displayed.
   - Press the ON/OFF key and check that LED at the top of the Remote Control is lit. If the LED is not lit, it is an indication that the Remote Control is not receiving power. Check the connections and the 5 amp fuse in the back panel.
   - As a check to see if the Remote Control is functioning, you may use the STANDBY key. Activating this key will turn all of the CRTs on or off if it is working properly.
   - A second check can be made using the ON/OFF button on the registration panel.
f. Check the Sweep Mode --
   - Select code [1][1] ENTER. A crosshair pattern should appear on the screen. Remote Control display will read TEST.
   - Press key [2]. A large crosshatch pattern will appear. Press key [2] again and a smaller scale crosshatch pattern with one of the squares filled in will appear. For front projection. the indicator should be at the top right corner. For back or rear projection, the indicator should be in the upper left corner (viewed from the projector's side).

   - If the indicator is in the wrong corner, perform a sweep reversal.

   1. Press key [3]. Display will read 2nd OFF, then TEST.

2. Select code [3][2] ENTER. Display will read HORIZ REV. Projector will shut down, then come up in TEST. The sweep indicator should have changed sides.

NOTE: A "SECURE" prompt will require a code [2][9] ENTER to disable the security bit.

3. Select code [2][3] ENTER. Display should read 2nd ON, then TEST. Sweep reversal is complete.

NOTE: If the indicator is at the bottom of the pattern for ceiling mounted units, a failure of the automatic switching has occurred. Perform the sweep reversal procedure using codes [3][3] instead of code [3][2]. An alignment procedure must be accomplished any time sweep has been reversed. See paragraph 5.2.

g. Check Registration.
   - Select large crosshatch pattern using code [1][1] ENTER, then key [2].
   - Select [BRIGHT] control to mid range: Select [BRIGHT] on the Remote Control and adjust intensity with directional arrows.
   - Decrease [PICTURE] to minimum then increase it until a pattern is visible. The pattern should be white with little or no red,green or blue showing.
   - If colors are visible and lines are separated, go to the Alignment and Adjustment Procedure, paragraph 5.2.

h. Check Keystone.
   - Pattern squares should be uniformly shaped. If the image has a keystone effect, refer to the Keystone Correction procedure, paragraph 5.6.

i. Check Focus.
   - Enter code [1][1]. Crosshair pattern should be displayed.
   - If the image is blurry or fuzzy, attempt to adjust using the [DETAIL] and arrow controls of the Remote Control. If the image remains unacceptable, the control limits may have been reached. Refer to Mechanical Lens Focus, paragraph 5.4.

j. Pulse key [2]. Crosshatch should be displayed. The image on the screen should now be clear, sharp and white with evenly shaped squares. If it is not, go to the Alignment and Registration Procedure.

5.2 ALIGNMENT AND REGISTRATION PROCEDURE

This is a complete set up and checkout procedure.

Not every procedure will be required for every adjustment so the manual is structured to allow for bypassing unnecessary steps. It cannot cover all contingencies so individual procedures are included as separate paragraphs.

Perform this procedure for initial set up, any time the projector has been moved, or if the performance check indicates an adjustment need.

a. Power up.
   - Turn the projecto ON/OFF switch to ON. Cooling fan should start running.If the projector does not turn on, check power cord, power source and the 5 amp fuse in the back panel.
   - Turn on power at the Remote Control. Lights at the top of the Remote Control should come on. If not, check power cord and connections.
   - The projector can now be controlled from the Remote Control. Power down and restart are done from the Remote Control. The projector power switch can remain in the ON position without damaging the projector.

b. Turn the registration switch to OFF.
   - The sliding door on top of the projector must be opened for access to the registration panel.

NOTE: There is a light switch for registration panel illumination next to the registration switch.

c. Allow a fifteen minute warm up period.

d. Call up a crosshatch test pattern.
   - Select code [1][1] ENTER if display reads other than TEST, when the display reads TEST pulsing the [2] key will cycle through the three test patterns.

NOTE: The projector should be in the second level (single key entry) mode of operation. If single key functions appear not to be working, press key [3]. If the projector was in the second level of operation, a 2nd OFF display should appear, then TEST. If nothing happens to the display when key [3] is pressed, it is a sign that the projector is in the first level of operation. Select code [2][3] ENTER. The display should read 2nd ON, then TEST. Single key functions are now activated.

- Press the [BRIGHT] key on the Remote Control and adjust the intensity to maximum with directional arrow key commands.

- Press [PICTURE] on the Remote Control and, using the arrow keys, decrease intensity until the test pattern disappears. Increase intensity until the test pattern becomes visible again.

e. Check for parallax.
- This procedure is usually required after image size is changed and is a direct result of changing the distance between the projector and the screen. The GREEN image seems to become larger or smaller while the RED or BLUE images appear to move laterally.
- If these indications are showing on the screen, go to the Mechanical Lateral Lens Adjustment procedure, paragraph 5.3 after completing this procedure.

f. Check for overscanning.
- Look in the front of each lens. The test pattern should not be touching the vertical line on the right.

CAUTION
Severe overscanning requires a qualified technician to correct. Corrections require exposing high voltage components.

CAUTION
Minor overscanning may be corrected with electronic adjustments. However, continued operation at adjustment limits could damage the equipment.

- If there is no overscanning or if the raster is slightly offset, continue. Be aware that upcoming mechanical and electronic adjustments could be affected if overscanning is severe enough.

g. To check sweep reversal setting.
- Pulse the [2] key until the small scale crosshatch pattern with a solid white block is displayed. The solid square should be in the upper right corner for front projection, upper left corner for rear projection. If the solid square is in the wrong position, refer to paragraph 5.1.f. for the sweep reversal procedure.

h. Go to the Mechanical Lateral Lens Adjustment procedure, paragraph 5.3.

5.3 MECHANICAL LATERAL LENS ADJUSTMENT PROCEDURE.

This adjustment is needed whenever the image size is changed. The illustration shows the effect of moving the projector closer or further from the screen. The green image seems to become larger or smaller by moving the projector while the red and blue images move laterally. This condition is called parallax and can be corrected by moving the red and blue optic elements laterally after image size and throw distance have been decided.

This procedure is also used for correcting vertical linearity misalignments.

Preset: Power - ON, TEST mode. Registration switch off.

a. Select the crosshair test pattern.
   - Pulse the [2] key.
b. Adjust brightness to mid-range.
   - Select [BRIGHT] on the Remote Control and set brightness using the arrow keys.
c. Adjust picture.
   - Select [PICTURE] on the Remote Control. Using the arrow keys, decrease to minimum setting then increase until the crosshair becomes visible again.
d. Locate the registration switch on the registration panel and turn it OFF.
e. Open the front cover of the projector.
f. Locate the two 1/8" allen bolts on the optics holding channel and, if they are tight, loosen them one turn.

NOTE: These bolts are primarily for shipping but may be used in permanent installations to lock in lateral adjustments.

g. Adjust the RED lens.
   - Turn the knob above the red lens until the vertical lines of the RED test pattern overlap the vertical lines of the GREEN test pattern.
h. Adjust the BLUE lens.
   - Turn the knob above the BLUE lens until the vertical lines of the BLUE test pattern overlap the vertical lines of the GREEN and RED test patterns.
i. Select the crosshair test pattern
   - Pulse key [2] on the Remote Control.
j. Align the RED image.
   - Press key [7] and use directional arrow keys to overlay the RED pattern on the GREEN (vertical and horizontal).
k. Align the BLUE image.
   - Press key [9] and use the directional arrow keys to overlay the BLUE pattern on the RED and GREEN (vertical and horizontal).

NOTE: Crosshair should now be white.

l. Tighten the two allen bolts on the optics holding channel if desired.

m. Close and secure the front cover of the projector.

n. Check focus.
   - Pulse key [2].
   - Check focus using the crosshatch pattern.

o. If focus adjustments are required, refer to paragraph 5.4, Mechanical Lens Focus procedure. If focus adjustments are not required, go to paragraph 5.7, Registration procedure.

5.4 MECHANICAL LENS FOCUS PROCEDURE

This procedure is to be accomplished for all focus corrections or if the image is distorted on only one portion of the screen (center or edges). It assumes that the following has been accomplished.

Power ON
All CRTs on
Crosshatch test pattern selected (pulse key [2])
BRIGHT - mid-range
PICTURE - advanced from minimum until pattern is visible

Registration Switch - OFF

a. Open the front cover of the projector.
b. Turn off the BLUE and GREEN CRTs.
   - BLUE = Key [6] depressed on the Remote Control.
   - GREEN = Key [5] depressed on the Remote Control.
c. Locate the two focus locking wing nuts on the front and rear RED lens housing.
d. Focus image center.
   - Loosen rear wing nut and rotate the housing at the center of the lens assembly until the vertical bead pattern on the screen has a sharp clear image. Tighten the rear focus locking nut.
e. Focus edges and corners.
   - Loosen the front focus locking wing nut and rotate the forward section of the lens housing until the pattern at the edges of the screen has a sharp, clear image. Tighten the front focus locking wing nut.
f. Turn off the RED CRT.
   - Press key [4] on the Remote Control.
g. Turn off the GREEN CRT.
   - Press key [5].
h. Repeat steps c thru f for the GREEN CRT.
i. Turn off the GREEN CRT.

j. Turn on the BLUE CRT.
   - Press key [6].
k. Repeat steps c thru e for the BLUE CRT.
l. Turn on the RED and GREEN CRTs.
   - Keys [4] and [5].
m. The images should be clear and crisp. For fine adjustments go to paragraph 5.5, Electrostatic Lens Focus procedure.

5.5 ELECTROSTATIC LENS FOCUS PROCEDURE

This procedure should be performed if you are unable to obtain a satisfactory image from the RED and GREEN raster beads mechanically.

The Mechanical Lens Focus procedure should be used for all large adjustments. The electronic controls have range limitations. To achieve the best focus it may be necessary to alternate between mechanical and electrostatic procedures.

a. Power - ON.
   - Power should be on at the projector and CRTs activated and warmed up.
b. Select the crosshatch test pattern.
   - Press key [2] on Remote Control.
c. Set brightness to mid-range.
   - Select [BRIGHT] on the Remote Control and adjust brightness via up and down arrow keys.
d. Adjust image.
   - Select [PICTURE] on the Remote Control. Using the arrow keys decrease until the image disappears. Increase until the image becomes visible.
e. Turn off the GREEN and BLUE CRTs.
   - GREEN equals key [5] on Remote Control.
   - BLUE equals key [6] on Remote Control.
f. Open the back door of the projector.
g. Locate the electrostatic focus controls.
h. Adjust RED focus control until a sharp image is obtained.
i. Turn off the RED CRT.
   - key [4] on the Remote Control.
j. Turn on the GREEN CRT.
   - key [5] on the Remote Control.
k. Adjust the GREEN focus control until the best image is achieved.
l. Turn off the GREEN CRT.
   - key [5] on the Remote Control.
m. Turn on the BLUE CRT.
   - key [6] on the Remote Control.
n. Adjust the BLUE focus control until the best image is achieved.
o. Turn on the RED and GREEN CRTs.
   - RED equals key [4] on the Remote Control.
   - GREEN equals key [5] on the Remote Control.
p. If performing the Alignment and Adjustment procedure, go to paragraph 5.6, Keystone Correction procedure.

5.6 KEYSTONE CORRECTION PROCEDURE

This procedure assumes the following conditions:

Power - ON
Crosshatch TEST pattern displayed
Sliding door on top of projector open
Registration switch - OFF

a. Set BRIGHT to maximum
   - Select [BRIGHT] on the Remote Control and adjust brightness via up and down arrow keys.
b. Advance PICTURE from minimum until pattern is visible.
   - Select [PICTURE] on the Remote Control and adjust via up and down arrow keys.
c. Turn OFF the RED and BLUE CRTs.
   - RED equals Remote Control key [4]
   - BLUE equals Remote Control key [6]
d. Locate the master Keystone controls on the registration control panel. The master Keystone controls are the only controls on the registration panel which are usable with the registration switch OFF.
e. Adjust the master Keystone controls until all the square images are the same shape.
   - Use a plastic adjustment tool.
   - Vertical and horizontal corrections may be required.
f. Turn on the RED CRT.
   - key [4] on the Remote Control.
g. Locate the RED east/west keystone control.
h. Adjust the control until the RED overlays the GREEN pattern.

NOTE: The pots have a 30 turn capacity end to end. To establish the mid-range setting, turn in a clockwise direction until first 'click' is heard.
Then turn counter-clockwise 15 complete rotations.

WARNING -- There are no physical stops on these potentiometers. You have reached maximum limitation when the first clicking sound is heard. Once center has been established avoid over-correcting. Refer to paragraph 5.5.

i. Turn OFF the GREEN CRT.
   - Key [5] on the Remote Control.
j. Turn ON the BLUE CRT.
   - Key [6] on the Remote Control.
k. Repeat steps g and h for the BLUE CRT.
l. Turn ON the GREEN CRT (all CRTs are now ON).
m. Crosshatch pattern should be white with no keystone distortion.
n. Go to paragraph 5.7, Registration procedure.

5.7 REGISTRATION PROCEDURE

Prerequisites: Alignment and Adjustment procedures, paragraphs 5.2 - 5.6.

Preset: Power ON, CRTs - ON
Registration switch ON

a. Select crosshatch TEST patterns via key [2] on the Remote Control. The correct pattern for this procedure is the one with the larger squares with the ends of lines visible.
b. Set brightness to mid-range. Select [BRIGHT] on the Remote Control and adjust via up and down arrow keys.
c. Set TEST pattern.
   - Select [PICTURE] on the Remote Control. Using the arrow keys, decrease until the image disappears then increase until image becomes visible again.
d. Check registration switch -- should be in the ON position.

NOTE: CRTs must have been on at least three minutes before proceeding.

e. Turn the RED and BLUE CRTs OFF.
   - Red equals key [4] on the Remote Control.
   - Blue equals key [6] on the Remote Control.
f. Check keystone.
   - If keystone correction is required, adjust using the master keystone controls (par. 5.6).
g. Turn the RED CRT ON.
   - Key [4] on the Remote Control.
h. Using the centering controls on the Remote Control, offset the horizontal RED lines 2-3 scan widths.
i. Parallel the RED and GREEN lines horizontally.
   - Use the horizontal bow and horizontal skew controls to adjust the lines (if required).
j. Overlay the RED horizontal lines onto the GREEN TEST pattern via the Remote Control centering controls.

k. Offset the RED vertical lines 2-3 scan widths via the Remote Control centering controls.
l. Parallel the vertical RED and GREEN lines.
   - Use the vertical bow and vertical skew controls (if required).
m. Overlay the RED vertical lines onto the GREEN TEST pattern via the Remote Control centering controls.
n. Turn the GREEN CRT OFF.
   - Key [5] on the Remote Control.
o. Turn the BLUE CRT ON.
   - Key [6] on the Remote Control.
p. Repeat steps i - m for the BLUE CRT.
q. Turn the GREEN CRT ON.
   - Key [5] on the Remote Control
   - Pattern should be white with little or no RED, GREEN, or BLUE showing.
r. This is the last step in the Alignment and Registration procedure. Go to paragraph 6.0 for Image Adjustment procedures.

SECTION 6.0 VIDEO IMAGE ADJUSTMENTS

This section of the manual describes how to adjust the projection system to obtain the best video image when using a composite video input signal. It also describes how to make adjustments to eliminate deficiencies in the video image should these occur. ALL ADJUSTMENTS SHOULD BE MADE ONLY AFTER THE SYSTEM HAS WARMED UP app. fifteen minutes and the Performance Check has been completed.

6.1 SELECTING VIDEO

To change from any other mode to a video projection mode press VIDEO on the Remote Control. The projector will automatically select the video source. All image adjustments are now made with the Remote Control commands.

6.2 ADJUSTING THE VIDEO IMAGE

- Press the [PICTURE] control and the up/down arrows to obtain maximum balance.
- Press the [BRIGHT] control and the up/down arrows until the black parts of the video image appears the blackest. You may need to wait until the image shows something you are sure is black to make this adjustment. Be careful not to lose the details in the darkly shaded areas. Once this control is set properly, you should not have to adjust it further.
- Activate the [COLOR] control and the up/down arrows until the image reaches a pleasing level of color intensity. For different settings, the picture control may need readjustment to achieve the proper color intensity level.
- Press the [TINT] control and up/down arrows until good flesh tone colors are achieved (not active in RGB).
- Press the [DETAIL] control and up/down arrows until the edges of the object in the image appear sharp and well defined.

6.3 TIPS ON ADJUSTING IMAGE, COLOR AND TINT

In adjusting image color or tint, the following guidelines may be helpful.
- If color appears pale or weak, increase color intensity by bringing up the [COLOR] control.
- If color appears flushed or too bright, decrease color intensity by lowering the [COLOR] control.
- If facial tones or objects appear too GREEN, bring down the [TINT] control.
- If after registration has been accomplished a redish hue appears on the white parts of the image, a fine tune can be made using the white balance pots on the registration panel.
- RGB enhancements can be performed using the analog and digital pots and the analog blue enhance pot on the right side of the registration panel.

SECTION 7.0 SYSTEM TROUBLESHOOTING/MAINTENANCE

Only Trident authorized technicians may repair Trident projectors. Operator actions are limited to the procedures in this section of the manual.

This section of the manual describes the procedures for correcting operating problems. Locate the problem indicator (s) in the paragraph titles and follow the directions.

7.1 SYSTEM WILL NOT OPERATE

- Verify that power outlets are furnishing power.
- Verify that the projection unit power cord is plugged in firmly.
- Verify that the ON/OFF switch on the back panel is ON.
- Verify that the LED on the Remote Control is illuminated. If not, check the 5 amp fuse in the back panel.

7.2 SYSTEM STOPS DURING OPERATION

One of the projection systems's protection circuits may have activated, due to an AC power fault or a momentary projection fault.

- Check power cords.
- Turn the power ON/OFF switch to OFF.
- Check the 5 amp fuse in the back panel fuse box.
- Wait one minute to allow projection circuit to reset itself.
- Turn the power ON/OFF switch ON.

7.3 REMOTE CONTROL READOUTS DO NOT MATCH CODED INPUTS

The controlling logic in the T-100 has several levels of complexity. Because of this, the keys on the Remote Control have several functions depending on the level of operation. If the Remote Control readouts do not appear to relate to the commands entered, it is possible that the logic has somehow entered a different level of operation.

- If in the TEST mode, exit to another mode and reenter. Set the security bit. Check level two or level one operation (single digit or two digit plus ENTER commands required).
- If in any mode other than TEST, return to a VIDEO or RGB projection mode and set the security bit. Check first or second level of operation.
- If unable to obtain satisfactory results after changing modes, setting the security bit and confirming operating level, refer to the initializing procedure in Section 4.0.

7.4 POWER ON BUT NO PICTURE

- Verify that the CRTs are not in standby mode.

- If the color tubes are on, check video source. If the projector operates in TEST, the problem is either in the external source or the projector circuitry. Try a different input mode.
- If tubes are not on, turn on the ON/OFF switch on the registration panel.
- If everything appears to be working but still unable to get a picture, refer to the initializing procedure in Section 4.0.

7.5 PREVENTIVE MAINTENANCE

Lens cleaning -- Use a soft cloth and a mild commercial glass cleaner. Do not use abrasive cleaners which could scratch the lens.

* IBM PC/XT and PC/AT are Trademarks of International Business Machines.